REPORT NO. DOT-TSC-UM104-PM-80-49
DECEMBER 1980

DESIGN FEASIBILITY STUDY FOR MODIFYING AN EXISTING HEAVY RAPID RAIL TRUCK TO A STEERABLE CONFIGURATION

George Mekosh, Jr.

THE BUDD COMPANY
Technical Center
Fort Washington PA 19034

PROJECT MEMORANDUM

THIS DOCUMENT CONTAINS PRELIMINARY INFORMATION SUBJECT TO CHANGE. IT IS CONSIDERED AN INTERNAL TSC WORKING PAPER WITH A SELECT DISTRIBUTION MADE BY THE AUTHOR. IT IS NOT A FORMAL REFERABLE REPORT.

U.S. DEPARTMENT OF TRANSPORTATION
RESEARCH AND SPECIAL PROGRAMS ADMINISTRATION
Transportation Systems Center
Cambridge MA 02142

Acknowledgments

This work was conducted for the Urban Mass Transportation Agency (UMTA) through the Transportation Systems Center (TSC) in Cambridge, Massachusetts. Mr. Charles O. Phillips was the TSC technical monitor. Dr. H. Weinstock of TSC, also provided technical assistance and guidance for this work.

The author wishes to express thanks and appreciation to Mr. Harold A. List of Railway Engineering Associates for his contributions to the steerable truck design and the development and operation of the non-linear model.

The author also wishes to express thanks and appreciation to Dr. J. K. Hedrick, Dr. D. N. Wormley and their graduate students Mr. C. E. Bell and Mr. D. Horak at the Massachusetts Institute of Technology, for their technical assistance in the areas of curving, stability, and ride quality.

Thanks also to Mr. Bill Vigrass, Superintendent of Equipment and Mr. Don Wolfe, Superintendent of Power and Way at PATCO, for the information they provided concerning the operation, maintenance, and related costs for the trucks and rail system.

METRIC CONVERSION FACTORS

Approximate Conversions to Metric Measures

Symbol	When You Know	Multiply by	To Find	Symbol
	LENGTH			
in	inches	*2.5	centimeters	cm
ft	feet	30	centimeters	cm
yd	yards	0.9	meters	m
mi	miles	1.6	kilometers	km
	AREA			
in^2	square inches	6.5	square centimeters	cm^2
ft^2	square feet	0.09	square meters	m^2
yd^2	square yards	0.8	square meters	m^2
mi^2	square miles	2.6	square kilometers	km^2
	acres	0.4	hectares	ha
	MASS (weight)			
oz	ounces	28	grams	g
lb	pounds	0.45	kilograms	kg
	short tons (2000 lb)	0.9	tonnes	t
	VOLUME			
tsp	teaspoons	5	milliliters	ml
Tbsp	tablespoons	15	milliliters	ml
fl oz	fluid ounces	30	milliliters	ml
c	cups	0.24	liters	l
pt	pints	0.47	liters	l
qt	quarts	0.96	liters	l
gal	gallons	3.8	liters	l
ft^3	cubic feet	0.03	cubic meters	m^3
yd^3	cubic yards	0.76	cubic meters	m^3
	TEMPERATURE (exact)			
°F	Fahrenheit temperature	5/9 (after subtracting 32)	Celsius temperature	°C

*1 in = 2.54 (exactly). For other exact conversions and more detailed tables, see NBS Misc. Publ. 286, Units of Weights and Measures, Price $2.25, SD Catalog No. C13.10:286.

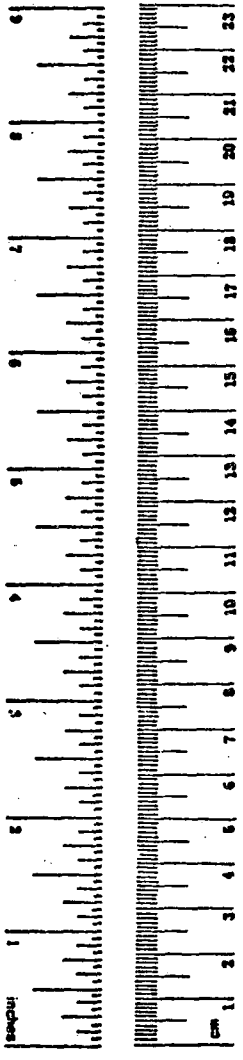

Approximate Conversions from Metric Measures

Symbol	When You Know	Multiply by	To Find	Symbol
	LENGTH			
mm	millimeters	0.04	inches	in
cm	centimeters	0.4	inches	in
m	meters	3.3	feet	ft
m	meters	1.1	yards	yd
km	kilometers	0.6	miles	mi
	AREA			
cm^2	square centimeters	0.16	square inches	in^2
m^2	square meters	1.2	square yards	yd^2
km^2	square kilometers	0.4	square miles	mi^2
ha	hectares (10,000 m^2)	2.5	acres	
	MASS (weight)			
g	grams	0.035	ounces	oz
kg	kilograms	2.2	pounds	lb
t	tonnes (1000 kg)	1.1	short tons	
	VOLUME			
ml	milliliters	0.03	fluid ounces	fl oz
l	liters	2.1	pints	pt
l	liters	1.06	quarts	qt
l	liters	0.26	gallons	gal
m^3	cubic meters	35	cubic feet	ft^3
m^3	cubic meters	1.3	cubic yards	yd^3
	TEMPERATURE (exact)			
°C	Celsius temperature	9/5 (then add 32)	Fahrenheit temperature	°F

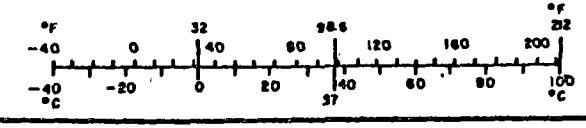

TABLE OF CONTENTS

TABLE OF CONTENTS (CONTINUED)

LIST OF ILLUSTRATIONS

LIST OF TABLES

NOMENCLATURE

a = one half track gauge

b = one half truck wheel base

d = one half primary suspension lateral spacing

C = damping rate

C_{px} = primary suspension longitudinal damping

C_{py} = primary suspension lateral damping

D_f = track curvature that can be negotiated without flange contact

f = Kalker coefficients

F_o = friction breakaway force

G = steering gain

K = spring rate

K_b = inter-axle bending stiffness

K_s = inter-axle shear stiffness

K_{fs} = effective shear stiffness of forced steering link

K_{px} = primary suspension longitudinal stiffness

K_{py} = primary suspension lateral stiffness

K_{rb} = bending stiffness of the steering arm

K_{rs} = shear stiffness of the steering arm

K_{sy} = secondary yaw stiffness

ℓ_1 = steering link offset

ℓ_s = one half truck center spacing

L/V ratio of lateral to vertical wheel/rail force

r_o = rolling radius

S = power spectral density

T_s = secondary yaw breakaway torque

V = velocity

V_{cr} = critical speed

V_o = initial velocity

$\dot{x}$ = longitudinal velocity

y = lateral displacement

θ = track curvature

λ = wheel tread conicity

μ = coefficient of friction

ξ = damping ratio

$\overline{\sigma_{\dot{x}}}$ = RMS relative velocity across damper

ϕ_d = cant deficiency

ψ_c = carbody yaw displacement

Ω = wavelength

EXECUTIVE SUMMARY

One of the problems confronting the transit industry is the curving performance of the powered conventional urban heavy rapid rail truck. Among the curving performance problems are the high rate of wheel flange wear and rail gauge wear associated with operating heavy rapid rail cars on sharp curves. An additional problem that may be even more objectionable than the high wear rate is the high pitch screech or squeal that is associated with negotiating sharp curves (usually greater than 8 degrees curvature or approximately 700-foot radius).

The squeal noise and most of the wheel flange wear and rail gauge wear experienced with conventional parallel axle trucks are due to the non-radial running position of the leading axle in sharp curves. The non-radial running position results in a tracking error or an angle of attack between the wheel and rail. It is the associated wheel/rail angle of attack and lateral motion (creep) that cause noise, wear, and an unnecessarily high lateral force between the wheel flange and the rail. In addition, in the non-radial running position, there is a substantial rubbing velocity between the rail and the flange which causes additional noise and wear.

The noise problem can be mitigated by using resilient wheels, various other noise suppression measures, and by lubricating the wheel/rail interface. Of course, resilient wheels or noise barriers do not relieve the wear problem and lubrication must be very carefully controlled or there will be an increase in the incidence of flat wheels due to wheel slide during braking.

The addition of steering, however, cures the problem at the source by eliminating the tracking error and the associated wheel/rail lateral motion. The vibration which causes the noise is not generated. Flange forces are lower and the rubbing action is eliminated. With the need for wheel/rail lubrication removed, traction and braking performance become more consistent.

The objective of this program is to determine the feasibility of modifying an existing urban rail vehicle truck to a steerable configuration for the purpose of improved curving performance. The anticipated benefits from the use of steerable trucks on urban transit vehicles are: reduced wheel flange wear, reduced rail gauge wear, reduced wheel/rail noise, and reduced energy consumption during curve negotiation. Where cars accumulate a high percentage of their mileage on curved track, the potential dollar savings on wheel and track wear could be quite substantial.

The existing urban rail vehicle trucks that were selected for this feasibility study are now in service on the Port Authority Transit Corp. (PATCO) system. Both the PATCO cars and trucks were designed and built by The Budd Company. These vehicles (75 in number) went into service during 1967. The basic truck design is known as the Budd Pioneer-III (P-III) and is similar to thousands of other trucks built by Budd.

The PATCO System, known locally as the Lindenwold High Speed Line, runs between downtown Philadelphia and Lindenwold, New Jersey. In Philadelphia, the line runs east and west under Locust Street utilizing a tunnel with several sharp curves. There are additional curves and a grade as the line comes out of the tunnel and up to cross the Delaware River on the Benjamin Franklin Bridge. In Camden, New Jersey, the line is again underground with several sharp curves. From Camden to Lindenwold, the curves are gradual. Even though the stations are relatively close together, the cars often reach 75 mph in this area. The PATCO System would be an excellent place to test a steering type truck because it has both sharp curves and a high speed section.

The basic approach taken in the design performance studies was to first establish various performance indices for the existing PATCO truck design. The performance indices included high

speed stability, curving, and ride quality. Several different computer models were used for these studies. The major portions of the stability and ride quality studies were made using linear models that employ eigen value-eigen vector techniques. Linear models can also be used to study curving performance, however, the main set of curving studies used, instead, a non-linear tracking model. The Budd non-linear model can accommodate flange contact, apply an arbitrary creep characteristic, and use non-linear wheel profiles.

The studies indicate that the existing PATCO truck has a high critical speed which results in a rather conservative stability margin and this is confirmed by field experience. Although, the curving performance of the existing PATCO truck is similar to that of other conventional (square) trucks, there is room for improvement. The existing PATCO truck experiences significant angles of attack during curve negotiation and generates the squeal or screech that is so typical of the sharp curves.

Once the baseline performance data for the existing PATCO truck was established, steering was added to the analytical models. The steering concept that is most suitable to powered trucks employs "C"-shaped structures or sub-frames called steering arms. The steering arms are inter-connected at the truck center and inter-

face with the independent side frames at the corners. The corner connections must allow for the axle yaw motions which are ± 1.1 degree if positioned radially on a 30-degree curve (193 ft. radius). The resulting longitudinal deflection at the corner joint is ±0.44 inches

The steering arm concept can have two modes of operation which are known as self-steering and forced- (positive-) steering. In the self-steering mode, the steering input comes exclusively from the self-centering action of a tapered wheelset. The steering forces are generated by the creep forces developed at the wheel/rail contact patch. Therefore, the self-steering input is a direct function of the adhesion limits and contact geometry. In the forced-steering mode, the steering input comes from a linkage arrangement that responds to truck swivel with respect to the carbody during curve negotiation. The linkage geometry positions the axles radially when the car is in a curve. Self-steering action is also present and actually aids the positive-steering mode.

The longitudinal stiffness of the inter-connection between the steering arms and the truck frame corners became the major trade-off between high-speed stability margin and improved curving performance. A stiffness of 30,000 lb/in was the lowest value that could satisfy the stability requirements of this truck design. This required value is a function of the yaw inertia of

the wheelsets and steering arms. However, the value required for stability was not acceptable from a curving performance standpoint because of the large forces that would be required to deflect this joint $\pm$ 0.44 in. for radial positioning on a 30 degree curve. The self-steering mode could not possibly generate these force levels. The forced-steering mode could generate these force levels but the structural requirements of the steering linkage creates a packaging problem because of the space constraints. Therefore, a slide mechanism with a 2000-lb breakout force level was put in series with the longitudinal spring to limit the force levels. During high speed operation, the axle yaw motions would be handled within the spring element and breakout or sliding of the slide mechanism would not occur. However, during curve negotiation, the breakout force level would be developed so that the axles could assume the radial position.

In the self-steering mode, breakout could occur on rough track and possibly result in an instability. Also, in the self-steering mode, adequate curving performance required a minimum friction coefficient of 0.3 at the wheel/rail interface. Curving performance would degrade at the lower friction levels typical of wet or lubricated rail. Based on the above concerns, forced-steering is recommended for the proposed steerable truck design.

Forced-steering ensures radial positioning on curves down to 30 degrees and provides the proper inter-axle stiffness (bending and shear) parameters required for stability.

The proposed steerable truck design accommodates the existing truck bolster, wheel/axle assemblies, propulsion units, and tread brake units. A new side frame is required with the addition of steering arms. The new side frames are quite similiar to the existing truck frames with the exception of the corners. The four corners are designed to mate with the steering arms and allow the required yaw motions. The proposed steerable truck design will increase the weight of the truck by about 1560 lbs (approximately 12%). This increase is essentially the weight of two steering arm assemblies. It is quite possible that a new design that is not required to mate with existing equipment would not result in a weight increase.

The results of the analytical studies show that the proposed steerable truck design with forced-steering can dramatically improve curving performance on the PATCO system. High speed stability can be maintained by providing the required dynamic axle yaw restraint. Ride quality is preserved by retaining the existing secondary suspension without significantly modifying the input to this suspension. The potential does exist for improved ride quality because of the better tracking ability of the steerable truck. It is anticipated that many track irregularities typically encountered around switches and frogs can be avoided because of the improved tracking. Perhaps the most significant improvement of all will be the reduced noise levels associated with sharp curves.

A cost benefit analysis was made to determine the overall cost effectiveness or net worth of the proposed steerable truck for the PATCO system. The basic trade-off is the increased capital cost and increased maintenance cost because of added assemblies versus the potential savings from reduced wheel flange wear, reduced rail wear in curves, elimination of rail lubricators, elimination of wheel skid-flats caused by lubricant finding its way onto the rail head, and reduced energy consumption during curving. The results of the cost analysis show that the addition of steering to the PATCO system could reduce operating costs by about 6%. The estimated annual savings are approximately $50,000 from reduced wheel maintenance, $34,000 from reduced rail maintenance, and $20,000 from reduced energy consumption during curving. However, to realize these savings the entire fleet would have to be retrofitted. The capital cost to retrofit the PATCO trucks with steering has been estimated at approximatley $15,000 per truck. The base payback period for the retrofit would be about 21 years.

The cost analysis also looked at the cost impact of the addition of steering to a new truck design. The capital cost premium for steering on a new truck design was estimated at about $7000 per truck. Based on the potential savings at PATCO, the base payback period for steering on a new design was estimated at 11 years.

Clearly the cost benefit of steering is a direct function of the total number of sharp curves (over 4 degrees) on a particu-

lar transit system. On a transit system with more curves than PATCO, the potential operating cost savings could reduce the payback period and make steering much more cost effective.

Keep in mind that the cost analysis did not attempt to place a dollar value on reduced noise levels during curving.

1.0 INTRODUCTION

1.1 Background

The Office of Rail and Construction Technology, Urban Mass Transportation Administration (UMTA) Office of Technology Development and Deployment, is conducting research, development, test and evaluation programs directed toward the improvement of urban rail transportation systems. These programs will result in improved prototype vehicle, component and rail system designs, improved ways and structures and structural components, and will provide engineering design data on rail system component interaction.

The role of Transportation Systems Center (TSC) as System Manager for the necessary technical support to UMTA in these developmental areas includes its participation in the design of and technical monitoring of UMTA vehicle and component prototype development. In addition, TSC will participate in the analysis and testing of vehicles and components.

One of the problems confronting the transit industry is the curving performance of the powered conventional urban heavy rapid rail truck. Among the curving performance problems, are the high rate of wheel flange wear and rail gauge wear associated with operating heavy rapid rail cars on

sharp curves. An additional problem that may be even more objectionable than the high wear rate is the high pitch screech or squeal that is associated with negotiating sharp curves (usually greater than 8 degrees curvature or approximately 700-foot radius).

The squeal noise and most of the wheel flange wear and rail gauge wear experienced with conventional parallel axle trucks are due to the non-radial running position of the leading axle in sharp curves. The non-radial running position results in a tracking error or an angle of attack between the wheel and rail. It is the associated wheel/rail angle of attack and lateral motion (creep) that cause noise, wear, and an unnecessarily high lateral force between the wheel flange and the rail. In addition, in the non-radial running position, there is a substantial rubbing velocity between the rail and the flange which causes additional noise and wear.

The noise problem can be mitigated by using resilient wheels, various other noise suppression measures, and by lubricating the wheel/rail interface. Of course, resilient wheels or noise barriers do not relieve the wear problem and lubrication must be very carefully controlled or there will be an increase in the incidence of flat wheels due to wheel slide during braking.

One approach to reducing the wear problem and the associated noise is to make the trucks steerable. Steerable trucks can cure the wear problem at the source by eliminating the tracking error and the associated wheel/rail lateral motion. The vibration which causes the noise is not generated. Flange forces are lower and the rubbing action is eliminated. With the need for wheel/rail lubrication removed, traction and braking performance can become more consistent.

The addition of steering to the trucks in existing transit systems will eliminate the squeal problem in sharp curves and offer a reduction in operating and wheel/rail maintenance costs. The use of steering-type trucks in new systems will reduce engineering and construction costs by relieving the present need to use large radius curves which often involves very expensive modification of existing building foundations.

1.2 Objective

In July, 1979, The Budd Company was awarded one of two competing contracts let out by the Transportation Systems Center. The contract objective was to determine the feasibility of modifying an existing urban heavy rapid rail truck to a steerable configuration for the purpose of improved curving performance. The anticipated benefits from the use of steerable trucks on urban transit vehicles are: reduced

wheel flange wear, reduced rail gauge wear, reduced wheel/rail noise, and reduced energy consumption during curve negotiation. Where cars accumulate a high percentage of their mileage on curved track, the potential dollar savings on wheel and track wear could be quite substantial. The design and analysis, including technical and cost factors, will be utilized by the Government to determine the feasibility of subsequently fabricating one or more prototypes for test and evaluation.

1.3 Scope

The truck chosen for the modification studies is the Budd Pioneer - III now in service on the Port Authority Transit Corp. (PATCO) system. The basic approach taken in these studies was to first establish various performance indices for the existing PATCO truck design. The performance indices include high speed stability, curving performance, and ride quality. A cost benefit analysis was made to determine the overall cost effectiveness or net worth of the steerable truck concept with respect to the PATCO system. The basic trade-off is the increased capital cost versus the potential savings from reduced wheel flange wear, reduced rail wear and reduced power consumption in curves.

The existing truck design and the proposed steerable

truck design are described in Section 2.0. The Design Performance Specification is given in Section 3.0. The technical analysis of both the existing truck and the steerable truck with variations is presented in Section 4.0. The Cost Benefit Analysis is presented in Section 5.0. The Summary and Conclusions are presented in Section 6.0.

1.4 PATCO System Description

The PATCO System, known locally as the Lindenwold High Speed Line, runs between downtown Philadelphia and Lindenwold, New Jersey. Figure 1-4.1 is a schematic system map. The line is 14.2 miles long.

In Philadelphia, the line runs east and west under Locust Street utilizing a tunnel constructed many years before the line went into service. There is a very sharp (28-degree) curve where the route turns north under 8th Street to the 8th and Market Streets station. From here to City Hall, Camden, the route has been in use for many years - the service having been known as the "Bridge Train". There are additional sharp curves and a grade as the line comes up to cross the Delaware River on the Benjamin Franklin Bridge. In Camden, the route is again underground with several sharp curves.

Just beyond Camden City Hall, there is a new construction

connecting the old "Bridge" route with an existing railroad right-of-way. From here to Lindenwold, the curves are gradual and the line is generally elevated. Even though the stations are relatively close together, the cars often reach 75 - 80 mph in this area.

The line includes a wide variety of operating conditions from sharp curves in the tunnels to a long section along a railroad alignment with gentle curves. A summary of the PATCO curves, both east and west bound, is shown in Figure 1.4.2. This figure shows that the majority of the curves are in the 2-degree range; however, there are several curves in the tunnels which are in the 20- to 28-degree range. These sharp curves definitely generate the high pitch squeal or screech.

Operating with 75 vehicles, the PATCO system accumulated 3,983,000 car-miles and serviced 11,078,000 passengers during 1979. The total traffic has been estimated at 6 million gross tons per year past any given point along the system.

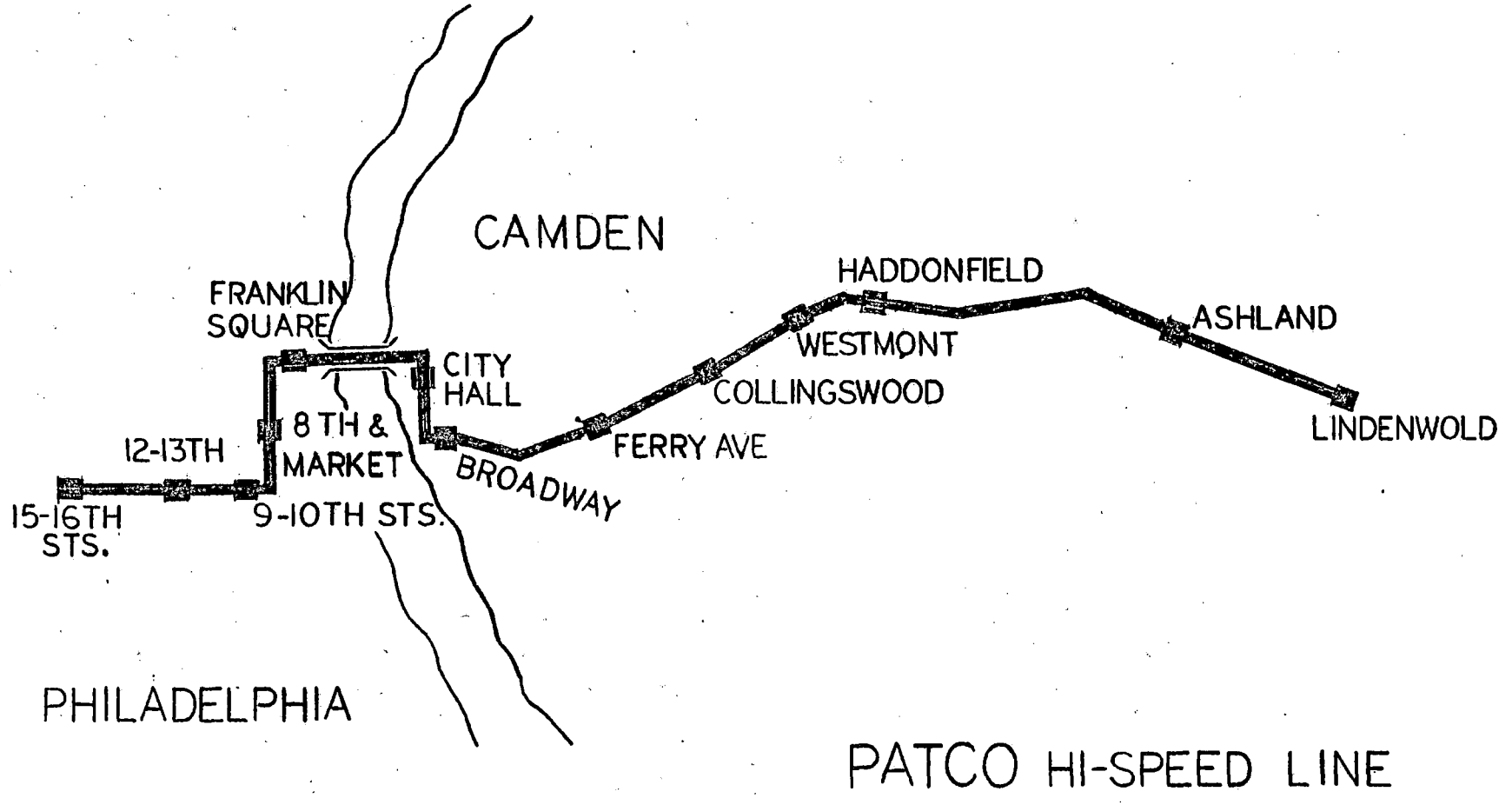
CAMDEN
FRANKLIN SQUARE
HADDONFIELD
ASHLAND
WESTMONT
CITY HALL
COLLINGSWOOD
LINDENWOLD
12-13TH
8 TH & MARKET
FERRY AVE
BROADWAY
15-16TH STS.
9-10TH STS.
PHILADELPHIA
PATCO HI-SPEED LINE

Figure 1.4.1

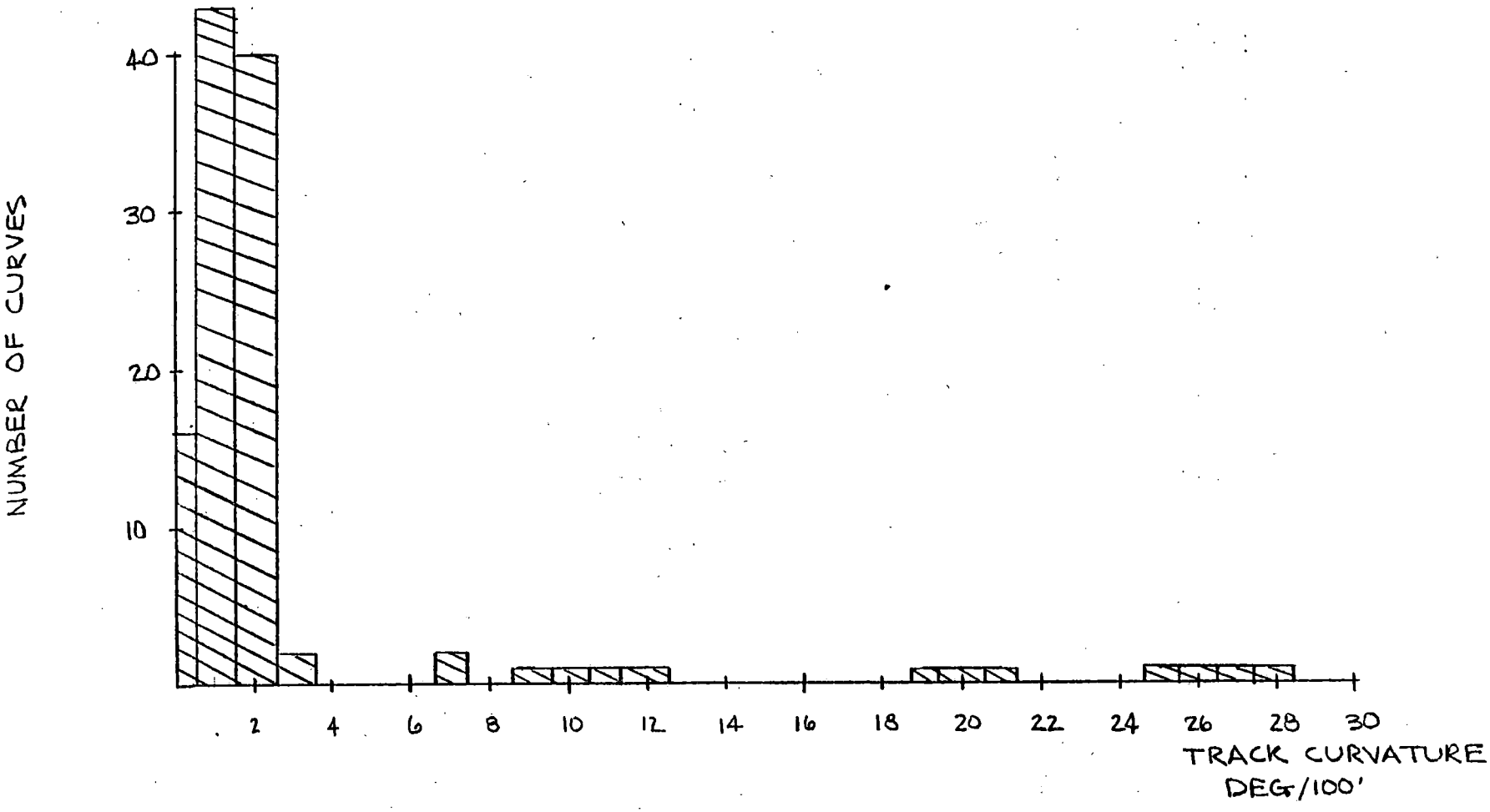

DISTRIBUTION OF CURVES - PATCO HI-SPEED LINE

BANDWIDTH = 1°

FIGURE 1.4.2

2.0 Design Description

2.1 Introduction

A general description of the PATCO cars and trucks are given in this section. Both the cars and trucks were designed and built by The Budd Company. These vehicles (75 in number) went into service during 1967.

This section also presents a description of the design modification to add steering capability to the existing PATCO trucks. A self-steering configuration is discussed in detail as well as a forced- (or positive-) steering configuration. In the self-steering mode, the steering input comes exclusively from the self-centering action of a tapered wheelset. In the positive-steering mode, the steering input comes from a linkage arrangement that responds to truck swivel with respect to the carbody during curving. Self-steering action is also present and actually aids the positive-steering mode.

2.2 Existing Truck

The basic dimensions of the cars and trucks are shown in Table 2-2.1. Figures 2-2.1 and 2-2.2 are plan and side views of the truck. The suspension parameters are shown in Table 2-2.2. Table 2-2.3 lists the weights and radii of gyration of the major truck assemblies.

TABLE 2-2.1: PATCO VEHICLE DIMENSIONS AND WEIGHTS

Maximum Scheduled Speed	75 MPH
Length of car over anticlimbers at the centerline of car	67 ft. 6 in.
Length of car over coupler faces	67 ft.10 in.
Distance center to center of trucks	47 ft. 6 in.
Maximum width of car body over threshold	10 ft. 0 in.
Height rail to top of floor, new wheels	3 ft.10-1/2 in.
Maximum height rail to top of roof, new wheels, empty car	12 ft. 4 in.
Height of high level station platform above top rail	3 ft.10 in.
Centerline of track to edge of high level platform	5 ft. 3 in.
Coupler height above rail	28-1/2 in.
Maximum number of cars in train	8
Maximum superelevation	10 in.
Minimum horizontal curve radius - with cars coupled	125 ft.
Minimum vertical curve radius	2,000 ft.
Length of minimum radius vertical curve	90 ft.
Wheel diameter	28 in.
Track gauge	56-1/2 in.
Wheel gauge	55-11/16 in.
Truck wheelbase	7 ft. 6 in.
Vehicle weights	
Carbody	54,340 lbs.
Truck	12,860 lbs.
Ready to run	80,060 lbs.
Full seated (80 passengers @ 155 lbs.)	92,460 lbs.
Normal maximum (125 @ 155 lbs.)	99,435 lbs.
Crush load (195 @ 155 lbs.)	110,285 lbs.

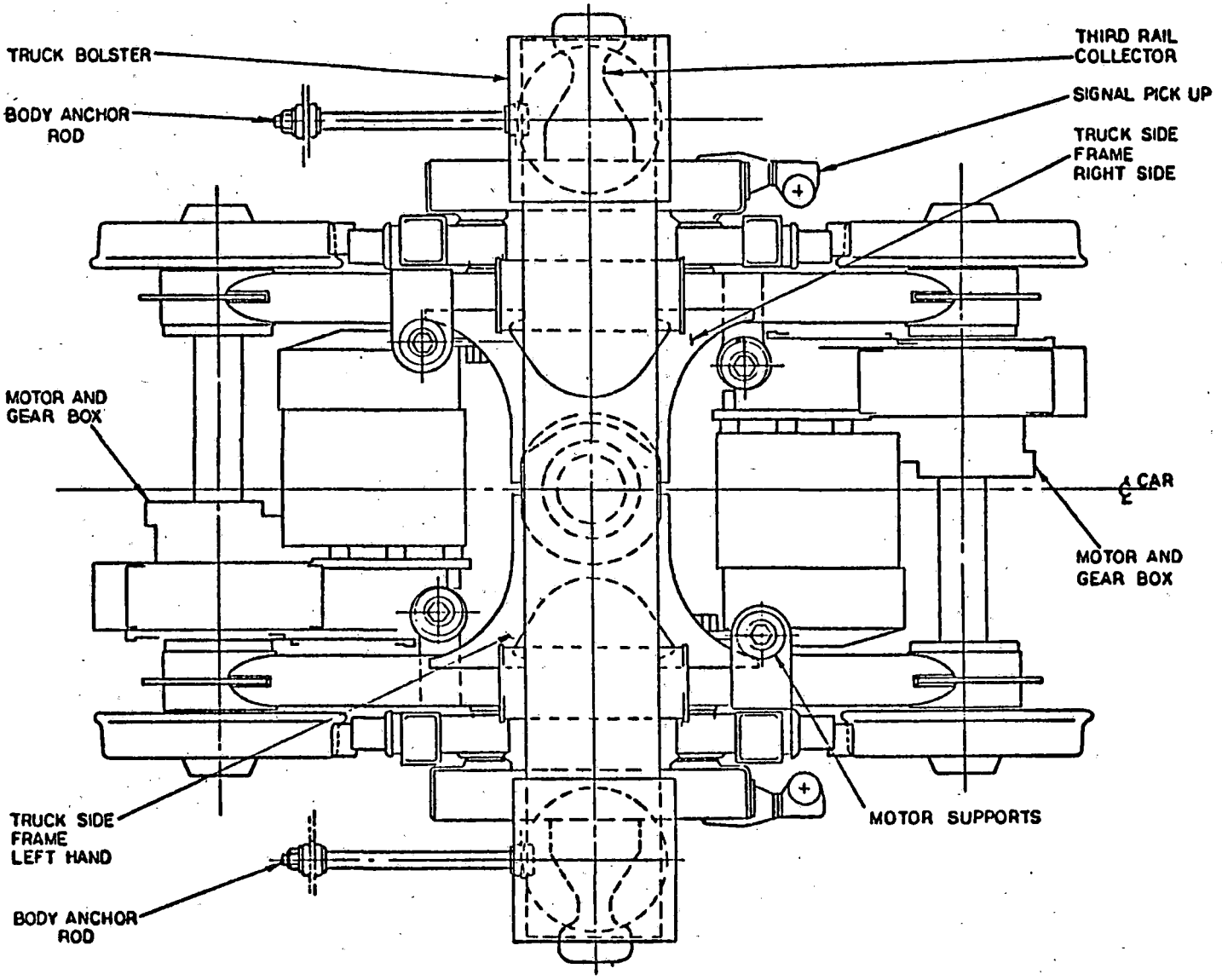

FIGURE 2-2.1: EXISTING PATCO P-III TRUCK, PLAN VIEW

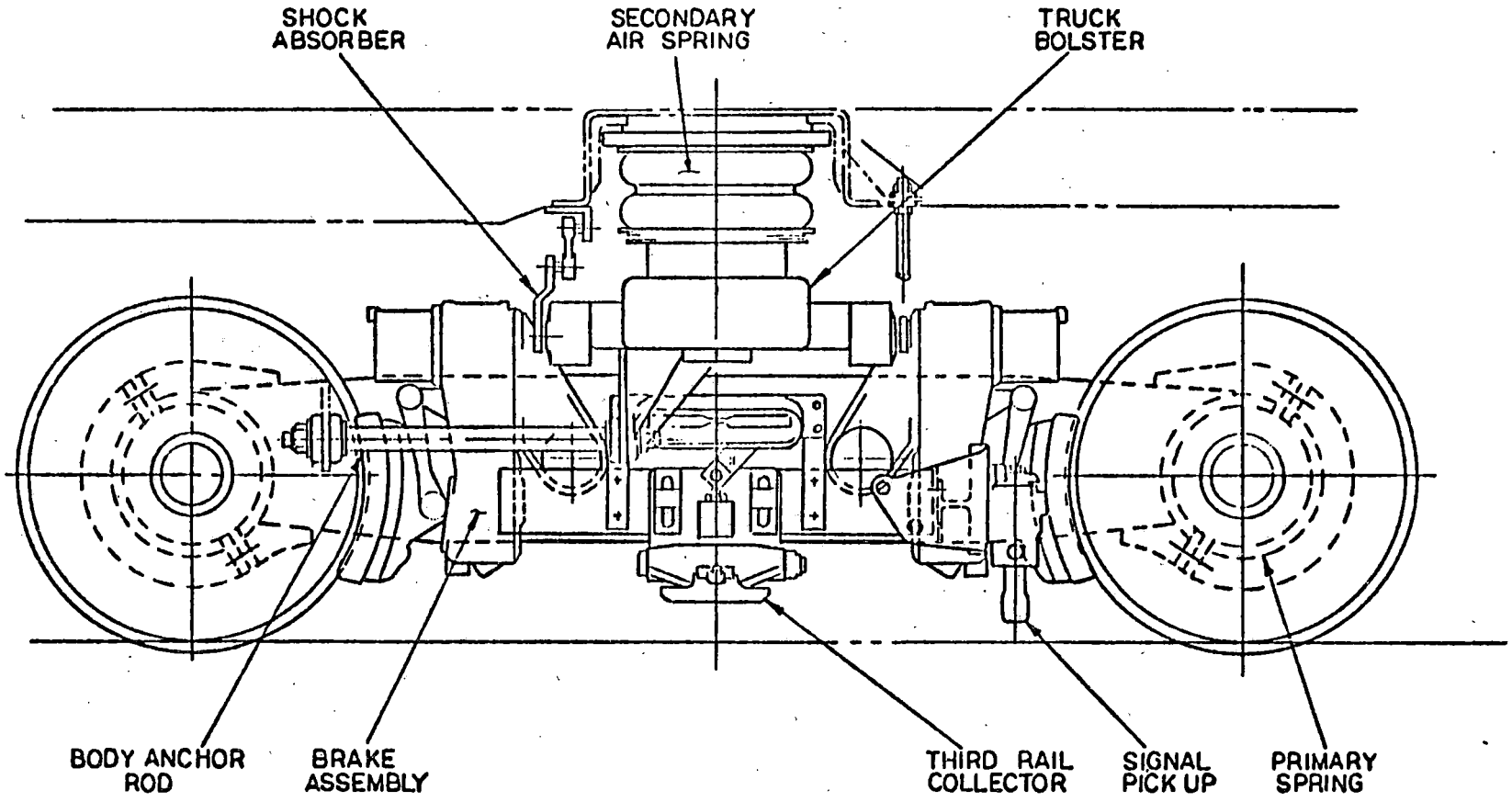

FIGURE 2-2.2: EXISTING PATCO P-III TRUCK, SIDE VIEW

		Stiffness Per Truck (LB/IN)	Damping Per Truck (LB-SEC/IN)	Spring Spacing (IN)			Damper Spacing (IN)		
				Vertical From Rail	Lateral	Long	Vertical From Rail	Lateral	Long
PRIMARY	VERTICAL	645×10^3	220	NA	46	90	NA	46	90
	LATERAL	400×10^3	170	14	NA	90	14	NA	90
	LONG	1.18×10^6	375	14	46	NA	14	46	NA
SECONDARY	VERTICAL	5×10^3	200	NA	89	0	NA	89	0
	LATERAL	2×10^3	180	38	NA	0	30	NA	0
	LONG	50×10^3	50	17	109	NA	17	109	NA
		STIFFNESS (IN-LB/RAD)	DAMPING (IN-LB-SEC/RAD)	FRICTION TORQUE BREAKAWAY (IN-LB)					
	YAW	18×10^6	NA	66×10^3					

INTER-AXLE LATERAL STIFFNESS = $43. \times 10^3$ LB/IN

INTER-AXLE YAW STIFFNESS = $156. \times 10^6$ IN-LB/RAD

TABLE 2-2.2: SUSPENSION PARAMETERS OF THE EXISTING PATCO PIONEER III TRUCK

			RADII OF GYRATION (IN)			C.G. SPACING (IN)		
UNSPRUNG PARTS, U SPRUNG PARTS, S		WEIGHT (LB)	YAW	ROLL	PITCH	VERTICAL FROM RAIL	LATERAL	LONG
WHEELSET	U	1771	28.3	28.3	8.5	14	0	90
WHEELSET AND TRACTION EQUIP.	U	4073	22.4	21.3	13.1	14	0	68
SIDE FRAME	S	1534	36.9	23.5	29.3	16	46	0
BOLSTER	S	1645	31.8	34.3	13.7	28	0	0
TRUCK FRAME ASSEMBLY AND BOLSTER	S	4713	49.2	39.5	38.8	22	0	0
TOTAL TRUCK WEIGHT		12859						

TABLE 2-2.3: TRUCK PARAMETERS OF THE EXISTING PATCO PIONEER III TRUCK

The basic truck is a three-piece inboard bearing design consisting of two side frames and a bolster. The side frames are independent of one another in the pitch direction and provide equalization even though the primary stiffness values are relatively high. The equalization characteristics of this truck are such that with the truck on level track under "empty car" load, jacking one journal bearing housing 2 inches does not result in a change of more than 25% in the load on any journal. In curves, truck swivel occurs between the bolster and the side frames at the bolster center pivot and the side bearings. The bolster fits between the two side frames at the center of the truck and rests on the side bearings which are located on the centerline of the side frames.

The connection of the two side frames to the center pivot is very stiff in the longitudinal direction, preventing lozenging of the side frames in plan view. This connection also transmits longitudinal and lateral loads between the side frames and bolster. Vertical load is transmitted from the bolster to the side frames by side bearings directly over the side frame.

The bolster is prevented from moving longitudinally and from swiveling with respect to the carbody by bolster

radius rods between the ends of the bolster and carbody.

The secondary suspension is contained within the bolster assembly. This system is primarily responsible for the ride quality of the carbody as it determines the vertical, lateral, and roll suspension parameters of the carbody. The secondary suspension consists of two air springs, located one at each end of the bolster. The bolster acts as an air reservoir, connected through orifices to the air springs. Orifice resistance to the transfer of air between the air springs and the reservoir will provide vertical damping. In addition to orifice damping and reservoirs, vertical hydraulic shock absorbers are used. The carbody is permitted to move laterally by the distortion of the air springs. Lateral hydraulic shock absorbers are used to dampen this motion. The maximum lateral movement is limited by rubber bump stops.

The powered P-III truck has two separate motor/gear box assemblies with the motor parallel to the axles. Each gear unit is supported from the axle at one end and by a vertical resilient hanger to the side frame at the other end. Each motor is resiliently mounted to its gear unit at one end and by a vertical and longitudinal resilient hanger system to the side frame at the other end.

2.3 Modified Truck

Figure 2-3.1 shows the side view of the steerable truck, Figure 2-3.2 shows a plan view of the steering arm assemblies, Figure 2-3.3 shows a plan view of the modified truck frame, Figure 2-3.4 shows a schematic drawing of the steering arm controls, and Figure 2-3.5 is the general truck arrangement drawing. The truck suspension parameters are given in Table 2-3.1. The truck weights, radii of gyration and center of gravity locations are given in Table 2-3.2.

Basically, the proposed truck is quite similar to the original with modification of side frames and the addition of steering arms. The proposed truck is designed to accommodate the existing truck bolster, wheel axle assemblies, propulsion units, and tread brake units.

The steering arms are "C"-shaped structures and are shown with the motors, axles, and gearing in Figure 2-3.2. The steering arms are connected together at the center of the truck by a Metalastic bushing. This connection insures equal but opposite yaw motion of the two steering arms. This connection also transfers lateral, longitudinal, and vertical loads between the steering arms. The steering arms are attached to the wheel/axle assemblies by a clamping arrangement which engages the existing shock ring around the axle journal bearing. This attachment is quite similar to the design that is used on the existing truck.

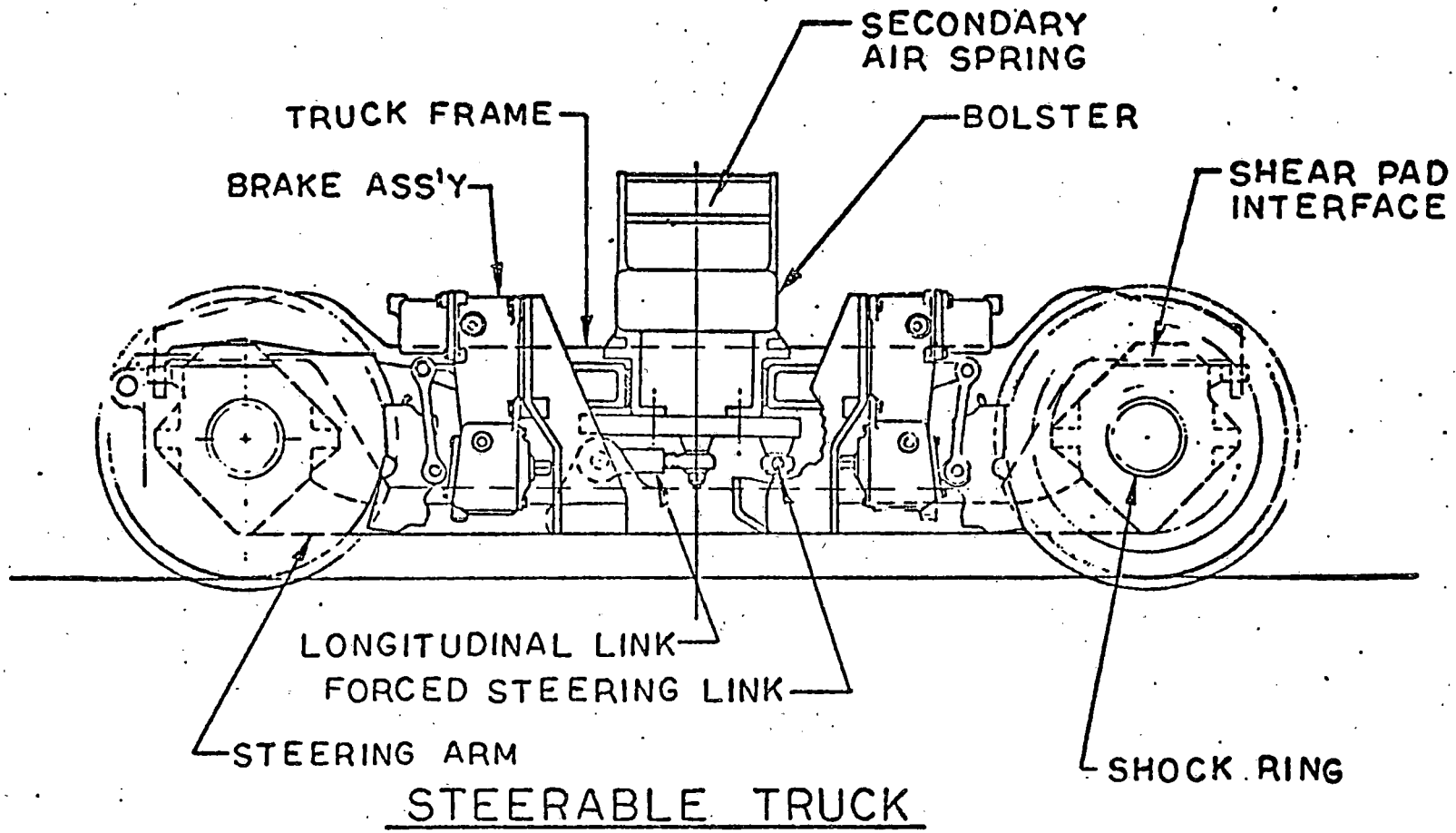

STEERABLE TRUCK

Figure 2-3.1

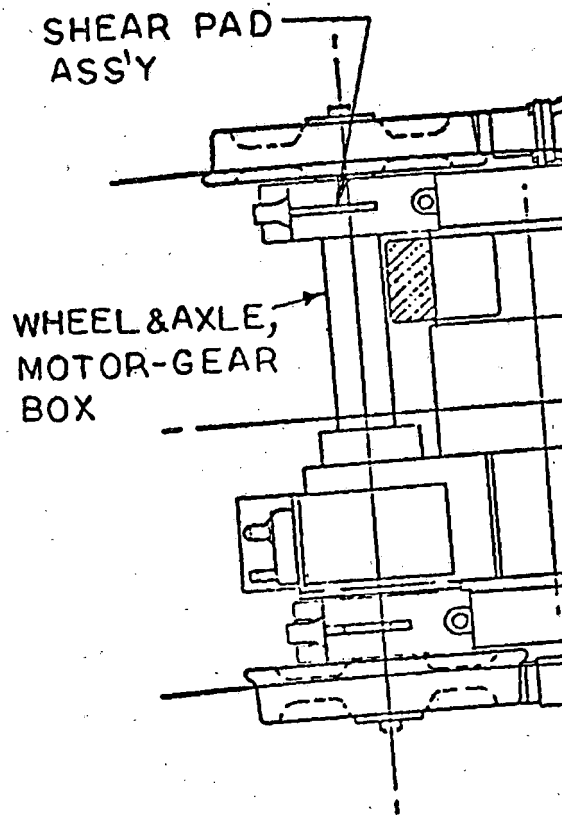
SHEAR PAD
ASS'Y
WHEEL & AXLE,
MOTOR-GEAR
BOX

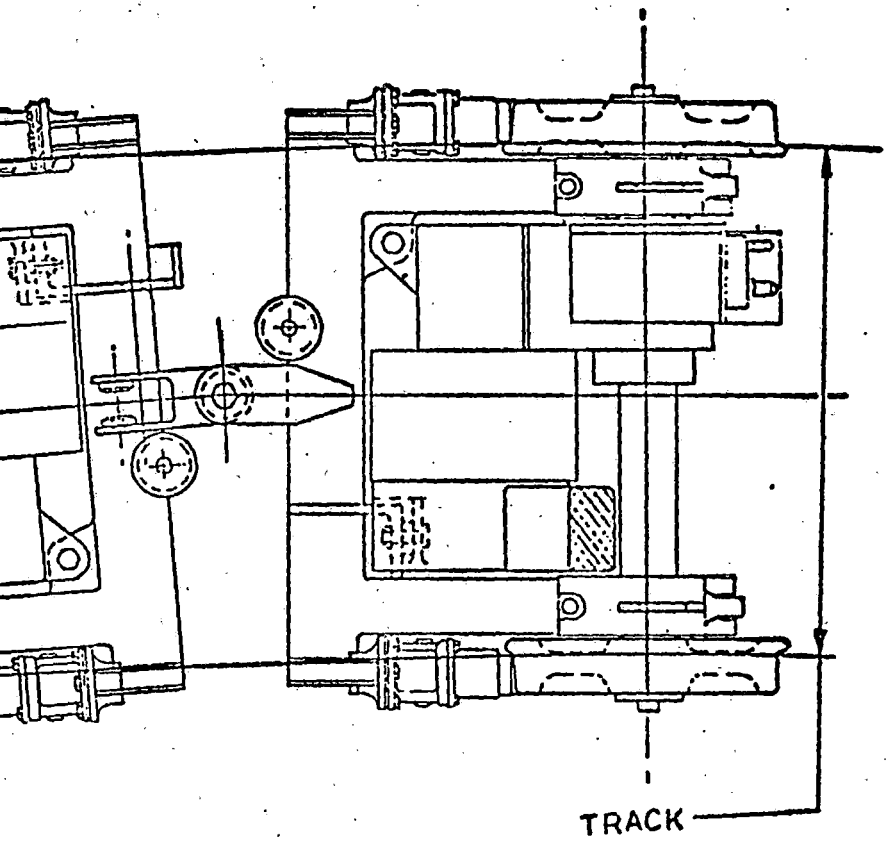

STEERING ARMS

TRUCK ON RADIUS TRACK

Figure 2-3.2

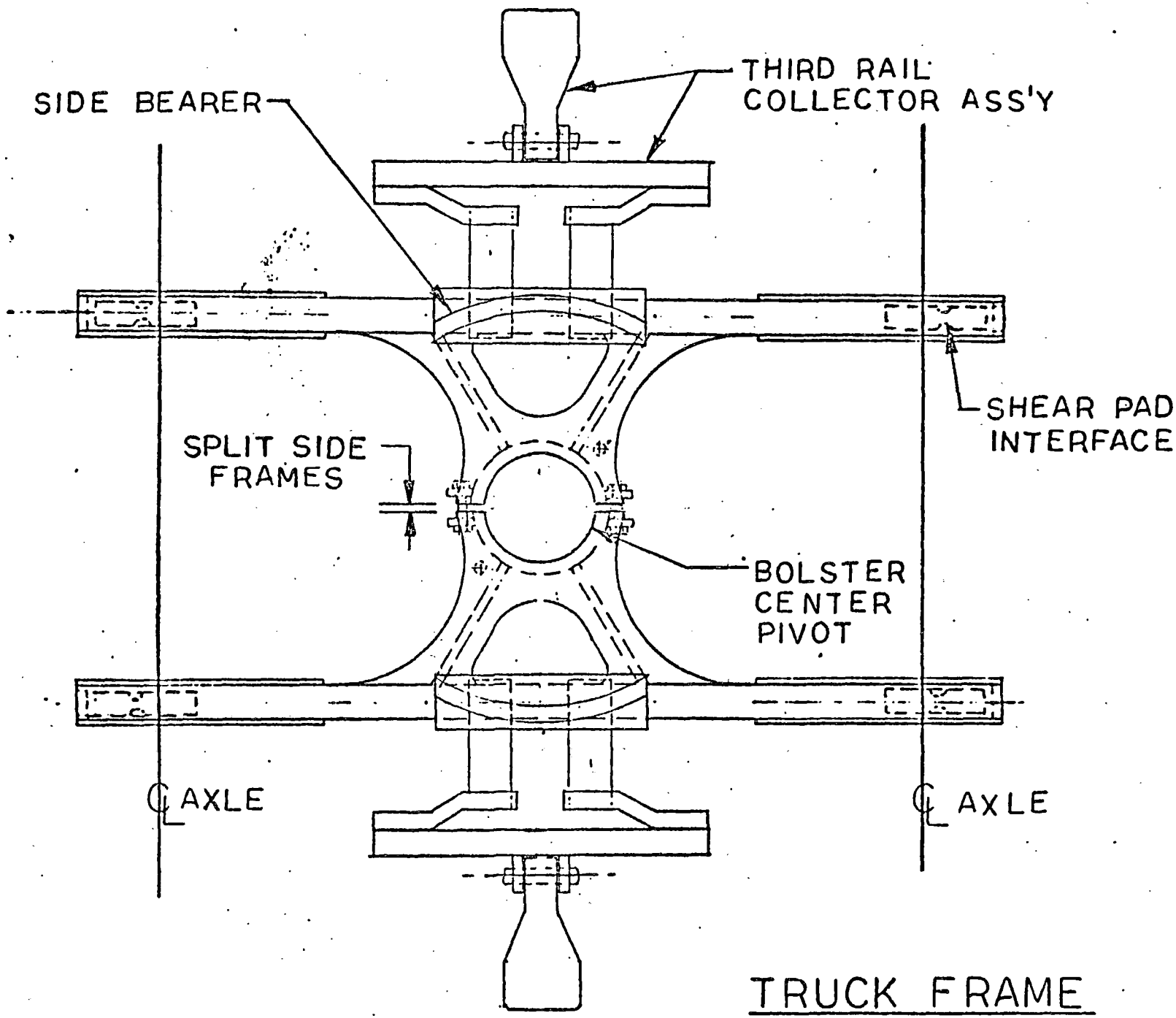
SIDE BEARER
THIRD RAIL
COLLECTOR ASS'Y
SHEAR PAD
INTERFACE
SPLIT SIDE
FRAMES
BOLSTER
CENTER
PIVOT
℄ AXLE
℄ AXLE
TRUCK FRAME

Figure 2-3.3

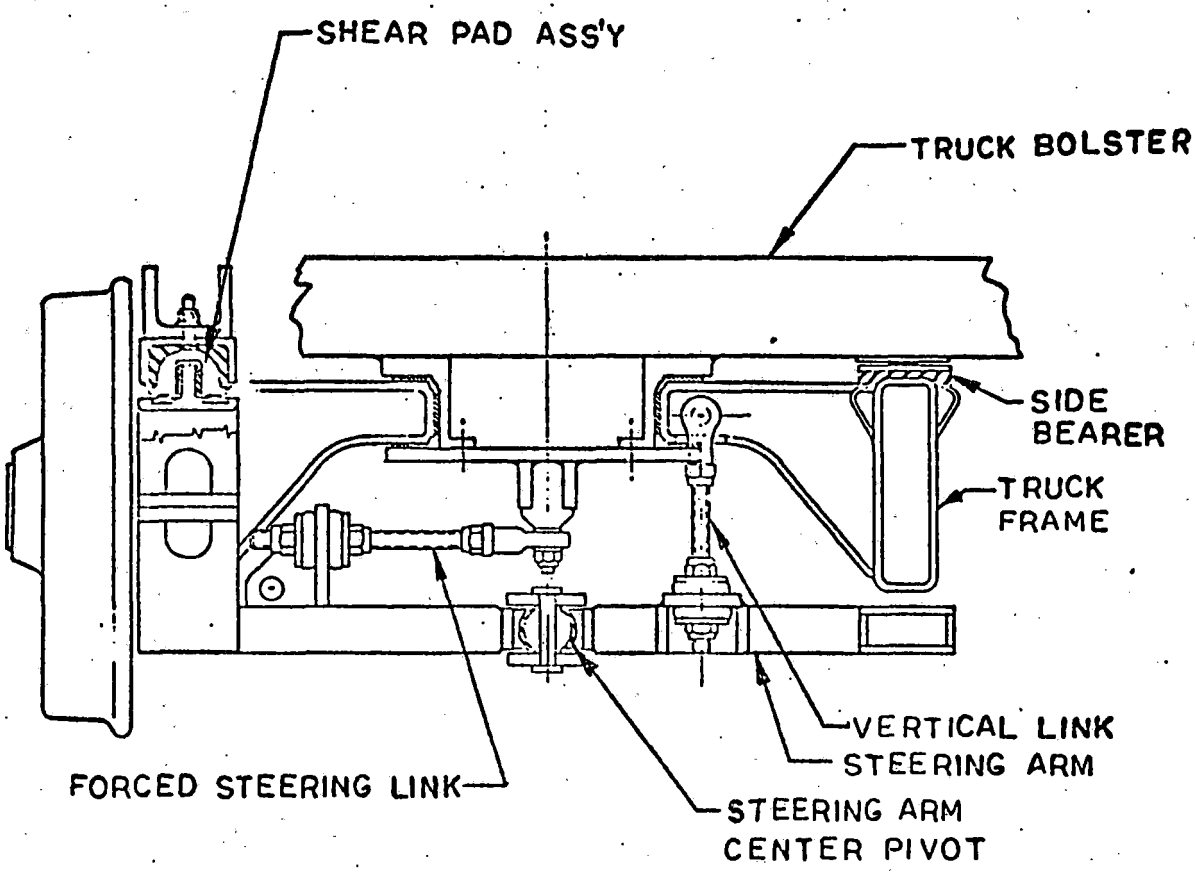

STEERING ARM CONTROLS

Figure 2-3.4

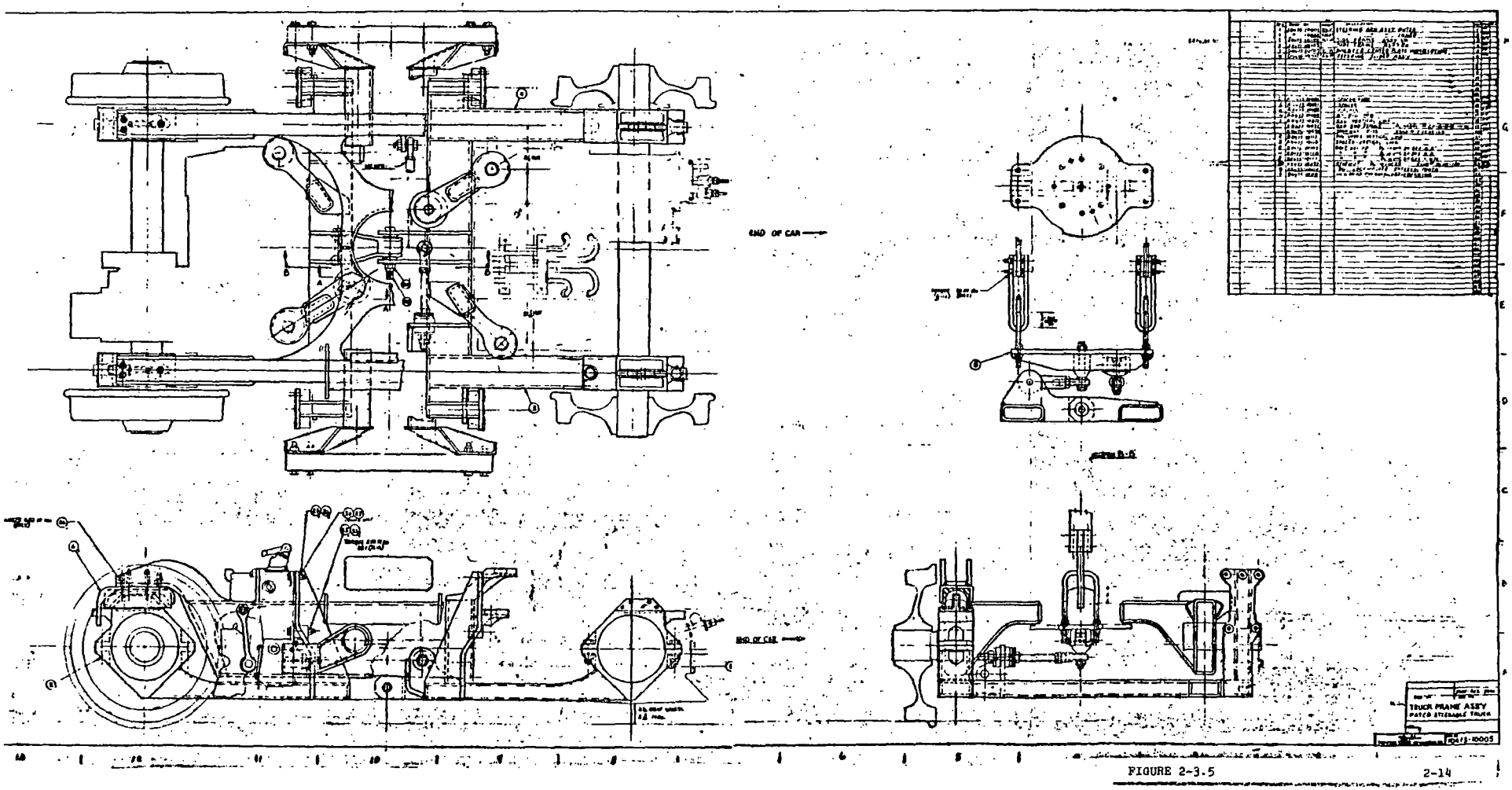

FIGURE 2-3.5

		Stiffness Per Truck (LB/IN)	Damping Per Truck (LB-SEC/IN)	Spring Spacing (IN)			Damper Spacing (IN)		
				Vertical From Rail	Lateral	Long	Vertical From Rail	Lateral	Long
PRIMARY	VERTICAL	645×10^3	220	NA	46	90	NA	46	90
	LATERAL	400×10^3	170	14	NA	90	14	NA	90
	LONG	1.18×10^6	375	14	46	NA	14	46	NA
SHEAR PAD	VERTICAL	800×10^3	360	NA	46	90	NA	46	90
	LATERAL	200×10^3	180	22	NA	90	22	NA	90
	LONG	120×10^3*	140	22	46	NA	22	46	NA
SECONDARY	VERTICAL	5×10^3	200	NA	89	0	NA	89	0
	LATERAL	2×10^3	180	38	NA	0	30	NA	0
	LONG	50×10^3	50	17	109	NA	17	109	NA
		STIFFNESS (IN-LB/RAD)	DAMPING (IN-LB-SEC/RAD)	FRICTION TORQUE BREAKAWAY (IN-LB)					
	YAW	18×10^6	NA	66×10^3					

* The shear pad longitudinal stiffness is in series with a friction slider with a breakaway force of 2000 lbs.

TABLE 2-3.1: SUSPENSION PARAMETERS OF THE PROPOSED STEERABLE TRUCK

			RADII OF GYRATION (IN)			C.G. SPACING (IN)		
UNSPRUNG PARTS, U SPRUNG PARTS, S		WEIGHT (LB)	YAW	ROLL	PITCH	VERTICAL FROM RAIL	LATERAL	LONG
WHEELSET	U	1771	28.2	8.2	8.5	14	0	0
STEERING ARM AND BRAKING EQUIPMENT	U	780	23.8	22.4	12.4	6	0	0
STEERING ARM WITH BRAKING AND TRACTION EQUIPMENT	U	4853	23.3	13.1	11.6	13	0	52
SIDE FRAME	S	1534	36.9	23.5	29.3	16	46	0
BOLSTER	S	1645	31.8	34.3	13.7	28	0	0
TRUCK FRAME ASSEMBLY AND BOLSTER	S	4713	49.2	39.5	38.8	22	0	0
TOTAL TRUCK WEIGHT		14,419						

Table 2-3.2: TRUCK PARAMETERS OF THE PROPOSED STEERABLE TRUCK

The propulsion unit/axle assemblies are not modified in any way. The three links which presently connect the motor and gearbox to the truck side frames are connected instead to the associated steering arm using the existing resilient links. This was done so that the motor/gear unit would remain interchangeable with the modified cars. This is certainly a desirable approach when considering a retrofit of two trucks. However, if a large number of trucks were to be retrofitted, a simpler propulsion unit/steering arm interface design could be provided by supporting the assembly from below.

The steering arms interface with the side frames at the four corners of the truck through shear pad/slider assemblies. The shear pad portion of the assembly acts to provide a spring stiffness in all directions. The longitudinal stiffness is important to the steering stability of the truck. The roll and pitch stiffnesses are selected to be compatible with the equalization requirements for the truck. The lateral and yaw stiffnesses must be chosen to allow the axles to yaw.

The slider portion of the shear pad/slider assembly is designed to limit the longitudinal forces associated with large yaw motion of the axles in sharp curves. For the best

possible steering performance, the coefficient of friction should be low in comparison with the wheel/rail creep coefficient. On the other hand, the slider friction must be high enough to prevent sliding for small yaw displacements so that the longitudinal spring rate of the assembly can make its contribution to high-speed stability.

The studies made to establish initial values for the longitudinal stiffness and the slider friction are discussed in the design performance analysis (Section 4.0 of this report).

Under normal conditions, the axles operate in a self-steering mode. The steering action is the result of wheel/rail creep forces acting in combination with the inter-axle parameters designed into the truck. The slider, with its 2000-lb. breakaway force, allows the self-steering mode to perform quite adequately on all curves as long as the wheel/rail friction coefficient is approximately equal to or greater than 0.3. However, if the wheel/rail friction coefficient is significantly less than 0.3, then self-steering alone is not sufficient for adequate steering. Since reduced friction coefficients are a possibility, forced- or

positive-steering has also been incorporated into the design. The positive-steering feature allows the self-steering input to initiate the steering input of yawing the axles. However, if the axles do not assume the radial position because of adverse adhesion, then the positive-steering feature will insure that the axles are properly aligned in the radial position during curving.

The positive-steering arrangement consists of a lateral link between the bolster pivot and the steering arms for the end axle. The positive-steering action is generated by the lateral motion of the link attachment point on the bolster relative to the side frame when the truck swivels relative to the bolster. The amount of this lateral motion depends on the longitudinal eccentricity of the steering link from the center of truck swivel and the amount of truck swivel. The longitudinal eccentricity is chosen to give radial axle positions in a circular curve. The amount of eccentricity required to do this is a function of truck wheel base and truck center spacing.

The lateral link is attached to the bolster with a ball joint. At this location, angular motion can be several degrees. The other end of the link, where angular motion is much less, is attached to the steering arm with a threaded

connection and rubber washers so that the effective length can be adjusted for a parallel axle position on straight track. An adjustable free zone for the positive-steering restraint is also provided. This free zone adjustment capability is provided so that the self-steering input can lead the forced-steering input.

There is also a longitudinal link between the bolster pivot and one steering arm to take normal longitudinal loads associated with propulsion and braking. The crash longitudinal loads will be carried through stops in the steering arm/side frame connection to the side frame and then to the bolster as is the case with the original truck.

Most of the steering arm pitching moments associated with normal propulsion and braking are balanced out between the two steering arms by an exchange of vertical forces at the point of steering arm interconnection. Any unbalance of these pitching moments and the weight of the steering arms are supported by vertical hangers from the side frames.

The side frame end of the vertical hanger is a ball joint and the steering arm end is a threaded bolt attachment with rubber washers. The vertical hangers will give the steering arms a certain amount of restoring moment due to the pendulum effect.

The steering arms also incorporate mounting brackets for the existing tread brake units. Because the brake units are mounted on the steering arms, they are always properly positioned with respect to the axle and will not interfere with the steering operation.

The side frames are modified at the four corners to interface with the shear pad/slider assembly as described previously. The side frames are shown in elevation in Figure 2-3.1 and in plan in Figure 2-3.3. The side frame is a fabricated rectangular tube measuring 14 in. x 6 in. with a thickness of 1/2 in. Stiffening ribs are added to the truck frame corners. Each shear pad/slider assembly is attached to the side frame by three threaded fasteners and two guide pins. The side frame/bolster interfaces are unchanged. The third rail power shoe collector is mounted from the side frame, which is quite similar to the existing design configuration.

The bolster remains unchanged with respect to the secondary suspension and its interfaces with the side frames. (See description of existing truck for more information.) However, there is a modification to the bolster center pivot bottom plate and safety strap arrangement. These changes are shown in the general truck arrangement drawing, Figure 2-3.5. The bolster pivot bottom plate provides a vertical up stop between the bolster and side frame. The bottom plate is

also attached to the carbody through safety straps. The safety straps provide a safety connection between the trucks and the carbody in the event of a derailment. All operational loads are transferred from the axles through the steering arms and the longitudinal drag link into the bolster, using the bottom plate connection. The loads are then transferred into the carbody using the longitudinal anchor rods between the bolster and the carbody. The positive-steering input position is generated by truck swivel and is transferred from the bolster bottom plate to the steering arms using the lateral steering link.

The proposed design will increase the weight of the existing truck by about 1560 lbs (approximately 12%). This increase is essentially the weight of the steering arms themselves. The side frame modifications have little effect on the total truck weight. As was mentioned earlier, the proposed truck is designed to accommodate the existing bolster, wheel/axle assemblies, propulsion units and tread brake units. It is quite possible that a new design that is not required to mate with existing equipment could produce a weight savings. The primary area for potential weight savings is a simpler propulsion unit/steering arm interface. It is also quite possible that additional weight could be saved from a simpler side frame interconnection /bolster pivot interface.

The proposed steerable truck design will have improved curving performance without compromising high-speed stability, braking performance, or ride quality.

Figure 2-3.6 shows the axle yaw motion and journal deflection that is required to achieve the radial position for various curvatures.

The proposed steerable truck design is based on a concept that is patented by Mr. Harold A. List of Railway Engineering Associates, Inc. The related patent numbers are 4,131,069 and 3,789,770.

FIGURE 2-3.6: P-III TRUCK-PATCO RADIAL POSITION

3.0 Design Performance Specification

3.1 Introduction

This performance specification for a modified PATCO truck with steering capability is based on the performance goals given in the contract statement of work and on the specific characteristics and requirements of the PATCO system itself. The results of the performance analysis and a review of literature relating to wheel squeal were also factored into the performance specifications.

3.2 Stability

3-2.1 Speed

The steerable truck design shall be capable of operating over the full range of speeds on the PATCO System from 0 to 75 mph (121 kph).

3-2.2 Damping Factor

The critical hunting speed characteristic of the steerable truck design shall provide a minimum damping factor of 10% for the least damped mode while operating at 80 mph (129 kph). This performance shall be obtainable under all varying conditions of components and wheels from new to fully worn and under crush load to empty car conditions.

3.3 Curving Performance

3-3.1 Angle of Attack

The steerable truck design shall be such that an angle of attack of less than $\pm$ 0.5 degrees shall be maintained

on all curves on the PATCO System down to a minimum radius of 190 ft. (59 meters) which is equivalent to a curvature of 30 degrees. This condition shall be obtained under maximum allowable acceleration, deceleration and constant speed.

3-3.2 Curve Negotiation

The steerable truck design shall permit negotiation of curves down to 125-ft. (30-meter) radius. This radius is a function of the truck center spacing (47.5 ft. for PATCO) and the maximum truck swivel angle permitted by clearance between the bolster and truck mounted equipment (usually less than 12 degrees for rapid transit vehicles). A car with a smaller truck center spacing would permit negotiation of sharper curves.

3.4 General Considerations

3-4.1 Track

The steerable truck design modification shall be suitable for operation on standard gauge of 4 ft. - 8-1/2 in. (1435 mm).

3-4.2 Fabrication Techniques and Materials

Selection of materials and fabrication techniques shall conform to standard rapid rail truck specifications and, in addition, shall operate over an ambient temperature range of minus 40 to 120 degrees Fahrenheit (-40 to 50 degrees Centigrade).

3-4.3 Capability to Withstand Stress

The design of the modification for the steerable concept shall include the capability of the truck structures and components to withstand, without structural degradation, the maximum stresses imposed from both static and dynamic loads acting on the truck. The loads include, but are not limited to, track shocks from rail joints, defects in rail geometry, braking, lateral unbalance forces and carbody/truck interface forces.

3-4.4 Truck Height

The design of the steerable feature of the truck shall ensure that the height of the floor, coupler and draw bars shall not change from the existing PATCO truck design.

3-4.5 Braking Capability

The braking performance of the steerable truck shall be equal to the braking performance of the existing PATCO truck (which is -3.0 mph/sec). Improved braking performance for the steerable truck could arise from two sources: (1) higher adhesion limits resulting from the elimination of the need for wheel/rail lubricators, (2) higher longitudinal friction values available due to the reduction of lateral wheel/rail creep in curves.

3-4.6 Ride Quality

The overall ride quality of the steerable truck shall not be less than that provided by the existing PATCO truck when measured by ISO standards. Improved ride quality for

the steerable truck could arise from the improved tracking that is expected, especially in curves. Improved tracking will help avoid certain fixed rail perturbations around switches, etc.

4.0 Design Performance and Structural Analysis

4.1 Introduction and Background

The basic approach taken in the design performance studies was to first establish various performance indices for the existing PATCO P-III truck design. These results were then used as a baseline for comparative analysis with the proposed steerable truck design. Both self-steering and forced-steering design configurations were considered.

The design performance areas that were studied include curving performance, high-speed stability, and ride quality. A finite element analysis was made on the proposed steerable truck design to verify structural integrity and determine the inter-axle shear and bending stiffness parameters.

Several different computer models were used in the design performance studies. The stability and ride quality studies were done primarily with linear models that employ eigen value-eigen vector techniques. The vertical ride quality model is presented in Appendix A and the lateral stability model is presented in Appendix B of Reference 1. The curving performance studies were primarily done with a non-linear tracking model that generates a time domain solution. This model is considered proprietary by

The Budd Company; therefore, a complete program listing is not included in this report. However, a general description of its operation, capabilities, and data input is presented in the next section (4.2, Curving Performance). The structural analysis was made using a commercially available computer program named ANSYS, capable of solving finite element structural problems.

4.2 Curving Performance

4-2.1 Introduction and Background

Improved curving performance is brought about by yawing the axles to a radial position during curve negotiation for the purpose of reducing or eliminating the angle of attack between the wheel and rail. The squeal noise, rail corrugations, and much of the wheel flange wear and rail gauge wear experienced with conventional parallel axle trucks are due to the non-radial running position of the leading axle in sharp curves. The addition of steering can improve curving performance substantially in sharp curves by eliminating the tracking error (angle of attack) and the associated wheel/rail lateral motion. Flange forces are lower and the rubbing action is greatly reduced.

The basic approach taken in the curving studies was to first establish the curving performance of the existing P-III truck. A preliminary look was taken at the prospect for improving curving simply by reducing the longitudinal primary stiffness of the existing truck to the lowest value practically attainable in the space available.

Steering arms were then added to the analysis. The geometrical implications of keeping both axles in a radial position were tabulated (see Figure 2-3.6). The steering arms can be designed to provide the inter-axle shear stiffness parameter required for stability while providing an appropriate inter-axle yaw stiffness parameter for improved curving. The axle yaw restraint required for stability is provided by a spring in series with a slider construction which also allows for the large yaw motion in sharp curves. The forced response of such a system was studied to determine the amount of friction required in the slider to make the axle yaw restraint dynamically effective. This value of friction was then used in the curving studies, particularly when evaluating the self-steering properties of the proposed truck.

4-2.2 Non-Linear Tracking Model - Time Domain

Curving performance can be studied in a limited way with an extension of the linear models and methods used to study stability. A few of these studies were made. These studies, however, are limited to flange-free curving, linear creep characteristics, and conical wheel tread profiles. These limitations make the linear studies of little value when looking at curvatures greater than 4 to 6 degrees. The main set of curving studies presented by this report use instead the Budd non-linear tracking model. This model can accommodate flange contact, apply an arbitrary creep characteristic, and use non-linear wheel profiles. As a result, this model can be applied to the sharper curves of the PATCO system in which flange contact does occur.

The non-linear model is a digital computer program that is set up to simulate the dynamics of rail vehicles. The dynamic input is generated by various track features such as tangent track, spirals, constant radius curvature, superelevation, track twist, and track defects which may be lateral and/or vertical. The program computes the dynamic behavior of the major truck components being

modeled and the forces and torques acting at various points where these parts are interconnected. Each major component is allowed to move in all six degrees of freedom: lateral, longitudinal, vertical, yaw, roll, and pitch. The program can be run at zero speed to study the vertical response of the vehicle to a vertical step input or the program can be run at constant speeds over various track features.

The equations of motion are solved by numerical integration so that the many non-linearities of the wheel/rail interface and the usual non-linearities of the interconnections among the component parts of the vehicle can be realistically represented. Several different numerical integration techniques have been used; however, the Corrected-Euler method seems to be the best. For each part and each time step, the net force along each axis and the net torque around each axis are computed taking into account all of the forces and torques acting at the interfaces. Based on these forces, a set of six accelerations is computed for each part and then integrated to compute a new set of velocities. The velocities are then integrated to compute a new set of positions. The program has built-in error criteria which permit large integration

time steps during periods of steady state operation and very small integration time steps during transient conditions.

A schematic drawing of the model that was developed for studying the existing P-III truck is shown in Figure 4-2.1. This model has six major parts: two motor/axle assemblies, two side frame assemblies, a bolster, and a carbody. The model also has four other parts: a track part under each truck axle, a track part under the trailing end of the carbody, and a master coordinate system. The part numbers are shown circled on the schematic and are also listed in Table 4-2.1. The numbers that are not circled in the schematic represent the various interfaces that were modeled and are described in Table 4-2.2.

The model parts are interconnected by interfaces which can be located in three dimensional space with respect to the centroid of each part. There are seven different interface types available to the model builder. These are listed in Table 4-2.3.

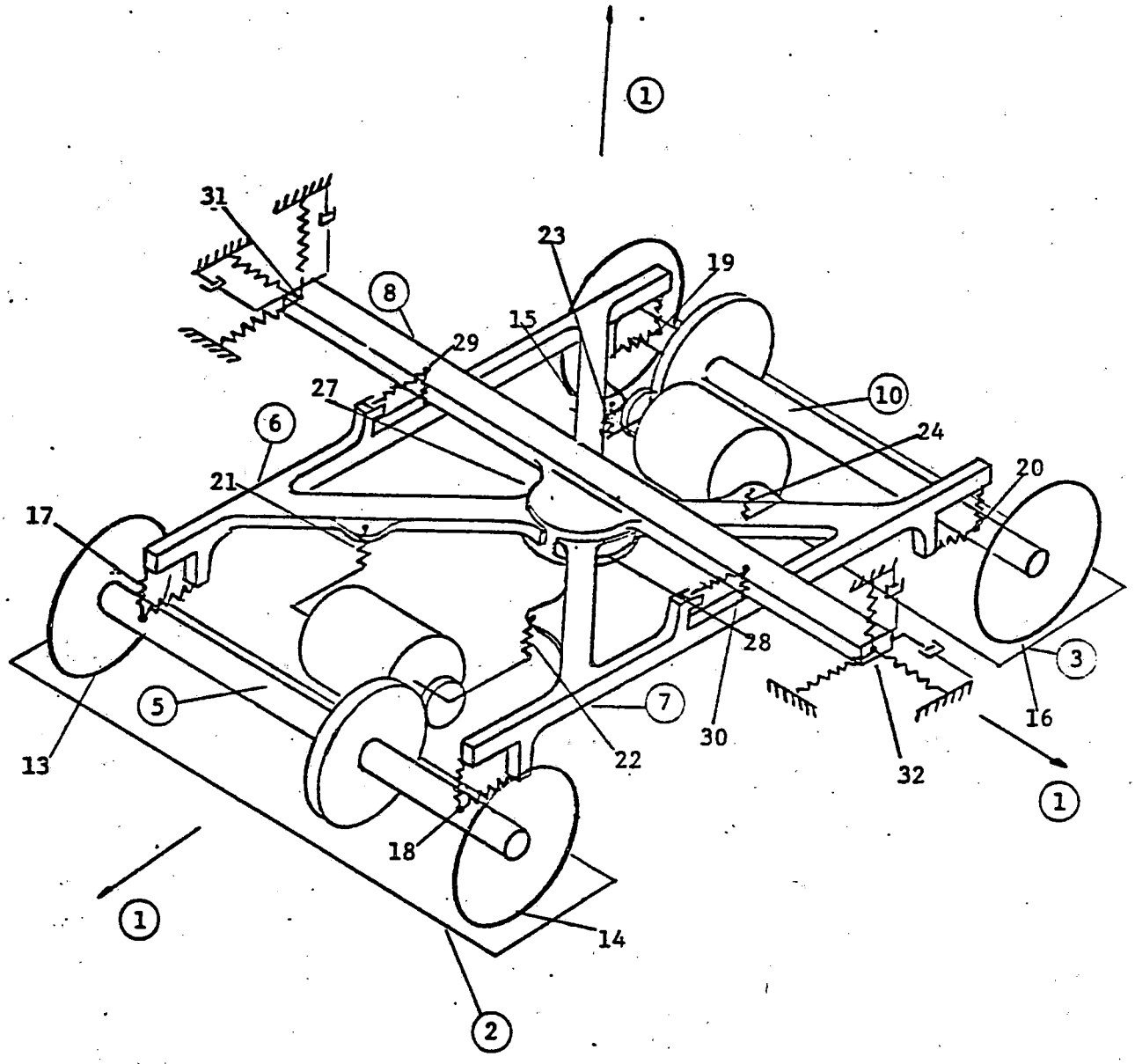

FIGURE 4-2.1: EXISTING P-III TRUCK MODEL

TABLE 4-2.1: PARTS MODELED FOR EXISTING P-III TRUCK

No.		Description
1		Master Coordinate System
2		Lead Track Part (Lead Truck)
3		Trail Track Part (Lead Truck)
4		End of Car Track Part
5	*	Lead Motor/Axle Assembly
6		Right Side Frame
7		Left Side Frame
8		Bolster
9		Carbody
10	*	Trail Motor/Axle Assembly

* Parts 5 and 10 are lead and trail steering arm/motor/axle assemblies for the steerable truck model. The weights and inertias were adjusted accordingly.

TABLE 4-2.2: INTERFACES MODELED FOR EXISTING P-III TRUCK

No.		Type	Spring/Dashpot Group No.
1-6	Gravity Force on Real Parts 5-10	1	-
7-12	Centrifugal Force on Real Parts 5-10	2	-
13	Right Leading Wheel/Rail	6	1
14	Left Leading Wheel/Rail	6	1
15	Right Trailing Wheel/Rail	6	1
16	Left Trailing Wheel/Rail	6	1
17	Right Lead Primary Suspension	3	2
18	Left Lead Primary Suspension	3	2
19	Right Trail - Primary Suspension	3	2
20	Left Trail - Primary Suspension	3	2
21	Lead Motor Mount	3	3
22	Lead Gear Box Mount	3	3
23	Trail Gear Box Mount	3	3
24	Trail Motor Mount	3	3
25	Not Used	-	-
26	Not Used	-	-
27	Right Spider to Center Pivot	3	5
28	Left Spider to Center Pivot	3	5
29	Right Side Bearer	3	6
30	Left Side Bearer	3	6
31	Right Lead Secondary Suspension	3	7
32	Left Lead Secondary Suspension	3	7
33	Right Trail Secondary Suspension	3	7
34	Left Trail Secondary Suspension	3	7

TABLE 4-2.3: INTERFACE TYPES

Identifying No.	Description
1	Weight
2	Centrifugal Force
3	Piecewise Linear
4	Dominant Direction Piecewise Linear
5	Half-Linear
6	Wheel/Rail
7	Spring in Series with Damper

Interface Types 1 and 2 are used to apply forces at the centroid of the modeled parts. The numerical value of these forces depend on the mass of the part and the system of units specified by the user.

The most basic part interconnection interface is Type 3. This provides for two different user specified spring and damper rates in all six directions. The location of the break point between the two rates can also be user specified. The kind of non-linearities that are available to the user with this interface type are shown in Figure 4-2.2.

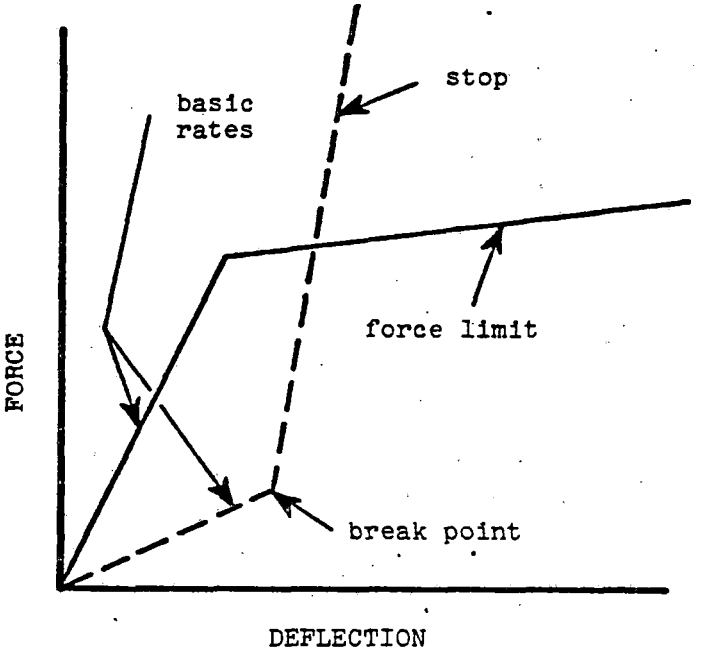

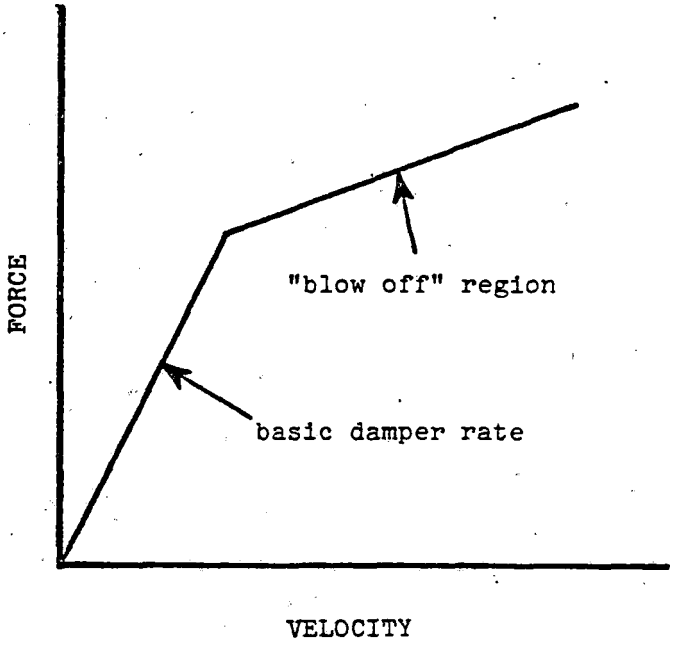

FIGURE 4-2.2: INTERFACE TYPE 3 - PIECEWISE LINEAR

Each of the six possible springs and six possible dampers can have two different rates. The transition point between the two rates can be specified by the user, e.g., the stiffening action of a bump stop or the action of a damper blow-off.

Interface Type 4 is a variation of Type 3 which allows the reactions in all directions to be zero if the force in a specified direction goes to zero. This can be used, for example, to represent a rubber pad which is weight loaded. It would have a full set of elastic and damping properties when under vertical load, but these would all be zero if the vertical load is zero.

A Type 5 interface provides for a guided vertical spring element in which the lateral and longitudinal characteristics would continue even if the vertical force goes to zero. It differs from the Type 3 interface in that the force in the specified direction can only be compression; a relative motion which would call for tension with Type 3 is clamped at zero.

The Type 6 interface provides for the special situation at the wheel/rail interface. This interface computes wheel/rail forces based on wheel/rail geometry

and wheel/rail creep as well as specified values for vertical and lateral rail stiffnesses.

The user can specify rolling radius difference and wheel/rail contact angle versus lateral displacement. See Figure 4-2.3 for more information. This permits exploring the effect of worn wheel profiles as well as new wheel profiles. The user can also specify the creep characteristic. This can be either a theoretical curve or values obtained from experimental data.

Interface 7 provides for representing the hysteresis, or memory effect, associated with having a friction damping element in series with an elastic element. This action can occur in any user specified direction while the action of the interfaces in the other direction will be as described for Type 3.

A schematic drawing of the model that was used for studying the proposed steerable truck is shown in Figure 4-2.4. This model added the steering arms to the existing motor/axle assemblies and made the necessary adjustments to the interfaces. The interfaces that were used for the steerable model are given in Table 4-2.4. Note that when interface 26 is not included (zeroed out), the truck model configuration is self-steering and when interface 26 is included, the truck model configuration is positive- or forced-steering.

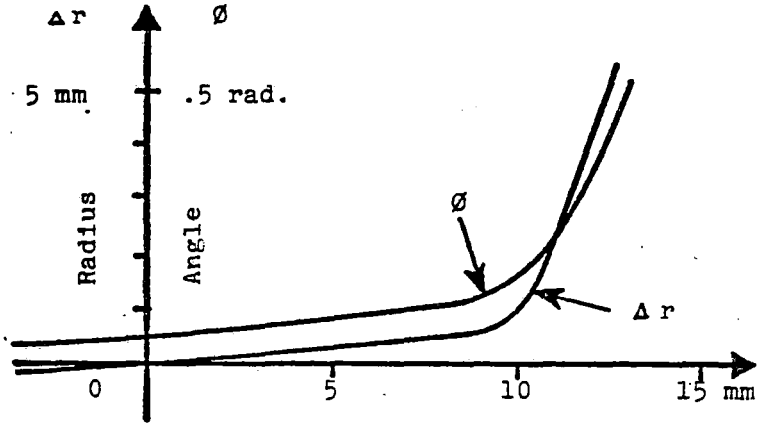

Lateral Displacement

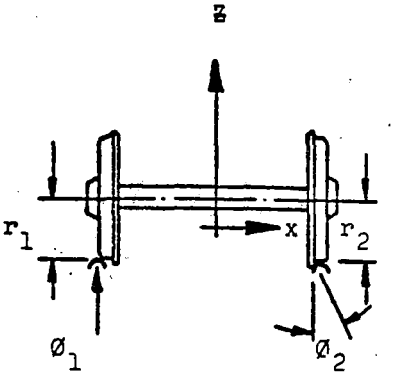

Diagram of Rolling Radii and Wheel/Rail Contact Angle

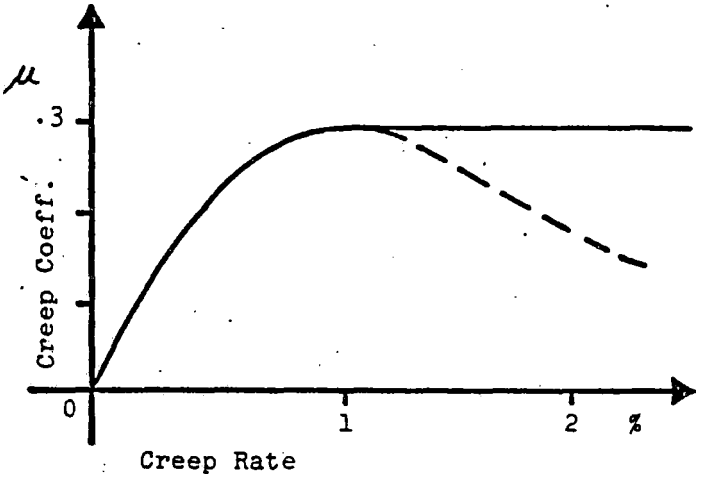

Creep Rate

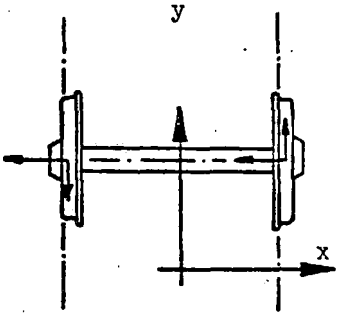

Diagram of lateral and longitudinal Creep Forces

FIGURE 4-2.3: INTERFACE TYPE 6 - WHEEL/RAIL

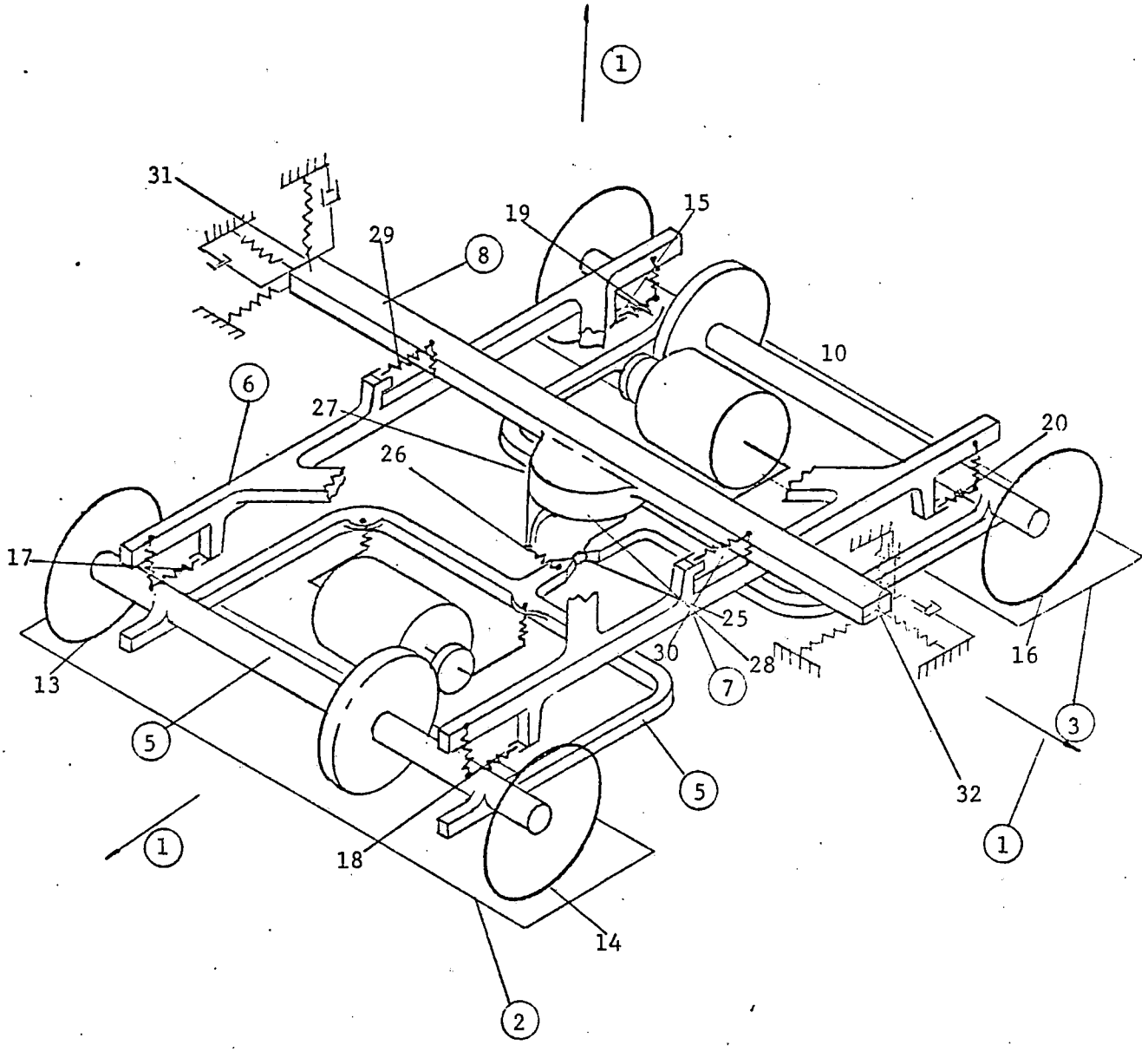

FIGURE 4-2.4: PROPOSED STEERABLE TRUCK MODEL

TABLE 4-2.4

INTERFACES MODELED FOR PROPOSED STEERABLE TRUCK

No.		Type	Spring/Dashpot Group No.
1-6	Gravity Force on Real Parts 5-10	1	-
7-12	Centrifugal Force on Real Parts 5-10	2	-
13	Right Leading Wheel/Rail	6	1
14	Left Leading Wheel/Rail	6	1
15	Right Trailing Wheel/Rail	6	1
16	Left Trailing Wheel/Rail	6	1
17	Right Lead Shear Pad/Slider	3	2
18	Left Lead Shear Pad/Slider	3	2
19	Right Trail Shear Pad/Slider	3	2
20	Left Trail Shear Pad/Slider	3	2
21	Lead Steering Arm Vertical Hanger	3	3
22	Not Used	-	-
23	Trail Steering Arm Vertical Hanger	3	2
24	Not Used	-	-
25	Steering Arm Interconnection	3	4
26	Positive Steering Link	3	9
27	Right Spider to Center Pivot	3	5
28	Left Spider to Center Pivot	3	5
29	Right Side Bearer	3	6
30	Left Side Bearer	3	6
31	Right Lead Secondary Suspension	3	7
32	Left Lead Secondary Suspension	3	7
33	Right Trail Secondary Suspension	3	7
34	Left Trail Secondary Suspension	3	7

4-2.3 Curving Performance Results - General Case

Wheel/rail contact geometry and friction coefficient levels have strong effects on curving performance. The contact geometry is a function of the wheel tread profile and the rail head profile. The existing PATCO trucks use the standard AAR profile which is a 1 in 20 tread taper and permits two-point contact. This particular profile lasts approximately 3000 to 5000 miles on the PATCO system. The resulting profile has a slightly higher effective conicity and no longer exhibits two-point contact. This profile was actually measured at PATCO. The profile was named "moderately worn 1 in 20". This profile appears to be quite stable with respect to wear patterns and does remain the predominant profile during the life of the wheel. Therefore, the moderately worn 1 in 20 profile was used for the general case curving performance studies.

Figure 4-2.5 shows the rolling radius difference and the wheel/rail contact angle as a function of lateral offset from the centered rail position for the moderately worn 1 in 20 profile. Note that the contact angle changes slightly even for small displacements. This gives rise to a wheel centering action often called gravitational stiffness.

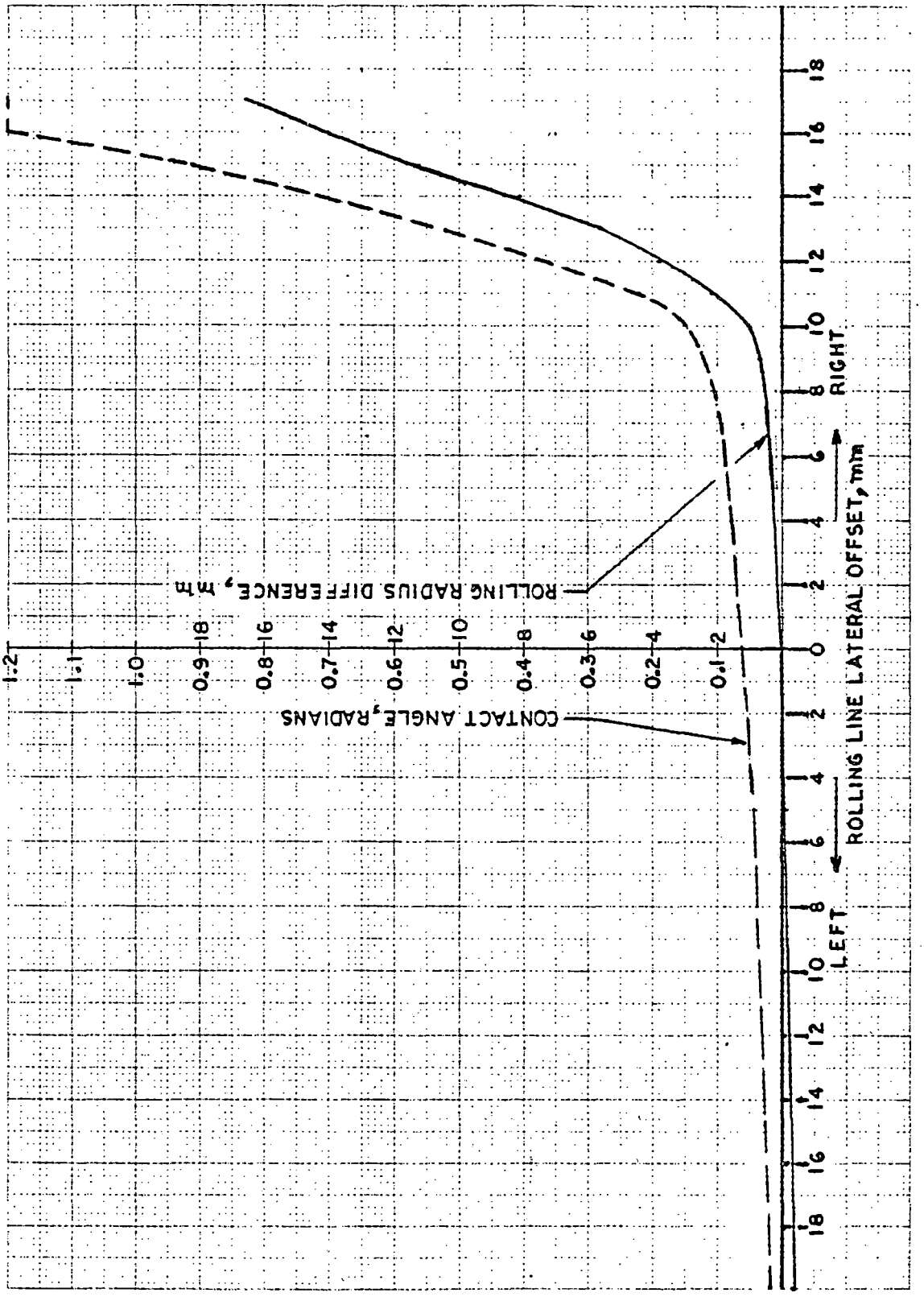

FIGURE 4-2.5: MODERATELY WORN 1 IN 20 PROFILE

Figure 4-2.6 shows the three creep characteristics used for the curving performance studies. Note that the maximum friction values are μ = 0.1, 0.3, and 0.5. The general case curving performance studies were done using the 0.3 maximum friction coefficient curve. Note also that the curve shapes are based on the Vermuelen-Johnson formulations.

While the model itself is three dimensional with all six degrees of freedom for each part of the truck or vehicle being studied, the principal curving performance results are shown using the variables defined in Figure 4-2.7.

The general case studies were run at curvatures that are typical of the PATCO system. The specific curvature, speed, and cant deficiency are given in Table 4-2.5. This series was run at zero superelevation because many of the sharp curves at PATCO are flat.

* Computed assuming $f_{11} = f_{33} = 1.875 \times 10^6$ LB. and wheel load N = 12, 240. LB.

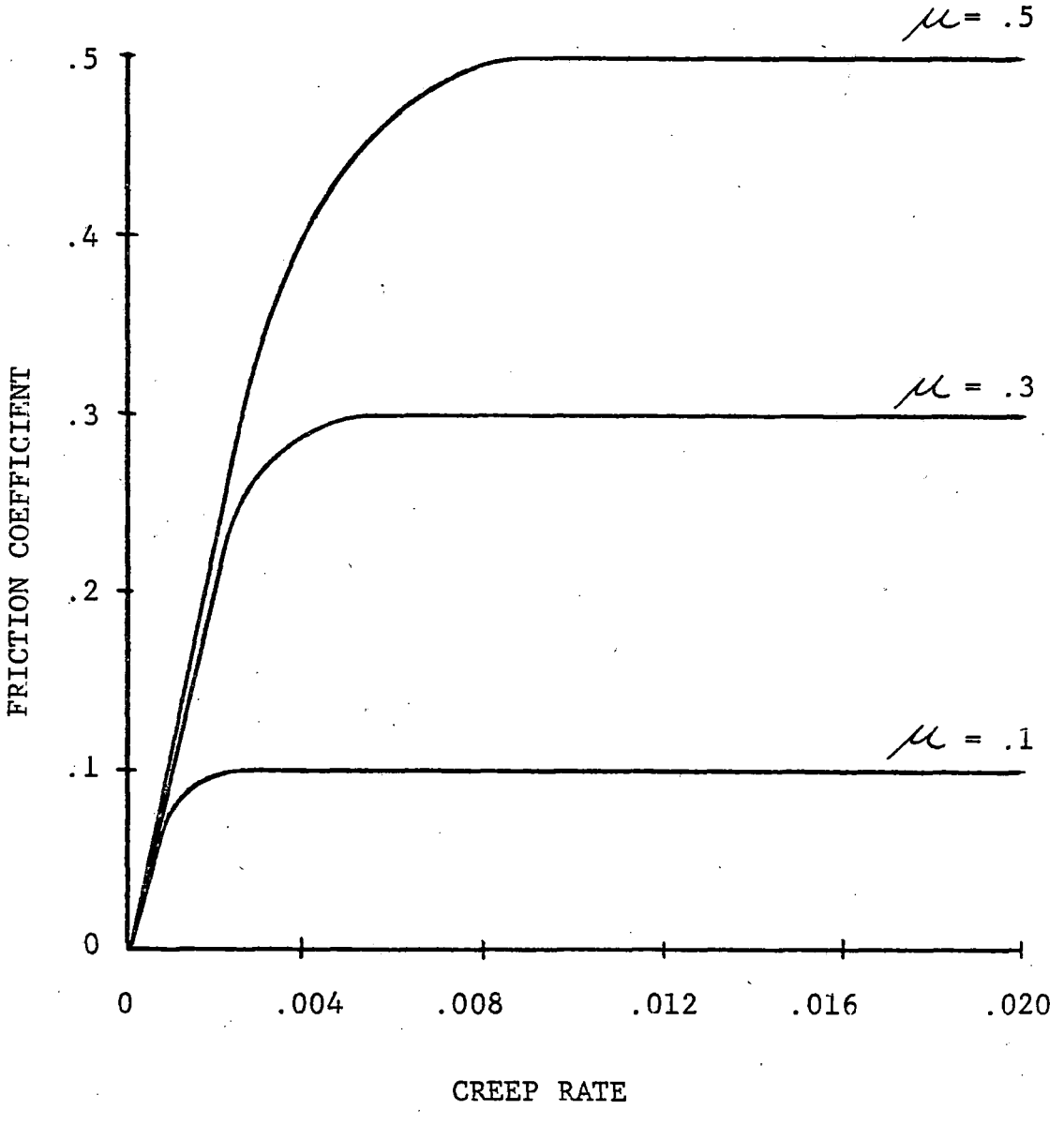

FIGURE 4-2.6: COEFFICIENT OF FRICTION VERSUS CREEP RATE (Vermuelen-Johnson formulation)*

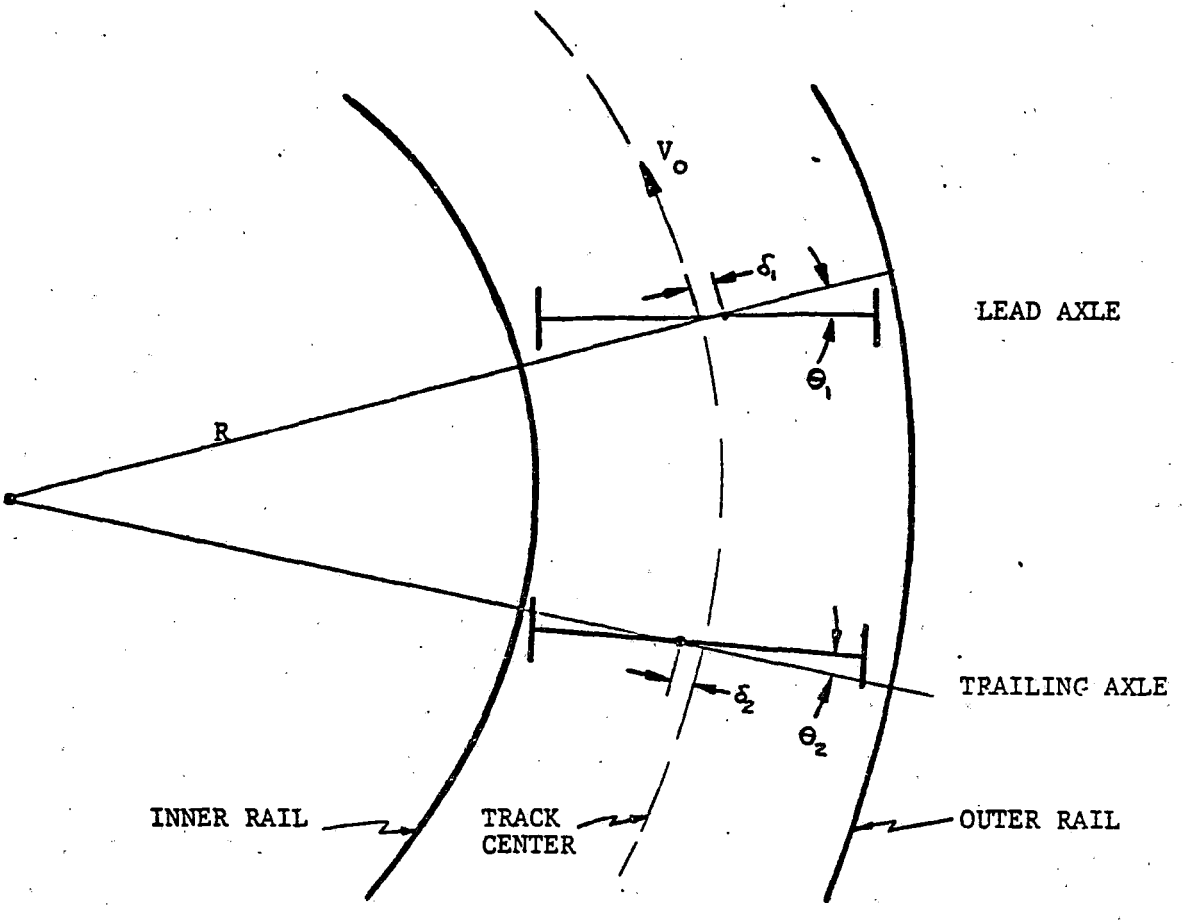

V_o = FORWARD VELOCITY

R = CURVE RADIUS

δ_1 = ROLLING LINE LATERAL OFFSET OF LEAD AXLE, SHOWN TOWARD OUTER RAIL

δ_2 = ROLLING LINE LATERAL OFFSET OF TRAILING AXLE, SHOWN TOWARD INNER RAIL

Θ_1 = ANGLE OF ATTACK OF LEAD AXLE, SHOWN TOWAPD OUTER RAIL

Θ_2 = ANGLE OF ATTACK OF TRAILING AXLE, SHOWN TOWARD INNER RAIL

FIGURE 4-2.7: Curving Performance Definitions

TABLE 4-2.5: GENERAL CASE OPERATING CONDITIONS

CURVATURE (Deg/100 ft)	RADIUS (M)	VELOCITY (M/S) (mph)	SUPERELEVATION (in)	CANT DEFICIENCY (in)
1	1746	29	0	2.94
2	873	20	0	2.82
3	582	17	0	3.06
4	437	15	0	3.18
8	218	10	0	2.82
12	146	8	0	2.70
20	88	6	0	2,52
28	63	5	0	2.40

The general case curving studies were run for four sets of inter-axle parameters, representing four different truck configurations. One set of truck parameters is labeled "PATCO" and represents the steering behavior of the existing truck. These results would also be typical of most conventional transit car trucks.

The set of parameters labeled "MODIFIED" represents the steering behavior of a truck in which the only modification from "PATCO" is the reduction of primary longitudinal stiffness to 30,000 lb/in, which is the lowest value consistent with stability.

The set of parameters labeled "SELF-STEERING" represents the curving performance of a self-steered truck with a 30,000 lb/in longitudinal primary stiffness in series with a slider having a breakout force level of 2,000 lb. The 30,000-lb/in stiffness was required to satisfy the stability requirements. Note that both the self-steered design and the modified require the same value

for longitudinal stiffness for stability. This results from the fact that an increase in unsprung mass must have an increase in the inter-axle bending stiffness to maintain the same stability margin. In the case of the steerable truck, the unsprung mass increased considerably because of the added weight of the steering arms and the mounted braking equipment. However, the additional bending stiffness that is required comes from the steering arm interconnection leaving the primary longitudinal stiffness unchanged.

A similar set of parameters with the addition of a positive-steering link is labeled "POSITIVE-STEERING". The positive-steering link ensures radial alignment under all curving conditions.

Figure 4-2.8 shows the offset of the leading and trailing axles from the track centerline during curve negotiation. Note that in all cases, the lead axles are against the outer rail in curves sharper than 8 degrees. The fact that the offset is somewhat greater for the non-steering configurations is explained by the fact that the lateral wheel/rail forces are higher and there is a greater deflection of the rail itself.

The behavior of the trailing axle is quite different for the steering trucks as compared with the non-steering trucks. In the steering cases, the trailing axles remain offset toward the outer rail even in the sharpest curves while the trailing axles of the non-steering configurations move toward the inner rail. The modified truck behaves much better than the original design in this regard, but is not nearly as good as the steering designs.

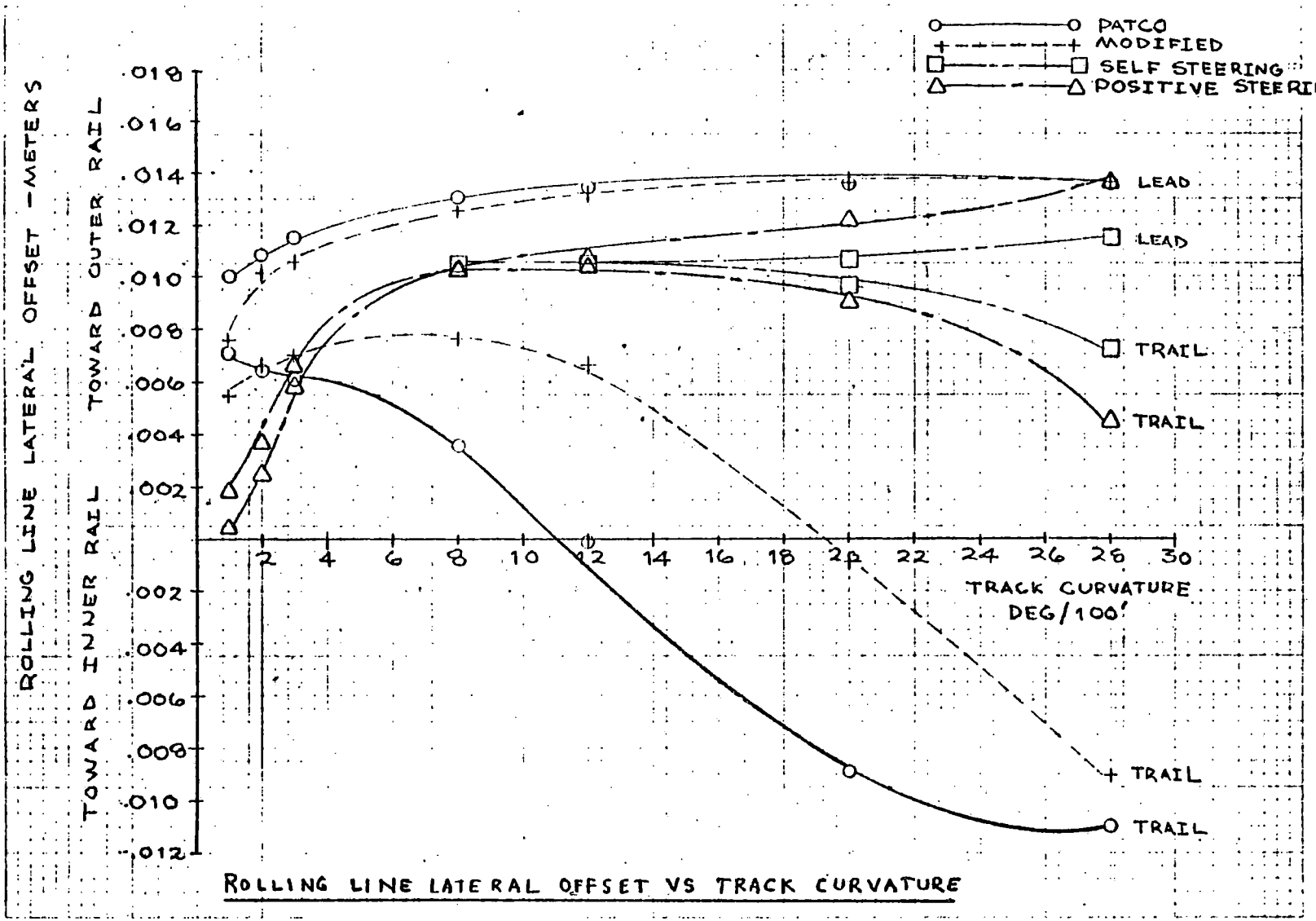
PATCO
MODIFIED
SELF STEERING
POSITIVE STEERING
LEAD
LEAD
TRAIL
TRAIL
TRAIL
TRAIL
ROLLING LINE LATERAL OFFSET -METERS
TOWARD OUTER RAIL
TOWARD INNER RAIL
.018
.016
.014
.012
.010
.008
.006
.004
.002
.002
.004
.006
.008
.010
.012
2
4
6
8
10
12
14
16
18
20
22
24
26
28
30
TRACK CURVATURE
DEG/100'
ROLLING LINE LATERAL OFFSET VS TRACK CURVATURE

FIGURE 4-2.8

Figure 4-2.9 shows the angle of attack for the leading axle as a function of track curvature for the four sets of truck parameters studied. The angle of attack reaches the critical value for noise (0.01 rad.) at 8.5 degrees for the PATCO truck 12 degrees for the modified conventional set. This result is consistent with observed curvature for the onset of screech with conventional trucks. On the other hand, the steering designs stay well below the critical value in the sharpest curve.

Figure 4-2.10 shows angle of attack data for the trailing axles. Note that none of them approaches the critical value.

Figure 4-2.11 shows the lateral wheel rail force for the lead outer wheel. Note that there is a substantial reduction of the force level for the steerable trucks for intermediate curvatures. In gradual curves, all configurations show low forces. In sharp curves, the creep forces finally become saturated for all trucks and the forces are again the same, but this time at a relatively high value.

Figure 4-2.12 shows the lateral force on the lead inner wheel. The primary contribution to this force is lateral creep. The non-steering truck configurations have higher values in intermediate curves because the angle of attack is much higher.

Figures 4-2.13 and 4-2.14 show lateral forces acting on the trailing axles. For all truck configurations, they are quite modest.

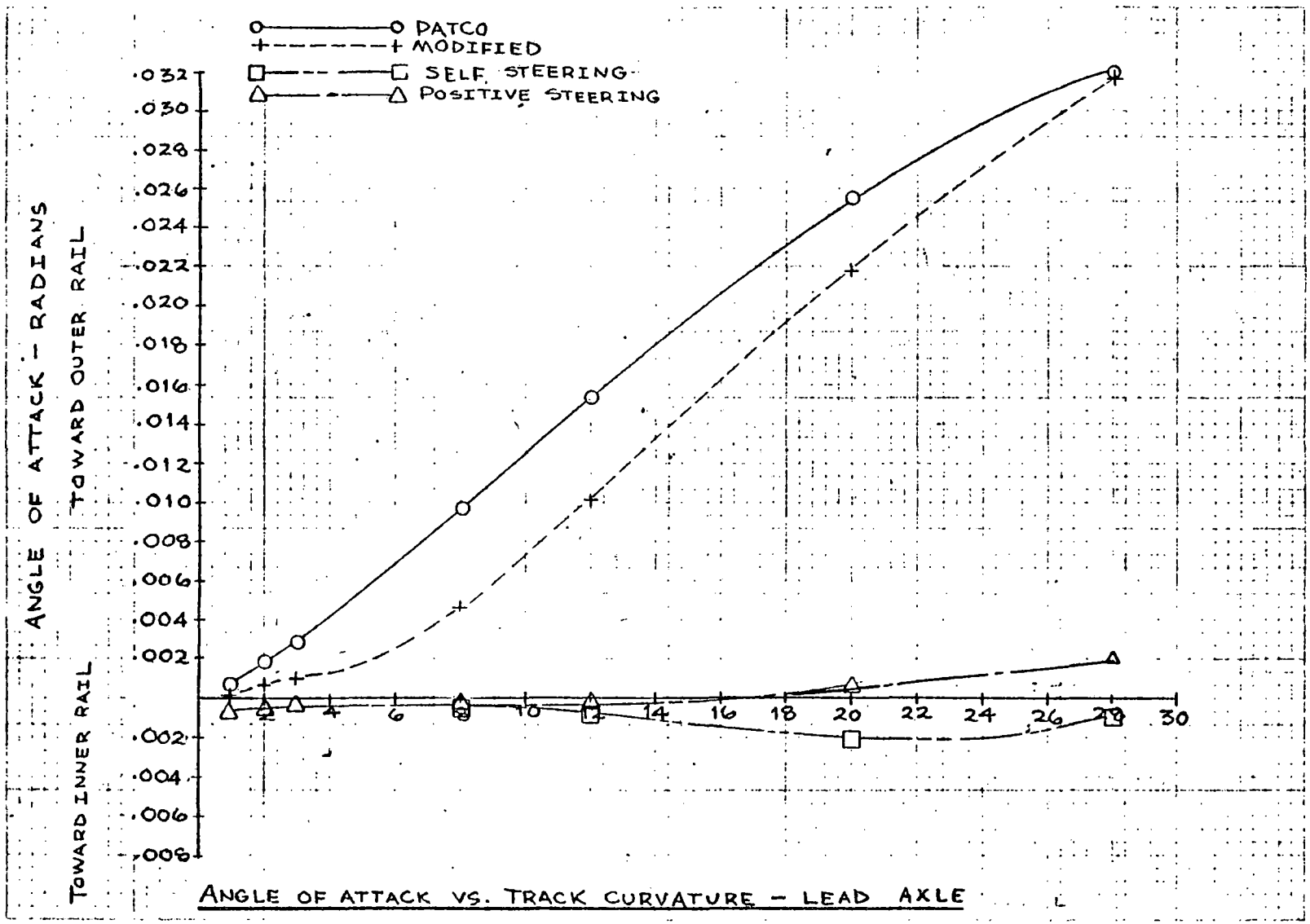
PATCO
MODIFIED
SELF STEERING
POSITIVE STEERING
ANGLE OF ATTACK - RADIANS
TOWARD OUTER RAIL
TOWARD INNER RAIL
.032
.030
.028
.026
.024
.022
.020
.018
.016
.014
.012
.010
.008
.006
.004
.002
.002
.004
.006
.008
2
4
6
8
10
12
14
16
18
20
22
24
26
28
30
ANGLE OF ATTACK VS. TRACK CURVATURE - LEAD AXLE

FIGIRE 4-2.9

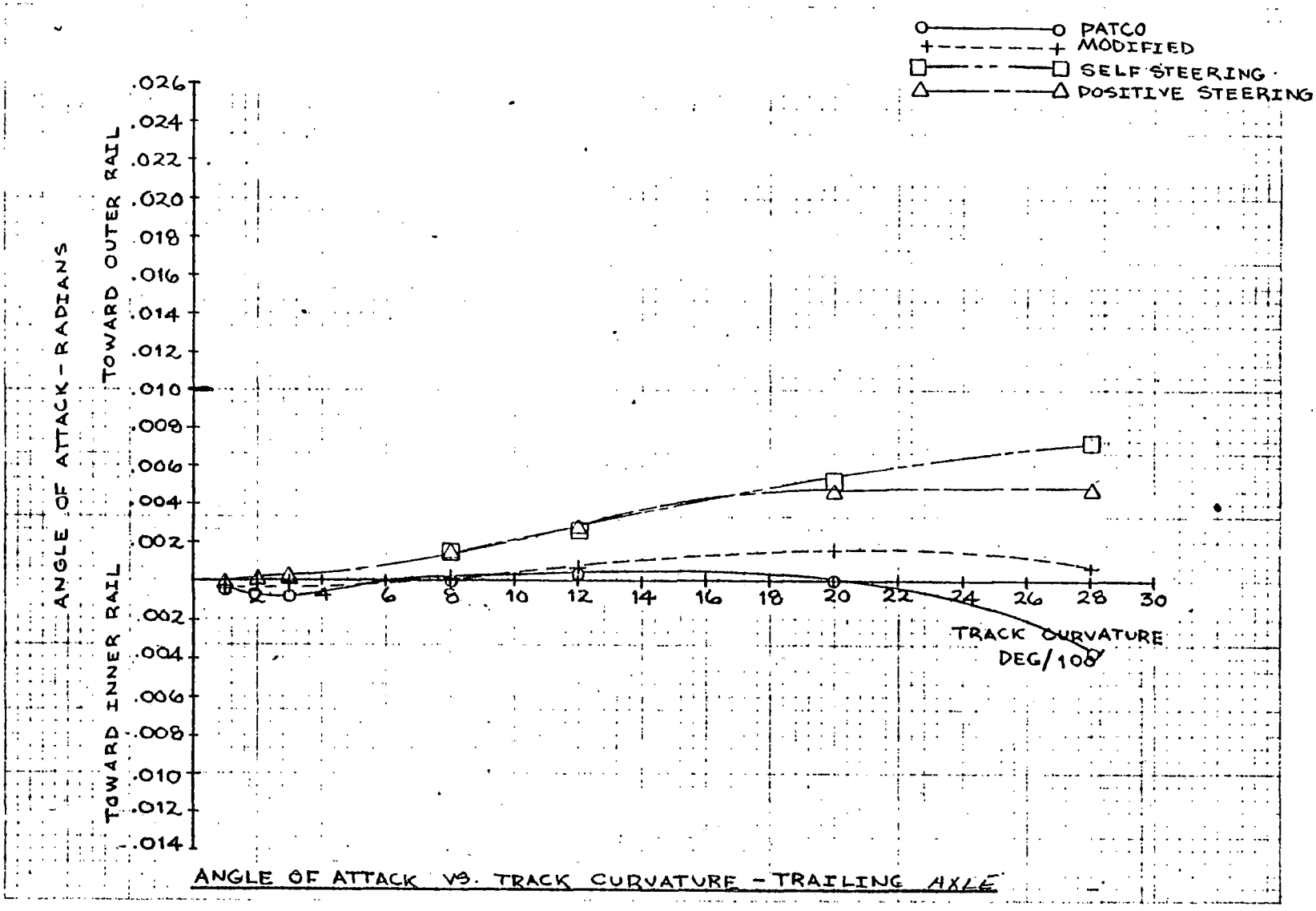
PATCO
MODIFIED
SELF STEERING
POSITIVE STEERING
ANGLE OF ATTACK - RADIANS
TOWARD OUTER RAIL
TOWARD INNER RAIL
.026
.024
.022
.020
.018
.016
.014
.012
.010
.008
.006
.004
.002
.002
.004
.006
.008
.010
.012
.014
0
2
4
6
8
10
12
14
16
18
20
22
24
26
28
30
TRACK CURVATURE
DEG/100'
ANGLE OF ATTACK VS. TRACK CURVATURE - TRAILING AXLE

FIGURE 4-2.10

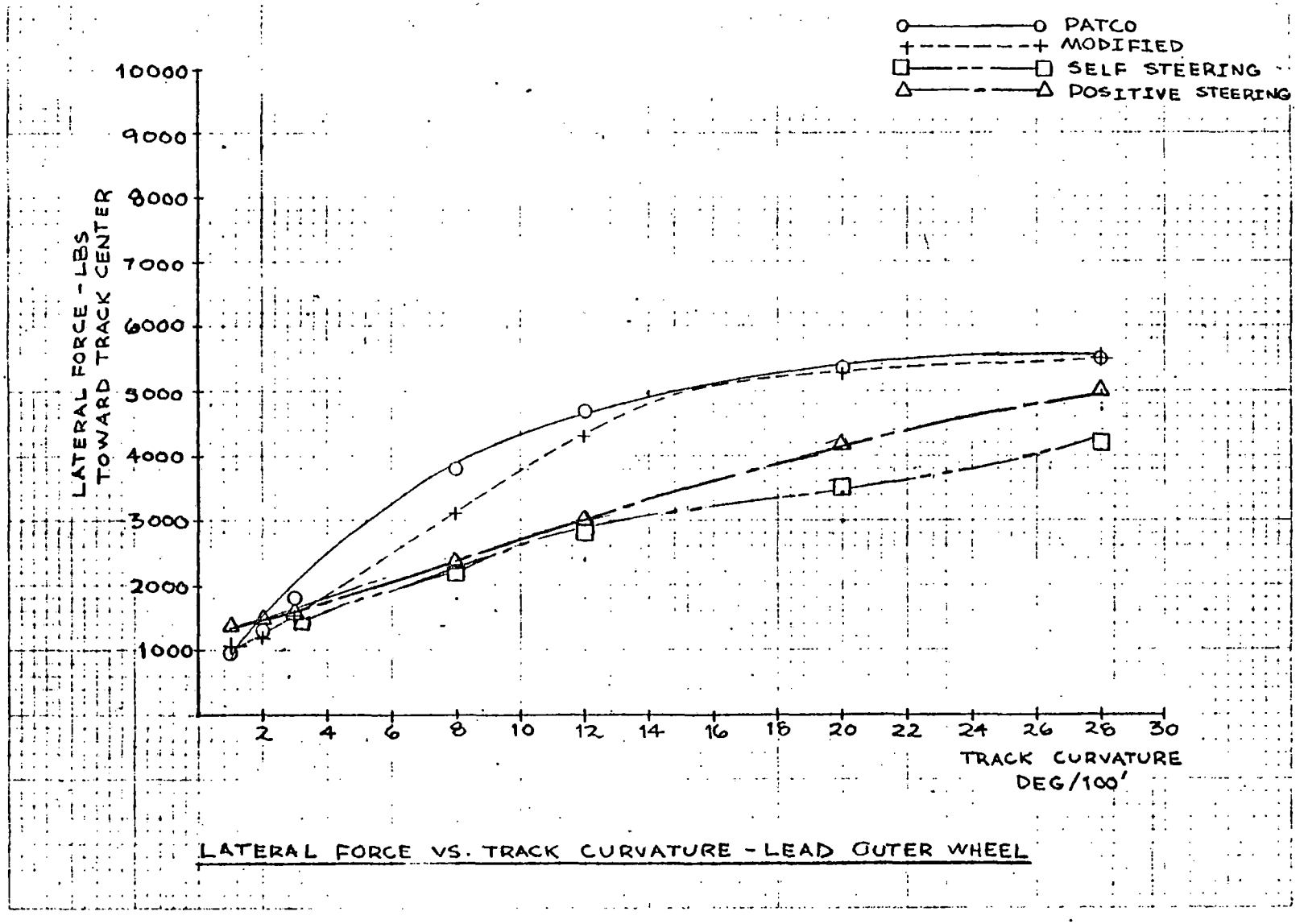
PATCO
MODIFIED
SELF STEERING
POSITIVE STEERING
LATERAL FORCE - LBS
TOWARD TRACK CENTER
10000
9000
8000
7000
6000
5000
4000
3000
2000
1000
2
4
6
8
10
12
14
16
18
20
22
24
26
28
30
TRACK CURVATURE
DEG/100'
LATERAL FORCE VS. TRACK CURVATURE - LEAD OUTER WHEEL

FIGURE 4.2.11

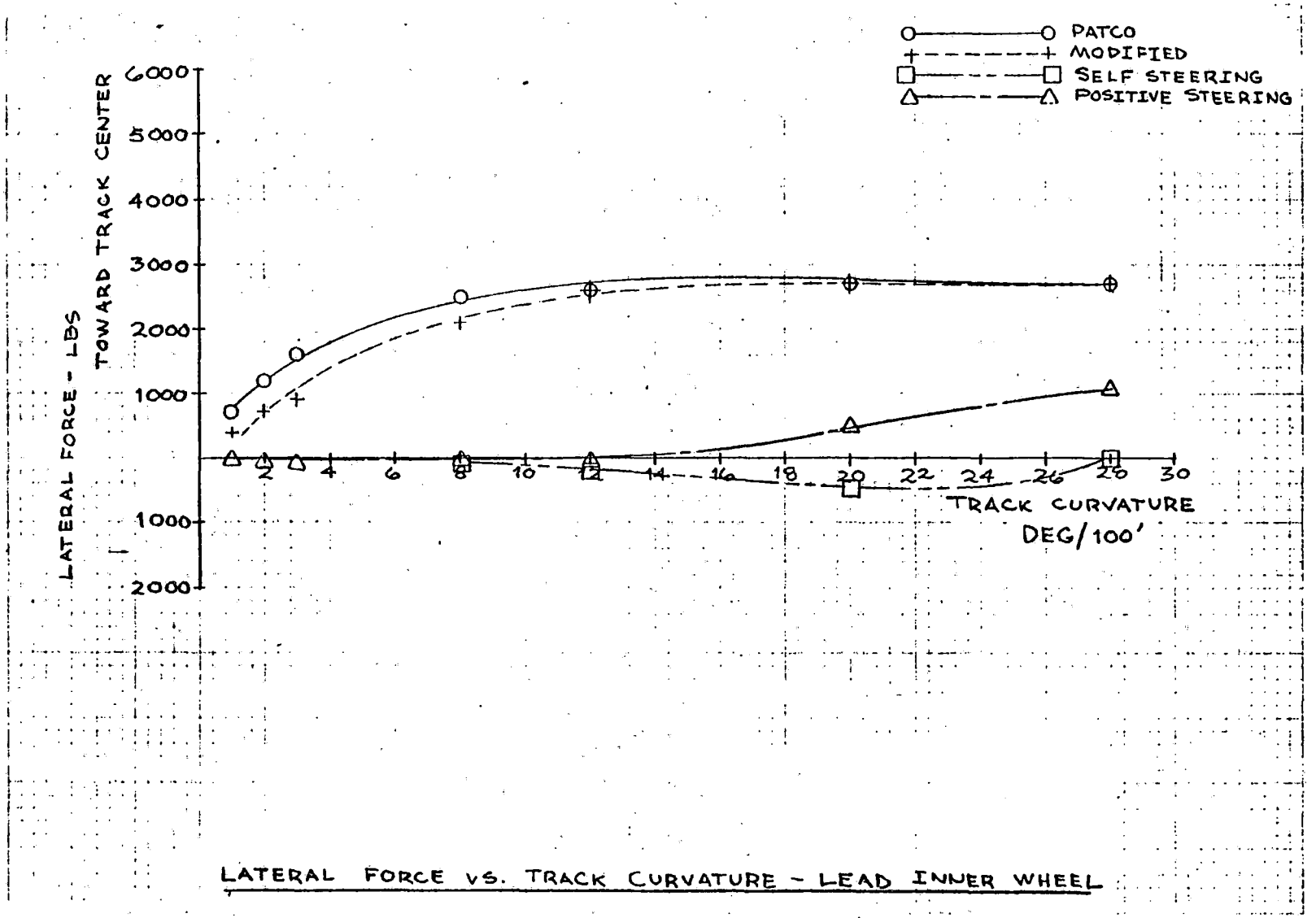

LATERAL FORCE VS. TRACK CURVATURE - LEAD INNER WHEEL

FIGURE 4.2-12

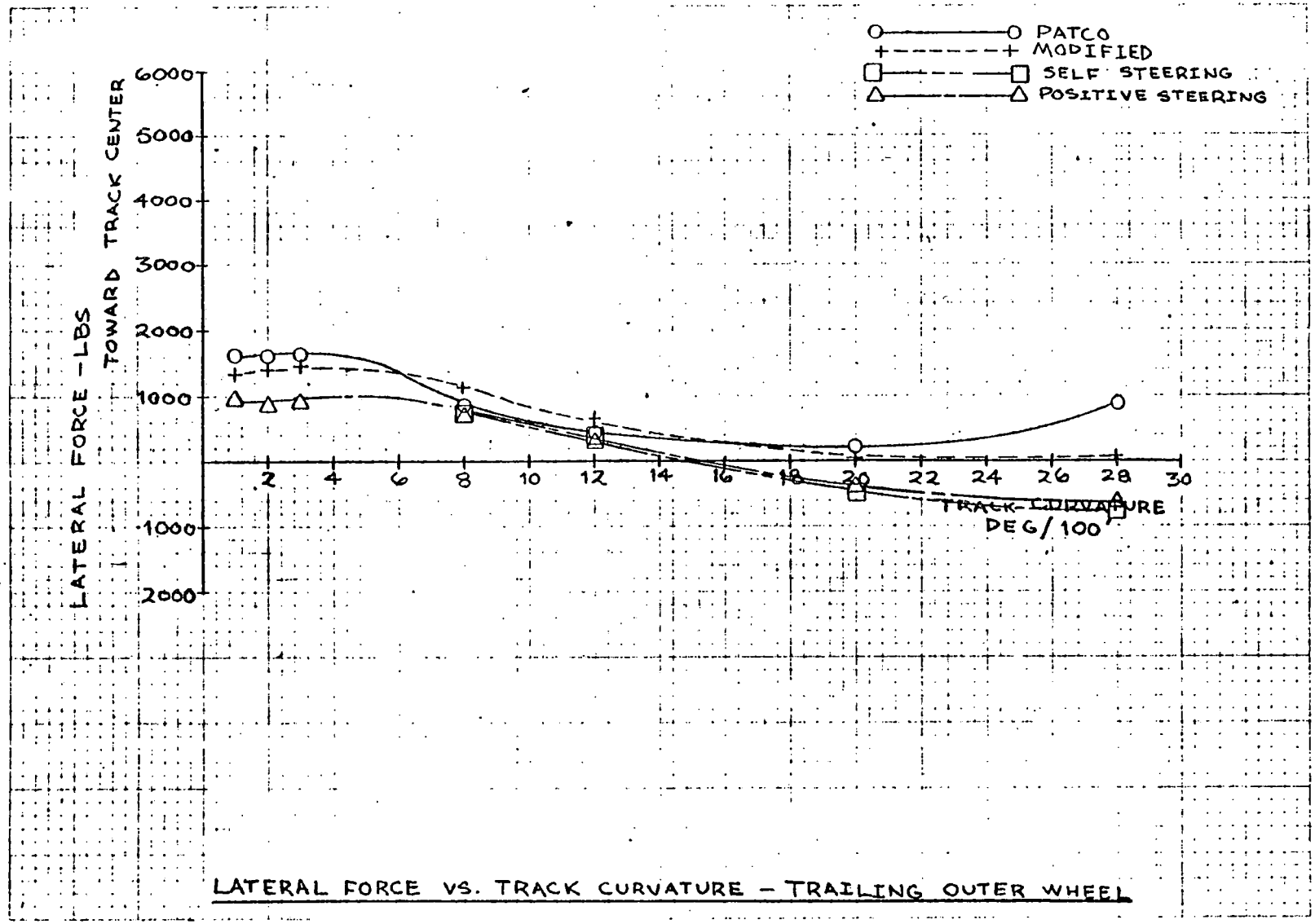
PATCO
MODIFIED
SELF STEERING
POSITIVE STEERING
LATERAL FORCE - LBS
TOWARD TRACK CENTER
6000
5000
4000
3000
2000
1000
1000
2000
2
4
6
8
10
12
14
16
18
20
22
24
26
28
30
TRACK CURVATURE
DEG/100
LATERAL FORCE VS. TRACK CURVATURE - TRAILING OUTER WHEEL

FIGURE 4.2-13

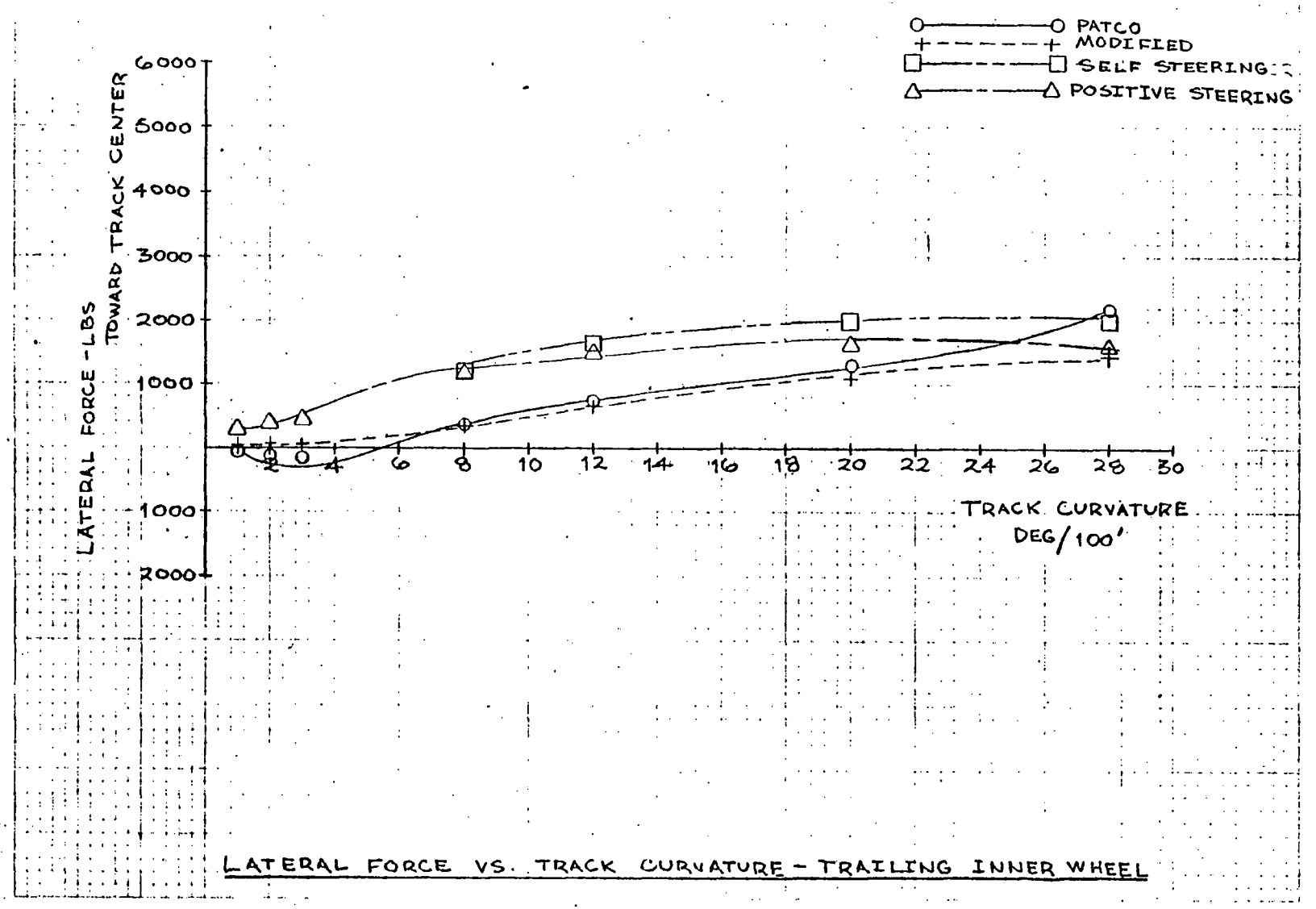
PATCO
MODIFIED
SELF STEERING
POSITIVE STEERING
LATERAL FORCE - LBS
TOWARD TRACK CENTER
6000
5000
4000
3000
2000
1000
1000
2000
0
2
4
6
8
10
12
14
16
18
20
22
24
26
28
30
TRACK CURVATURE
DEG/100'
LATERAL FORCE VS. TRACK CURVATURE - TRAILING INNER WHEEL

FIGURE 4.2-14

Figures 4-2.15 through 4-2.18 show the longitudinal creep forces at each of the four wheels for each of the parameter sets. In reviewing these curves, it should be kept in mind that a force of 3000 lb is the approximate limit set by the maximum value available on the creep curve. A review of the trailing axles (Figures 4-2.17 and 4-2.18) shows this value is approached in sharp curves by all configurations where the axles are all nearly radial. This behavior on a smaller scale can also be observed with the lead axle of the steering trucks. Note that the lead axle of the PATCO truck shows an early peak and then falls back to very low values. The early peak represents the effort being made by this axle to pull the truck around the curve. The lower values in sharper curves are the result of creep being saturated by lateral motion associated with the high angle of attack.

The general case studies show that significant improvements in curving performance can be expected from steerable trucks. However, the self-steering configuration depends on the wheel/rail adhesion for its performance. The next set of figures shows this sensitivity.

4-2.4 Effect of Friction Coefficient on Self-Steering

The curving performance of the self-steering configuration was studied for two additional friction levels (μ= 0.1 and 0.5). The case of μ_{max} = 0.5 was studied to provide assurance that wheel rail wear rates (angle of attack and lateral force) would remain low even under high adhesion conditions which would result

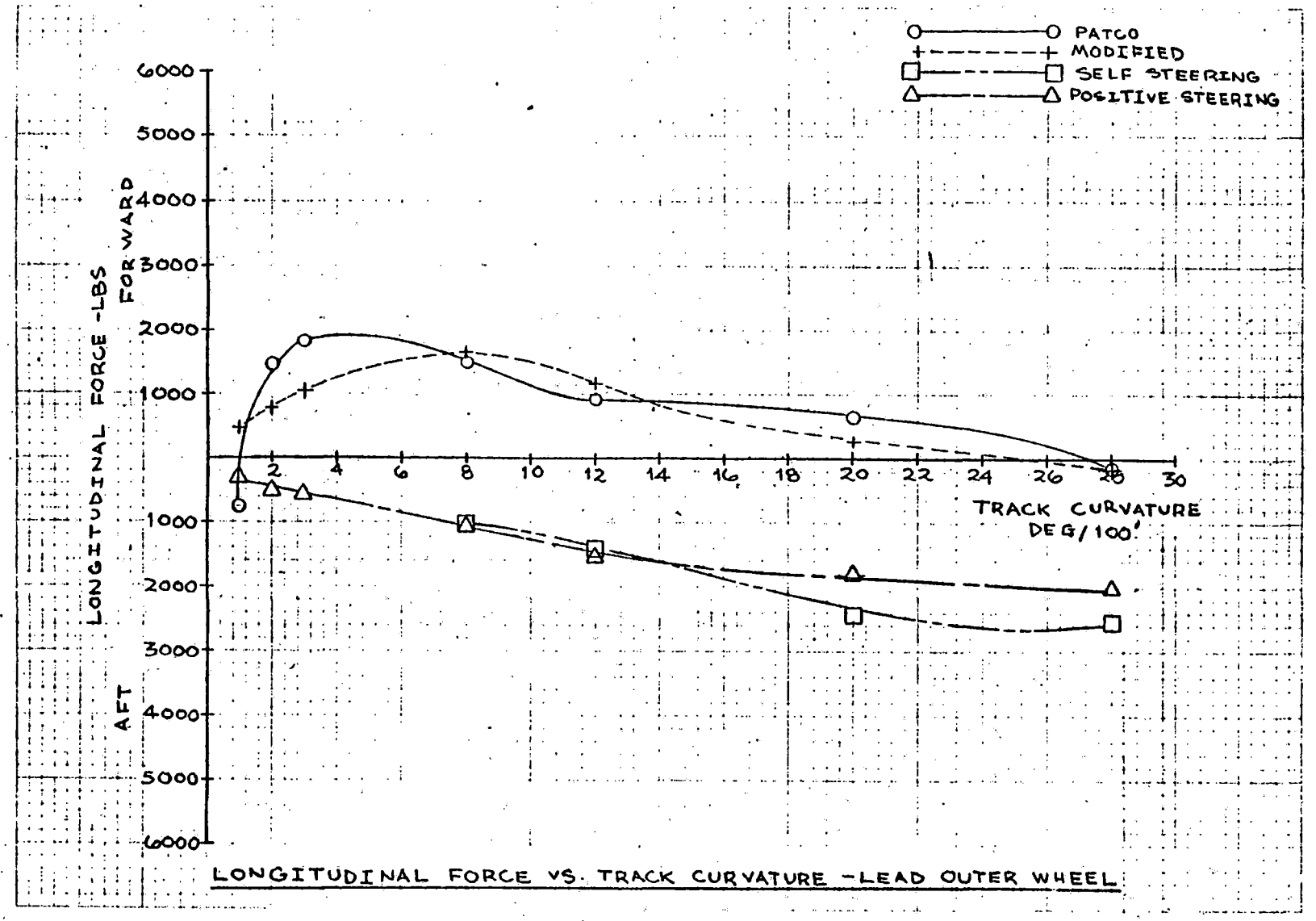
PATCO
MODIFIED
SELF STEERING
POSITIVE STEERING
LONGITUDINAL FORCE -LBS
FORWARD
AFT
6000
5000
4000
3000
2000
1000
1000
2000
3000
4000
5000
6000
2
4
6
8
10
12
14
16
18
20
22
24
26
28
30
TRACK CURVATURE
DEG/100'
LONGITUDINAL FORCE VS. TRACK CURVATURE -LEAD OUTER WHEEL

FIGURE 4.2-15

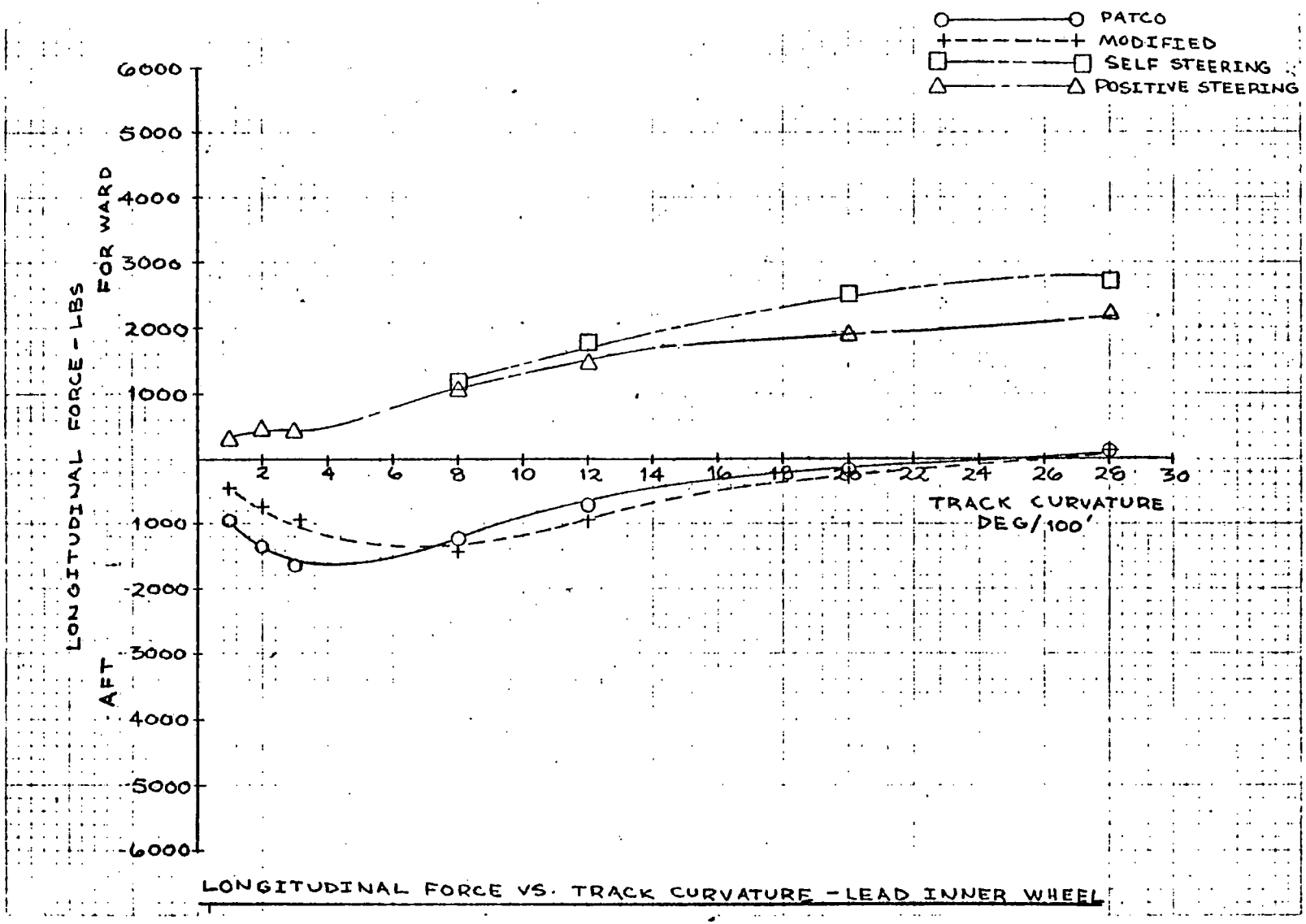
PATCO
MODIFIED
SELF STEERING
POSITIVE STEERING
6000
5000
4000
3000
2000
1000
1000
2000
3000
4000
5000
6000
LONGITUDINAL FORCE - LBS
FOR WARD
AFT
2
4
6
8
10
12
14
16
18
20
22
24
26
28
30
TRACK CURVATURE
DEG/100'
LONGITUDINAL FORCE VS. TRACK CURVATURE - LEAD INNER WHEEL

FIGURE 4.2-16

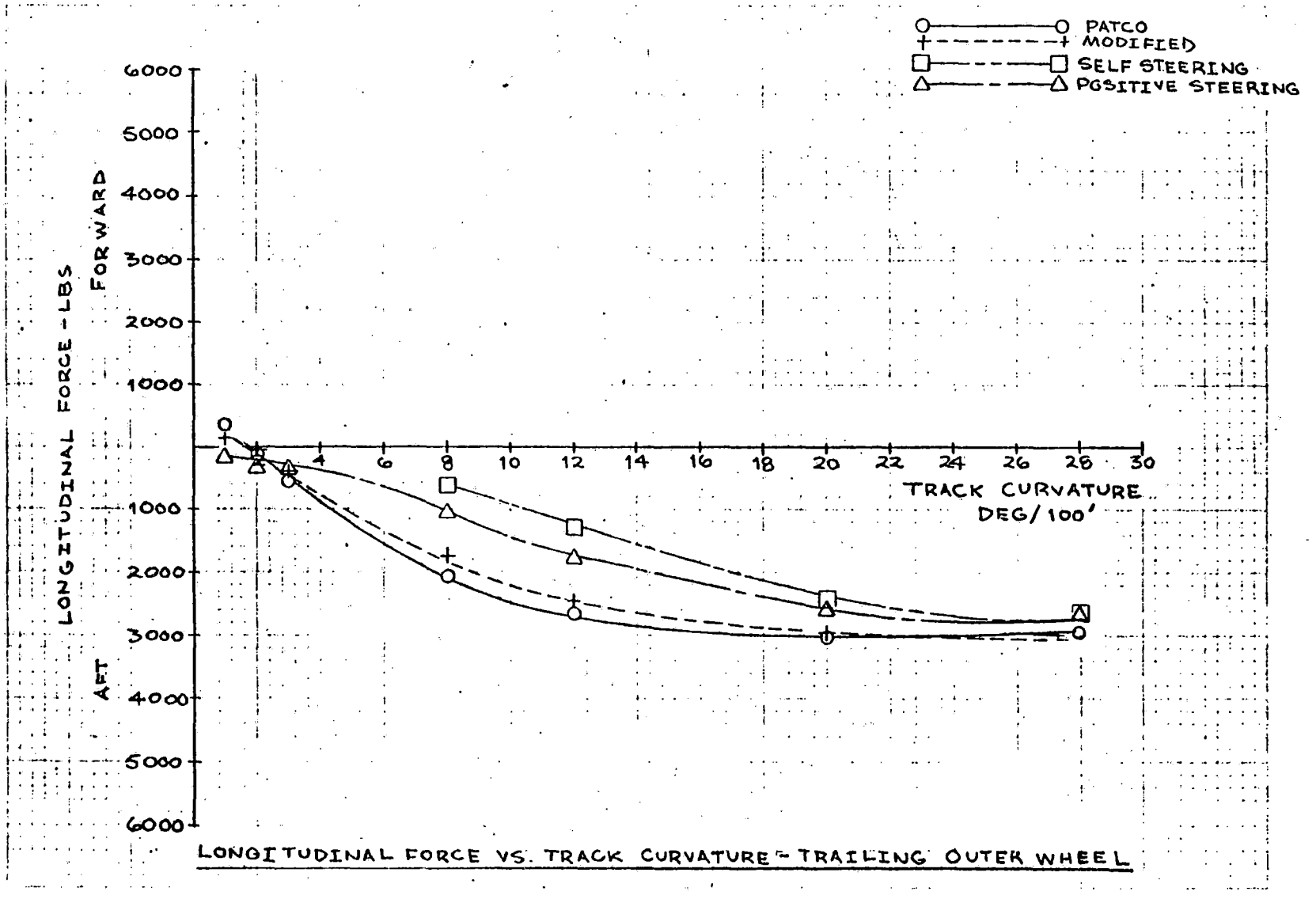
PATCO
MODIFIED
SELF STEERING
POSITIVE STEERING
LONGITUDINAL FORCE - LBS
FORWARD
AFT
6000
5000
4000
3000
2000
1000
1000
2000
3000
4000
5000
6000
4
6
8
10
12
14
16
18
20
22
24
26
28
30
TRACK CURVATURE
DEG/100'
LONGITUDINAL FORCE VS. TRACK CURVATURE - TRAILING OUTER WHEEL

FIGURE 4.2-17

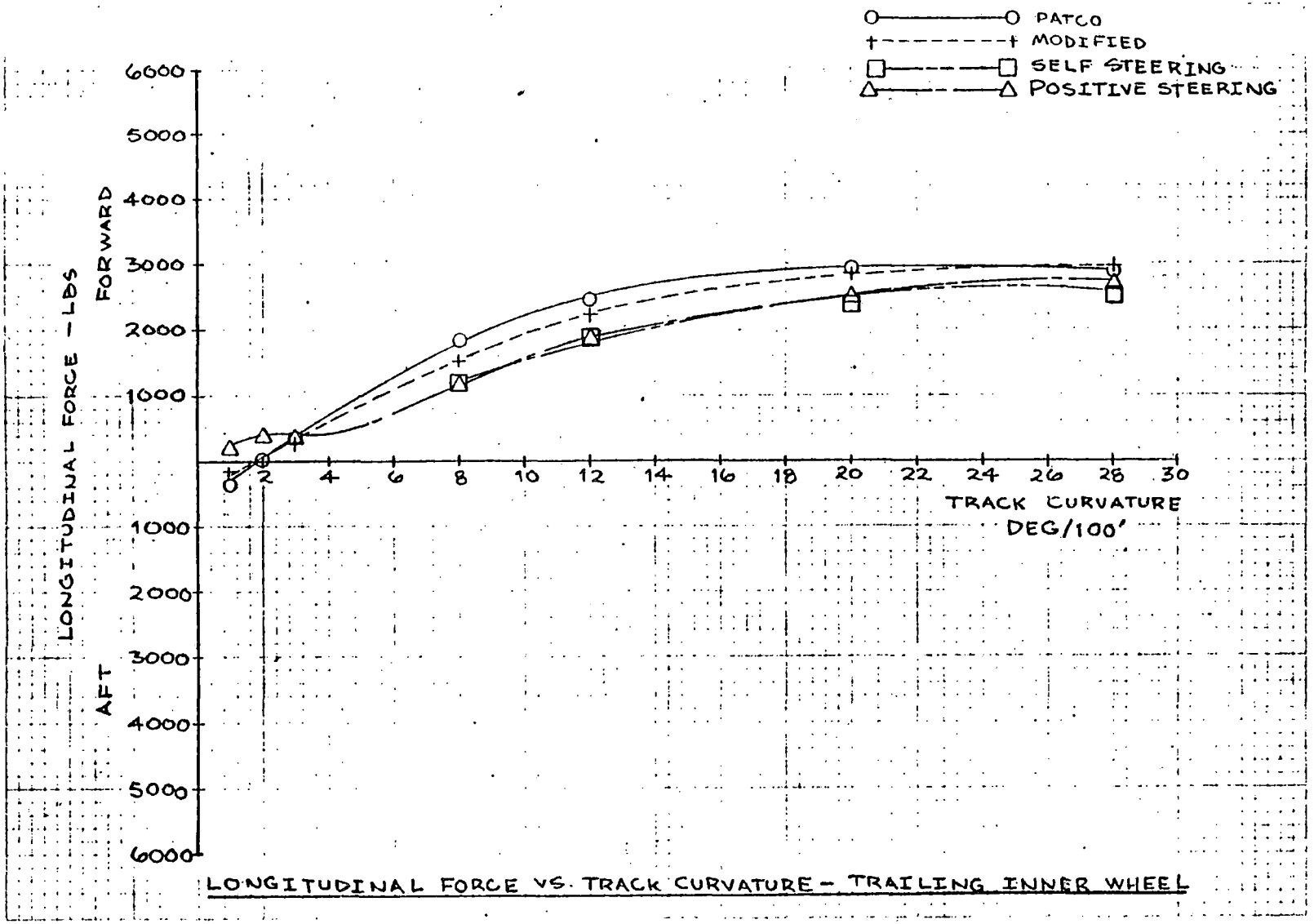
PATCO
MODIFIED
SELF STEERING
POSITIVE STEERING
LONGITUDINAL FORCE - LBS
FORWARD
AFT
6000
5000
4000
3000
2000
1000
1000
2000
3000
4000
5000
6000
0
2
4
6
8
10
12
14
16
18
20
22
24
26
28
30
TRACK CURVATURE
DEG/100'
LONGITUDINAL FORCE VS. TRACK CURVATURE - TRAILING INNER WHEEL

FIGURE 4-2.18

from removal of track lubricators. The case of μ_{max} = 0.3 was run in the general case studies and is shown here again for comparison as being a typical value. The case of μ_{max} = 0.1 was run to represent the effect of traction and braking torques on steering behavior. The presence of traction torques will tend to saturate wheel/rail creep forces. This is represented by imposing a low limit on the maximum friction force. This level would also be typical of wet or lubricated rail.

Figure 4-2.19 shows that increasing friction has little effect on the running position of the axles. At low friction (creep saturation), the trailing axle shows a tendency to behave somewhat like a conventional truck.

Figure 4-2.20 also shows that increasing friction has little effect on angle of attack of the lead axle. This is good in that it predicts that eliminating track lubrication will not increase track or wheel wear. Lowering friction shows the expected result that the self-steering action is weak, allowing the angle of attack to build up in sharp curves. This result confirms the need to provide at least some amount of positive-steering action for a powered truck.

Figure 4-2.21 shows that the angle of attack for the trailing axle remains relatively low for all friction values.

Figure 4.2-22 shows that the maximum value for lateral wheel force increases with friction. The force level associated with the highest friction is still quite modest in terms of track strength or L/V; and because the angle of attack is near

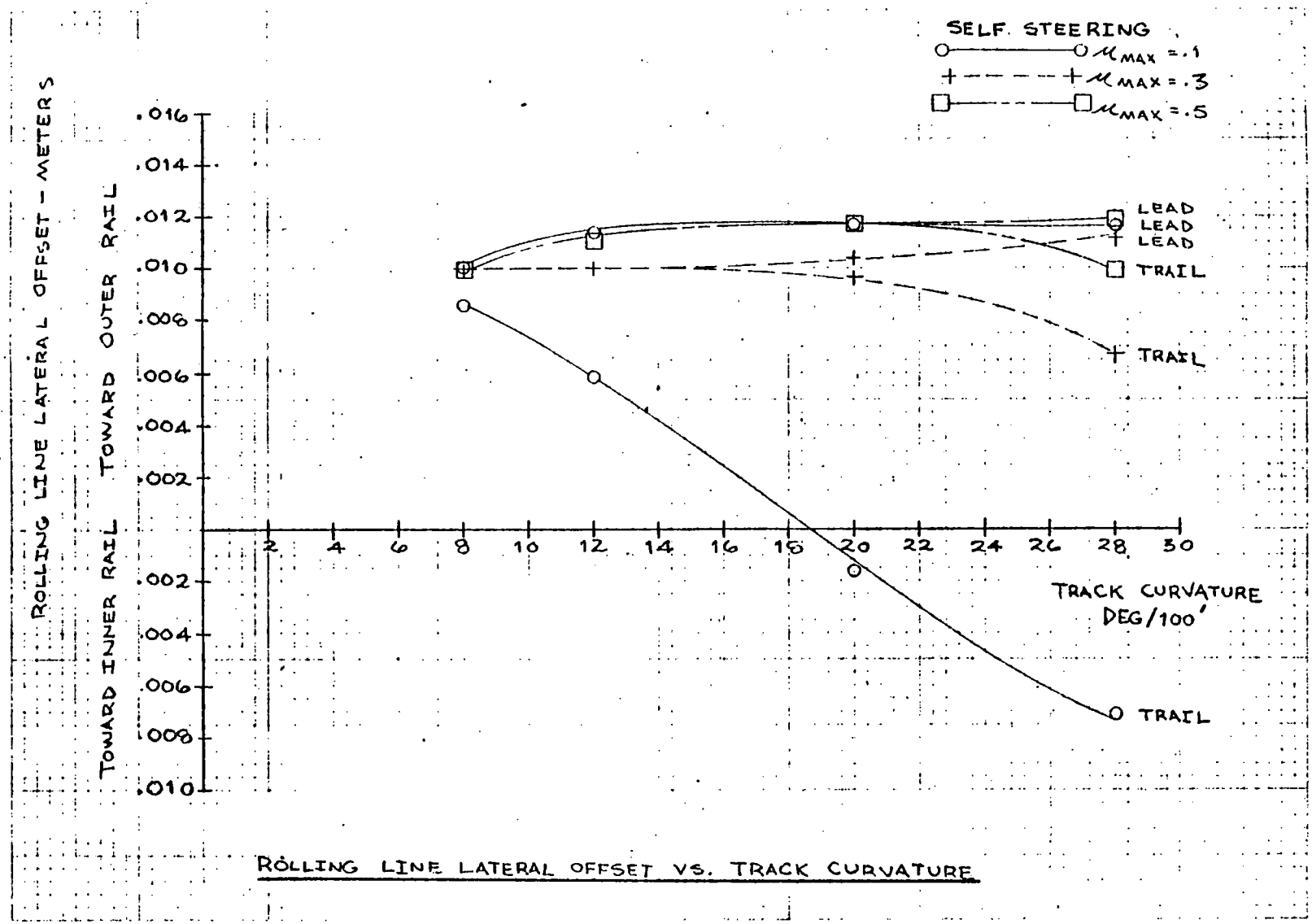

ROLLING LINE LATERAL OFFSET VS. TRACK CURVATURE

FIGURE 4-2.19

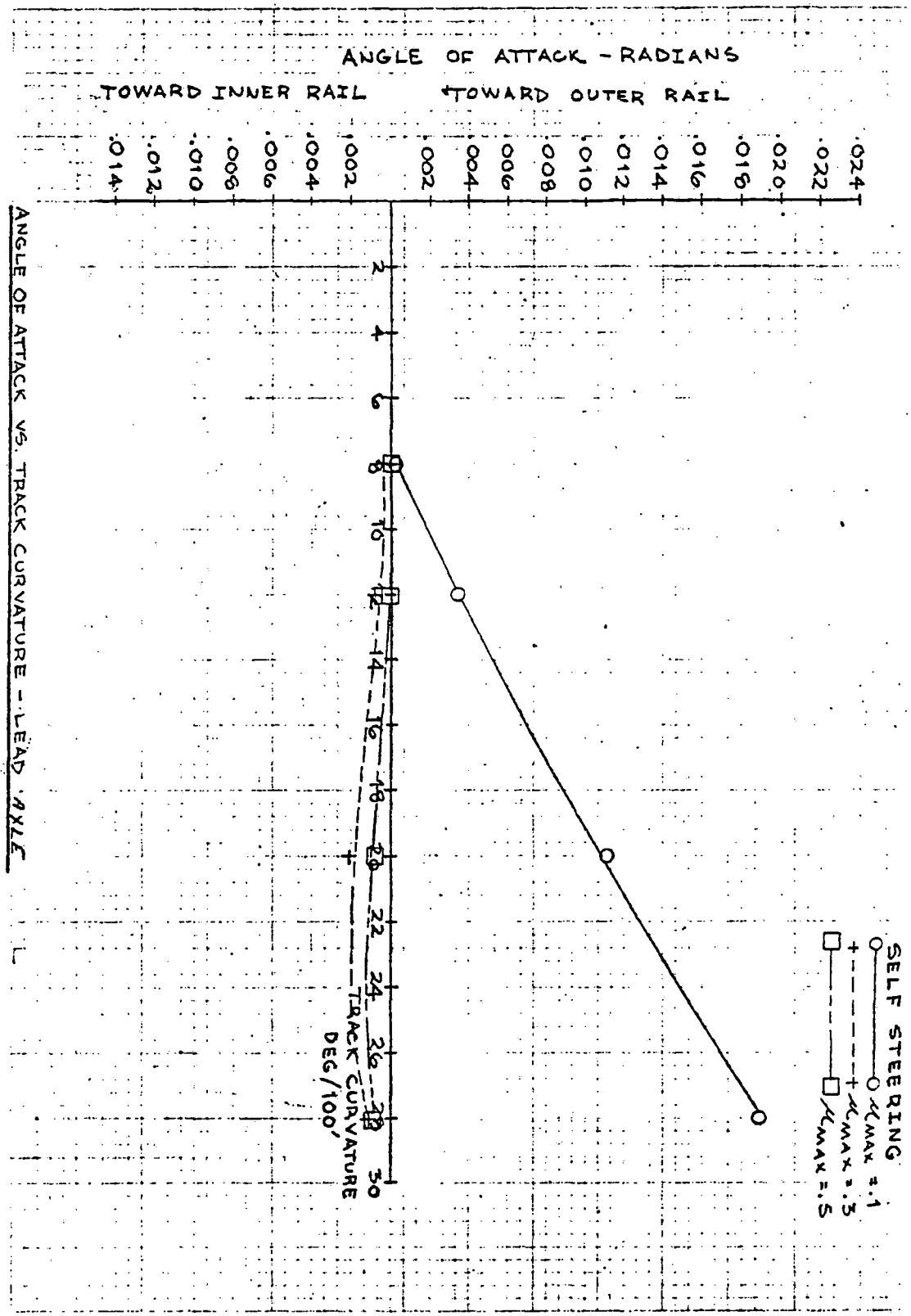
ANGLE OF ATTACK - RADIANS
TOWARD INNER RAIL
TOWARD OUTER RAIL
.024
.022
.020
.018
.016
.014
.012
.010
.008
.006
.004
.002
.002
.004
.006
.008
.010
.012
.014
2
4
6
8
10
12
14
16
18
20
22
24
26
28
30
TRACK CURVATURE DEG/100'
SELF STEERING
α MAX = .1
α MAX = .3
α MAX = .5
ANGLE OF ATTACK VS. TRACK CURVATURE - LEAD AXLE

FIGURE 4-2.20

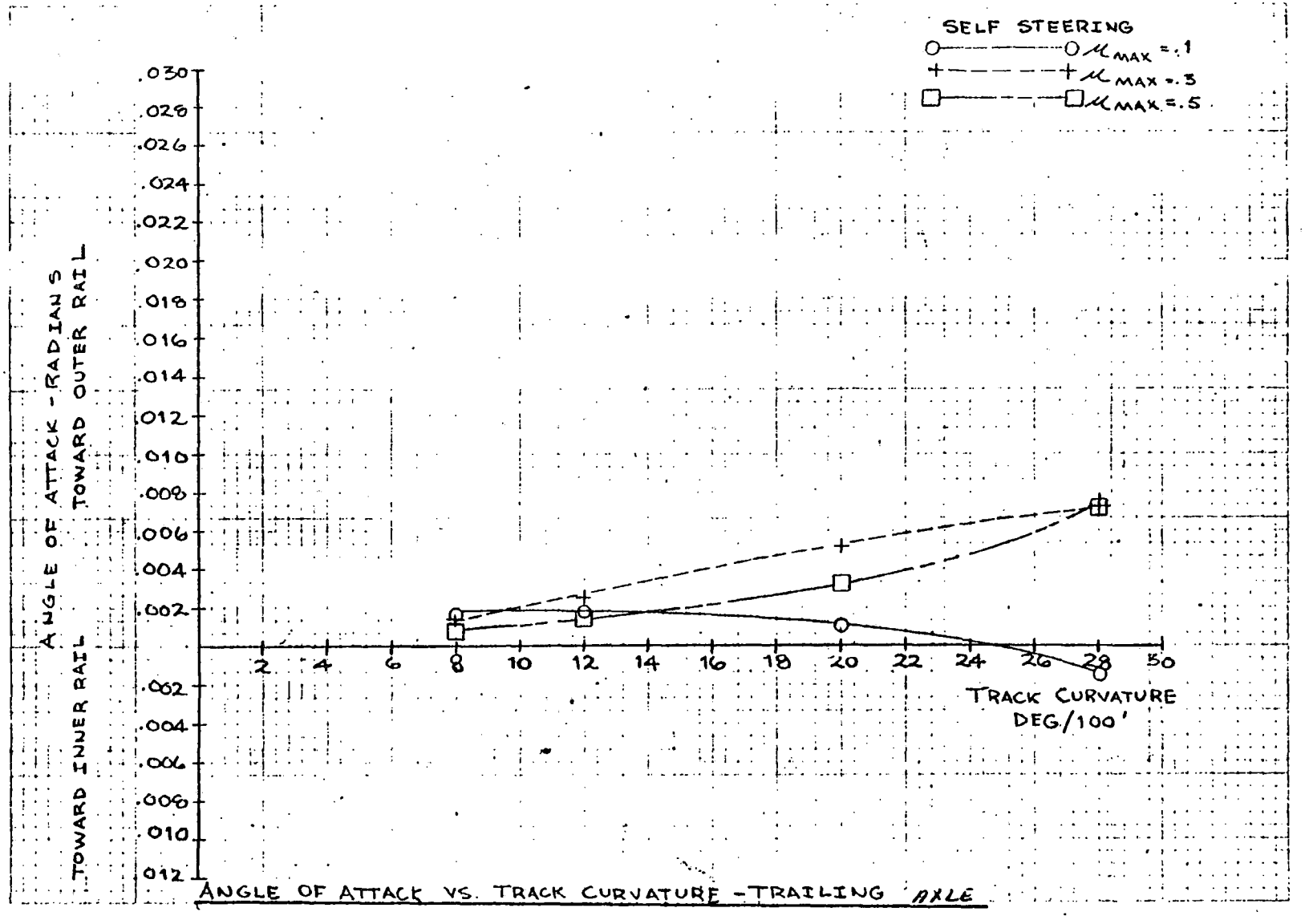
SELF STEERING
μ MAX = .1
μ MAX = .3
μ MAX = .5
ANGLE OF ATTACK - RADIANS
TOWARD OUTER RAIL
TOWARD INNER RAIL
.030
.028
.026
.024
.022
.020
.018
.016
.014
.012
.010
.008
.006
.004
.002
.002
.004
.006
.008
.010
.012
2
4
6
8
10
12
14
16
18
20
22
24
26
28
30
TRACK CURVATURE
DEG/100'
ANGLE OF ATTACK VS. TRACK CURVATURE - TRAILING AXLE

FIGURE 4-2.21

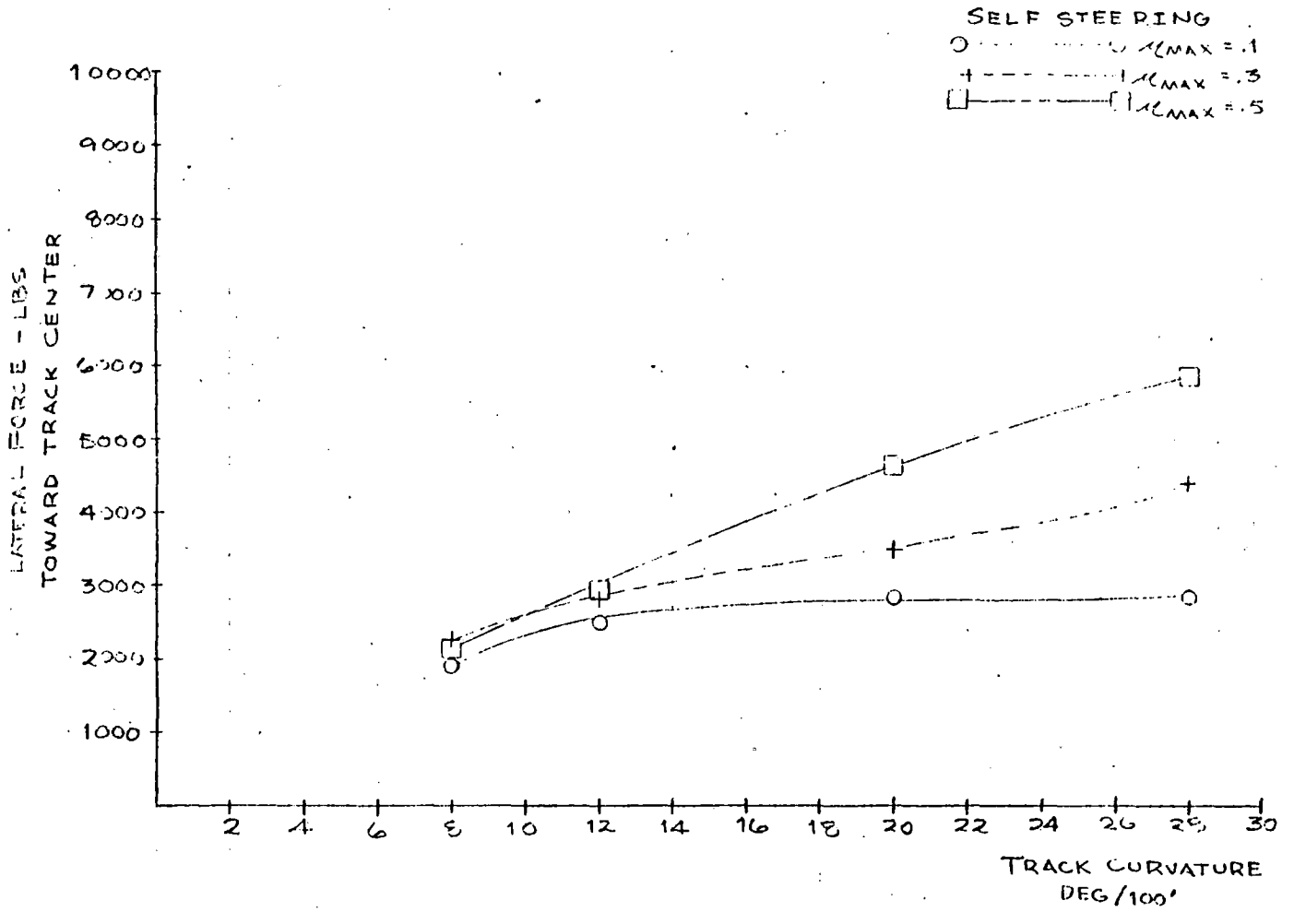

LATERAL FORCE VS. TRACK CURVATURE - LEAD OUTER WHEEL

FIGURE 4-2.22

zero, there would not be a wear problem.

Figures 4-2.23 and 4-2.24 show the expected result that these forces are low at all times.

Figure 4-2.25 shows the increase in lateral force at the trailing inner wheel that is associated with increasing adhesion levels. This increase is required to balance the yaw moments for the truck. The peak values are, however, modest and will not result in high wear rates because the attack angles are low.

Figures 4-2.26 through 4-2.29 show the increase in longitudinal wheel/rail forces with increasing adhesion. Because the range of curvatures shown are sharper than could be accommodated by a free wheelset, the direction of the forces is to the rear (aft) for the outer wheels (Figures 4-2.26 and 4-2.28) and forward for the inner wheels (Figures 4-2.27 and 4-2.29). It is the requirement to balance these forces that prevents the lateral forces of Figures 4-2.22 and 4-2.25 from being zero even with steering.

Based on the drop-off in curving performance of the self-steering configuration at low friction levels, positive-steering is recommended. The positive- or forced-steering configuration will ensure radial alignment under all curving conditions.

A second reason for recommending forced-steering is that the self-steering design with the 2000-lb slider may have a stability problem if breakout occurs at high speed. To prevent breakout, a higher slide force level would be required and this would have a negative effect on curving performance.

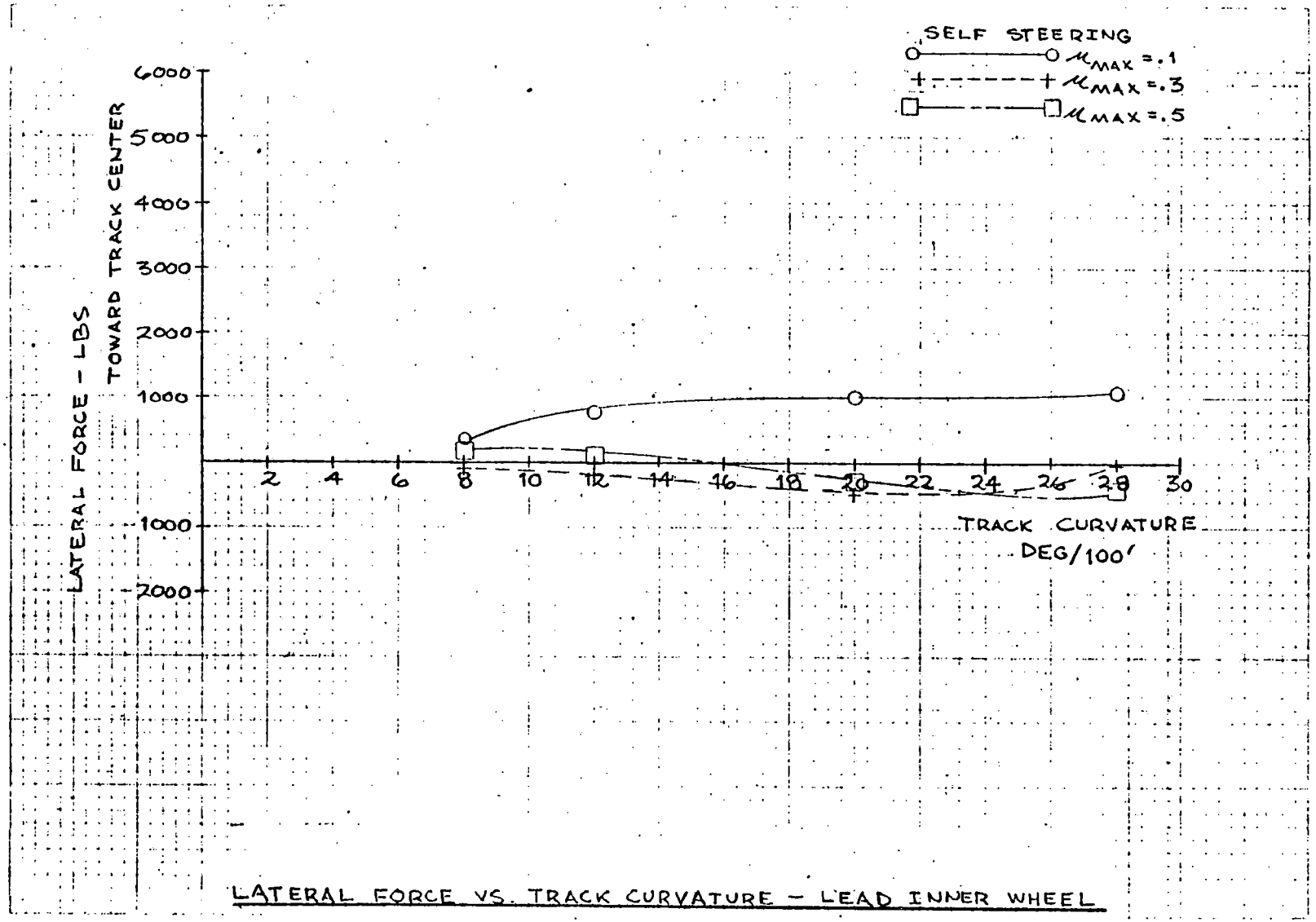

LATERAL FORCE VS. TRACK CURVATURE - LEAD INNER WHEEL

IGURE 4-2.23

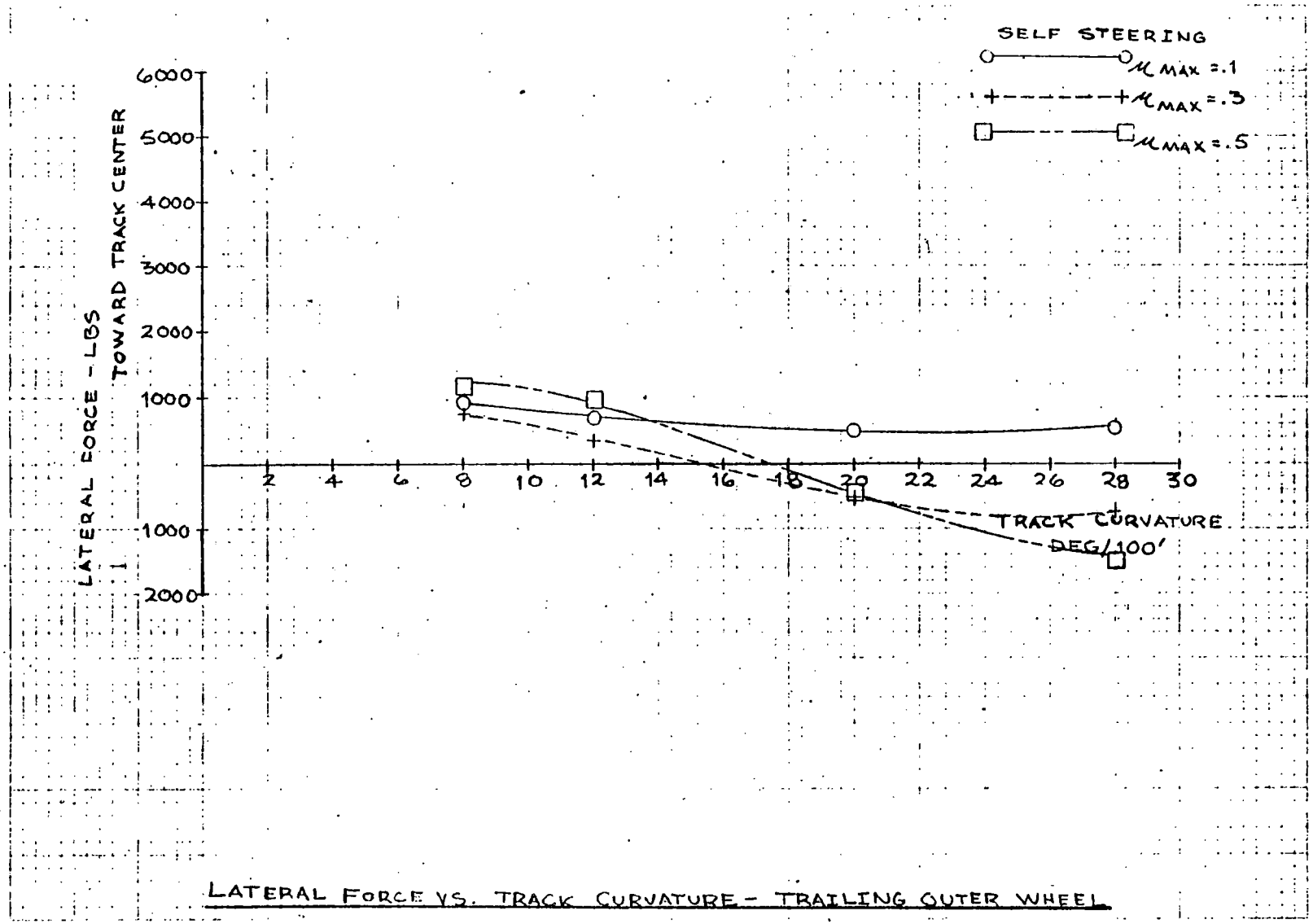
SELF STEERING
μ MAX =.1
μ MAX =.3
μ MAX =.5
LATERAL FORCE - LBS
TOWARD TRACK CENTER
6000
5000
4000
3000
2000
1000
1000
2000
2
4
6
8
10
12
14
16
18
20
22
24
26
28
30
TRACK CURVATURE
DEG/100'
LATERAL FORCE VS. TRACK CURVATURE - TRAILING OUTER WHEEL

FIGURE 4-2.24

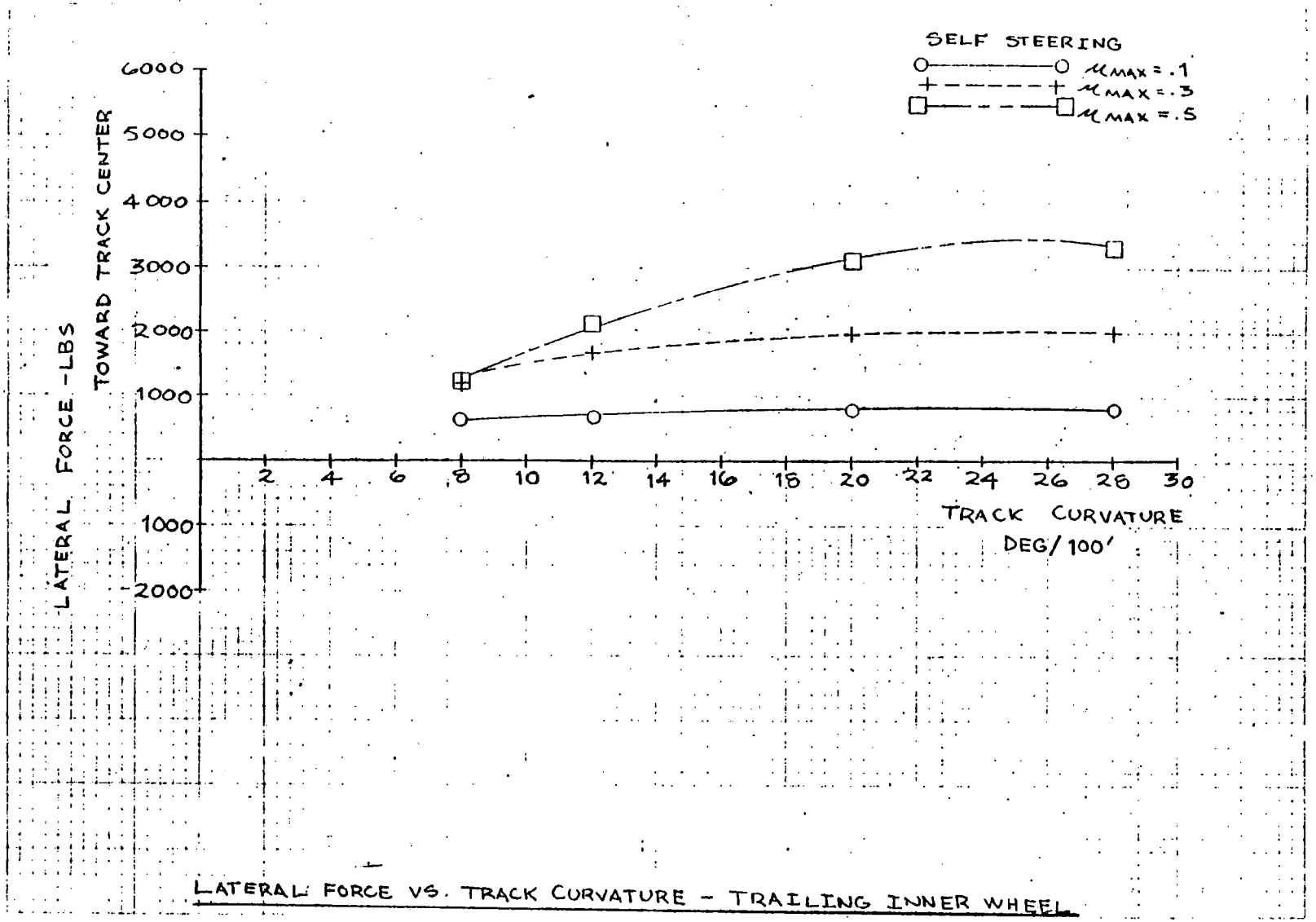

LATERAL FORCE VS. TRACK CURVATURE - TRAILING INNER WHEEL

FIGURE 4-2.25

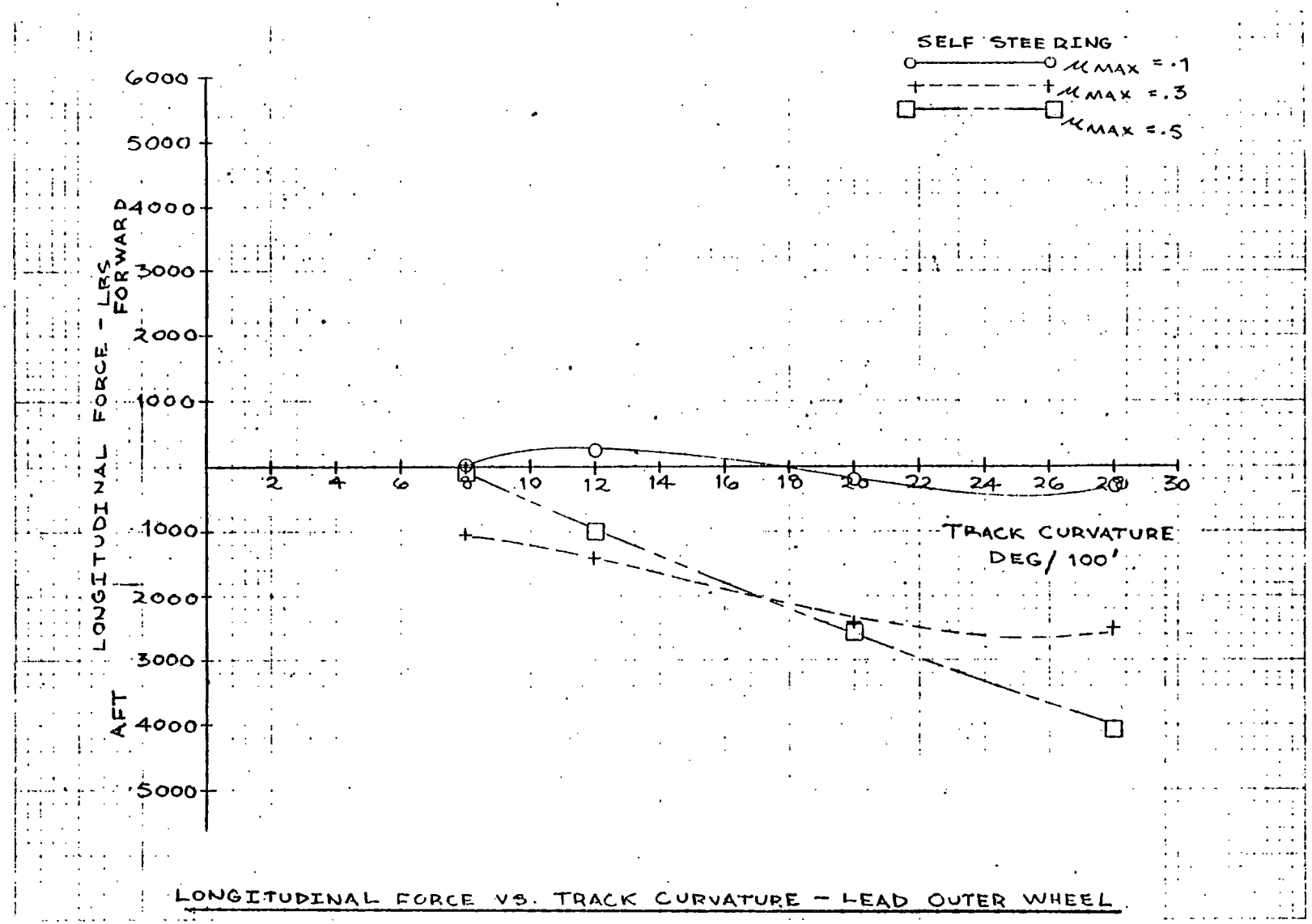
SELF STEERING
μMAX = .1
μMAX = .3
μMAX = .5
LONGITUDINAL FORCE - LBS
FORWARD
AFT
6000
5000
4000
3000
2000
1000
1000
2000
3000
4000
5000
2
4
6
8
10
12
14
16
18
20
22
24
26
28
30
TRACK CURVATURE
DEG/ 100'
LONGITUDINAL FORCE VS. TRACK CURVATURE - LEAD OUTER WHEEL

FIGURE 4-2.26

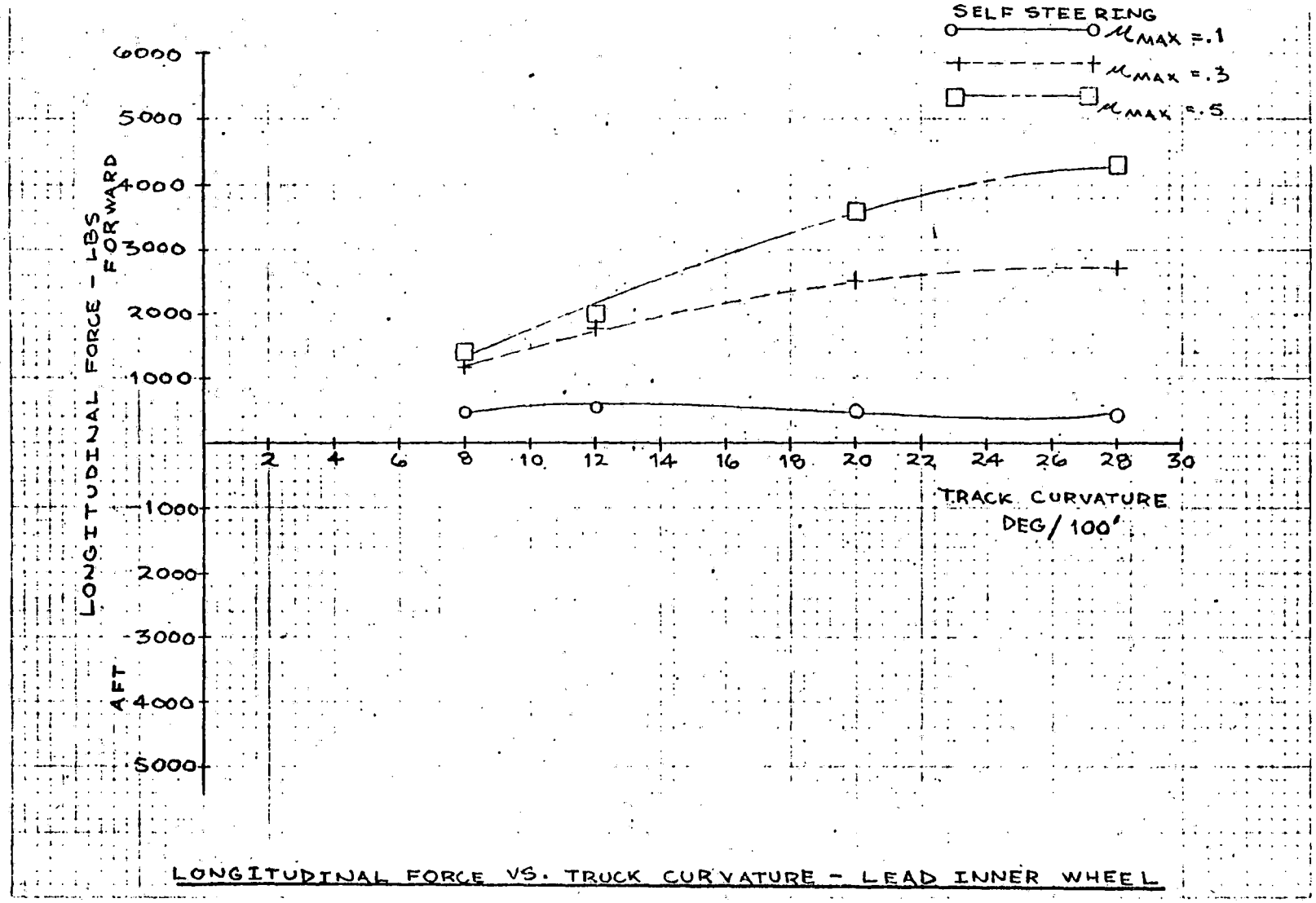
SELF STEERING
μ_{MAX} = .1
μ_{MAX} = .3
μ_{MAX} = .5
LONGITUDINAL FORCE - LBS
FORWARD
AFT
6000
5000
4000
3000
2000
1000
1000
2000
3000
4000
5000
2
4
6
8
10
12
14
16
18
20
22
24
26
28
30
TRACK CURVATURE
DEG/100'
LONGITUDINAL FORCE VS. TRUCK CURVATURE - LEAD INNER WHEEL

FIGURE 4-2.27

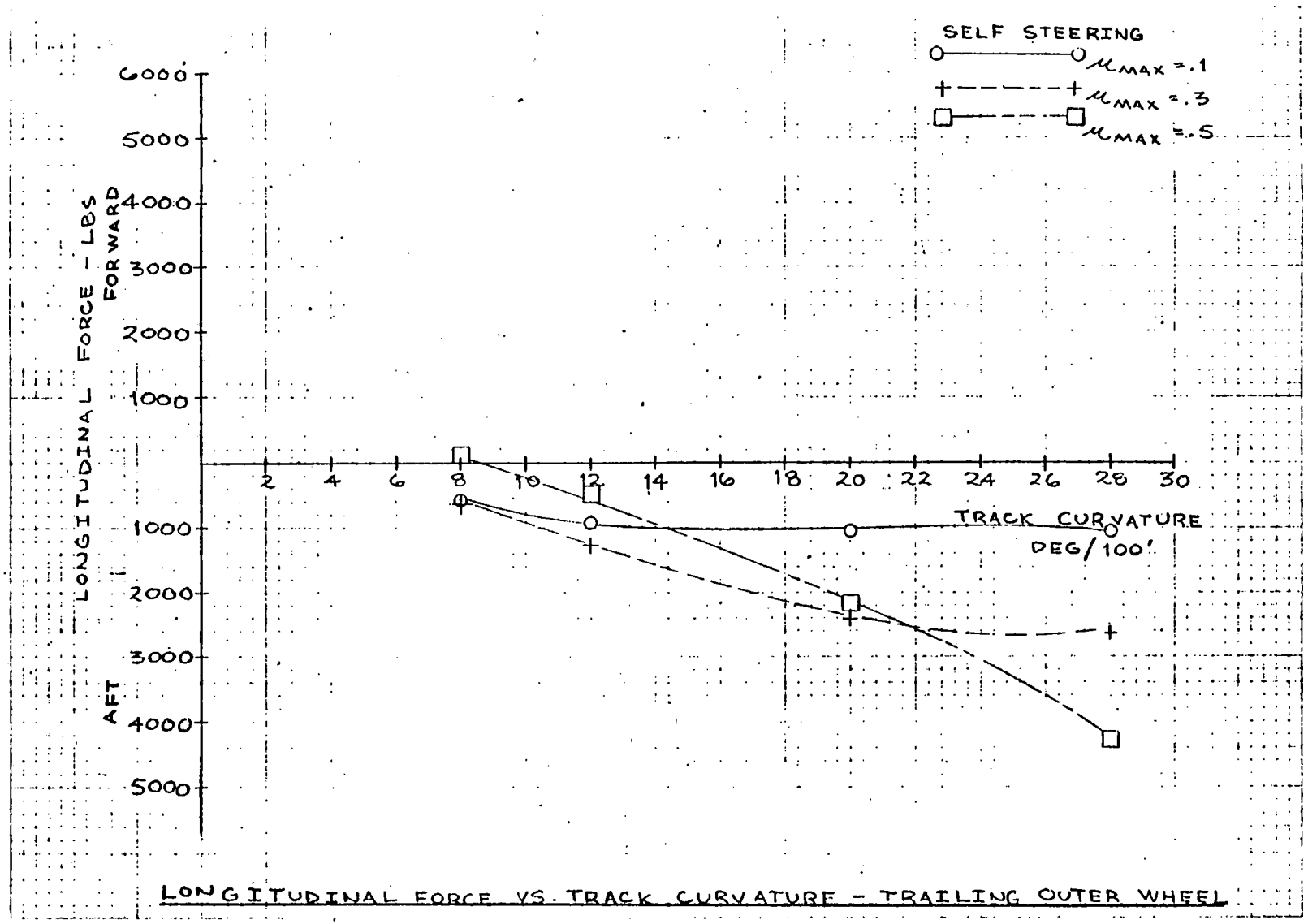
SELF STEERING
μ_{MAX} = .1
μ_{MAX} = .3
μ_{MAX} = .5
LONGITUDINAL FORCE - LBS
FORWARD
AFT
6000
5000
4000
3000
2000
1000
1000
2000
3000
4000
5000
2
4
6
8
10
12
14
16
18
20
22
24
26
28
30
TRACK CURVATURE
DEG/100'
LONGITUDINAL FORCE VS. TRACK CURVATURE - TRAILING OUTER WHEEL

FIGURE 4-2.28

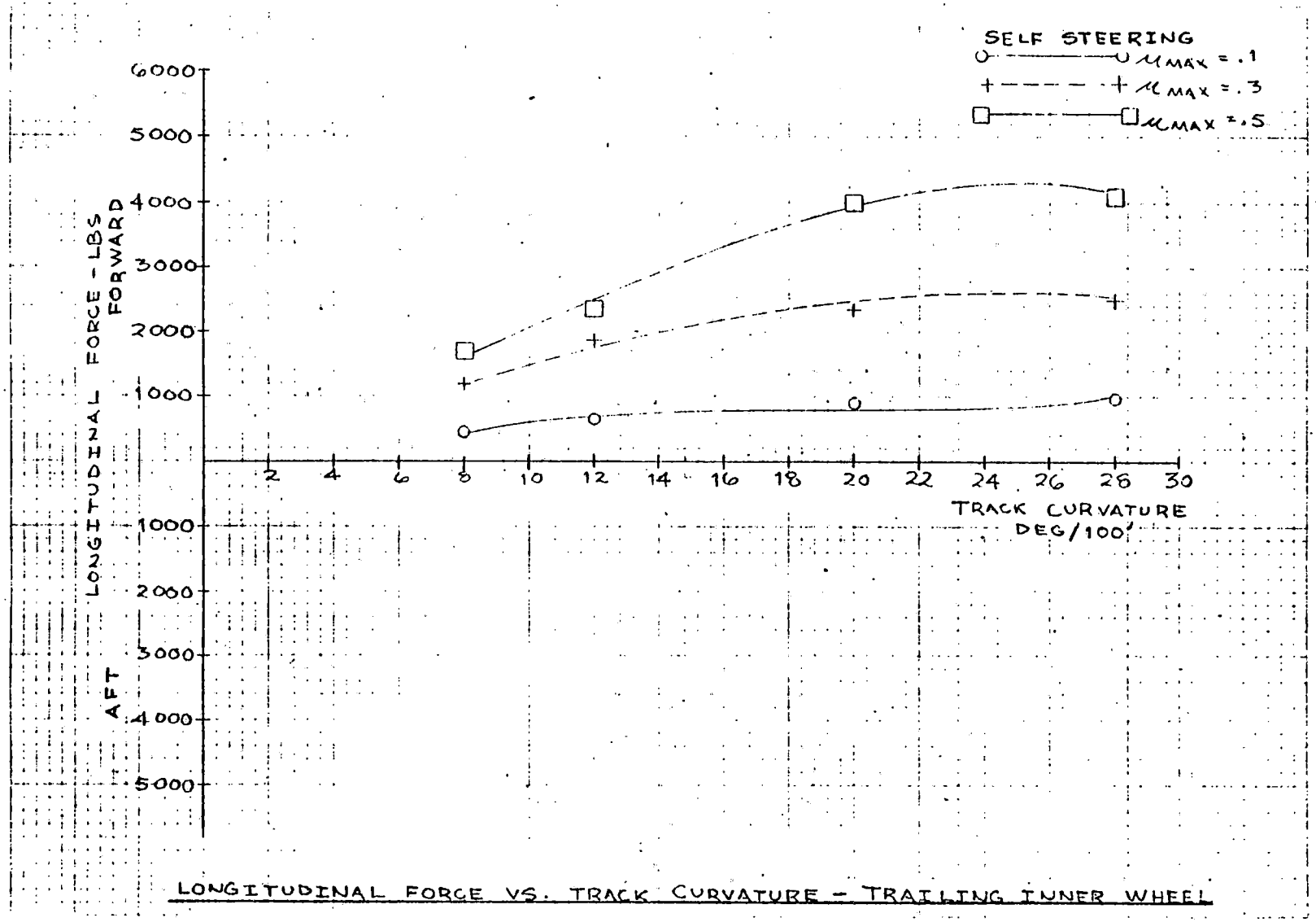

LONGITUDINAL FORCE VS. TRACK CURVATURE - TRAILING INNER WHEEL

FIGURE 4-2.29

4-2.5 Off-Flange Curving - General Case

A 15 degrees of freedom steady state linear curving program was used to compute the off-flange curving performance for three sets of conventional truck suspension values and six sets of self-steering suspension values as listed in Table 4-2.6. Design numbers 1 and 2 represent the existing PATCO truck with reduced primary longitudinal stiffness. Design number 3 represents the existing PATCO truck. The off-flange curving performance is given in terms of D_f, the maximum degree curve negotiable without flange contact.

Designs A through F are self-steering configurations with variations in primary longitudinal stiffness and the steering arm shear stiffness, K_s, at the steering arm interconnection. Self-steering designs A, B, and C show excellent off-flange performance with a 3000-lb/in primary longitudinal stiffness; however, this stiffness level is not compatible with the stability requirements. Designs D, E, and F have a longitudinal primary stiffness of 30,000 lb/in which is compatible with stability; however, the off-flange curving performance is reduced. This is further indication that self-steering needs a slider for curving performance or a very low primary longitudinal stiffness, both of which can cause stability problems. Positive-steering can provide performance without sacrificing stability.

The data is plotted in the plane of total shear stiffness in Figure 4-2.30, along with lines of constant off-flange curving performance index, D_f. For all design points except

TABLE 4-2.6: OFF-FLANGE CURVING PERFORMANCE

Design #	k_{px} (lb/ft)	k_{py} (lb/ft)	k_b (ft-lb/rad)	k_s (lb/ft)	D_f (^{o})
1	360,000	1.22E7	0	0	4.50
2	720,000	1.22E7	0	0	2.78
3	3,540,000	1.22E7	0	0	2.13
A	36,000	600,000	2,083	180,000	7.63
B	36,000	600,000	2,083	360,000	7.27
C	36,000	600,000	2,083	720,000	6.70
D	360,000	600,000	2,083	180,000	3.55
E	360,000	600,000	2,083	360,000	3.11
F	360,000	600,000	2,083	720,000	2.78

CONICITY, λ = 1/7

Yaw Breakaway Torque, T_s = 5730. ft-lb

Flange Clearance, y_{fc} = 0.029 ft = 0.35 in

Cant Deficiency, ϕ_d = 0. (balanced running)

Coefficient of friction, μ = 0.4

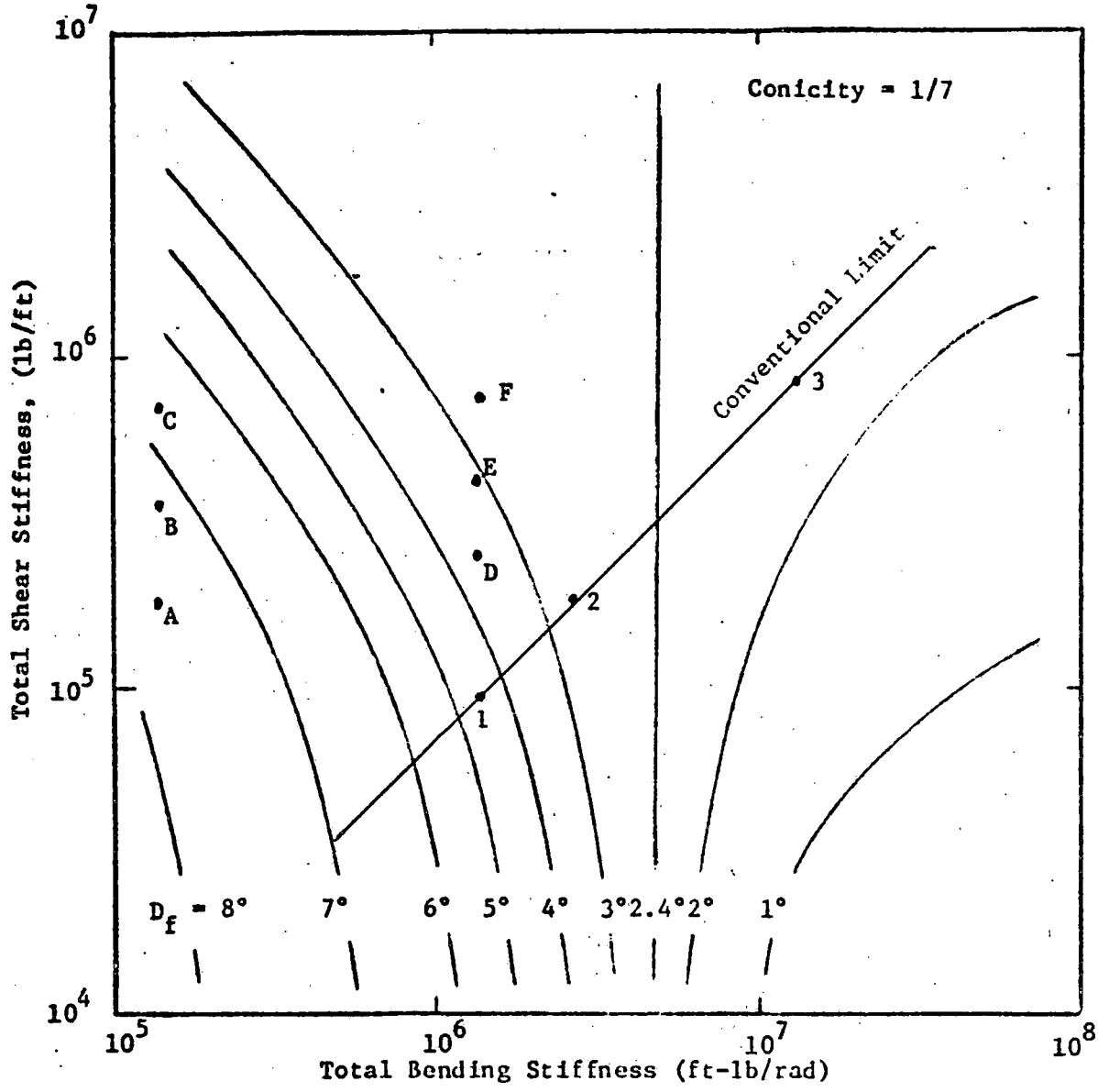

FIGURE 4-2.30: MAXIMUM DEGREE CURVE NEGOTIABLE WITHOUT FLANGE CONTACT, AS COMPUTED WITH THE 15 D.O.F. MODEL

number 3, an increase in total shear stiffness causes a decrease in off-flange performance. For all the design points, a decrease in total bending stiffness improves off-flange curving performance.

4-2.6 Off-Flange Curving Performance of Forced-Steering

The curving performance of the forced-steering configuration was presented in the general case studies using the moderately worn 1 in 20 profile. These studies were done using the Budd non-linear tracking model. This section will look at the effect of forced-steering on curving using linear models. The major difference in the models is related to the wheel profile. The non-linear model uses the moderately worn 1 in 20 profile which represents single-point contact geometry. The flange root area is worn so that two-point contact is no longer possible. The linear model looks at two-point contact. The tread profile has a constant taper as well as the flange angle. This study also looks at the effect of different conicities and creep coefficients.

Simple geometry of a truck on curved track yields an estimate of the value of steering gain, G, which will provide radial alignment of the wheelsets, allowing them to track the pure rolling line in steady state curving. The proposed forced-steering configuration has a steering gain G = 0.16 Equation 1 below gives the steering gain relationship with truck wheelbase and truck center spacing.

$$G_{p.r.\ell.} = \frac{b}{\ell_s} = 0.16 \qquad (1)$$

$$(\ell_1 = 6.2 \text{ in})$$

where:

b = half of truck wheelbase

ℓ_s = half of truck spacing

ℓ_1 = steering link offset

For the case of high inter-axle shear stiffness, k_s, the wheelsets will track the centerline of the track if a small amount of oversteer is provided:

$$G_{c.\ell.} = \frac{b}{\ell_s} \left(\ell_1 + \frac{a_2}{b^2} \right) = 0.22 \qquad (2)$$

where: a = track gauge (ℓ_1 = 8.1 in)

Equation 1 minimizes tread creepages while Equation 2 minimizes flange contact. Effects such as secondary breakaway torque and lack of primary breakaway may necessitate higher values of G in order to achieve the desired degree of steering, as discussed below.

Figure 4-2.31 shows the effect of forced-steering on the front and rear trucks assuming free primary breakaway, as computed by the 6 D.O.F. curving model. The degree curve which can be negotiated without flanging is plotted against steering gain, G. The peak region in the center of each plot results from the wheelsets tracking the centerline of the track. Slight differences between the trucks result from the opposite secondary yaw torque directions on the two trucks and the fact that k_s is not infinite.

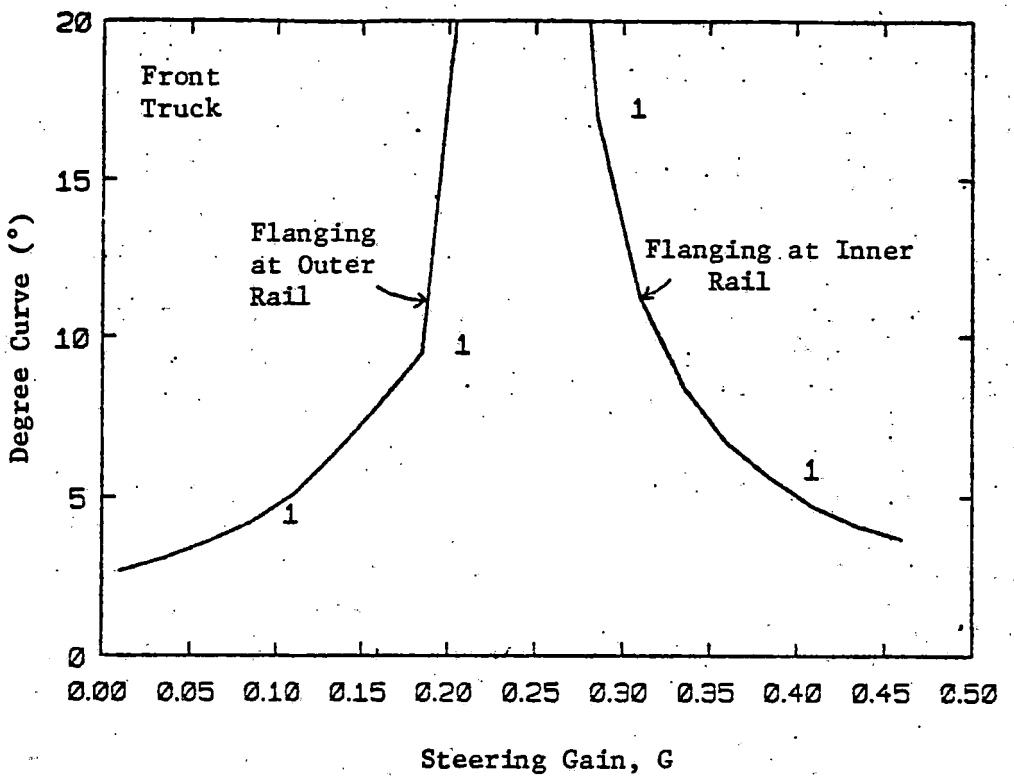

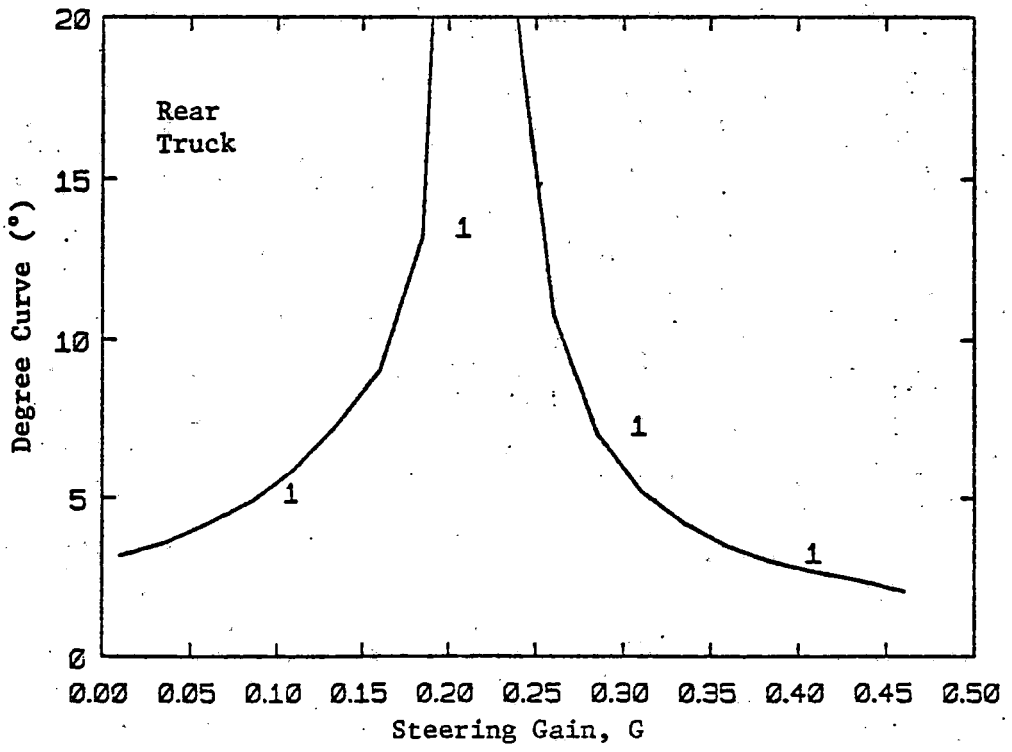

FIGURE 4-2.31: CURVING PERFORMANCE FOR FREE PRIMARY BREAKAWAY

A reduction of k_s would degrade this performance. The left axis of each plot represents a self-steering truck with no forced-steering action. Figure 4-2.31 is largely independent of creep coefficients and k_b (i.e., k_{fs}).

Figure 4-2.32 shows the detrimental effect on the curving performance of the front and rear trucks if primary breakaway does not occur. However, a significant advantage over the self-steering truck is still observed. As a byproduct of the forced-steering effect, the steering link applies an overall truck moment which tends to hurt the front truck and help the rear truck. For smaller link stiffnesses (i.e., k_b), more steering gain is required to achieve peak performance.

Figures 4-2.33 a and b show the effects of primary breakaway force on curving performance. Even a 2000 lb slider force is enough to significantly change the steering gain required for off-flange curving compared with the case of free breakaway.

Figure 4-2.34 shows the influence of conicity on curving performance for the case of free primary breakaway. While the value of G required for off-flange curving does not vary with conicity, the off-flange curving window narrows with decreasing conicity, thus increasing the likelihood of flange contact.

Figure 4-2.35 shows the effect of halving the creep coefficients for the case of no primary breakaway. Compared with Figure 4-2.34, still higher steering gains are required to achieve the same performance.

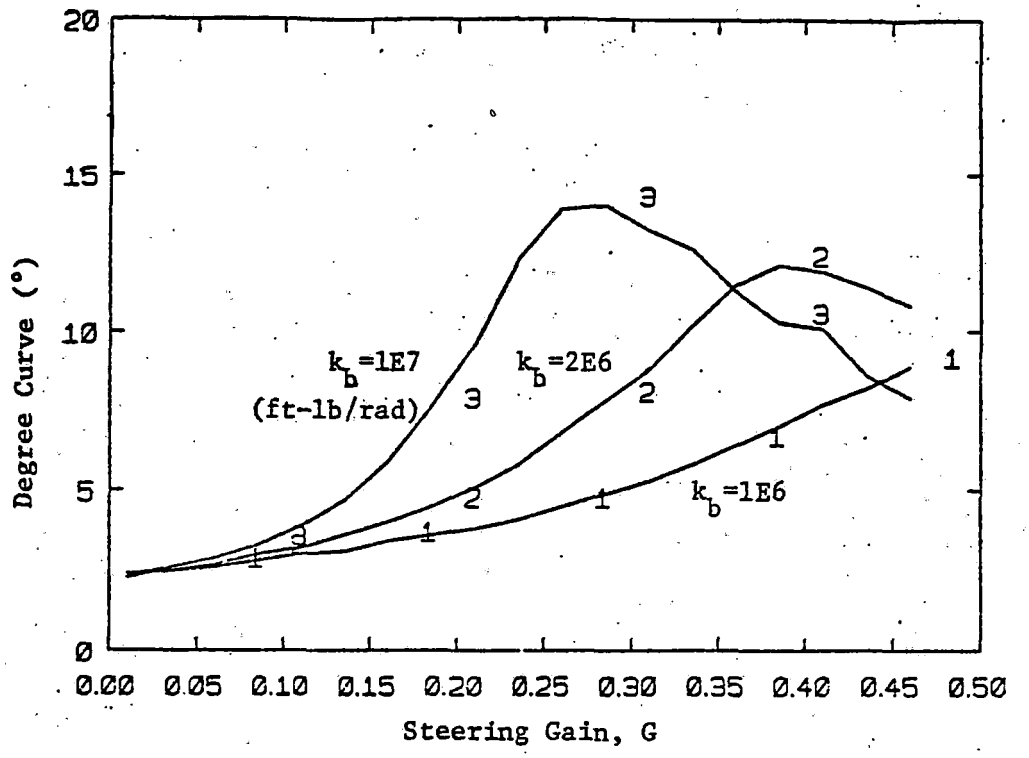

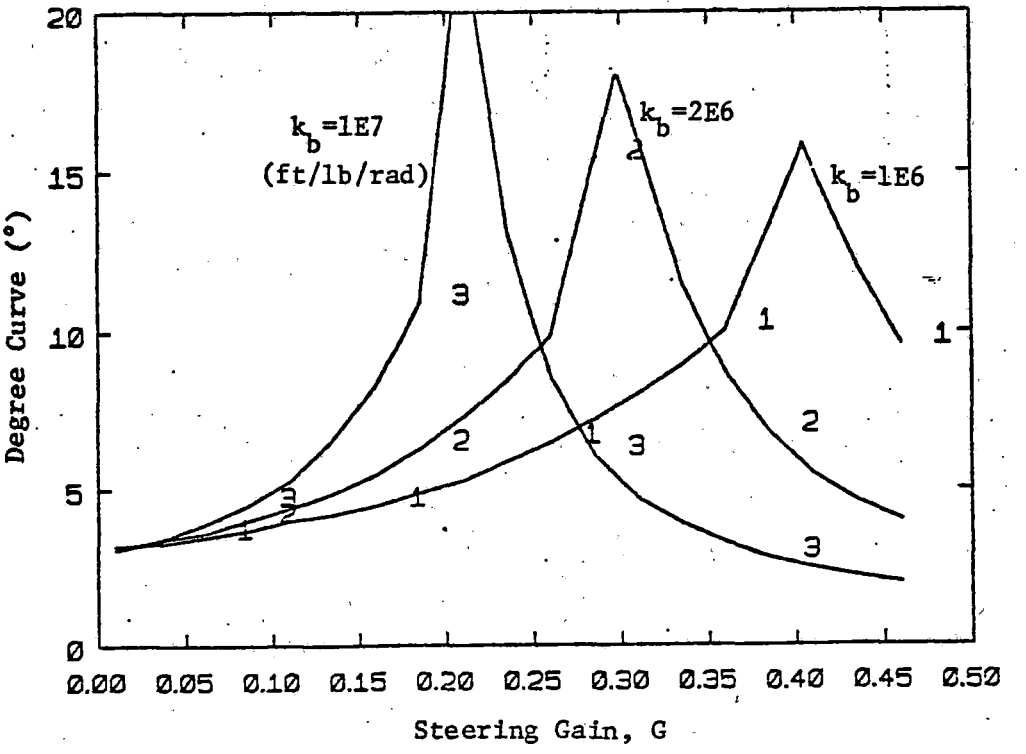

FIGURE 4-2.32: CURVING PERFORMANCE FOR NO PRIMARY BREAKAWAY

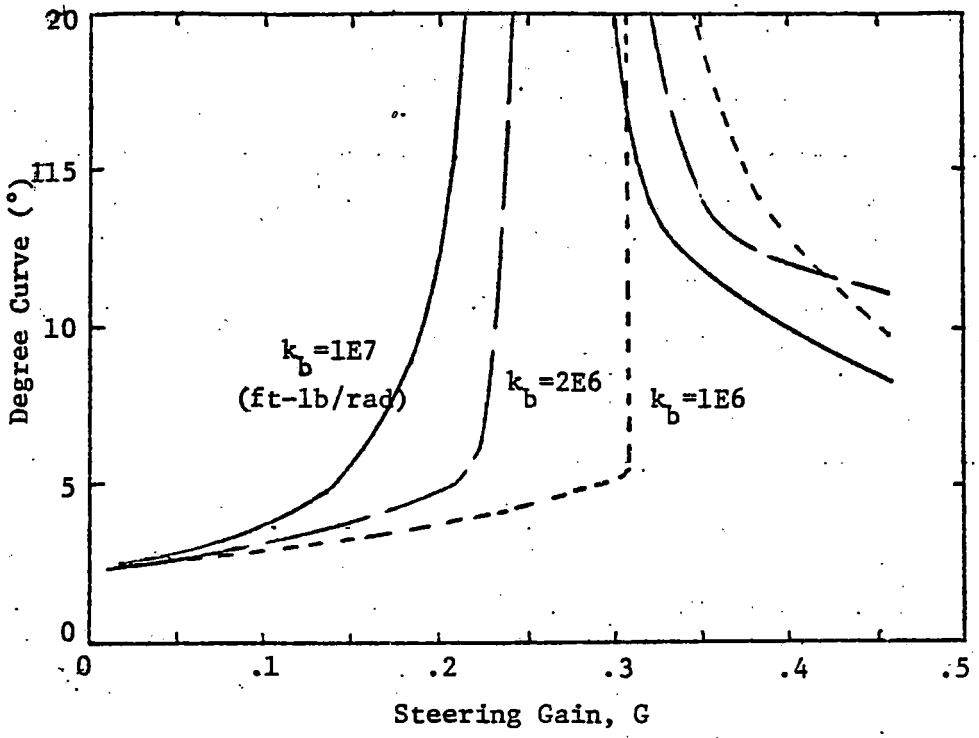

a) Primary Breakaway Force = 2000 lb.

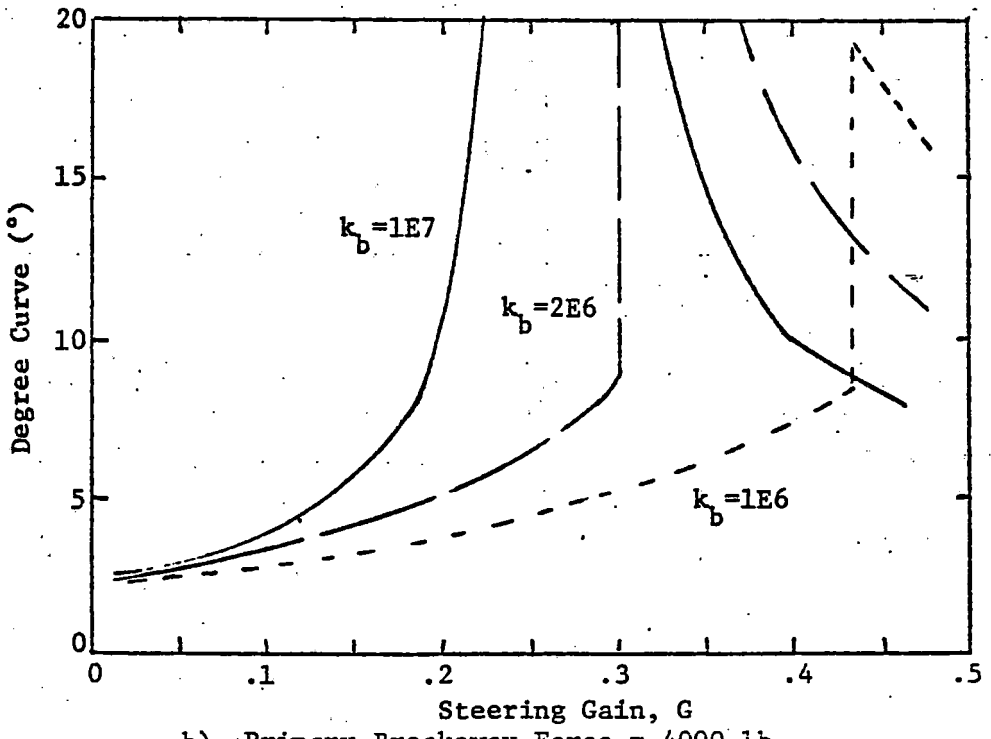

b) Primary Breakaway Force = 4000 lb

FIGURE 4-2.33: CURVING PERFORMANCE OF FRONT TRUCK AS INFLUENCED BY PRIMARY BREAKAWAY

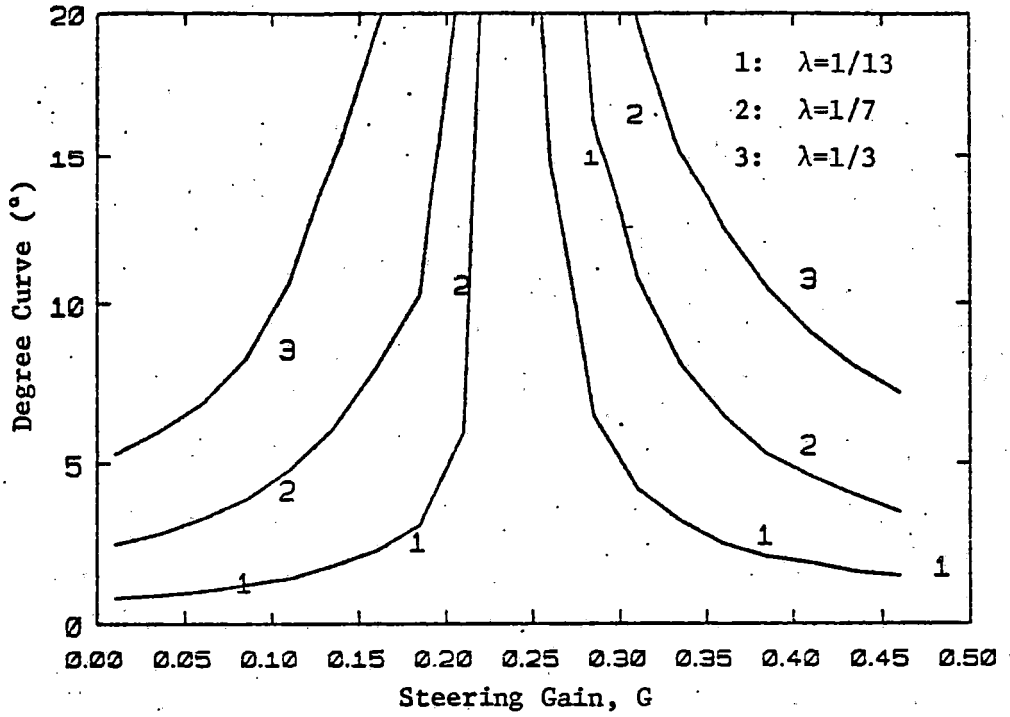

FIGURE 4-2.34: CURVING PERFORMANCE OF FRONT TRUCK WITH FREE PRIMARY BREAKAWAY FOR DIFFERENT CONICITIES

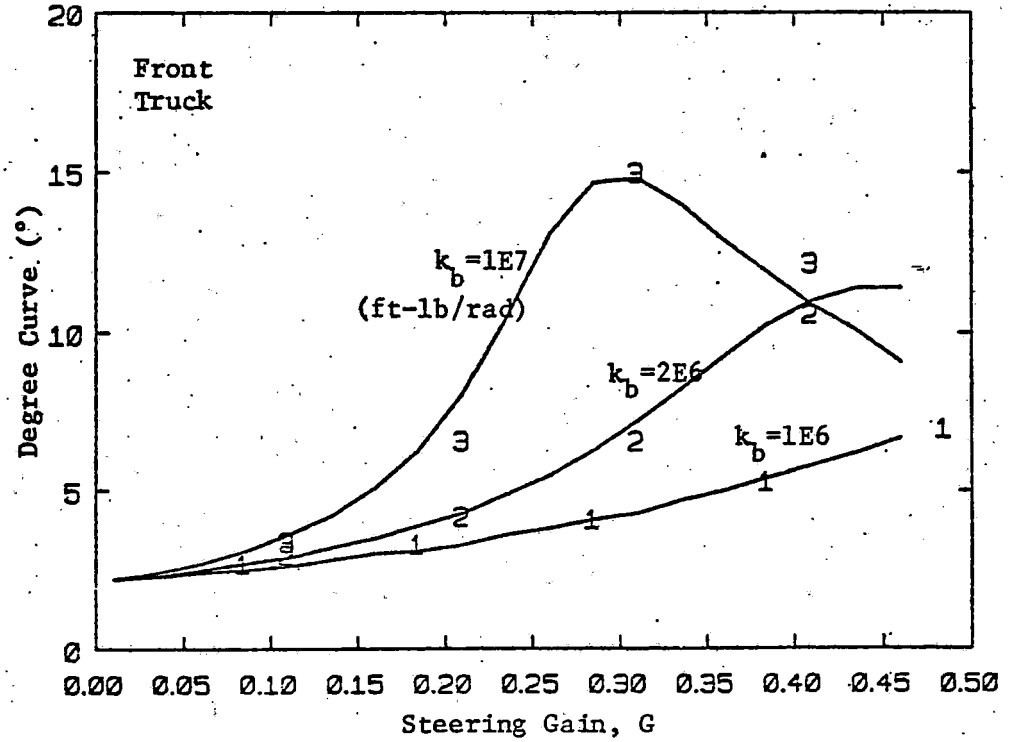

FIGURE 4-2.35: CURVING PERFORMANCE AT 1/2 NOMINAL CREEP COEFFICIENTS FOR NO PRIMARY BREAKAWAY

Finally, the forced-steering truck is better able to support cant deficiency loads than a self-steering truck with k_b. The effect of cant deficiency on the front and rear trucks is shown in Figure 4-2.36. Only a moderate decrease in performance occurs at $\gamma_d = 0.12$, which is more than twice the FRA limit.

4-2.7 Curving Performance Summary

Figure 4-2.37 summarizes the curving performance studies for both truck types. The angle of attack for the conventional truck crosses the screech boundary at about 8 degrees of track curvature, whereas the angle of attack for the steering truck is essentially zero at all curvatures. The lateral force for the conventional truck is consistently higher than the steering truck, but must be substantial in both cases to satisfy the requirement for summation of yaw moment to equal zero for the truck. Keep in mind that this lateral force is the summation of both the lateral wheel tread force and the flange force as predicted by the non-linear tracking model. These results were obtained by running the model at a cant deficiency angle of about 0.05 radians (approximately 3 inches). This level is considered worst case for PATCO. Separate studies by others have suggested that there is an "Index" of wheel and rail wear depending on the product of these two variables (angle of attack x lateral force). Because the angle of attack is nearly zero, wheel and rail wear will be very low for the steering

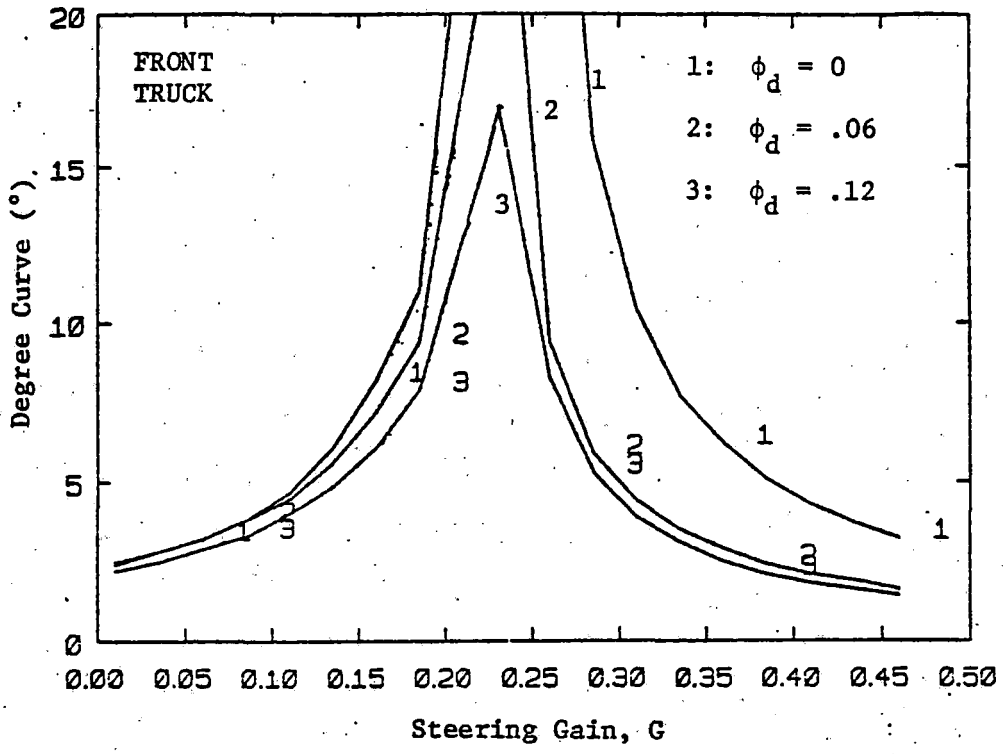

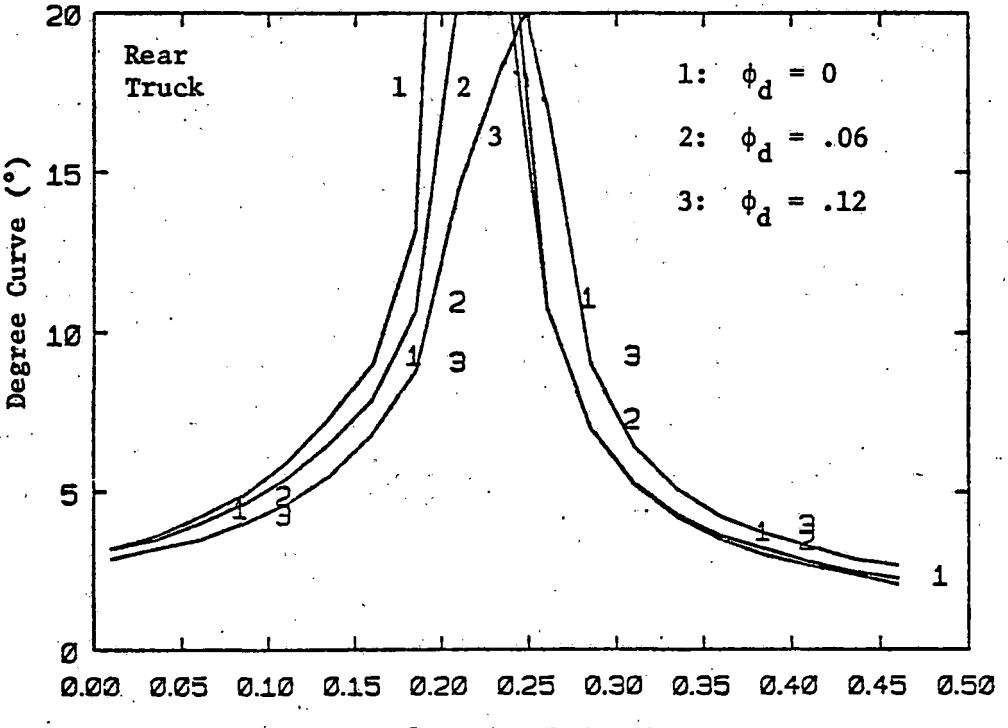

FIGURE 4-2.36: EFFECT OF CANT DEFICIENCY ON CURVING PERFORMANCE

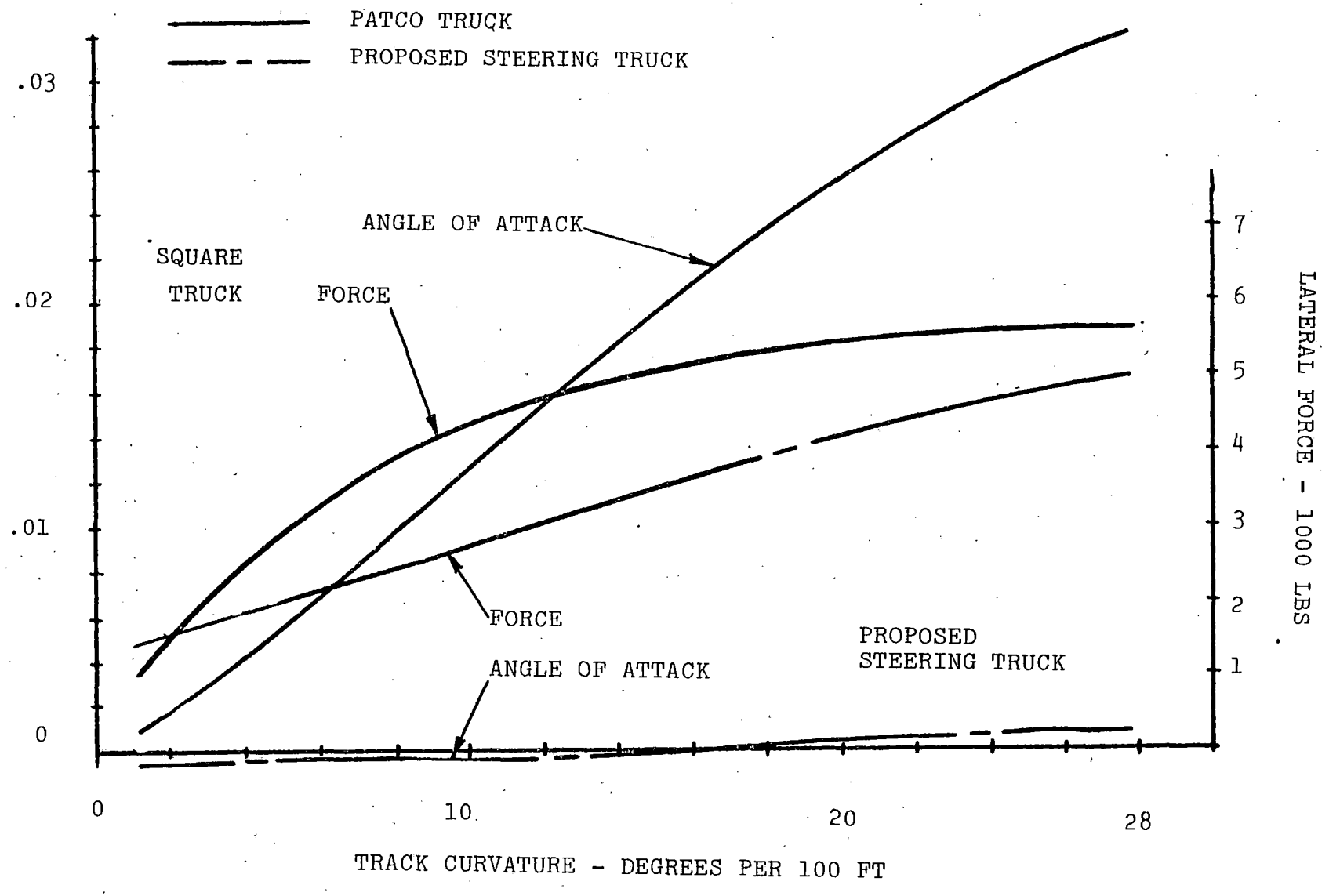

FIGURE 4-2.37: Angle of Attack and Lateral Force vs. Curvature (coefficient of Friction = 0.3)

truck even though the force is not zero. The wear index for the conventional truck is much greater than for other configurations because the angle of attack is greater. Plots of wear indices for the two truck configurations are shown in Figure 4-2.38.

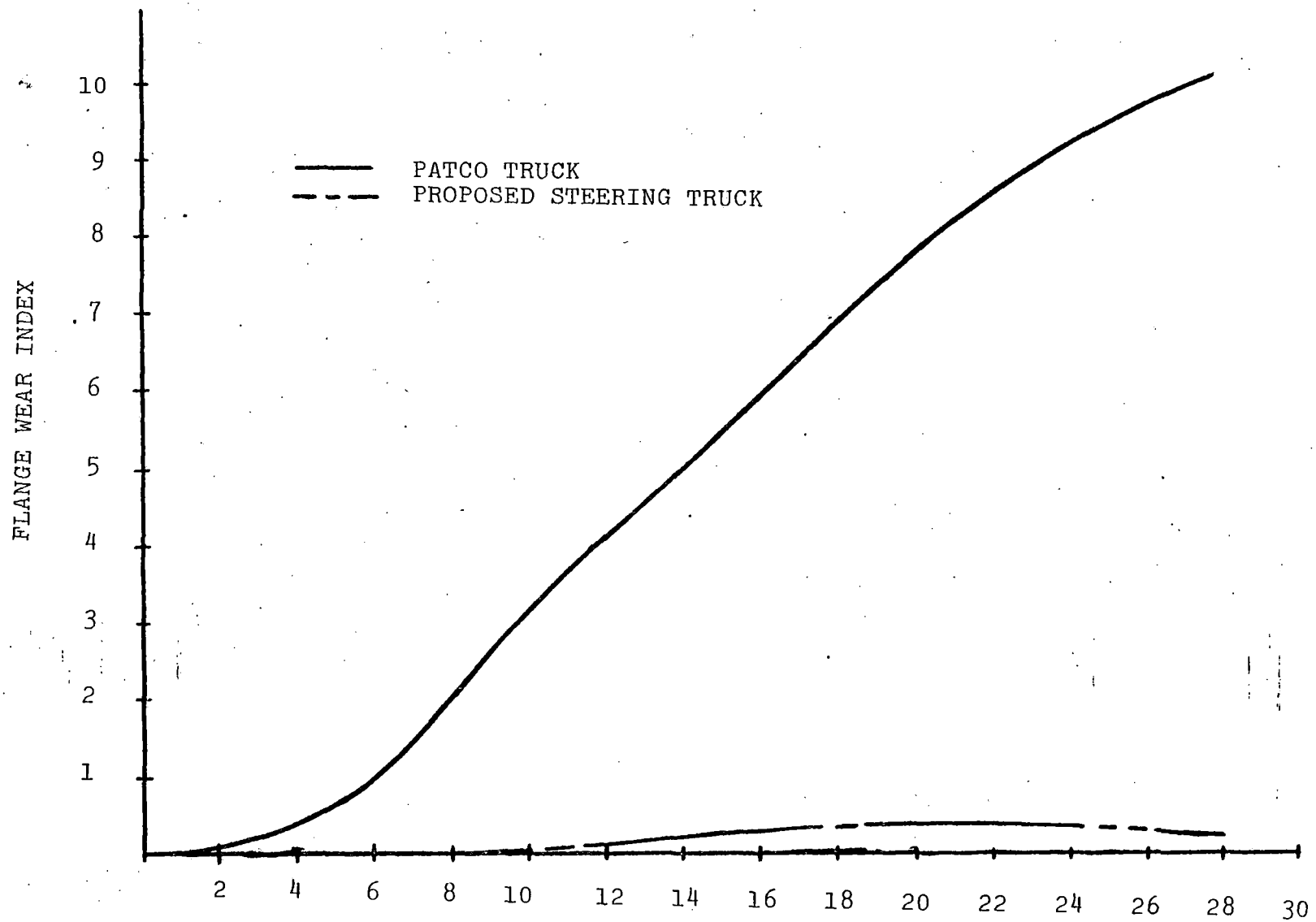

FIGURE 4-2.38:
FLANGE WEAR INDEX VS. TRACK CURVATURE

4.3 Stability

4-3.1 Introduction and Background

Rail vehicle lateral stability is usually associated with the well-known "hunting" phenomena. Hunting can be associated with either the truck or carbody. Carbody hunting involves large lateral, yaw, and roll motions of the carbody with very little truck motion. Carbody hunting usually occurs in a limited speed range with both lower and upper bounds. Carbody roll motions can be centered about a point above the carbody center of gravity (upper roll center) or about a point below the track (lower roll center). Truck hunting is significantly different from carbody hunting. In truck hunting, the wheelsets and truck frame can couple to produce sustained oscillations in the lateral and yaw directions with very little carbody motion resulting. The truck hunting phenomenon is inherent in the conventional wheelset which uses a tapered tread to provide lateral guidance or centering action. As the vehicle's speed is increased, a critical value can be reached at which the wheelset modes are undamped and sustained oscillation occurs. Increasing the vehicle's speed further results in a negative damping factor which then drives the system unstable.

The speed at which the system has zero damping is

defined as the critical speed and is used as a reference for vehicle instability. The damping ratio of the least damped mode of vibration at the vehicle's operating speed is used as a performance measure to assure a stable mode of operation. The stability criterion that has been adopted for this study can be stated as follows: The critical hunting speed characteristic of the proposed steerable truck design shall provide a minimum damping factor of 10% for the least damped mode while operating at 80 mph. This performance shall be obtainable under all varying conditions of components and wheels from new to full-worn and under crush load to empty car conditions. This criterion will assure minimum overshoot or oscillation in response to typical track irregularities.

4-3.2 Computational Models

Several different computer models were used to investigate the stability characteristics of the conventional truck and the proposed steerable truck design. The major portion of the stability analyses was done by Budd's consultants at the Massachusetts Institute of Technology using a 15 degrees of freedom linear model. The linear solutions were cross-checked with the Budd non-linear tracking model.

A schematic of the lateral stability model is shown in Figure 4-3.1. A complete derivation of this model is given in Appendix B of Reference 1. The 15 degrees of freedom include wheelset and truck frame lateral and yaw degrees, plus carbody lateral, yaw, and roll degrees. The wheelsets, trucks, and carbody are assumed to be rigid with no consideration of internal flexibility. There are four wheelsets, two trucks, and one carbody. The vehicle is made symmetric about the vertical plane.

The primary and secondary truck suspension systems are represented by lumped linear springs and dampers. The primary and secondary suspension systems can have different locations within the truck. However, the suspension values and locations represent the net effect of many elements which can individually contribute to the suspension system; e.g., the secondary lateral stiffness represents the total lateral stiffness in the secondary and combines the effects of airsprings, anchor rods, and rubber bushings.

The wheel/rail interface includes lateral, longitudinal, and spin components of creep. The gravitational forces and moments and the gyroscopic forces at the wheels

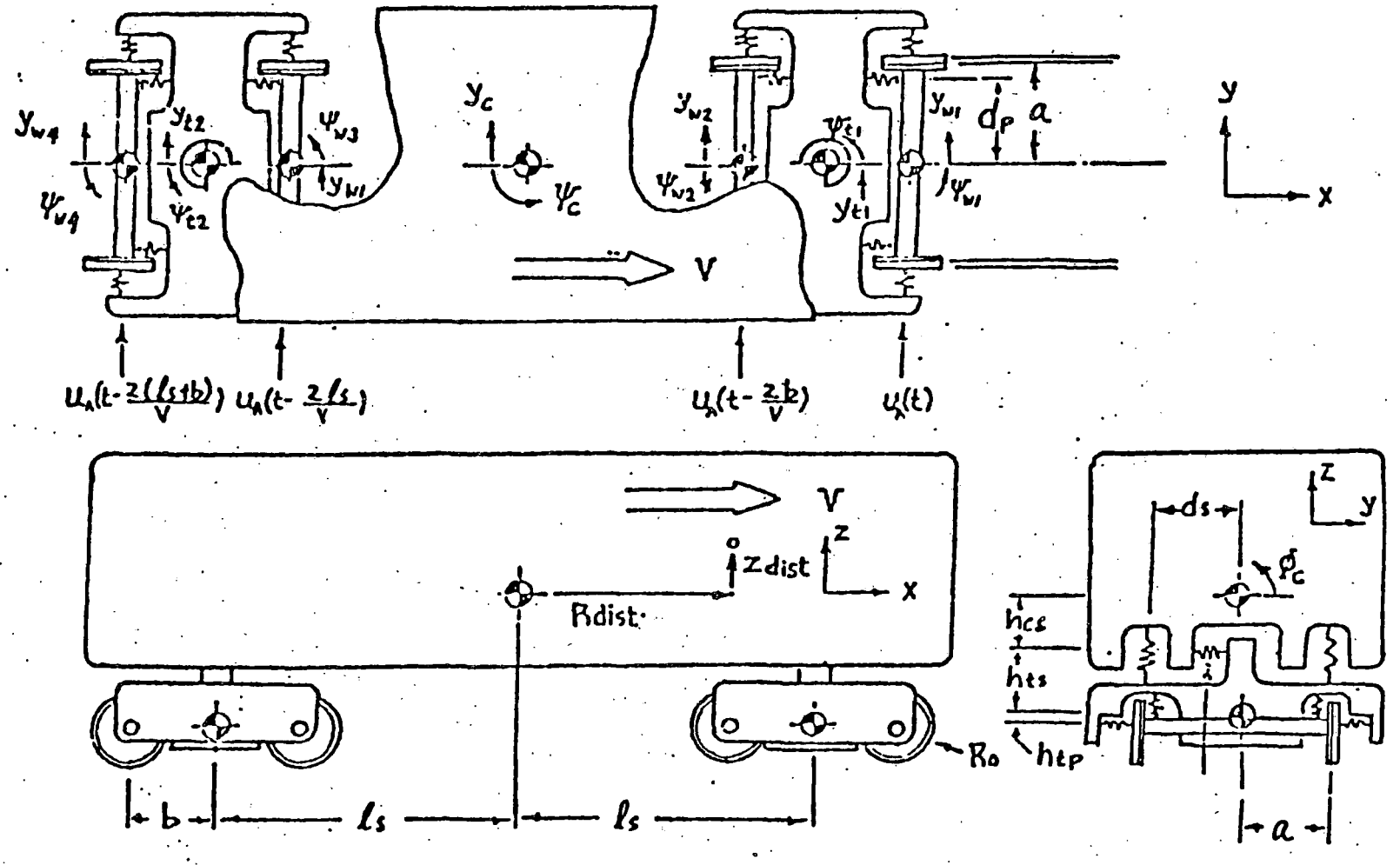

FIGURE 4-3.1: LATERAL RAILCAR MODEL

are considered as well. The wheel/rail geometry is represented as an effective tread taper; 1 in 20 for new wheel representation and 1 in 7 for worn wheel representation

The linear equations of motion for the lateral model can be summarized in matrix form as:

$$M\ddot{y} + C\dot{y} + Ky = 0$$

where

y is a 15 x 1 position vector

M, C, and K are the 15 x 15 inertia, damping, and stiffness matrices.

This model was also extended to include the steerable truck configuration by providing bending (K_b) and shear (K_s) stiffnesses between the wheelsets.

4-3.3 Stability Performance of Existing Truck

The existing truck is described in Section 2.2. The suspension parameters given in Table 2-2.2 and the weights and inertias given in Table 2-2.3 were used for the stability analysis. The primary suspension stiffness values for the longitudinal and lateral are K_{px} = 3.54×10^6 lb/ft and K_{py} = 1.2×10^6 lb/ft respectively. All stability runs were made with a worn wheel using a 1 in 7 wheel conicity. The stability study of the existing P-III truck is summarized in Figure 4-3.2. This curve shows

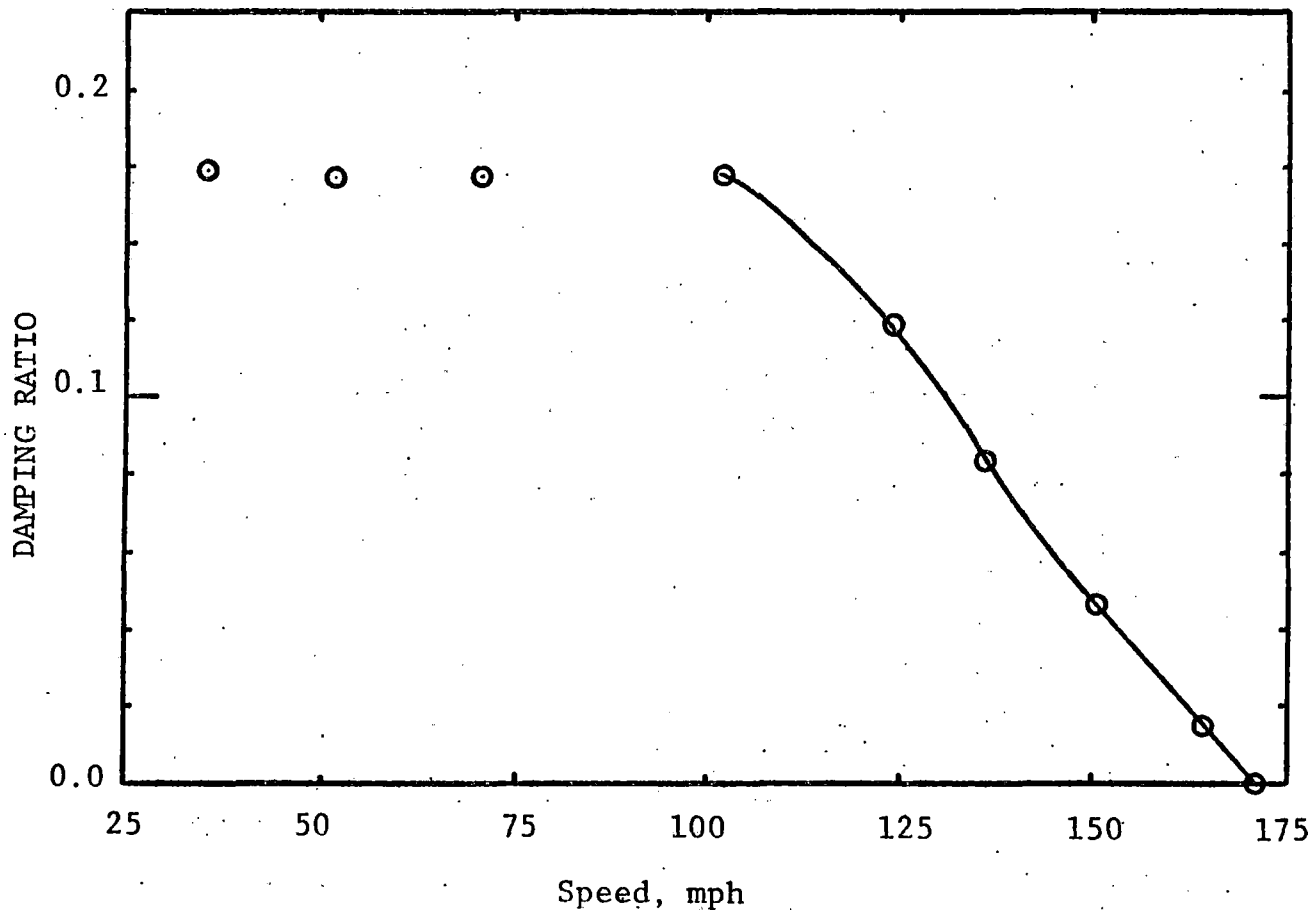

Figure 4-3.2 :Damping Ratio of the Least Damped Mode versus Speed - Conventional Truck

that the critical speed is about 170 mph and the 10% modal damping speed is about 135 mph. These theoretical speed predictions represent a very conservative stability margin with respect to the maximum operating speed of the PATCO system which is 75 mph. These predictions are quite consistent with the field observation that hunting is not a problem with the existing truck.

The stability study of the existing truck was extended to include critical speed as a function of inter-axle lateral stiffness, K_s (shear stiffness) and inter-axle yaw stiffness, K_b (bending stiffness). Figure 4-3.3 is a schematic drawing that describes the inter-axle shear and bending stiffness terms for a conventional (square) truck. Figure 4-3.4 shows the contours of constant critical speed in the inter-axle shear and bending plane (K_s - K_b plane). The existing conventional truck falls on the 170-mph speed contour. Shown also in Figure 4-3.4 is a modified truck, with a reduced longitudinal primary suspension, which falls on the 105-mph speed contour. This truck is similar in every way to the existing P-III truck except that the longitudinal primary stiffness was reduced to 3.6×10^5 lb/ft. This stiffness value was selected as the lowest practical value that could be

CONVENTIONAL TRUCK

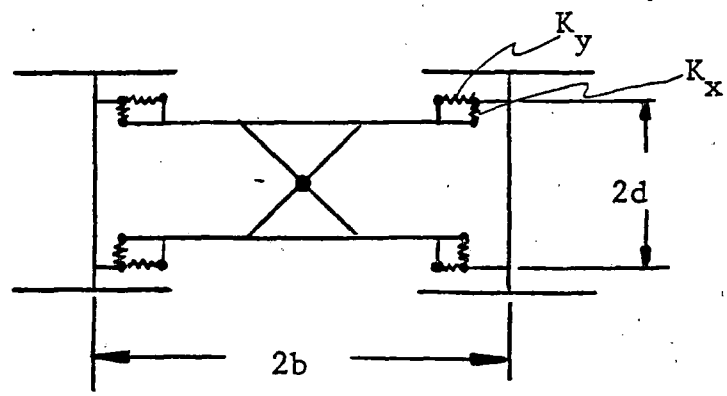

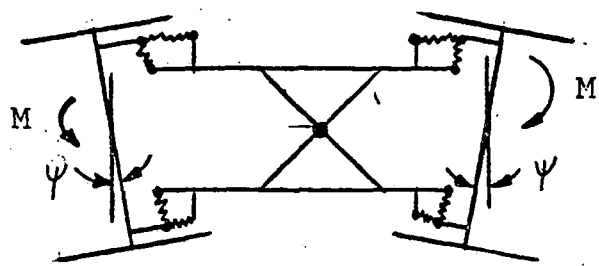

K_b = Bending Stiffness = $\frac{M}{\psi}$

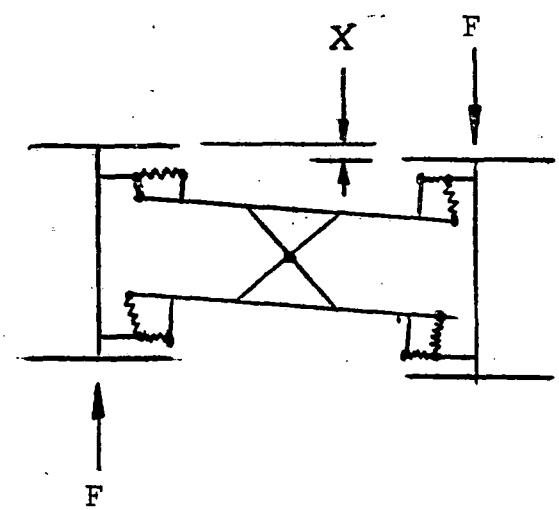

K_s = Shear Stiffness = $\frac{F}{X}$

$$K_b = d^2 K_y$$

$$K_s = \frac{K_x K_y d^2}{K_x b^2 + K_y d^2}$$

FIGURE 4-3.3: Inter-Axle Shear and Bending Stiffness Terms for a Conventional Truck

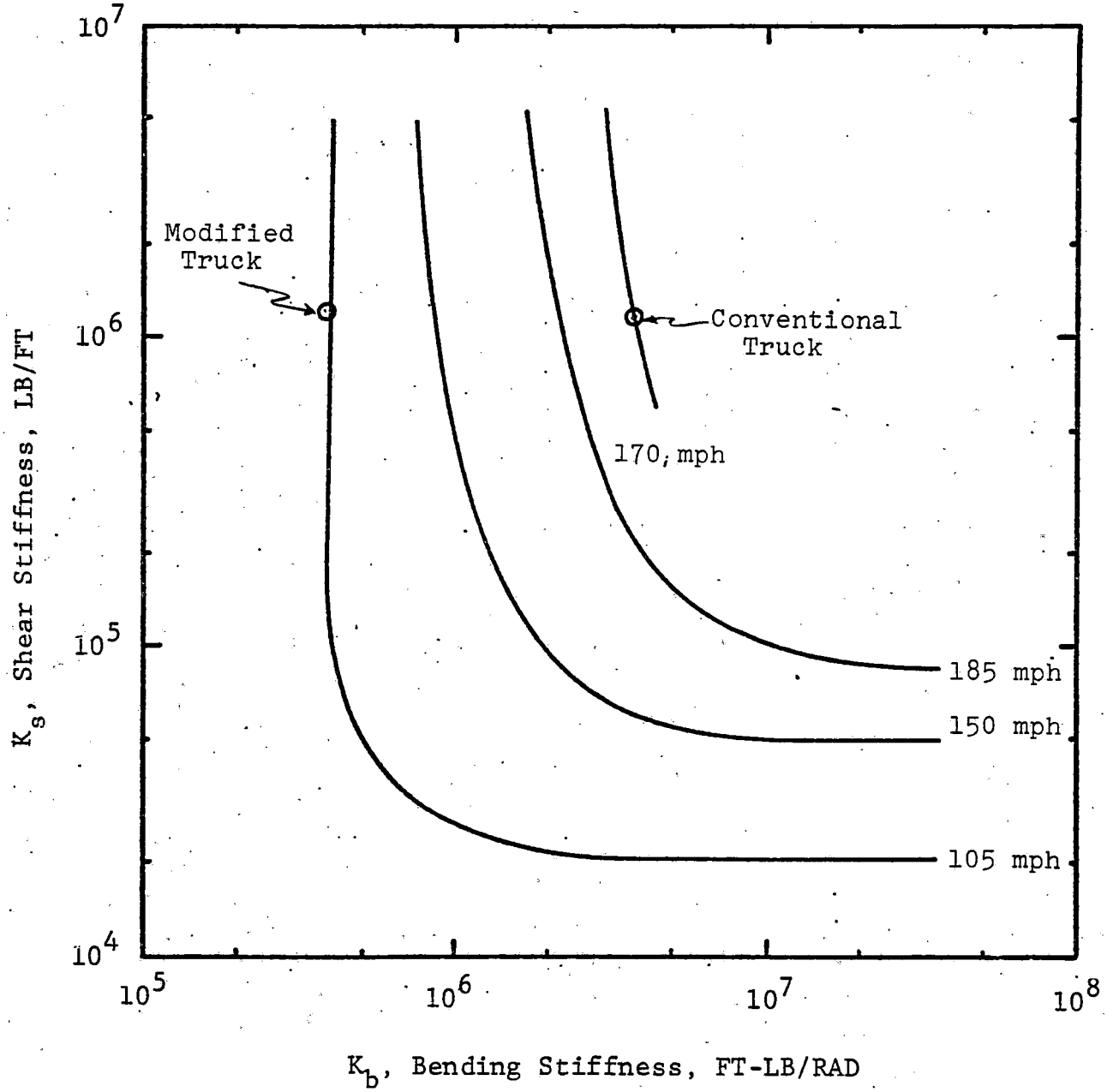

Figure 4-3.4; Contours of Constant Critical Speed for the Conventional Truck

packaged in the existing truck frame. This design configuration was primarily explored from a curving performance point of view and was discussed briefly in the curving performance section.

4-3.4 Stability Performance of Self-Steering Truck

The design configuration of the proposed steerable truck (self-steering mode) is given in Section 2.3. The suspension parameters are given in Table 2-3.1 and the weights and inertias are given in Table 2-3.2 Figure 4-3.5 shows the effect that the longitudinal primary stiffness has on critical speed assuming that the 2000-lb frictional slider does not breakaway. This figure also shows that a longitudinal stiffness of 3.6×10^5 lb/ft (30,000 lb/in) satisfies the stability requirement by providing 10% damping of the least damped mode while operating at 80 mph with worn wheels (1 in 7 tread taper). Figure 4-3.6 shows the damping ratio of the least damped mode as a function of speed for the proposed steerable truck with a primary longitudinal stiffness of 3.6×10^5 lb/ft. The critical speed of the proposed steerable truck design is about 123 mph in the self-steering mode if breakaway does not occur.

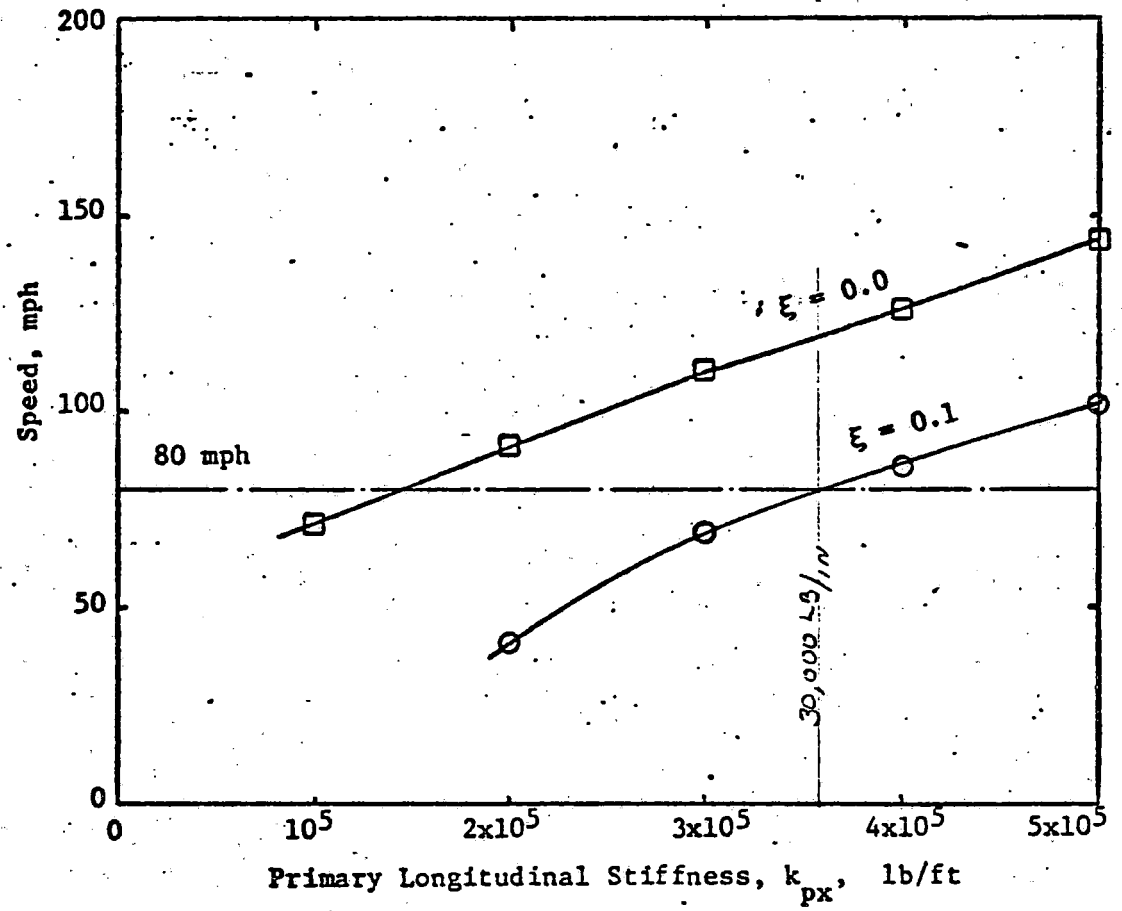

Figure 4-3.5: EFFECT OF k_{px} ON THE CRITICAL SPEED

where ξ = damping ratio:

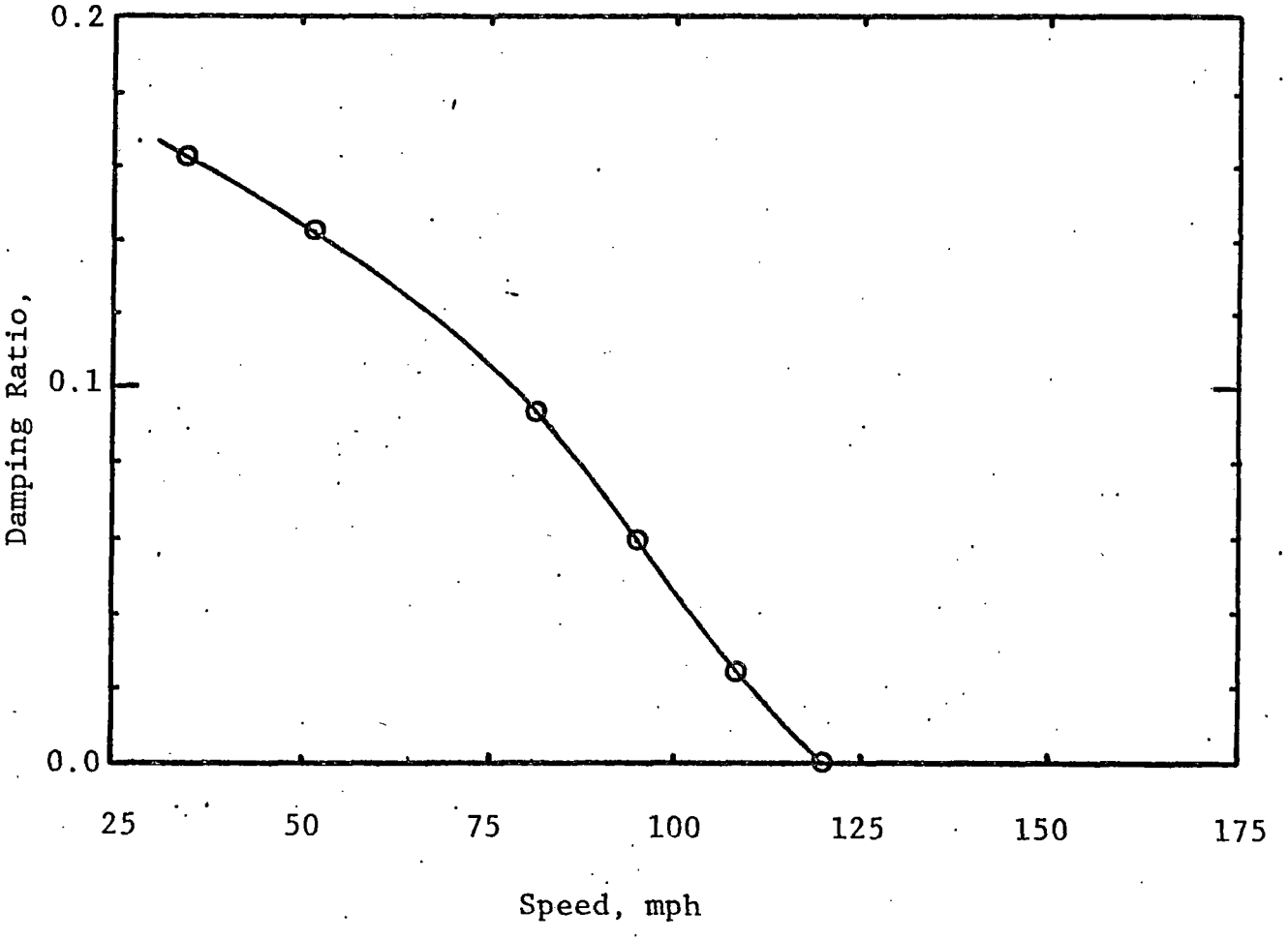

Figure 4-3.6: Damping Ratio of the Least Damped Mode versus Speed - Steerable Truck

The stability studies of the proposed steerable truck were extended to include critical speed as a function of inter-axle shear stiffness and inter-axle bending stiffness. Figure 4-3.7 describes the shear and bending stiffness terms for a steering arm truck that is self-steering. These terms are similar to those for the conventional truck except for the contribution of the steering arm interconnection. The bending stiffness is primarily a function of the longitudinal primary stiffness for both the conventional and steerable truck. However, the shear stiffness of the steerable truck is primarily a function of the lateral stiffness of the steering arms and the interconnection. The shear stiffness for a positive-steering truck would be higher because of the additional stiffness term due to the steering link.

Figure 4-3.8 shows contours of constant critical speed as a function of inter-axle shear and bending stiffness. All parameters were kept constant except the shear and bending stiffness (K_{rs} and K_{rb}) of the steering arm interconnection itself. For this study, it was assumed that the frictional slider does not breakaway.

Figure 4-3.9 shows critical speed as a function of the damping ratio for three different inter-axle shear

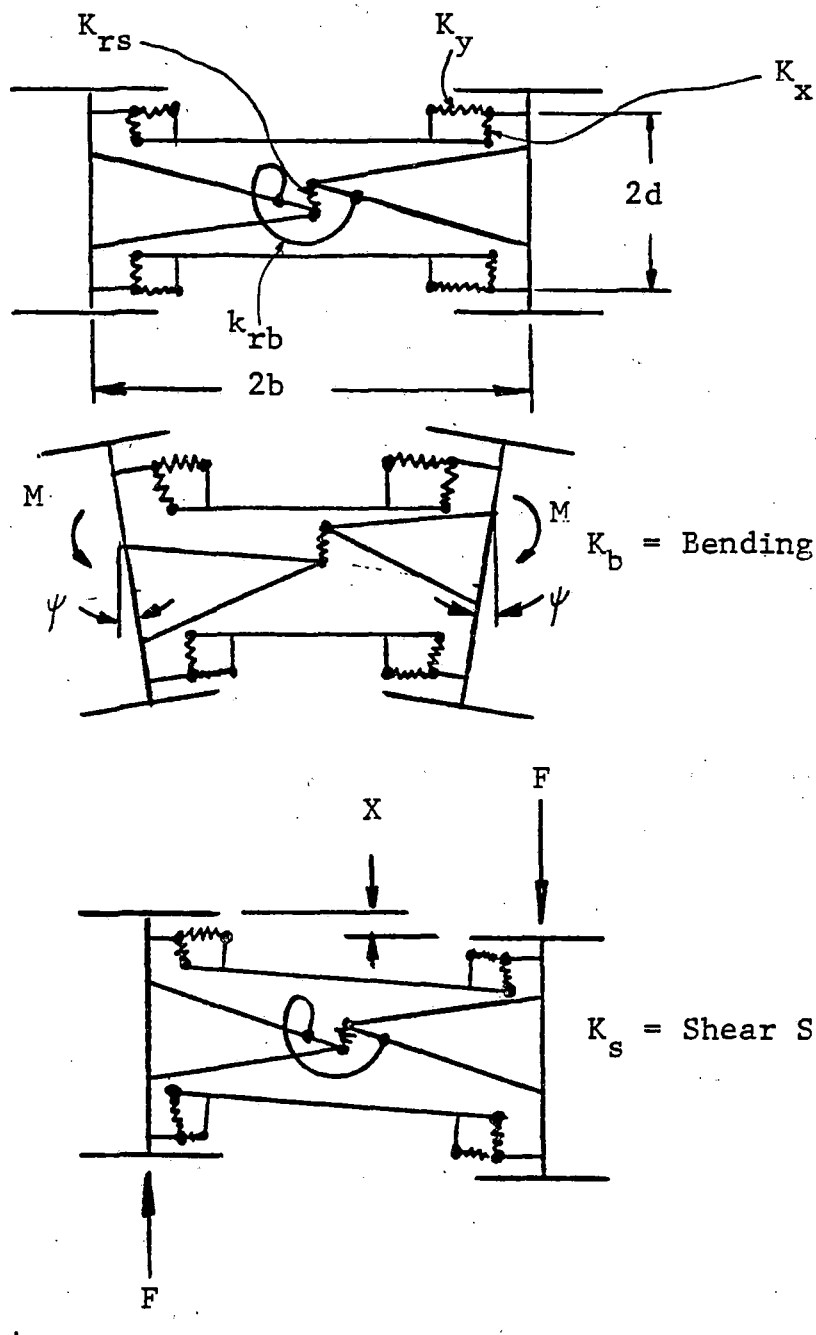

$$K_b = d^2 K_y^* + K_{rb}$$

$$K_s = \frac{K_x K_y}{K_x b^2 + K_y d^2} + K_{rs}^*$$

* dominant term

FIGURE 4-3.7: Inter-axle Shear and Bending Terms - Steerable Truck (Self-steering)

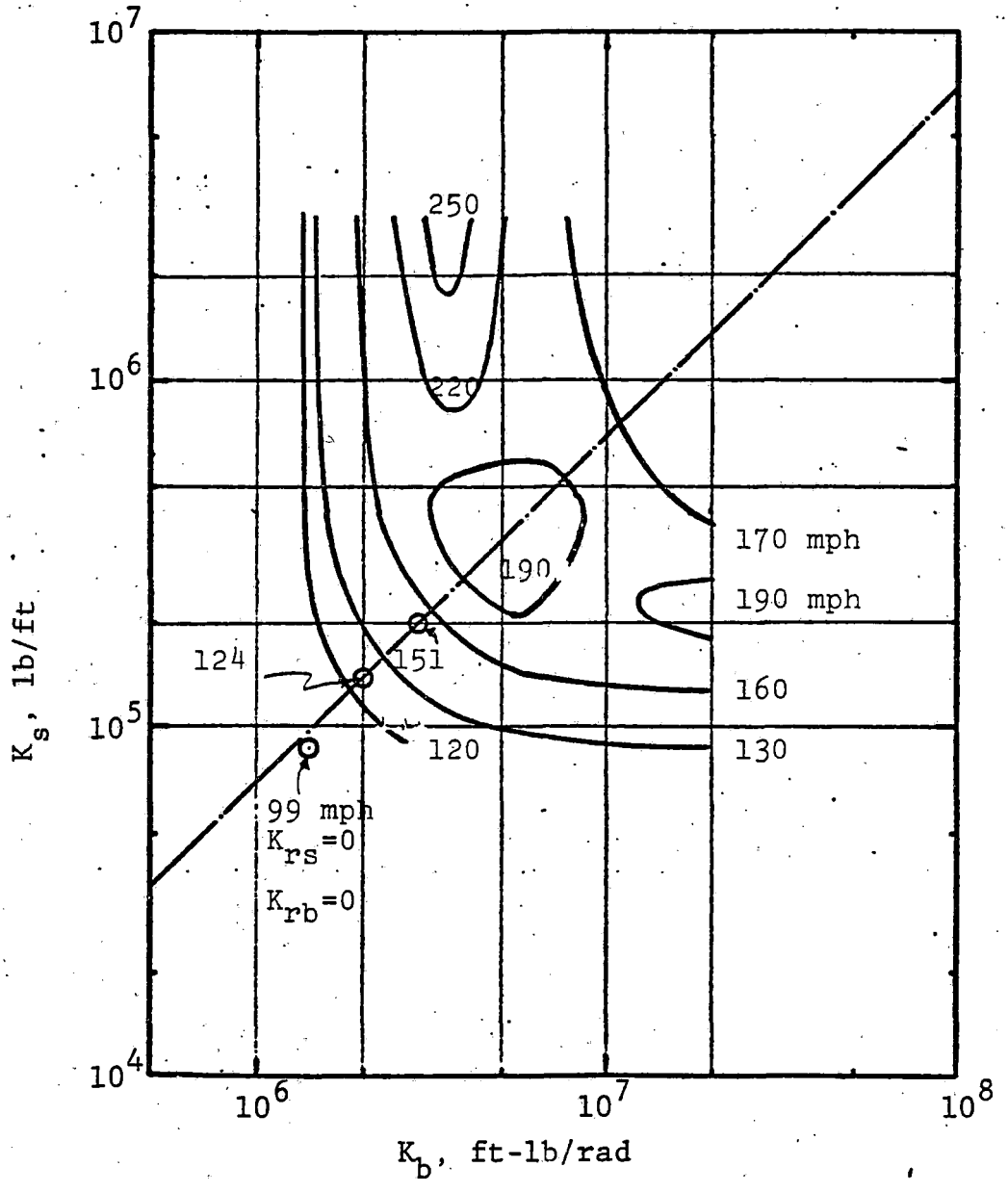

FIGURE 4-3.8: Contours of Constant Critical Speed (mph) - Steerable Truck

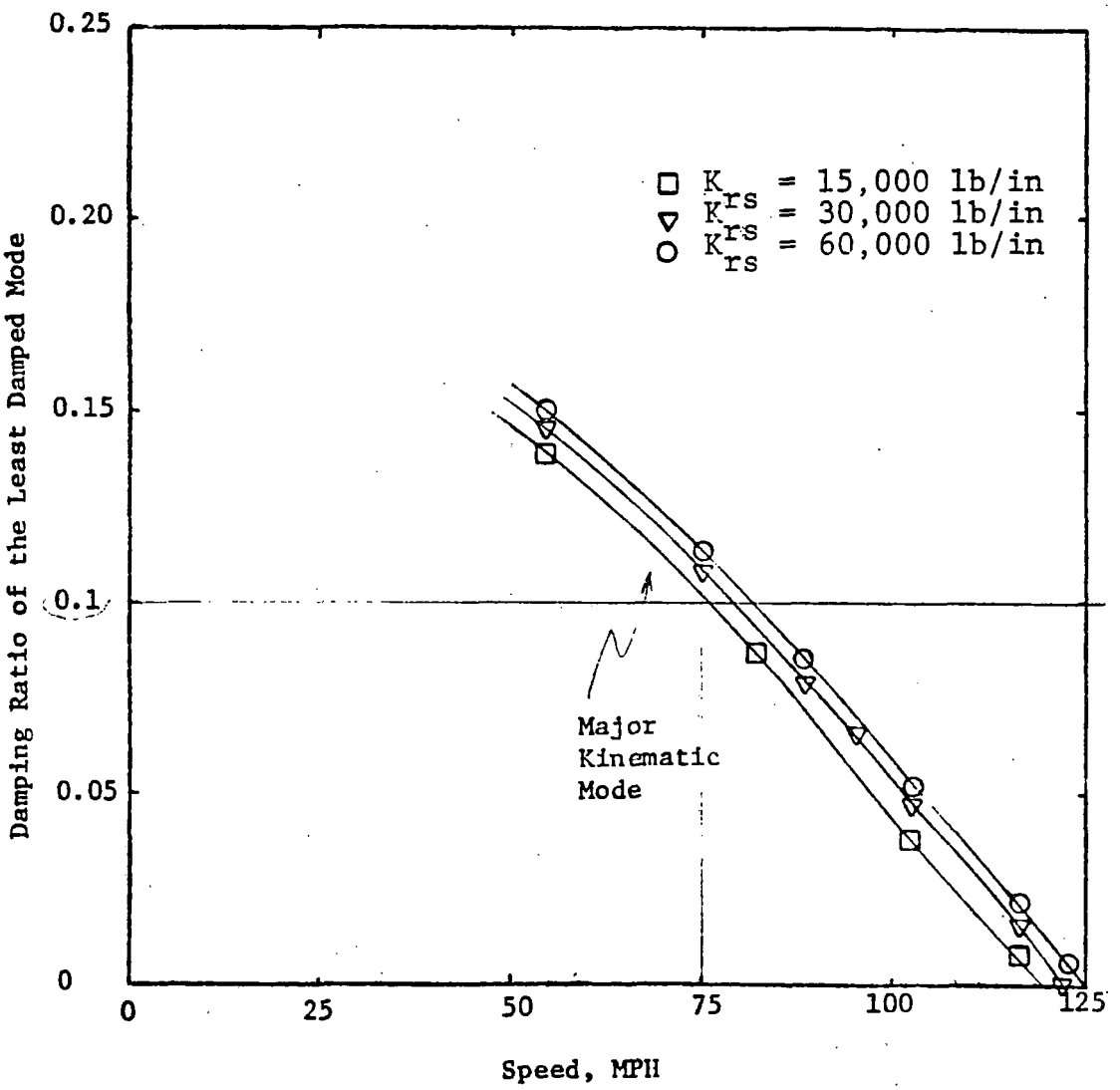

FIGURE 4-3.9: DAMPING RATIO OF THE LEAST DAMPED MODE VERSUS SPEED

stiffness values (K_{rs}) for the steering arm interconnection. Note that the influence of increasing the stiffness of the self-steering connection above the minimum of 15,000 lb/in is not great. Here again, it was also assumed that the frictional slider does not breakaway.

Several other stability investigations were made. For example, inter-axle damping was added in parallel with the bending stiffness. The results of this study are summarized in Table 4-3.1.

Table 4-3.1: Critical Speed vs. Damping for Primary Longitudinal Stiffness = 25,000 lb/in

Damping lb-sec/in	Critical Speed mph
0	112
100	110
400	107
1000	102
5000	94

Also, inter-axle damping without any bending stiffness was explored. These results are tabulated in Table 4-3.2.

Table 4-3.2: Critical Speed vs. Damping for No Longitudinal Stiffness

Damping lb-sec/in	Critical Speed mph
0	41
100	43
300	38
700	46
1700	52
10,000	85

From the above two tables, it can be seen that truck stability can be adversely affected by damping in parallel with a properly chosen longitudinal stiffness. Damping is only of limited value in the absence of adequate stiffness.

4-3.5 Influence of Frictional Slider on Stability

In the previous studies, the critical speed of the steerable truck (self-steering mode) was computed with the 15 D.O.F. linear model of Reference 1, assuming no breakaway in the frictional sliders. For computational purposes, the primary suspension consisted of a parallel combination of k_{px} and C_{px}. For k_{px} = 360,000 lb/ft the critical speed was 123 mph, and it was almost unaffected by C_{px}.

In this study, the case when breakaway occurs is considered. The method of Statistical Linearization is

used to replace the non-linear damping characteristics of the frictional damper, employed with the truck primary suspension and shown in Figure 4-3.10a by an equivalent linear damper shown in Figure 4-3.10b. The Statistical Linearization method chooses the damping rate of the linear damper so that the average square error between the outputs of the non-linear and the linear damper is minimum. If a Gaussian distribution of velocities across the damper is assumed, the equivalent linear damping coefficient is:

$$C = \frac{\sqrt{2/\pi}\, F_o}{\sigma_{\dot{x}}} \qquad (1)$$

where:

C = damping rate
F_o = breakaway force
$\sigma_{\dot{x}}$ = RMS relative velocity across the damper

Equation 1 is plotted in Figure 4-3.11 for two values of the breakaway force, F_o.

Self-Steering

The statistical linearization problem has a solution if the system in which the damper is installed has an operating point for which a value of C yields a value for

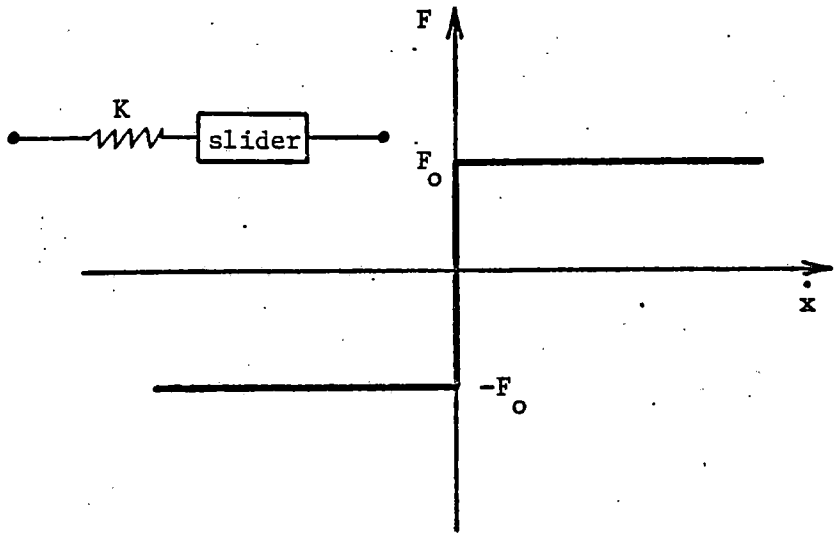

a) Frictional Characteristics of Slider

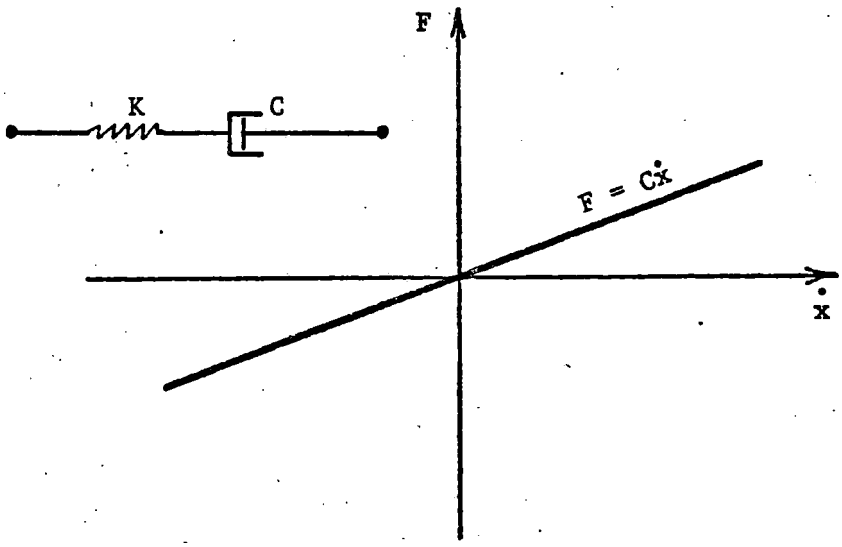

b) Equivalent Linear Element

FIGURE 4-3.10: FRICTIONAL AND LINEAR DAMPERS

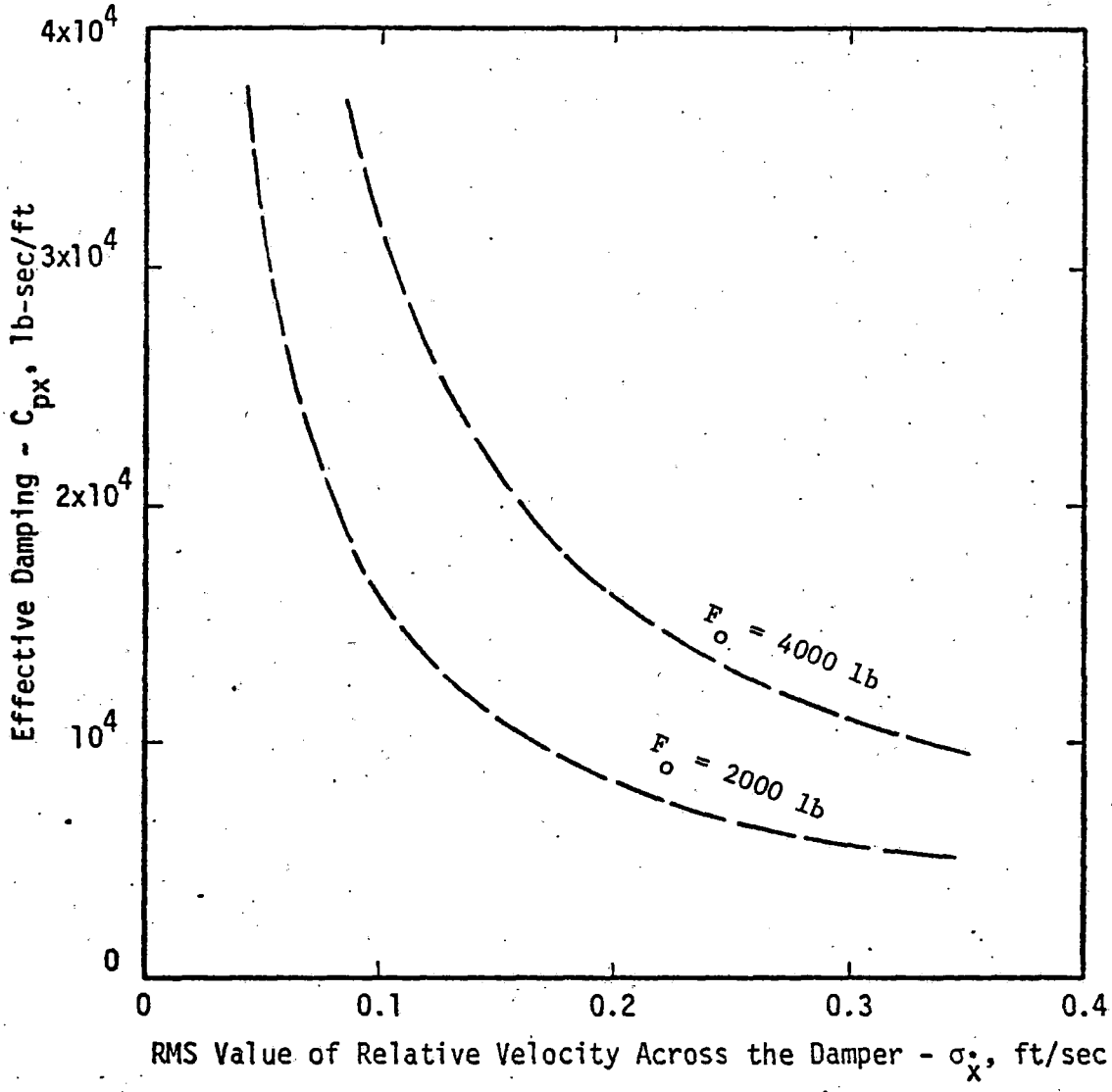

FIGURE 4-3.11: EQUIVALENT LINEAR DAMPING RATE FOR A FRICTIONAL SLIDER

$\overline{\sigma_{\dot{x}}}$ as predicted by Equation 1. Furthermore, this point must be stable for small variations in $\overline{\sigma_{\dot{x}}}$, and the system must be dynamically stable. The $\overline{\sigma_{\dot{x}}} = f(C)$ characteristics of the truck were computed using a 6 D.O.F. truck model derived from the 15 D.O.F. lateral vehicle model of Reference 1. This was accomplished by considering only the front truck of the model, and connecting the secondary suspension to a reference frame moving at the vehicle speed. The primary longitudinal suspension was changed from a parallel to a series combination of k_{px} and C_{px} to represent a spring connection to the slider. The quantity $\overline{\sigma_{\dot{x}}}$ was then computed for several values of equivalent damping, C_{px}.

Figure 4-3.12 shows the computed function for Class 6 track. The peak at about $C_{px} = 10^4$ indicates the point of instability. Theoretically, this peak is of infinite size, and for $C_{px} < 10^4$ the system is unstable. The values of $\overline{\sigma_{\dot{x}}}$ for $C_{px} < 10^4$, therefore, do not correspond to a practical solution.

The equivalent gains and the system characteristics are shown together in Figure 4-3.13 for three classes of track and two breakaway levels. The Class 6 curve and the F = 2000 lb curve intersect at points A and B, which

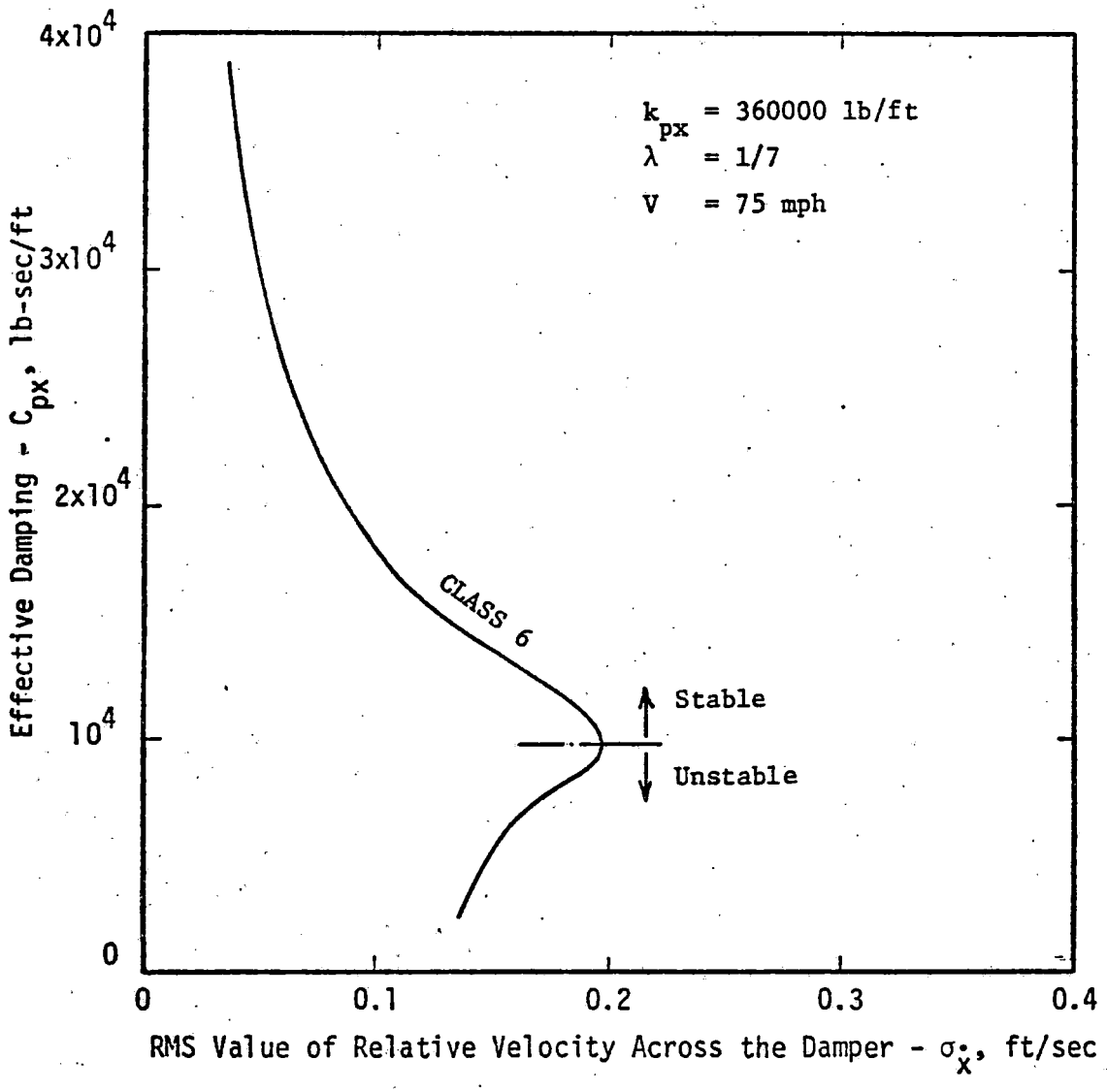

FIGURE 4-3.12: CHARACTERISTICS OF THE TRUCK WITHOUT FORCED-STEERING COMPUTED WITH A 6 D.O.F. MODEL

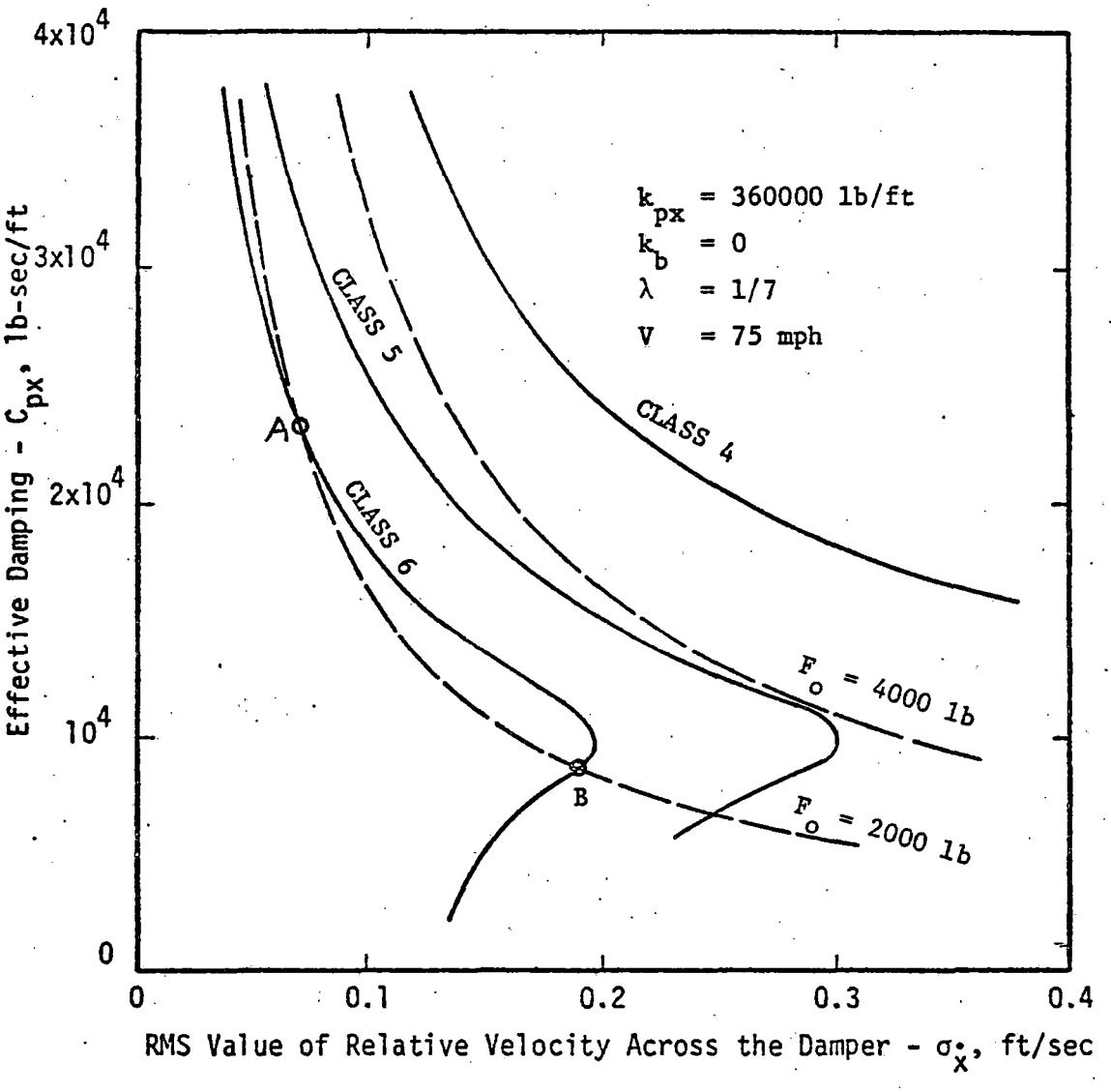

FIGURE 4-3.13: EQUIVALENT DAMPING AND TRUCK CHARACTERISTICS FOR THE TRUCK WITHOUT FORCED-STEERING

are the potential solutions of the statistical linearization problem. However, point A is not stable for variations in $\overline{\sigma_{\dot{x}}}$. If $\overline{\sigma_{\dot{x}}}$ increases, because of increased rail disturbances, the equivalent damping decreases. As the equivalent C_{px} decreases, the system generates even higher $\overline{\sigma_{\dot{x}}}$, and drifts away from point A. Point B is not a solution either, because it is in the unstable region of the system response. The conclusion is that F_o= 2000 lb and Class 6 track do not have a stable linear operating point. Because of the statistical nature of the problem, the slider is locked up part of the time (above point A) and breaks away part of the time (below point A). Sooner or later a low enough value of C_{px} develops to lead to an instability in the equivalent linear model. If F_o is increased to 4000 lb, there is no intersection of the Class 6 curve with the damping curve,* the slider is locked up, and the system is stable. The conclusion from Figure 4-3.13 is that the slider either stays locked or breaks away and results in instability in the model, with no operating mode between these extremes. Therefore, without the forced-steering connection, the slider friction connection is not effective in this model.

---

* Theoretically, there is an intersection, because the peak on the Class 6 curve is infinite. However, because of limits on suspension strokes and flange clearances all the motions remain finite. It is estimated that $\overline{\sigma_{\dot{x}}}$= 0.2 ft/sec is the highest practical value for all classes of track.

Forced-Steering

The effects of forced-steering have been represented by an equivalent bending stiffness $k_b = 10^6$ ft-lb/rad between truck wheelsets. The equivalent damping - truck characteristics plot is shown in Figure 4-3.14. The truck does not become unstable as $C_{px} \rightarrow 0$, because of the stabilizing influence of k_b. All the intersection points are as point A, i.e., unstable operating points. Therefore, the slider either never breaks away, or randomly shifts from locked to broken-away position. However, even if complete breakaway occurs, the truck remains stable. The critical speed is 188 mph if no breakaway occurs and 106 mph if breakaway occurs.

Evaluation of Vertical Dynamic Slider Force

The normal load on truck primary suspension slider bearings consists of a static load of 10,400 lbs. per slider due to the vehicle weight, and of a dynamic, zero mean load due to vehicle motions excited by rail irregularities. The dynamic normal forces were computed using a 14 D.O.F. vertical dynamic model. This model consists of the 12 D.O.F. vertical model of Reference 1, with two additional degrees of freedom: the pitch motions of the side frames of the two trucks.* With this addition, each truck frame has four degrees of freedom: heave, pitch,

* The out-of-phase pitch of the two frames is treated as a single D.O.F.

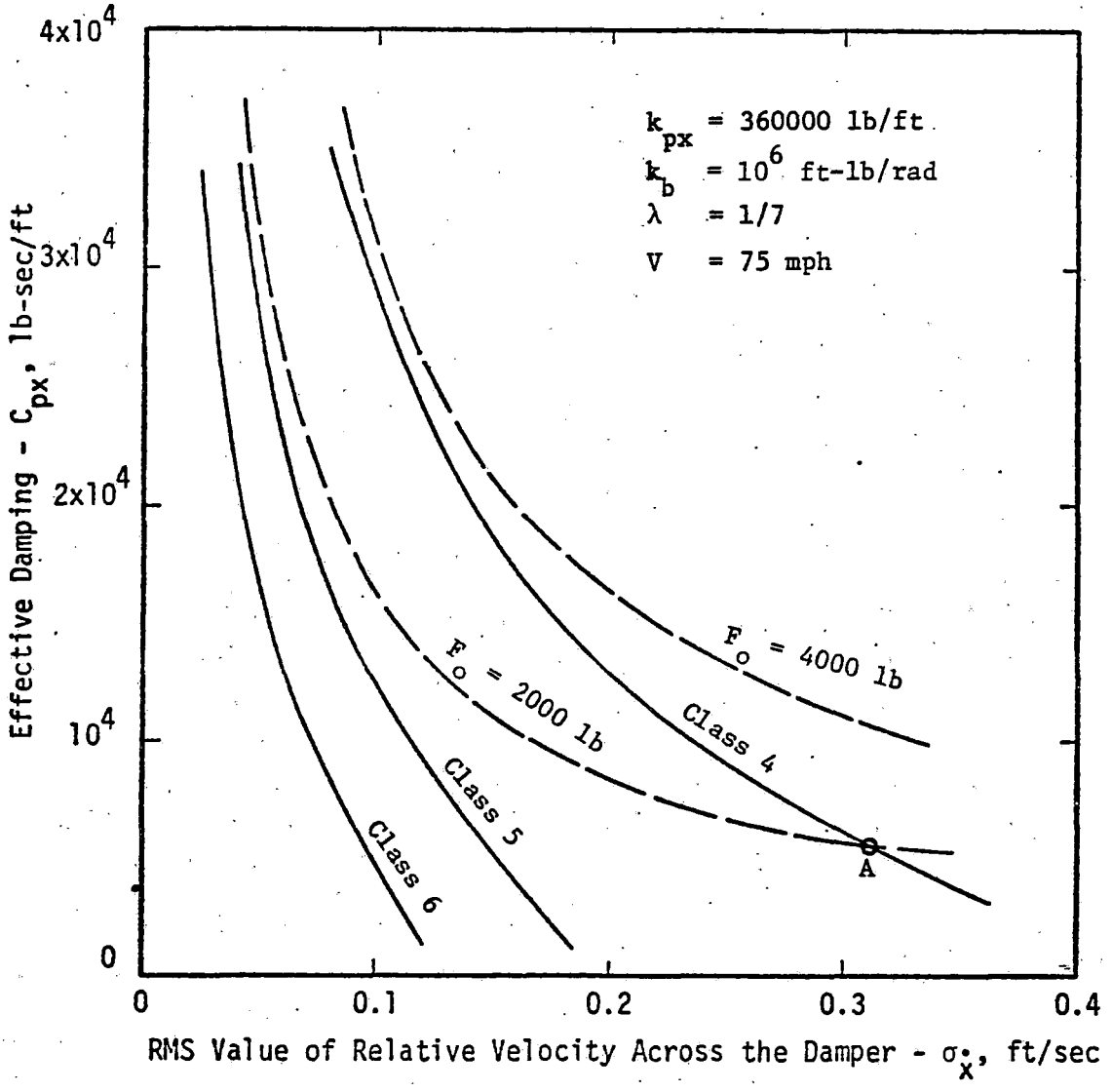

FIGURE 4-3.14: EQUIVALENT DAMPING AND TRUCK CHARACTERISTICS FOR THE TRUCK WITH FORCED-STEERING

roll and pitch of the side frames. This modification of the model of Reference 1 was required to accurately represent the load equalization mechanism.

The forces computed due to track irregularities in all eight primary vertical springs were almost equal, and are listed in Table 4-3.3. It is assumed that the force in a primary vertical spring also is the normal force on a frictional slider.

If Gaussian distribution of the dynamic forces is assumed, the force is within $\pm$ 1 RMS 68.26% of the time, within $\pm$ 2 RMS 95.44% of the time, and within $\pm$ 3 RMS 99.74% of the time. Since most of the RMS of the force is accumulated above 20 Hz, and the kinematic frequency is below 5 Hz, the average force in a cycle of the kinematic motion is expected to be close to the static value of 10,400 lbs. Therefore, the dynamic component of the normal force on the slider is expected to have little effect on the performance of the slider.

4-3.6 Kinematic Stability of Forced-Steering Truck

A forced-steering rail truck employs linkages which cause the wheelsets to develop a yaw angle between them as a result of a yaw angle between the truck and the carbody. This steering action is desirable for improved curving

TABLE 4-3.3: RMS NORMAL FORCE ON A FRICTIONAL SLIDER (lb)

Class of Track	6	5	4
RMS Force Due to Vertical Irregularities	837	2090	3345
RMS Force Due to Cross-Level Irregularities	820	1887	2914
Total RMS Force (lb)	1171	2816	4436

performance, but it can be a destabilizing effect. In the following paragraphs the stability of the proposed P-III truck with forced-steering is evaluated quantitatively. It shows that proper selection of the forced-steering link stiffness avoids a destabilizing effect in the range of realistic conicities and creep coefficient. Thus for a given primary axle box stiffness, the addition of the forced-steering link can improve both stability and curving performance.

Forced-steering terms were added to the 6 D.O.F.-stability model. The stability model assumes that the carbody remains fixed in the inertial reference frame.

The forced-steering terms used in this study were obtained from the following steering law representing carbody to wheelset connections:

$$\Delta\psi = 2G \left(\frac{y_1 - y_2}{2b} - \psi_c \right) \qquad (1)$$

where:

G = steering gain

$y_{1,2}$ = lateral wheelset displacements

b = half of truck wheelbase

ψ_c = carbody yaw displacement

The displacement $\Delta\psi$ acts in series with the wheelset interconnection bending stiffness, k_b, and in parallel with the primary longitudinal stiffness, k_{px}, as shown in Figure 4-3.15.

This model can be applied with accuracy to the P-III forced-steering truck shown in Figure 4-3.16 as long as k_{py} and k_s are reasonably stiff, as is the case with the current design. The bolster is assumed to be snugly pinned to the truck frame. The following relations result:

$$G = \frac{1}{b - \ell_1} \qquad (2)$$

$$k_b \cong \frac{(b-\ell_1)^2 k_{fs}}{4} \qquad (3)$$

where:

G = steering gain
ℓ_1 = steering link offset
b = half of truck wheelbase
k_b = interconnection bending stiffness
k_{fs} = effective stiffness of forced-steering link

The destabilizing tendency of forced-steering can lead to kinematic instability of the truck if the following condition is not met:

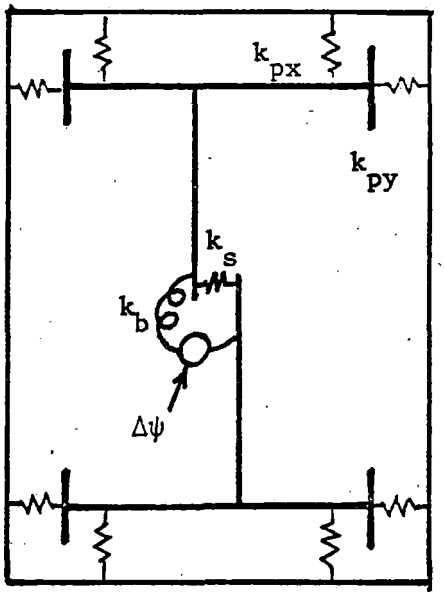

FIGURE 4-3.15: RADIAL TRUCK MODEL WITH FORCED-STEERING ADDED

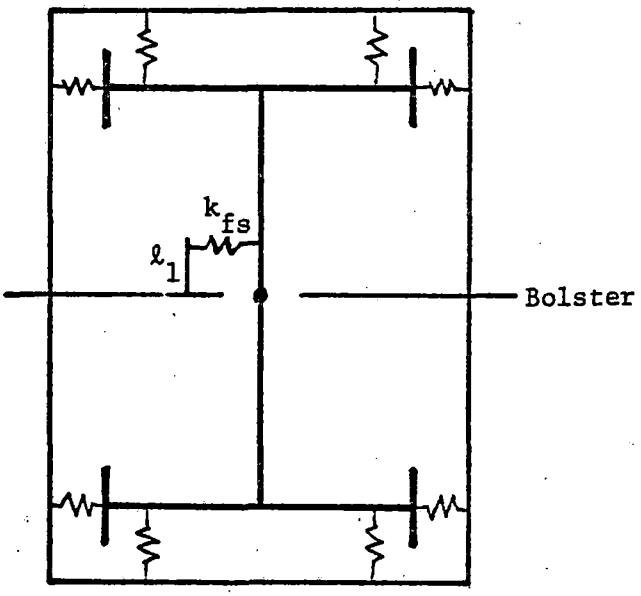

FIGURE 4-3.16: SCHEMATIC OF P-III FORCED-STEERING TRUCK

$$k_b \leq \frac{bf \quad \frac{\lambda a}{r_o}}{G} \qquad (4)$$

where:

k_b = interconnection bending stiffness

λ = conicity

a = track gauge

r_o = rolling radius

G = steering gain

This is a conservative condition which guarantees kinematic stability for the range of practical values of primary and secondary stiffnesses. It is least conservative when k_{sy}, $k_{s\psi}$, $k_{px} \rightarrow 0$ and $k_s \rightarrow \infty$. Thus in the following numerical stability studies the secondary stiffnesses have been set to zero to ensure conservative values of forced-steering link stiffness, k_{fs}, at which the truck becomes kinematically unstable. The remaining stiffness parameters are:

$$k_{px} = 360{,}000 \text{ lb/ft}$$
$$k_{py} = 1 \times 10^6 \text{ lb/ft}$$
$$k_s = 1 \times 10^6 \text{ lb/ft}$$

Figures 4-3.17 through 4-3.20 show stability performance results obtained from the 6 D.O.F. stability model for

different values of conicity, creep coefficients, and steering gain. All stability plots show critical speed vs bending stiffness k_b (or equivalently forced-steering link stiffness, k_{fs}). For each value of conicity, two extreme cases are considered: free primary breakaway and no primary breakaway.

Figure 4-3.17 represents the nominal conicity of $\lambda = 1/7$. The G=0 curve in each plot shows the performance of a radial truck without any forced-steering action. Increasing k_b causes critical speed to peak and then drop off gradually, with both trucks behaving the same. Increasing the steering gain, G, however, has a destabilizing effect on the rear truck when the forced-steering link stiffness is large.*

Bending stiffness, k_b, in the range of 1×10^6 to 3×10^6 (ft-lb/rad) ($k_{fs} \simeq$ 30,000 to 100,000 (lb/in)) is small enough that the steering gain has little detrimental effect, but large enough to provide good stability. Even with the primary slider force equal to zero (i.e., free breakaway), good stability is possible with the nominal conicity. When the slider force is large (i.e., no break away), stability improves in the low range of k_b due to

---

* Good curving performance is achieved in the range of G = 0.1 to 0.3.

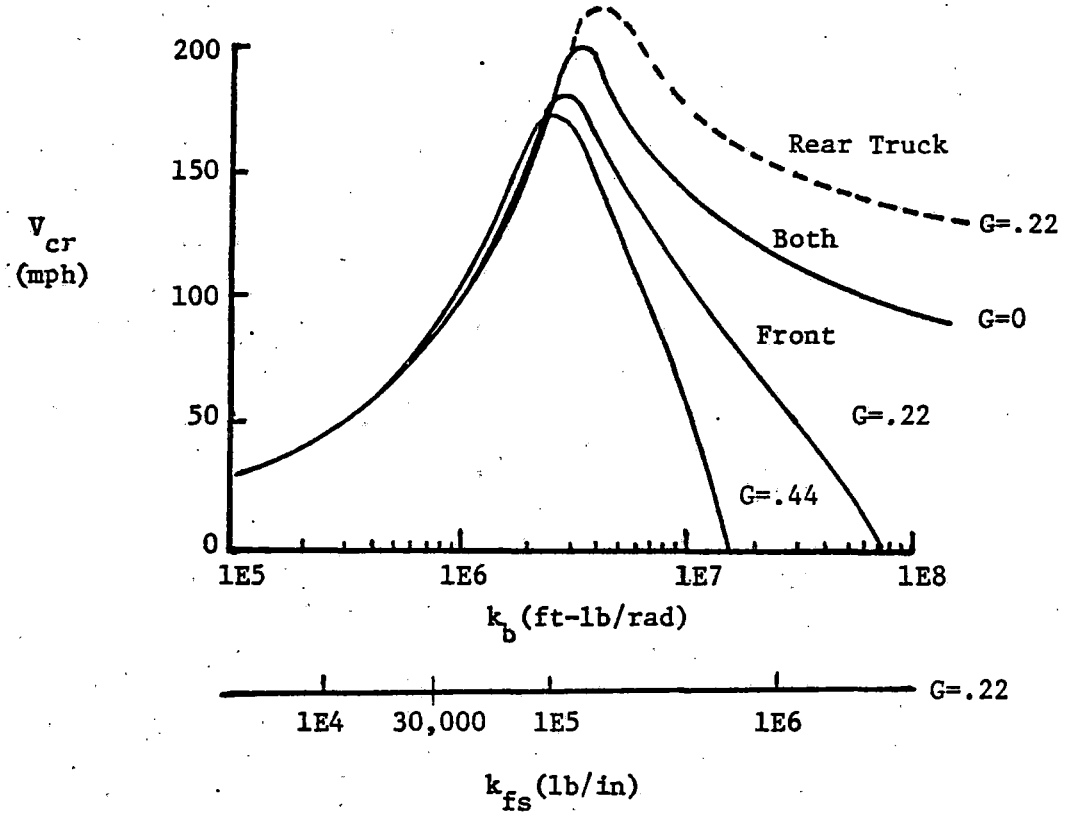

a) Free Primary Breakaway

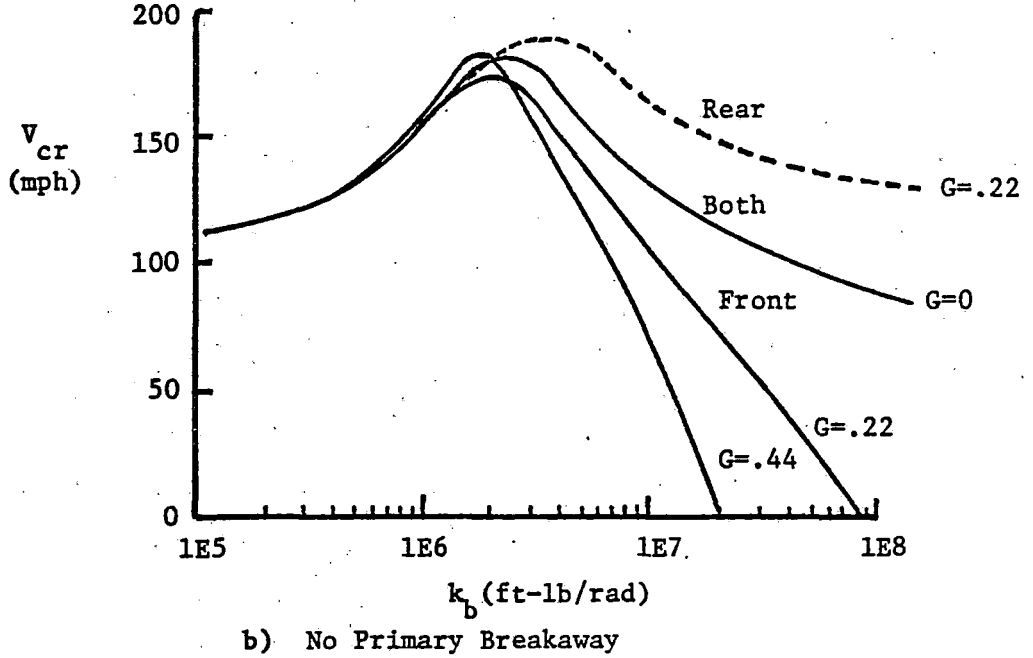

b) No Primary Breakaway

FIGURE 4-3.17: STABILITY PERFORMANCE FOR λ = 1/7

the increased primary yaw stiffness, but this is detrimental to curving performance.

Figures 4-3.18 and 4-3.19 show similar results for λ = 1/13 and λ = 1/3. The cutoff value of k_b at which kinematic instability occurs becomes more critical for the low conicity as indicated in Equation 4. For the high conicity, the cutoff value becomes less critical, but the critical speed which can be achieved in the desired range of k_b is reduced.

Figure 4-3.20 shows the effect on the results of Figure 4-3.17 of halving the creep coefficients. The cut-off value of k_b is halved as indicated by Equation 4, and critical speeds shift downward to the left as the truck stiffness increases relative to the creep force terms.

Figure 4-3.21 shows the extremely sharp nature of the drop in critical speed at low values of conicity and creep coefficients. It is not known what creep coefficient value corresponds to wet or lubricated rails. Also, it is not known if the wheel profile on a steerable truck could wear to a very low conicity. It is quite possible that low creep coefficients and low conicities are not realistic parameters for the steerable truck. Conducting field tests

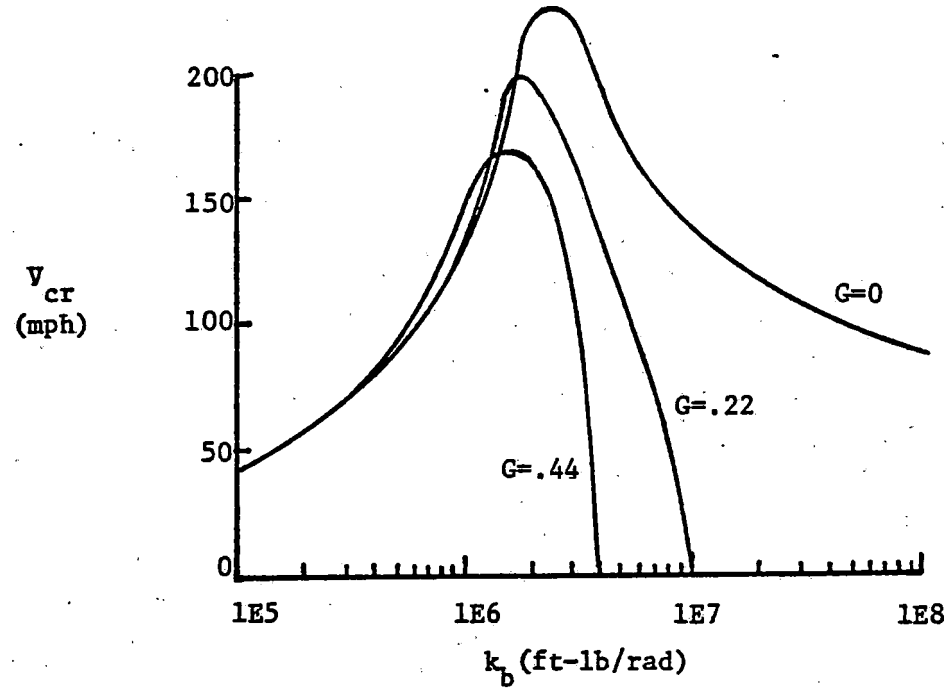

a) Free Primary Breakaway

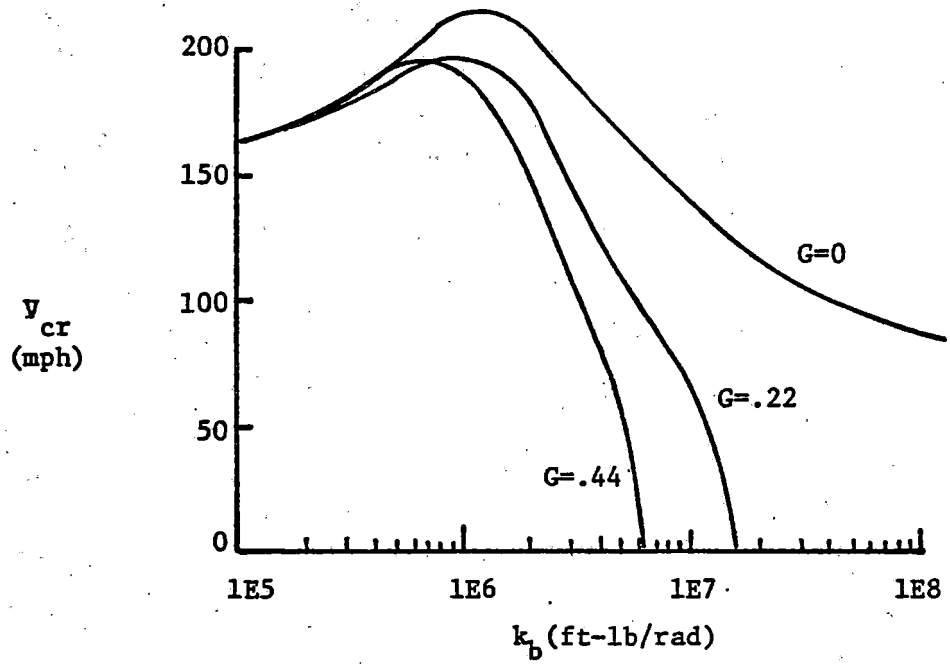

b) No Primary Breakaway

FIGURE 4-3.18: STABILITY PERFORMANCE FOR λ = 1/13

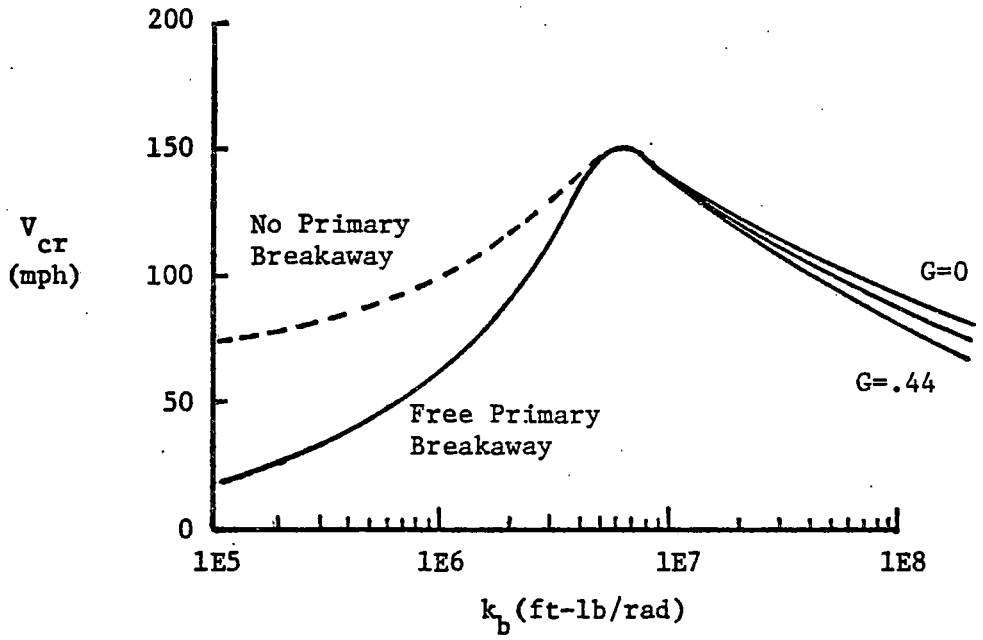

FIGURE 4-3.19: STABILITY PERFORMANCE FOR $\bar{\lambda}$ = 1/3

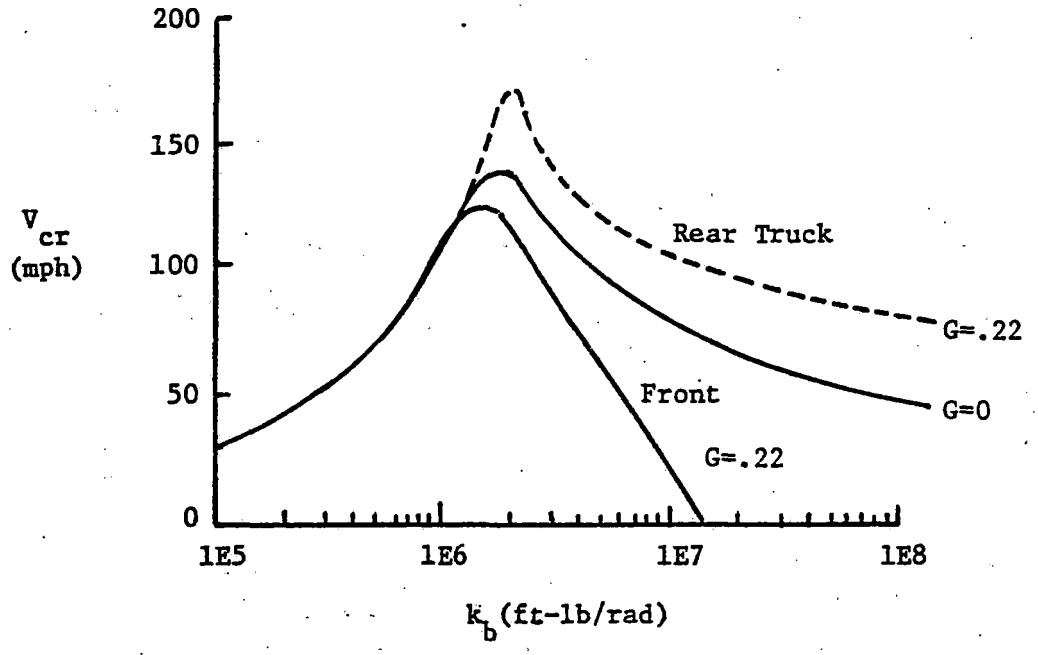

a) Free Primary Breakaway

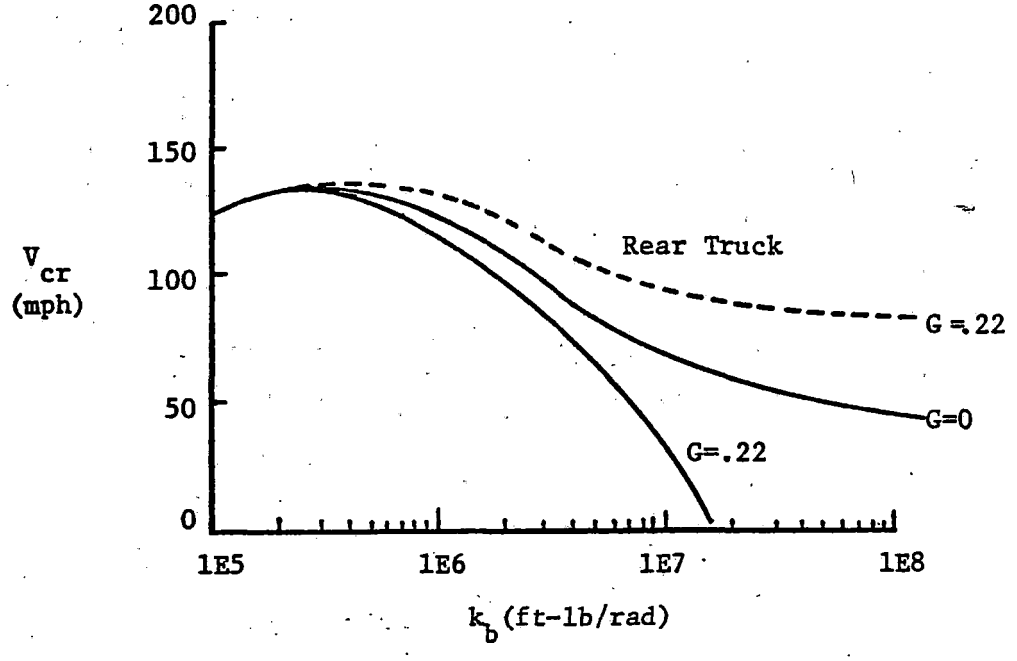

b) No Primary Breakaway

FIGURE 4-3.20: CONICITY PERFORMANCE FOR λ = 1/7 WITH 1/2 NOMINAL CREEP COEFFICIENTS

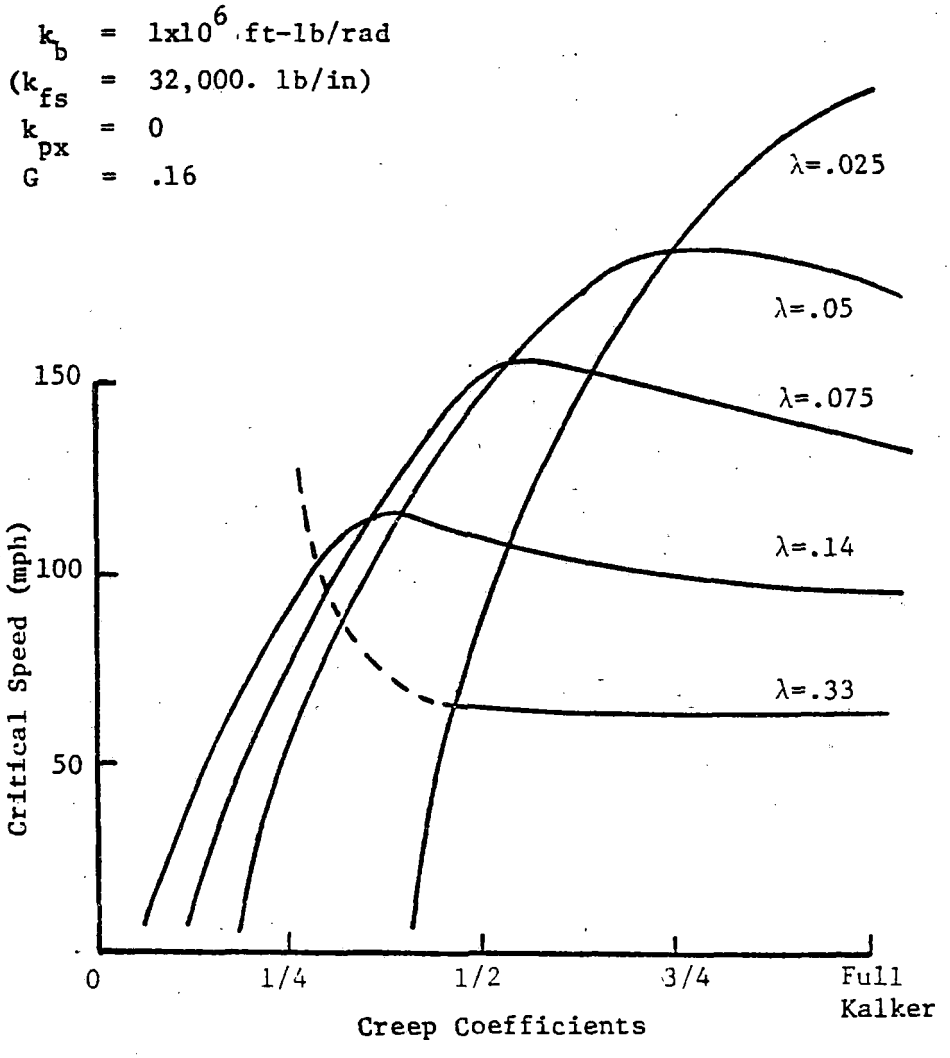

FIGURE 4-3.21: EFFECT OF CREEP COEFFICIENTS ON STABILITY PERFORMANCE OF THE FORCED-STEERING TRUCK

could answer these questions.

Assuming for the moment that low creep coefficients are not likely and that low effective conicities can be prevented, then the forced-steering configuration is a feasible design. A forced-steering design with 2000-lb. sliders can achieve a critical speed of 145 mph under the following assumptions:

k_{fs} = 32,000 lb/in
G = 0.16
k_b = 1.0 x 10^6 ft-lb/rad
λ = 0.05
f = 1/2 kalker

This design configuration is considered the best from overall curving performance and high speed stability criteria. However, if low creep coefficients and low effective conicities are possible, then the above forced-steering design configuration could have a tendency toward kinematic instability and alternate designs must be considered. Two alternate design configurations are discussed in the next section.

4-3.7 Forced-Steering Configuration Alternatives

If it is desired to design a forced-steering vehicle that is stable for 1/4 and full kalker coefficients then the steering linkage stiffness, k_{fs}, can be reduced to

10,000 lb/in (k_b = 3 x 10^5 ft-lb/rad) to ensure truck stability for conicities down to λ = 0.025. This alternate configuration would also require that the truck corner primary longitudinal stiffness, k_{px}, be set at 10,000 lb/in with no slider. These stiffnesses also provide adequate stability at the higher creep coefficients and conicities. The stability performance of the first alternative design is summarized in Table 4-3.4 below.

TABLE 4-3.4: Tangent Track Critical Speed for First Alternative Force-Steered Design

k_b = 3x10^6 ft-lb/rad
k_{fs}= 10,000 lb/in
G = 0.16

λ	1/40		1/7	
k_{px}(lb/in)	10,000	0	10,000	0
Full Kalker	205 mph	123	80	50
50% Kalker	176	133	84	51
25% Kalker	81	113	93	53

These results indicate that a very wide performance band is required to accommodate extremes of both conicity and creep coefficient. This design is definitely a com-

promise in the areas of both stability and curving performance.

It should also be mentioned that a quick study of the effect of 1/4 kalker on the self-steered design was also negative. Thus, the effect of such extremely low values of creep coefficients is a complex function of conicity and truck stiffness parameters. The negative effect is not limited to the forced-steering concept

The second alternate configuration is the basic forced-steered design with clearance in the lateral link. This configuration has been referred to by some as "sloppy" steering. The intent of this design is to allow the truck to behave as a self-steered truck on tangent track and to force it to behave as a force-steered truck on curved track. A preliminary analysis has shown that a 1/16 in. clearance would be sufficient to keep the excursion from closing if motion of the wheelsets relative to the truck frame is neglected. If a 1/8 in. clearance were used to allow a safety margin, then the truck would behave as a self-steered truck for curves less than 4 degrees and as a forced-steered truck for curves greater than 4 degrees. If k_{px} is set at 30,000 lb/in and a 4000-lb slider breakout level is used, the stability performance as is shown in Table

4-3.5 below:

TABLE 4-3.5: Tangent Track (self-steered) Critical Speed (mph)

% Kal. \ λ	1/40	1/20	1/7
100%	258	186	106
50%	160	152	113
25%	83	82	81

4-3.8 Steerable Truck Stability Performance Summary

The initial stability studies were concerned with finding the optimum primary longitudinal stiffness for the self-steering configuration. Because of the high unsprung mass of the steering arms and the traction and braking equipment mounted on the steering arms, a k_{px} of 30,000 lb/in was required to satisfy the stability requirement. The critical speed (assuming λ = 1/7 and F = full Kalker) was 123 mph. While this value satisfied the stability criteria, curving performance was not significantly improved over that of the conventional truck.

In order to improve the curving performance, a slider was placed in series with the 30,000-lb/in spring. A

slider with a 2000-lb breakout was ideal for curving. This permitted radial positioning for wheel/rail friction levels down to 0.2.

Running the self-steered configuration through a forced response study showed that a 2000-lb slider would breakout during tangent track operation and possibly lead to an instability. In order to prevent or minimize breakout on class 5 or 6 track, a 4000-lb slider is requried Even a higher level would be required for class 4 track. Increasing slider breakout force levels would reduce the curving performance of the self-steered configuration. For this reason, the use of forced-steering was investigated.

The forced-steered design allows the addition of truck bending stiffness (by the lateral stiffness of the forced-steered link, k_{fs}) so that the truck can be stabilized even if $k_{px} = 0$. Excellent curving performance can be expected. The stability of the forced-steered design with k_{px} = 30,000 lb/in, 2000-lb slider, and k_{fs} = 32,000 lb/in is 188 mph if no breakaway occurs and 106 mph if breakaway occurs. These results are for λ = 1/7 and f = full Kalker. However, these critical speeds rapidly decrease with decreasing conicities and creep coefficients. Since there is considerable uncertainty as to the possibility of low

creep coefficients, the above design is the recommended approach until field testing proves otherwise.

If field testing indicates that the forced-steered configuration has a tendency toward kinematic instability caused by low creep coefficients and conicities, then the alternative designs can be implemented. However, it should be noted that the alternate concepts do trade-off curving performance for improved stability at low creep coefficients.

4.4 RIDE QUALITY

4-4.1 Introduction and Background

Ride quality is very subjective as perceived by individual passengers. Such factors as vibration, noise, temperature, passenger space constraints, and passenger compartment measures can enter into the overall perception of ride quality. However, only the dynamic vibration environment resulting from the effect of track irregularities on the vehicle response is considered in this study. There are two measures that are generally used to quantitatively describe vibration environment: the root mean square acceleration levels and the distribution of the RMS acceleration in one-third octave frequency bands weighted by ISO standards as described in ISO guidelines for lateral motion.

Figure 4-4.1 illustrates the ISO recommended limits for the lateral and vertical one-hour reduced comfort boundaries. When the vehicle vibration environment is broad band, i.e., has a frequency content over a wide range, the recommended procedure is to compute the RMS accelerations in one-third octave bands and to compare them to the recommended ISO levels at the one-third octave band center frequency. Although these criteria are not exact, they are generally accepted as a useful indicator of passenger ride comfort.

The acceleration levels are computed using lateral and vertical linear eigen value programs modified to compute vehicle response to forced input in the form of random track irregularities. The track irregularities that were used for this study were alignment and cross-level defects representative of class 6 track. The defects or irregularities are represented by their spectral densities. Spectral densities are statistical measurements which describe random irregularities. Figures 4-4.2 and 4-4.3 present the alignment and cross-level spectral densities that were used. The equations of the spectras are shown in the figures, where $S(\Omega)$ is the spectral density as a function of wavelength Ω, Ω_c and Ω_s are wavelength parameters and A is a roughness parameter.

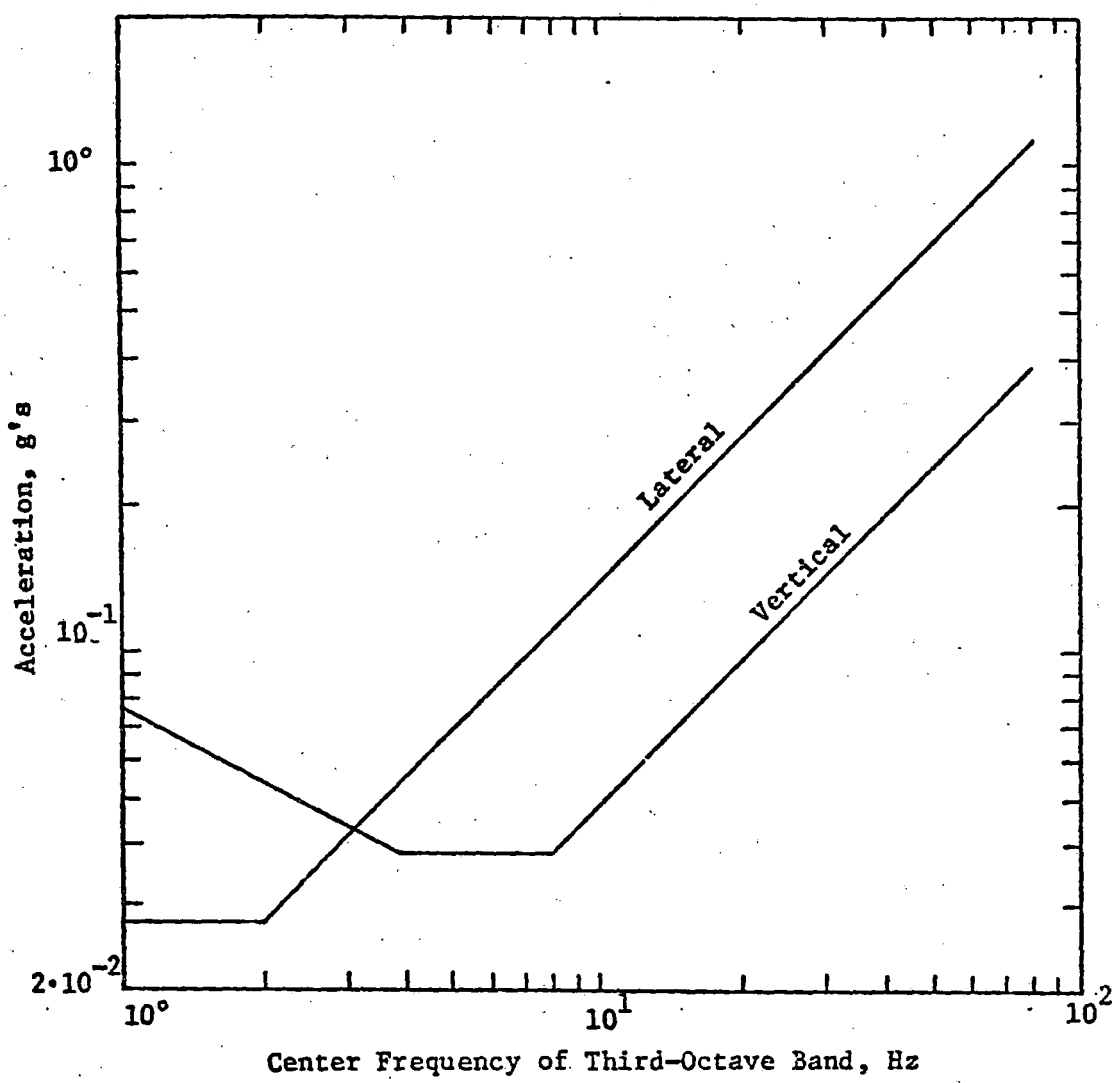

Figure 4-4.1: LATERAL AND VERTICAL ACCELERATION LIMITS AS A FUNCTION OF FREQUENCY FOR 1 HOUR EXPOSURE TIME; "REDUCED COMFORT BOUNDARY"

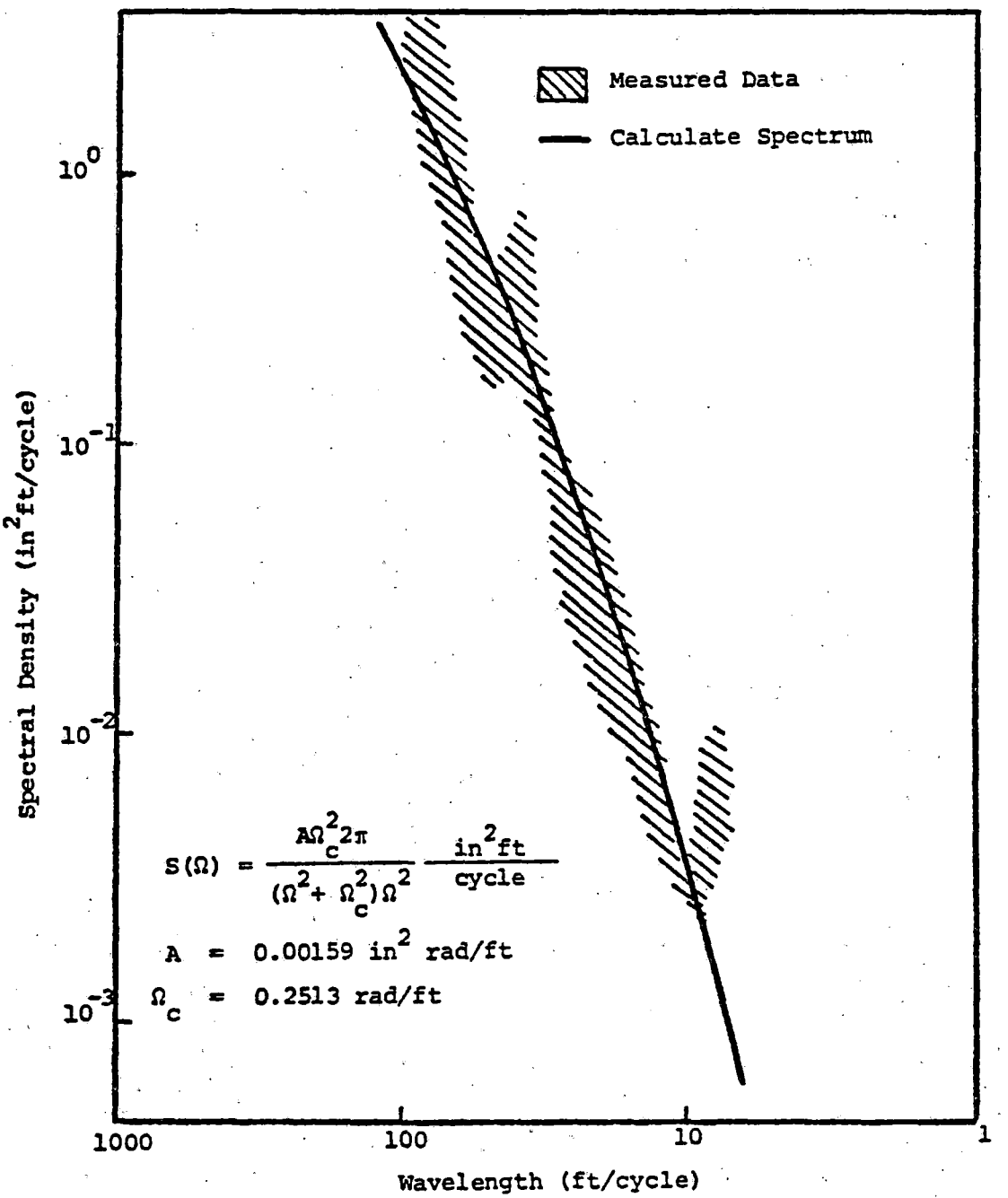

Figure 4-4.2: CLASS 6 ALIGNMENT SPECTRAL DENSITY

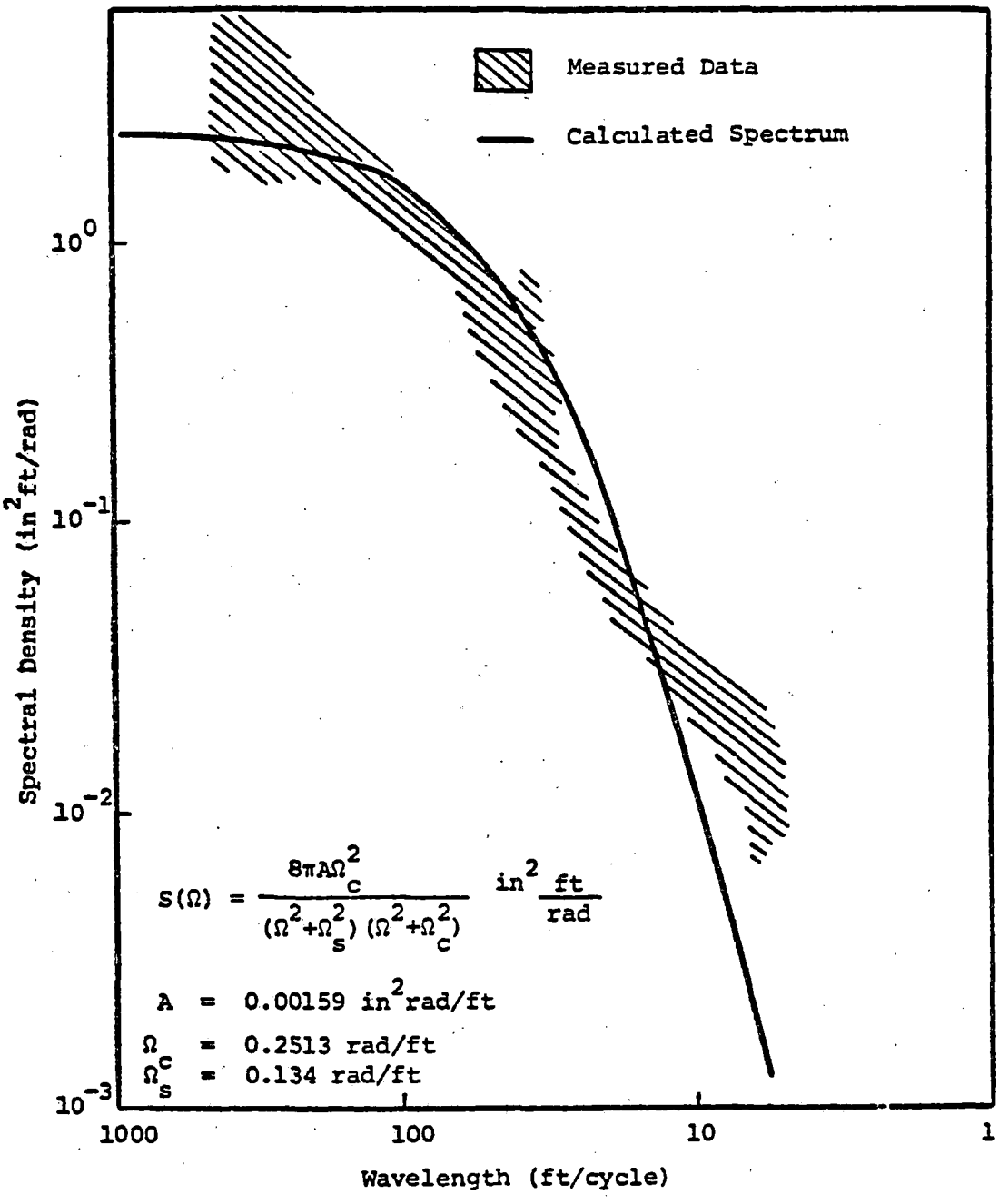

Figure 4-4.3: CLASS 6 CROSSLEVEL SPECTRAL DENSITY

4-4.2 Computational Models

The lateral response was computed using a 15 degrees of freedom model. Each wheelset and truck frame has lateral and yaw degrees of freedom and the carbody has lateral, yaw, and roll. A detail description of the lateral model and its equations are given in Reference 1.

The vertical response was computed using a 12 degrees of freedom model. The degrees of freedom represented include vertical, roll, and pitch of both trucks and the carbody. In addition to these rigid-body modes, carbody flexibility is incorporated by including the first bending mode and the first two torsion modes of the carbody. A description of the vertical model is also given in Reference 1.

4-4.3 Lateral Dynamic Response

Conventional Truck

The 15 degrees of freedom model was used to determine the lateral response of the existing P-III truck used on PATCO (conventional truck) for two different longitudinal primary stiffnesses. Three passenger locations were considered:

- Front passenger point - a point above a secondary spring of the leading truck, 3.5 ft above the carbody center of gravity

- e.g. passenger point - at carbody c.g.
- Rear passenger point - a point above a secondary spring of the trailing truck, 3.5 ft above the carbody center of gravity

The truck parameters used are given in Table 2-2.2 and 2-2.3 of the design description of the conventional truck. Table 4-4.1 summarizes the results of the lateral response. Figure 4-4.4 shows the acceleration spectral density at the front passenger point for the existing truck. Figure 4-4.5 shows the corresponding ISO ride quality plot. The reduced comfort time is about 1.8 hours. Figure 4-4.6 shows the acceleration spectral density for the existing truck with a lower primary longitudinal stiffness. Figure 4-4.7 shows the corresponding ISO ride quality plot. The resulting reduced comfort time is about 2.4 hours.

Steerable Truck

The 15 degrees of freedom model was also used to determine the lateral response of the proposed steerable truck. The truck parameters are given in Table 2-3.1 and 2-3.2 of the design description of the proposed steerable truck. Table 4-4.2 summarizes the results. Figure 4-4.8 shows the acceleration spectral density at the front passenger point for the proposed steerable truck. Figure 4-4.9 shows the corresponding ISO ride quality plot. The reduced comfort

TABLE 4-4.1: Summary of the Lateral Dynamic Response

Longitudinal Primary Stiffness

K_{px} (lb/ft)	360,000	3.54×10^6
CLASS OF TRACK	6	6
CONICITY, λ	1/7	1/7
SPEED (MPH)	75	75
Total Front Passenger Point RMS Acceleration (G)	0.055	0.043
Total C.G. Passenger Point RMS Acceleration (G)	0.021	0.019
Total Rear Passenger Point RMS Acceleration (G)	0.053	0.040
RMS Secondary Stroke Length, Leading Truck (in)	0.36	0.33
RMS Secondary Stroke Length, Rear Truck (in)	0.45	0.41
RMS Primary Stroke Length, 4th Wheelset (in)	0.00094	0.0017
RMS Wheelset Excursion, 1st Wheelset (in)	0.24	0.21

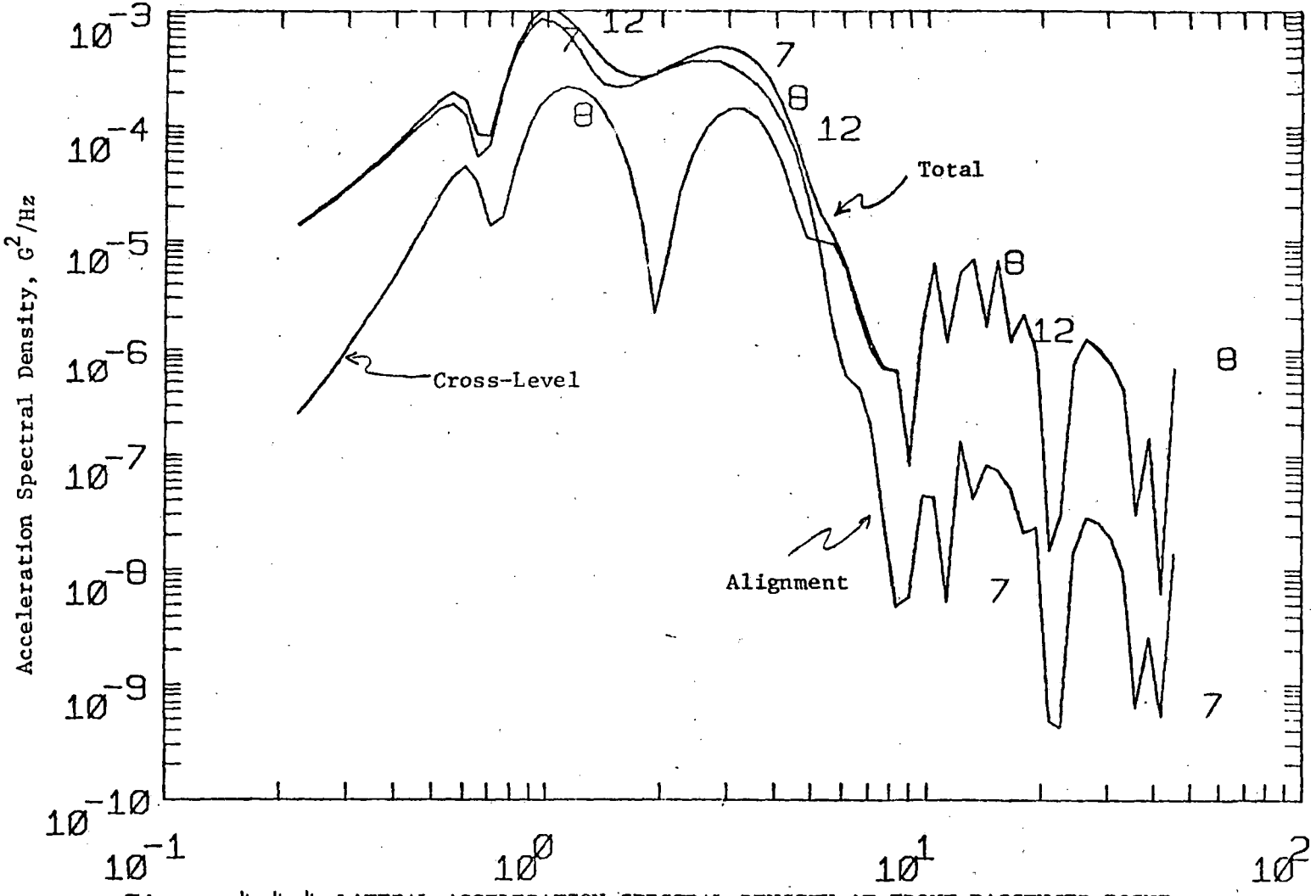

Figure 4-4.4: LATERAL ACCELERATION SPECTRAL DENSITY AT FRONT PASSENGER POINT
λ = 1/7, K_{px} = 3.54 x 10^6 lb/ft, V = 75 mph.

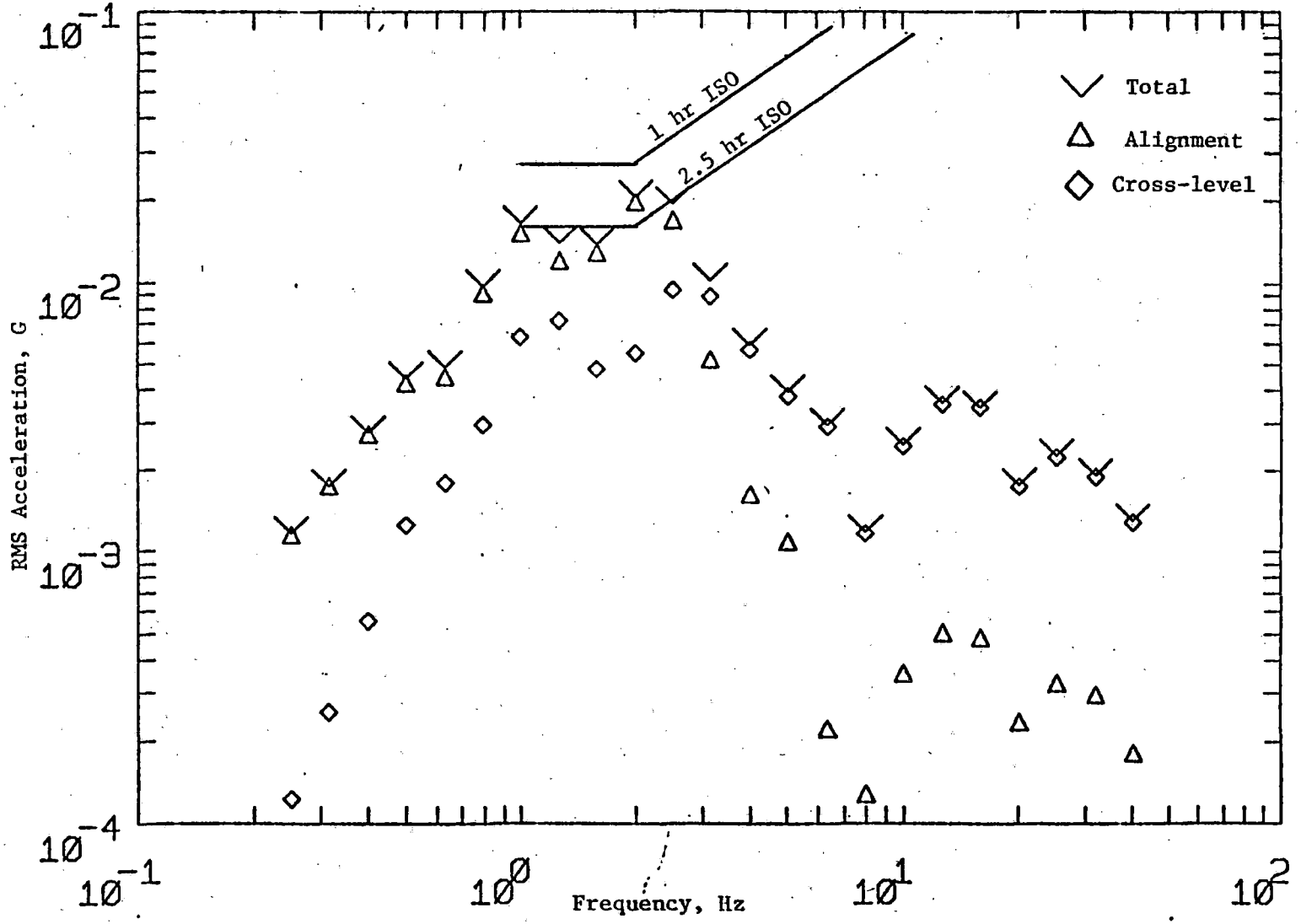

Figure 4-4.5: ONE-THIRD OCTAVE BAND RMS LATERAL ACCELERATIONS, FRONT PASSENGER POINT, $\lambda = 1/7$, $K_{py} = 3.54 \times 10^6$ lb/ft, V = 75 mph.

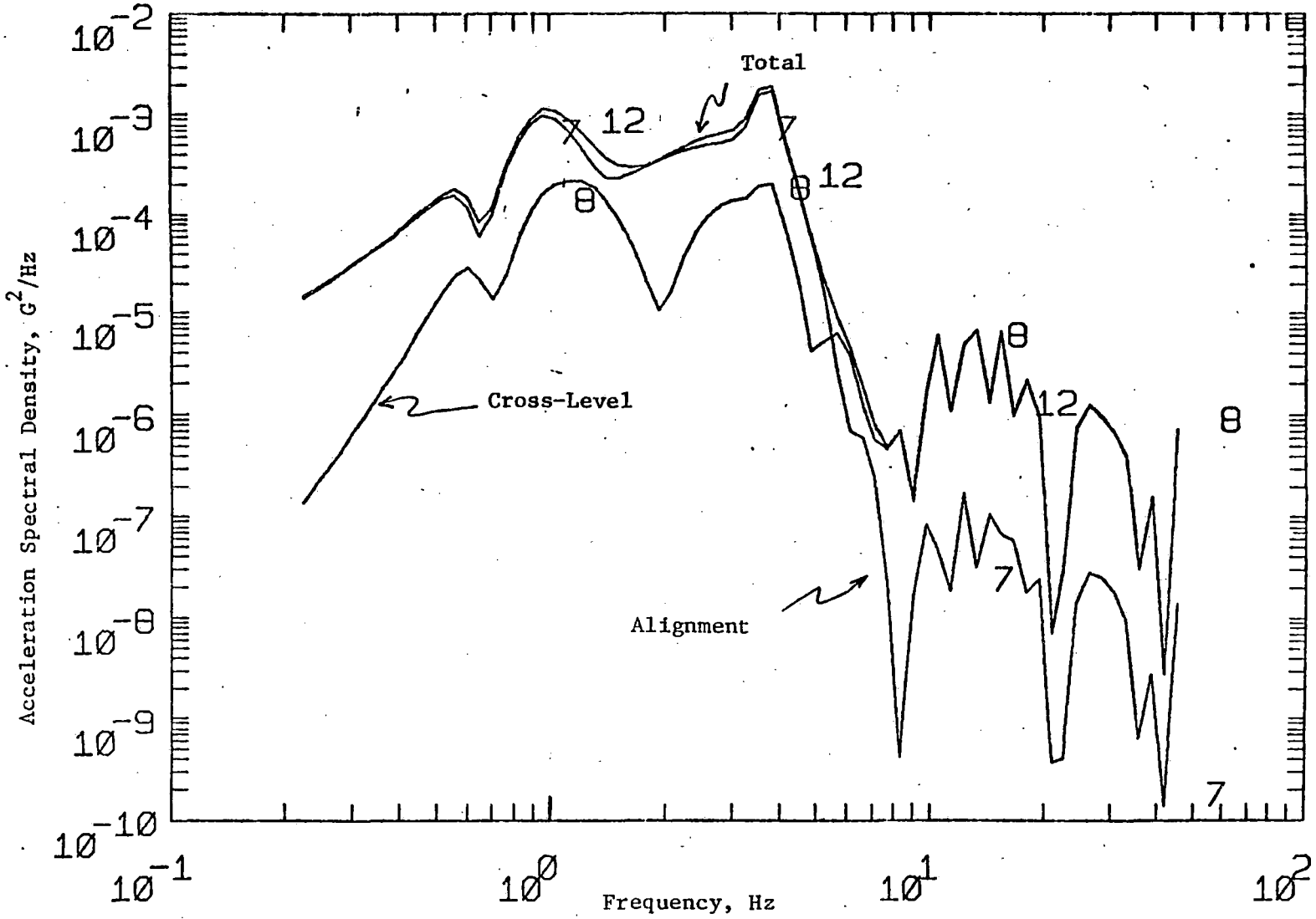

Figure 4-4.6: LATERAL ACCELERATION SPECTRAL DENSITY AT FRONT PASSENGER POINT, λ = 1/7, K_{px} = 360,000 lb/ft, V = 75 mph

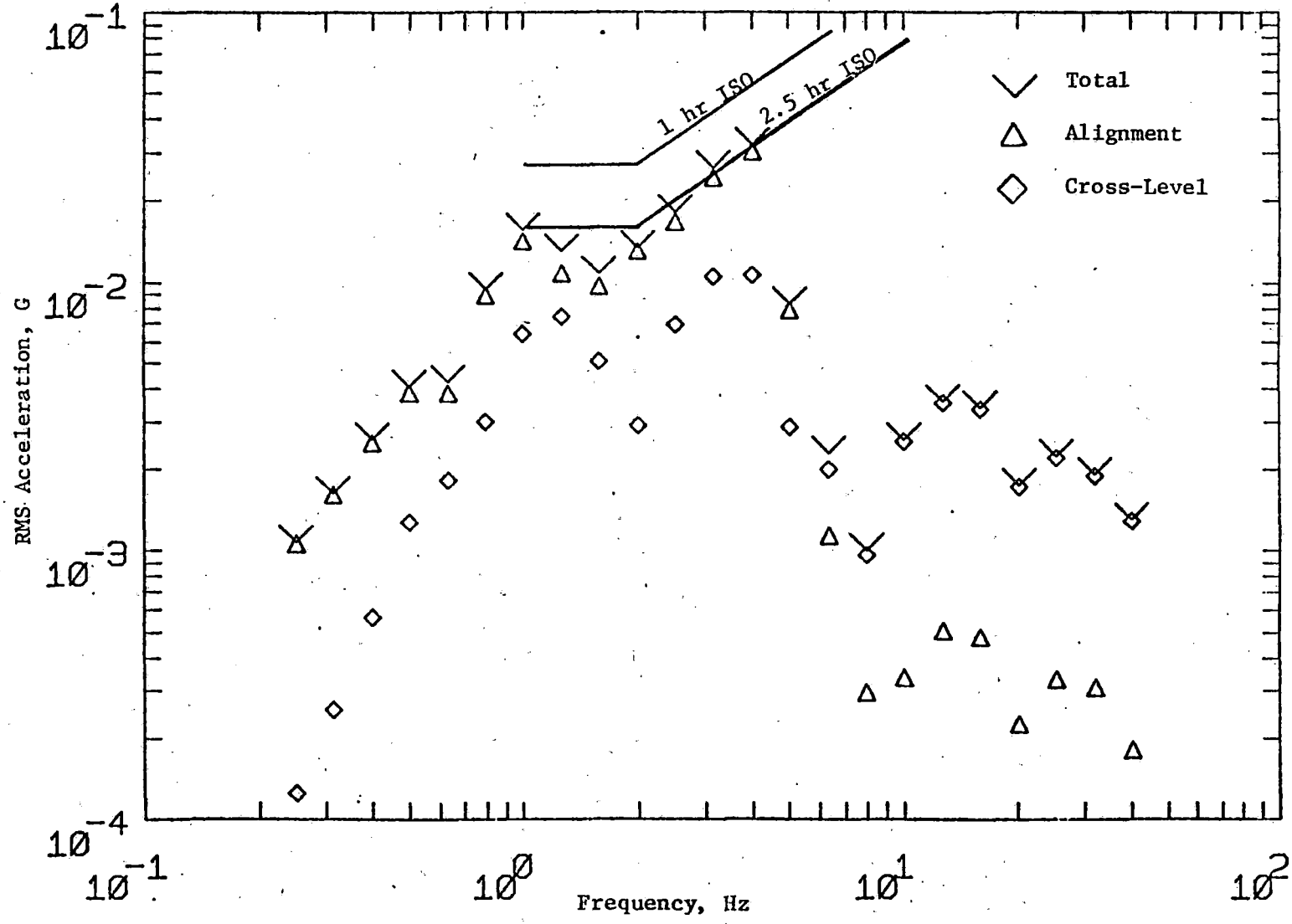

Figure 4-4.7: ONE-THIRD OCTAVE BAND RMS LATERAL ACCELERATIONS, FRONT PASSENGER POINT, λ = 1/7, K_{px} = 360,000 lb/ft, V = 75 mph.

TABLE 4-4.2: SUMMARY OF THE LATERAL DYNAMIC RESPONSE
STEERABLE TRUCK

CLASS OF TRACK	6
CONICITY, λ	1/7
SPEED (MPH)	75
Total Front Passenger Point RMS Acceleration (G)	0.0486
Total C.G. Passenger Point RMS Acceleration (G)	0.0208
Total Rear Passenger Point RMS Acceleration (G)	0.0473
RMS Secondary Stroke Length, Leading Truck (in)	0.35
RMS Secondary Stroke Length, Rear Truck (in)	0.46
RMS Primary Stroke Length, 1st Wheelset (in)	0.0107
RMS Wheelset Excursion, 1st Wheelset (in)	0.187

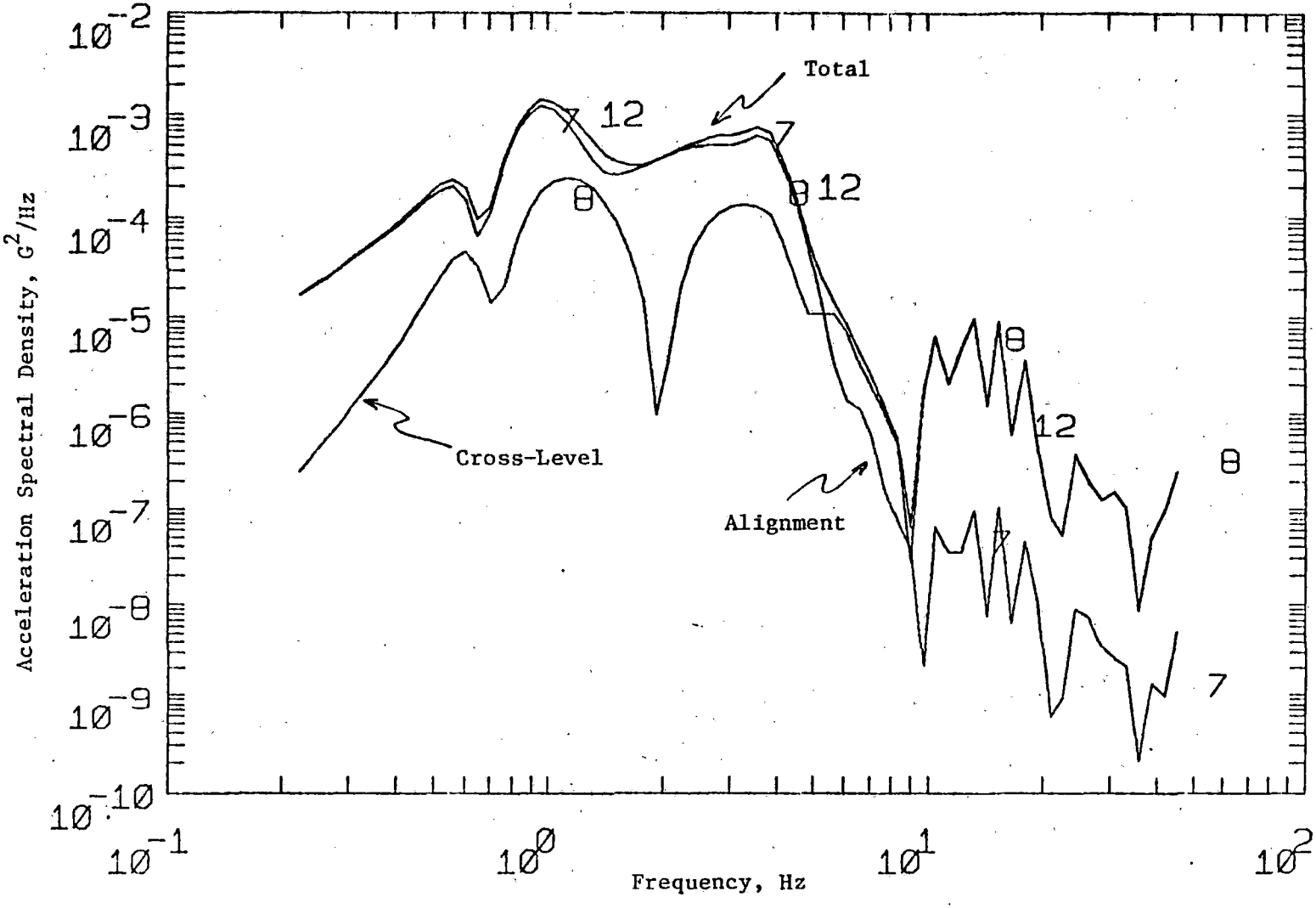

Figure 4-4.8 : LATERAL ACCELERATION SPECTRAL DENSITY AT FRONT PASSENGER POINT, , \ = 1/7, V = 75 mph.

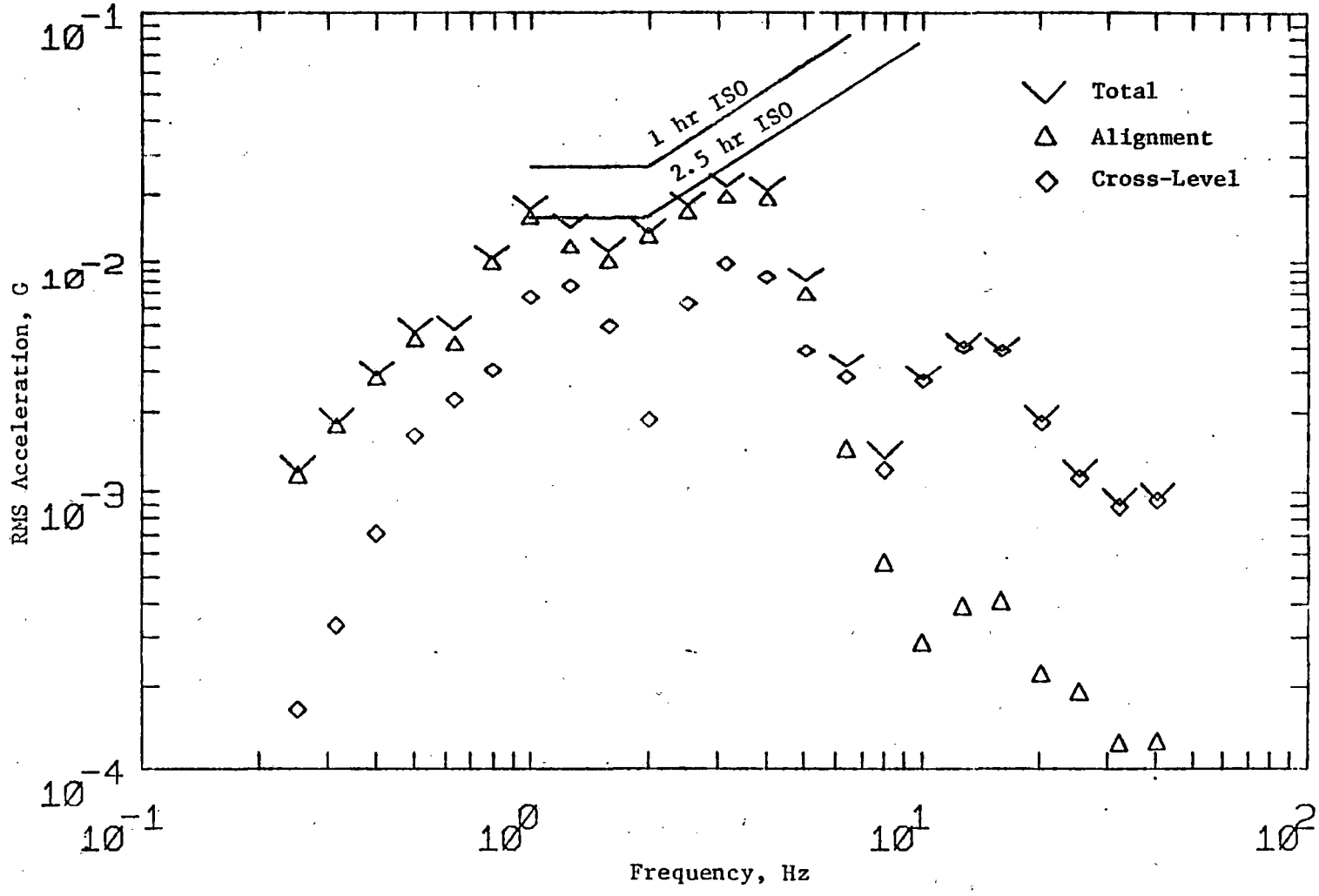

Figure 4-4.9: ONE-THIRD OCTAVE BAND RMS LATERAL ACCELERATION, FRONT PASSENGER POINT, , λ = 1/7, V = 75 mph.

time is about 2.2 hours.

4-4.4 Vertical Dynamic Response

The 12 degrees of freedom model was used to determine the vertical response of the existing P-III truck used on PATCO. Since the vertical response is independent of the primary longitudinal stiffness, the results are representative of both the existing P-III truck and the proposed steerable truck. The three passenger locations considered were the same as those for the lateral response. Table 4-4.3 summarizes the vertical response results. Figure 4-4.10 shows the vertical acceleration spectral density at the front passenger point for the existing P-III truck. Figure 4-4.11 shows the corresponding ISO ride quality plot. The resulting reduced comfort time is about 3.5 hours.

Table 4-4.3: Summary of Vertical Dynamic Response P-III Truck Speed (mph)

Speed (mph) - 75 Class of Track - 6

Total front passenger point RMS acceleration (G)	0.051
Total c.g. passenger point RMS acceleration (G)	0.027
Total rear passenger point RMS acceleration (G)	0.048
RMS secondary stroke length, front truck (in)	0.29
RMS secondary stroke length, rear truck (in)	0.26

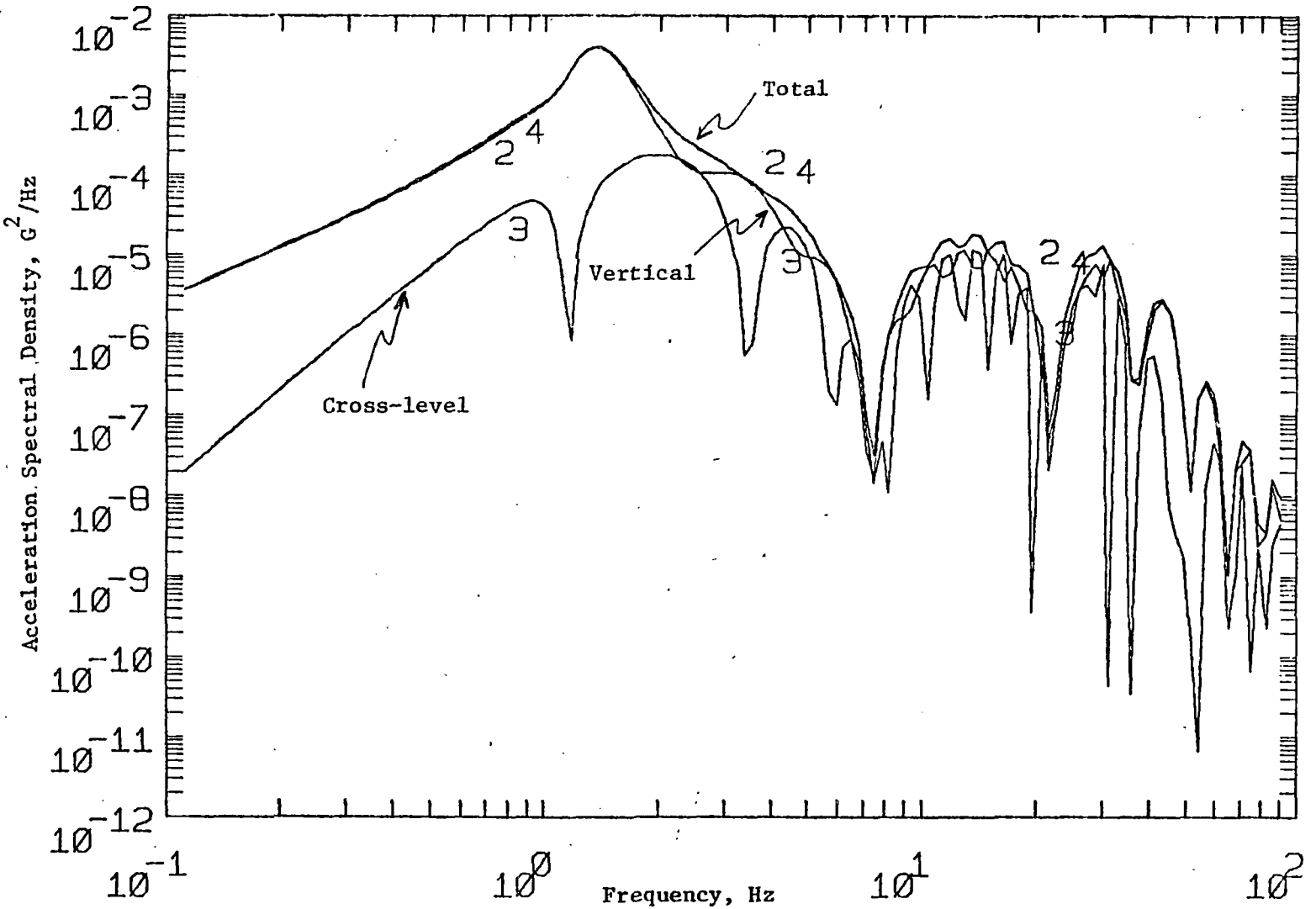

Figure 4-4.10: VERTICAL ACCELERATION SPECTRAL DENSITY AT FRONT PASSENGER POINT, 75 mph.

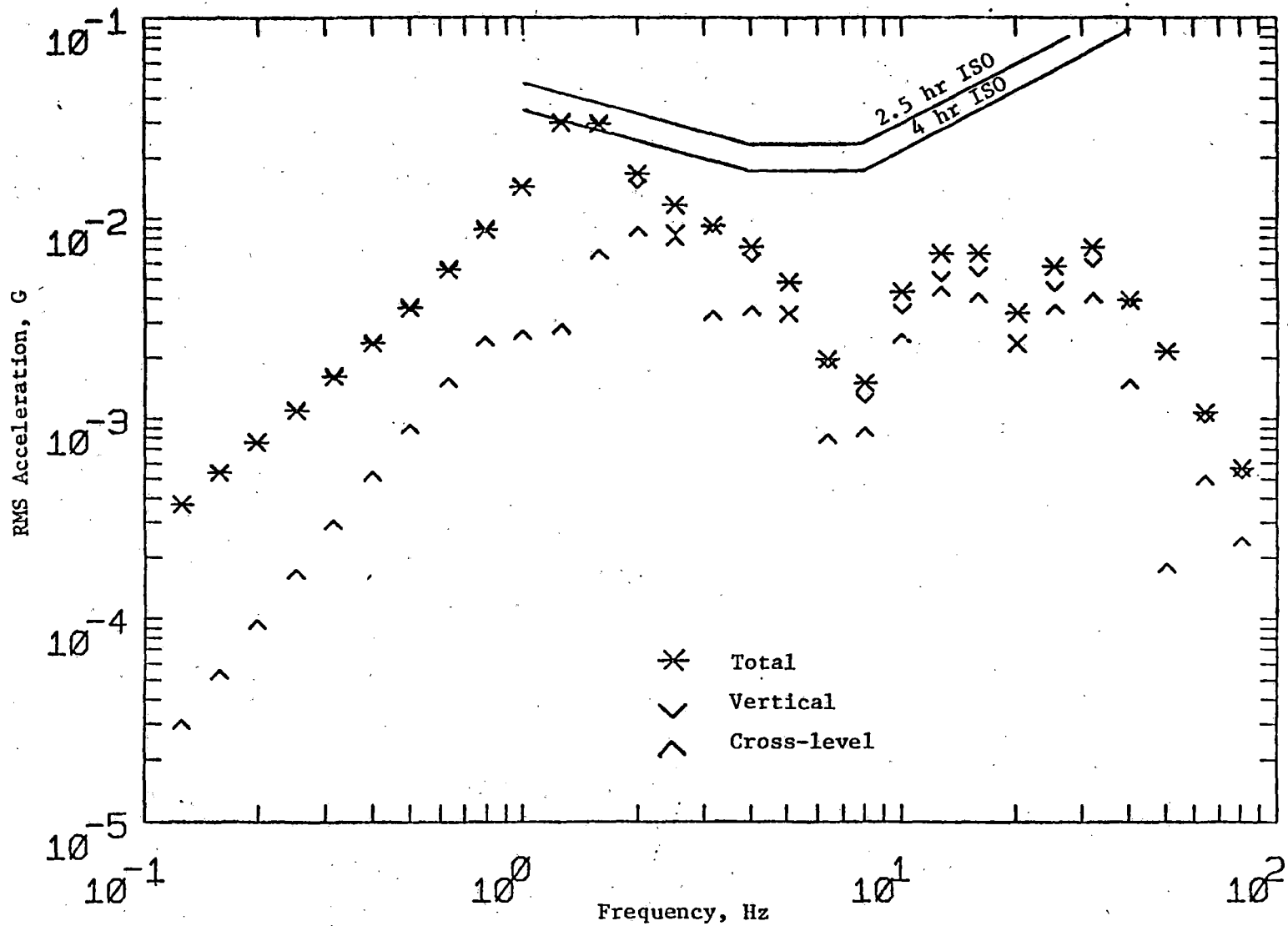

Figure 4-4.11: ONE-THIRD OCTAVE BAND RMS VERTICAL ACCELERATIONS, FRONT PASSENGER POINT, 75 mph.

4-4.5 Ride Quality Summary

Since the proposed steerable truck design uses the same secondary suspension as the existing truck, the ride quality should be similar to that of the existing truck. It should be mentioned that the steerable truck has the potential for improved ride quality because of its better tracking ability. It is anticipated that steering-type trucks operating on existing transit systems will avoid many track irregularities associated with switches, frogs, etc. thus improving the ride quality. Better tracking ability along with reduced noise levels associated with curving should tend to increase the overall ride comfort as perceived by passengers.

4.5 STRUCTURAL ANALYSIS - PROPOSED STEERABLE TRUCK

4-5.1 Introduction

In order to assure that the structural integrity of the proposed steerable truck design is adequate, a finite element stress analysis was performed and upgraded as the preliminary design progressed. A finite element model of the steerable truck structure was developed. The computer program used to solve the finite element model was ANSYS. The program was run for the following load cases: maximum static loads, maximum and minimum fatigue loads, equalization loads, and loads to provide inter-axle yaw and lateral stiffnesses.

4-5.2 Structural Model Description and Use

The major elements of the model are shown in Figure 4-5.1. The model is primarily a beam model with tension only, compression only members, and combination elements to provide the required stiffnesses at certain joints. The model consists of 147 nodes, 143 beams, 20 spars which can take tension but no bending, 22 compression only members with a specified gap, and 12 combination elements. The model represents 882 degrees of freedom. Figures 4-5.2 through 4-5.6 show all elements and nodes of the model. It is broken down into five major elements. All interfaces between elements are shown by letters in parenthesis () such as (A) on Figure 4-5.2 and 4-5.1 to show bolster to side frame interface.

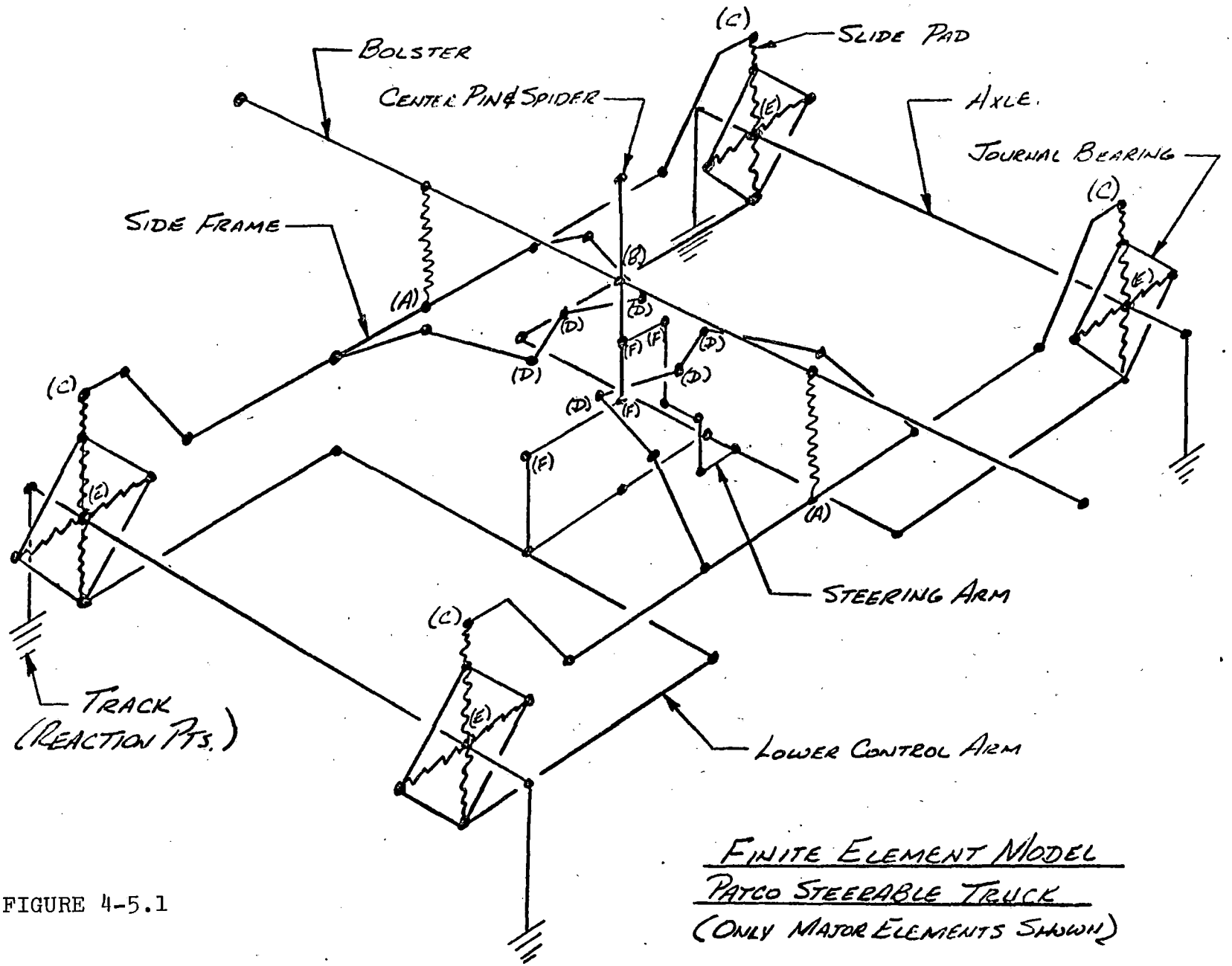

FINITE ELEMENT MODEL
PATCO STEERABLE TRUCK
(ONLY MAJOR ELEMENTS SHOWN)

FIGURE 4-5.1

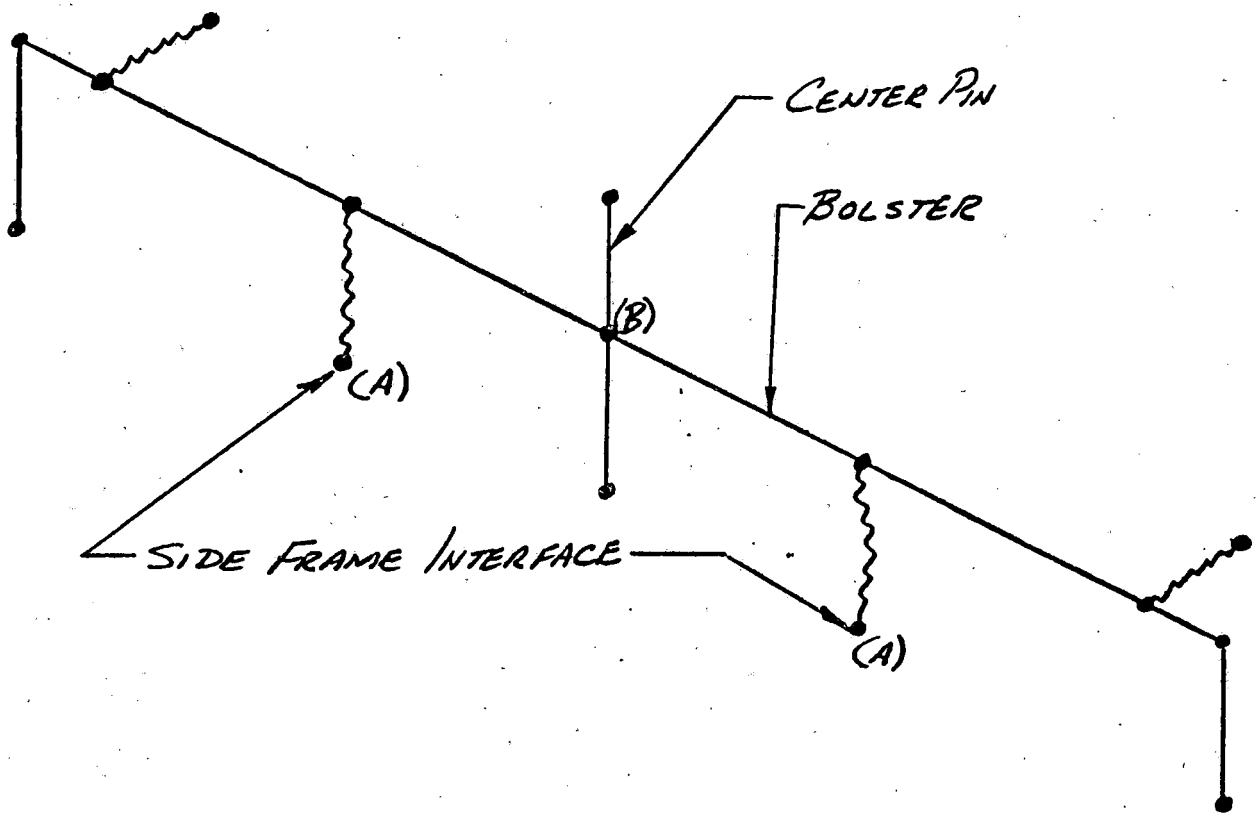

BOLSTER
FINITE ELEMENT MODEL
PATCO STEERABLE TRUCK

FIGURE 4-5.2

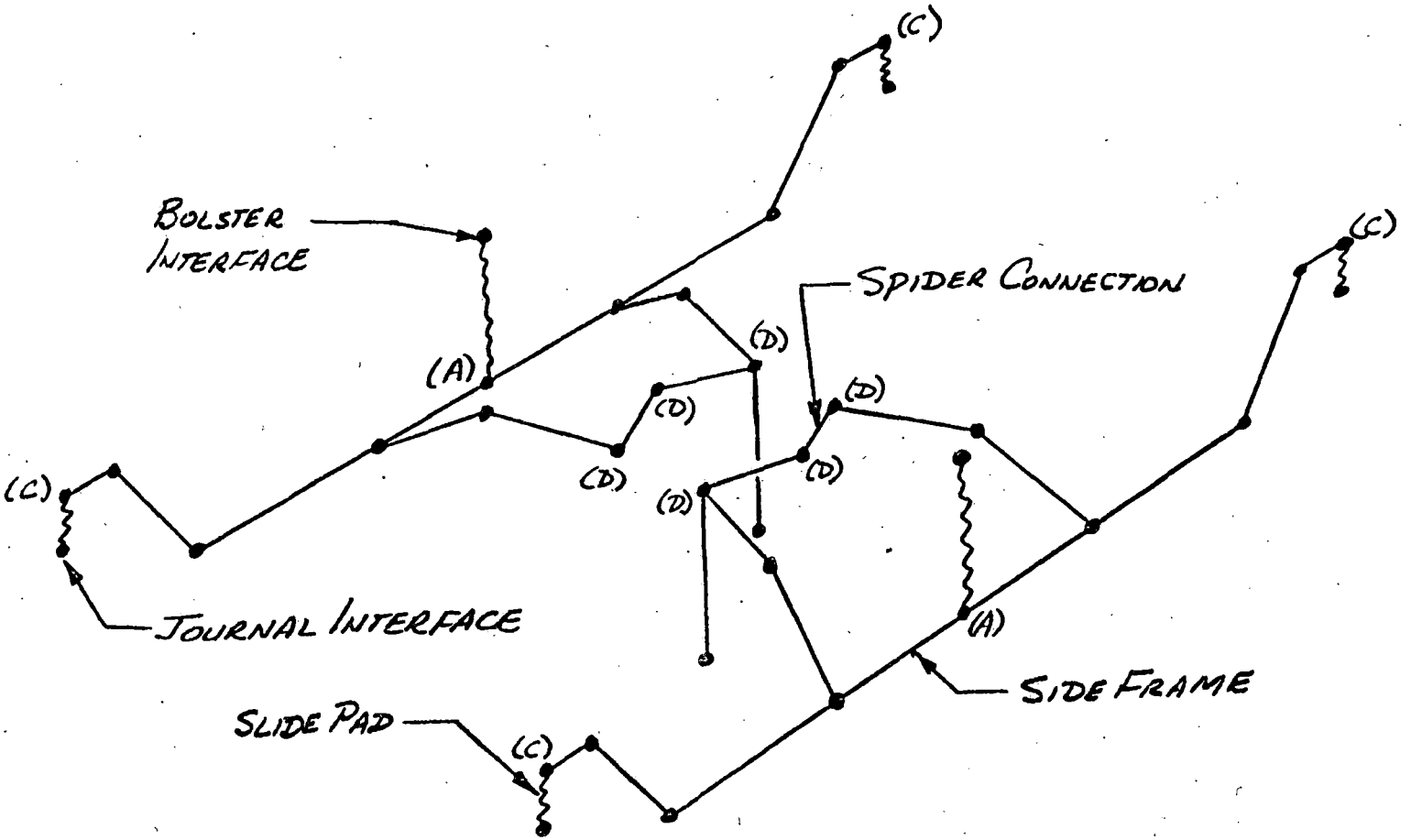
(C)
BOLSTER INTERFACE
SPIDER CONNECTION
(C)
(A)
(D)
(D)
(D)
(C)
(D)
(D)
(D)
(C)
JOURNAL INTERFACE
(A)
SIDE FRAME
SLIDE PAD
(C)
SIDE FRAMES
FINITE ELEMENT MODEL
PATCO STEERABLE TRUCK

FIGURE 4-5.3

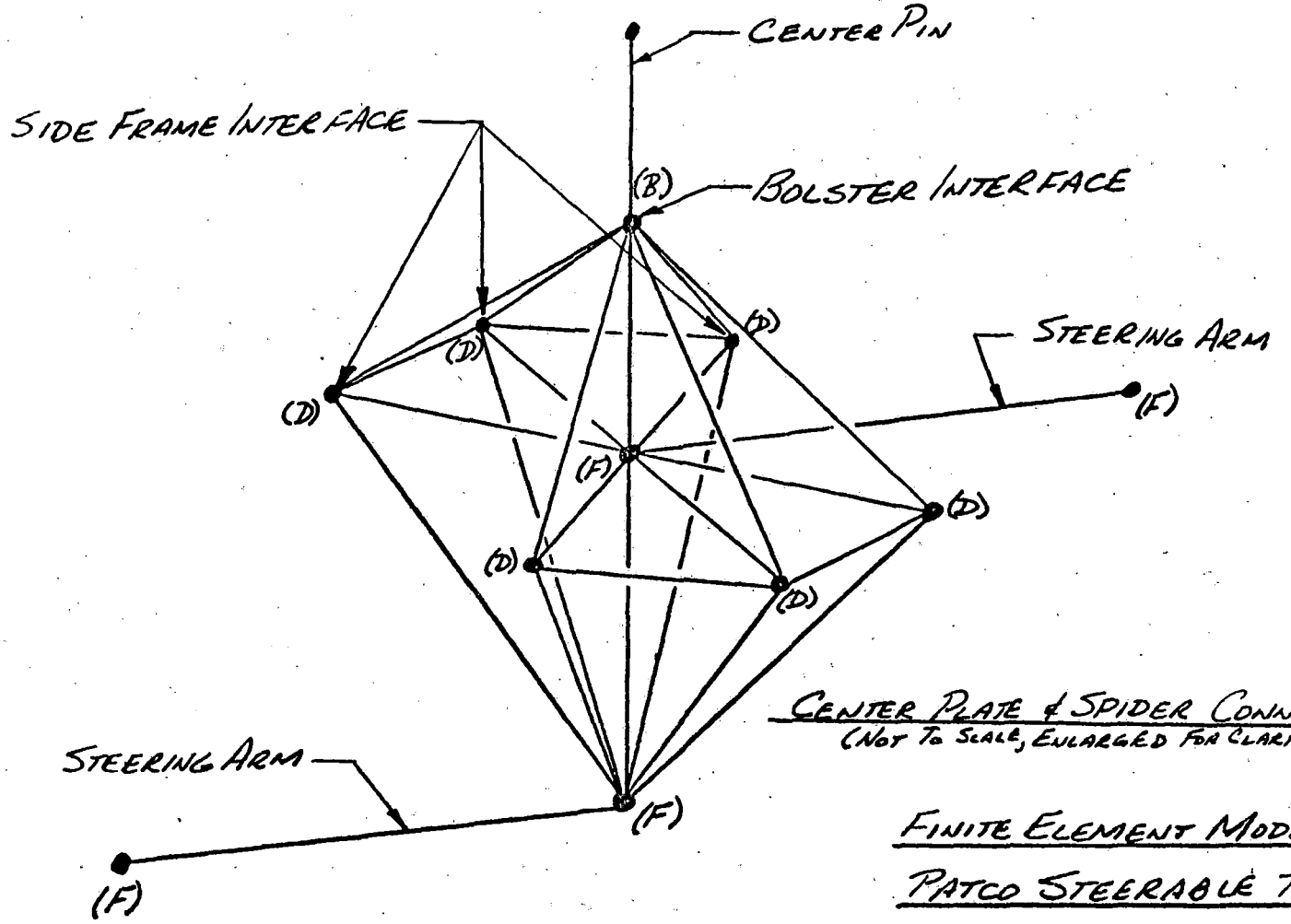
CENTER PIN
SIDE FRAME INTERFACE
(B)
BOLSTER INTERFACE
STEERING ARM
(D)
(D)
(D)
(F)
(F)
(D)
(D)
(D)
STEERING ARM
(F)
(F)
CENTER PLATE & SPIDER CONNECTION
(NOT TO SCALE, ENLARGED FOR CLARITY)
FINITE ELEMENT MODEL
PATCO STEERABLE TRUCK

FIGURE 4-5.4

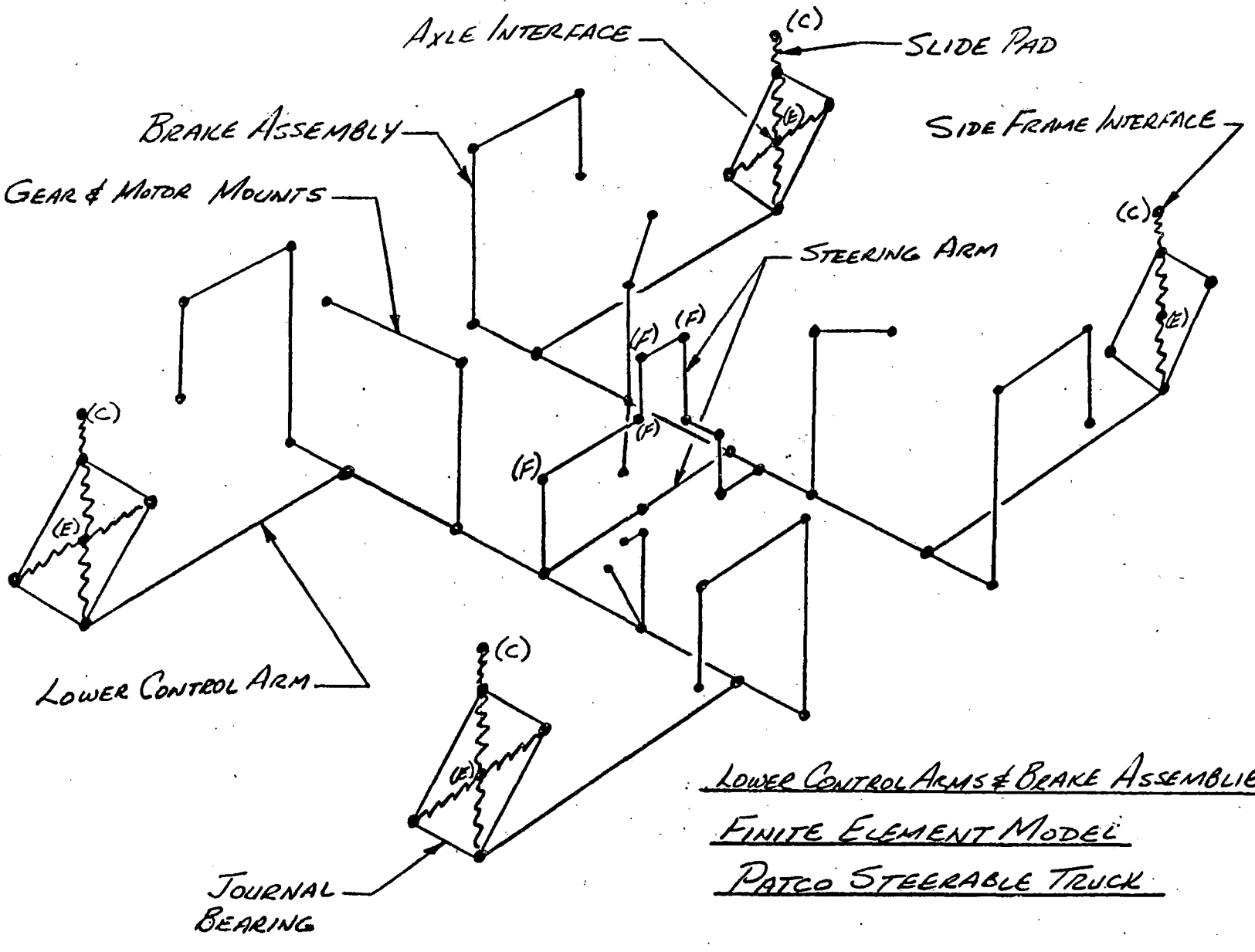
AXLE INTERFACE
(C)
SLIDE PAD
BRAKE ASSEMBLY
SIDE FRAME INTERFACE
GEAR & MOTOR MOUNTS
(C)
STEERING ARM
(F)
(F)
(F)
(F)
(C)
(E)
(E)
(E)
(C)
LOWER CONTROL ARM
(C)
(E)
JOURNAL BEARING
LOWER CONTROL ARMS & BRAKE ASSEMBLIES
FINITE ELEMENT MODEL
PATCO STEERABLE TRUCK

FIGURE 4-5.5

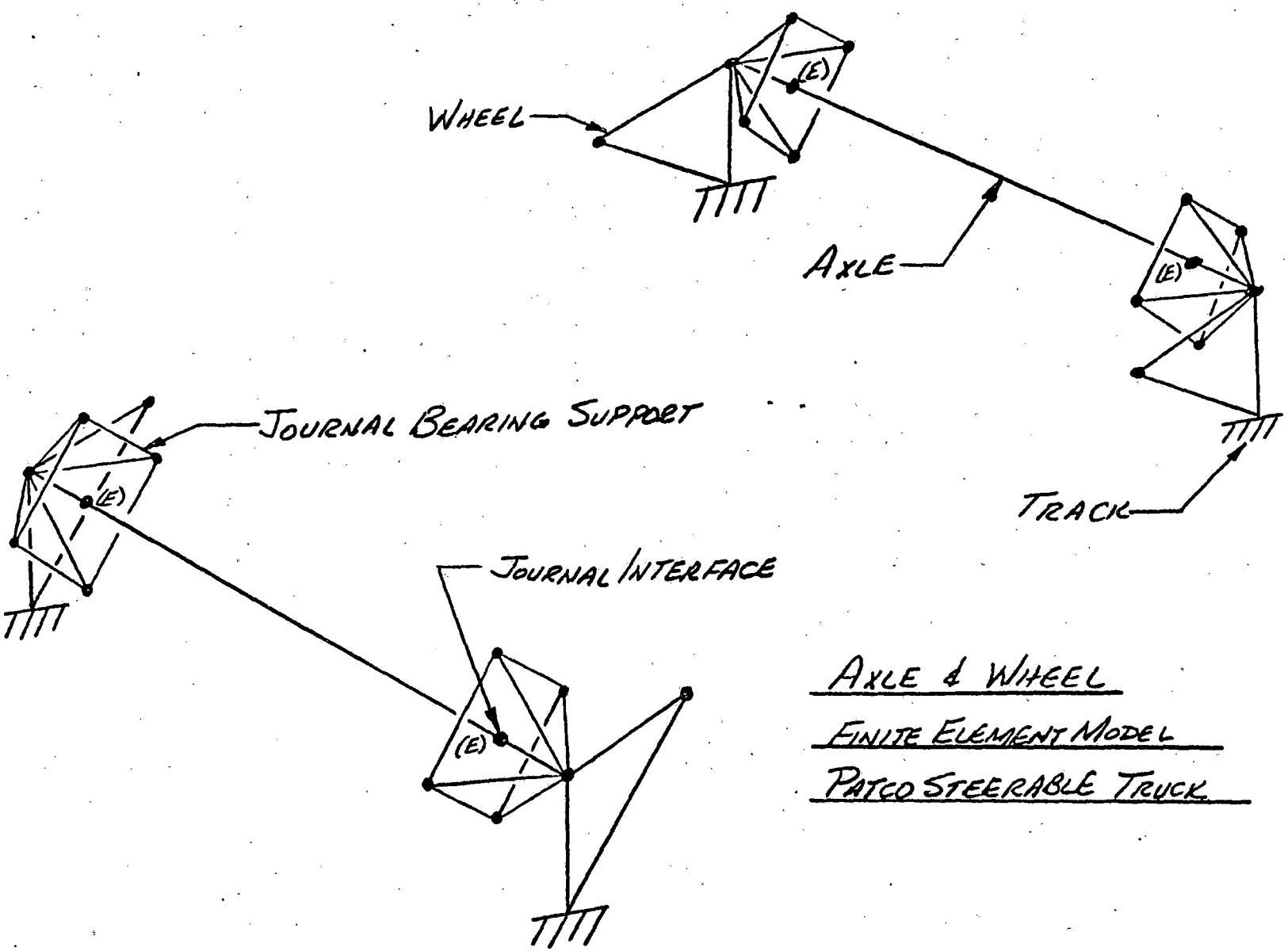
WHEEL
AXLE
TRACK
JOURNAL BEARING SUPPORT
JOURNAL INTERFACE
(E)
(E)
(E)
AXLE & WHEEL
FINITE ELEMENT MODEL
PATCO STEERABLE TRUCK

FIGURE 4-5.6

The initial static and fatigue load runs were able to locate the high stress areas. Design modifications were then made to the structural properties as necessary. The model was rerun and the results show that the stress levels are acceptable and very typical of good design practice.

The model was also used to predict the truck inter-axle lateral and yaw stiffnesses. The spring rates associated with the primary truck suspension and the shear pad/slider assembly and the steering arm inter-connection were incorporated into the finite element model. Necessary modifications to the section properties were made to achieve the required spring constants. The shear pad/slider constants were achieved by using the ANSYS combination element. This element allows a spring constant to be used for an element in one direction. Therefore, three separate elements were used at each shear pad/slider location to allow spring constants in the longitudinal, lateral, and vertical directions. Three nodes were incorporated at location (c) shown in Figures 4-5.1 and 4-5.3. These nodes were then coupled in all six degrees of freedom to assure uniform displacement of the point.

Inter-axle yaw stiffness was determined by applying equal and opposite 2000-lbs longitudinal loads to the ends of each axle as show in Figure 4-5.7. The truck was restrained in the vertical direction only at the four wheel track interfaces.

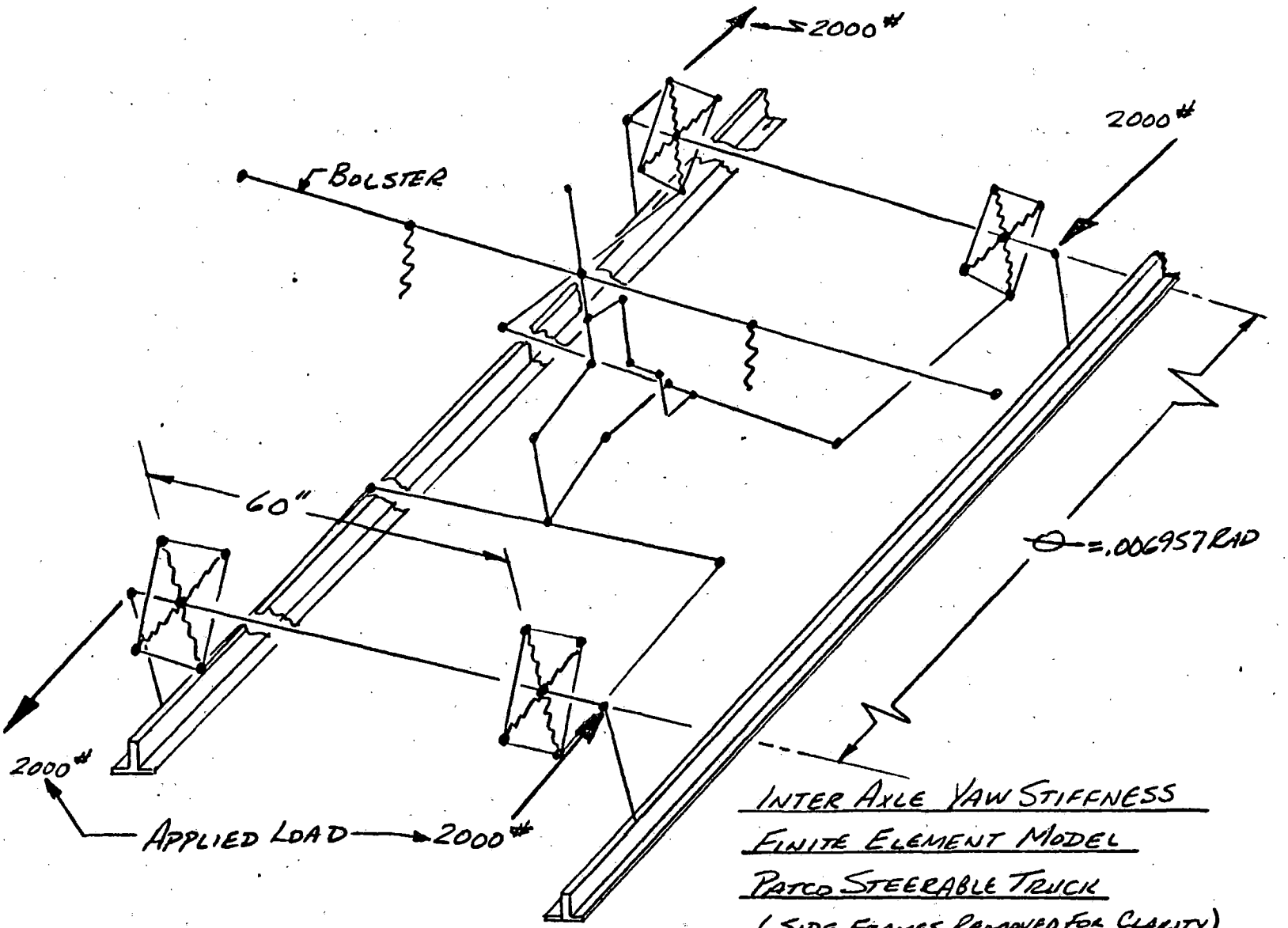
2000#
2000#
BOLSTER
60"
θ=.006957 RAD
2000#
APPLIED LOAD
2000#
INTER AXLE YAW STIFFNESS
FINITE ELEMENT MODEL
PATCO STEERABLE TRUCK
(SIDE FRAMES REMOVED FOR CLARITY)

FIGURE 4-5.7

Displacements were measured in the longitudinal direction at each end of the axle and the resultant angle 0 determined. The distance between applied loads was 60 inches.

Inter-axle lateral stiffness was determined by applying equal and opposite 2000-lb lateral loads to each axle as shown in Figure 4-5.8. The truck was restrained vertically and longitudinally at the four wheel track interfaces. Displacements at the ends of the axle were measured in the lateral direction.

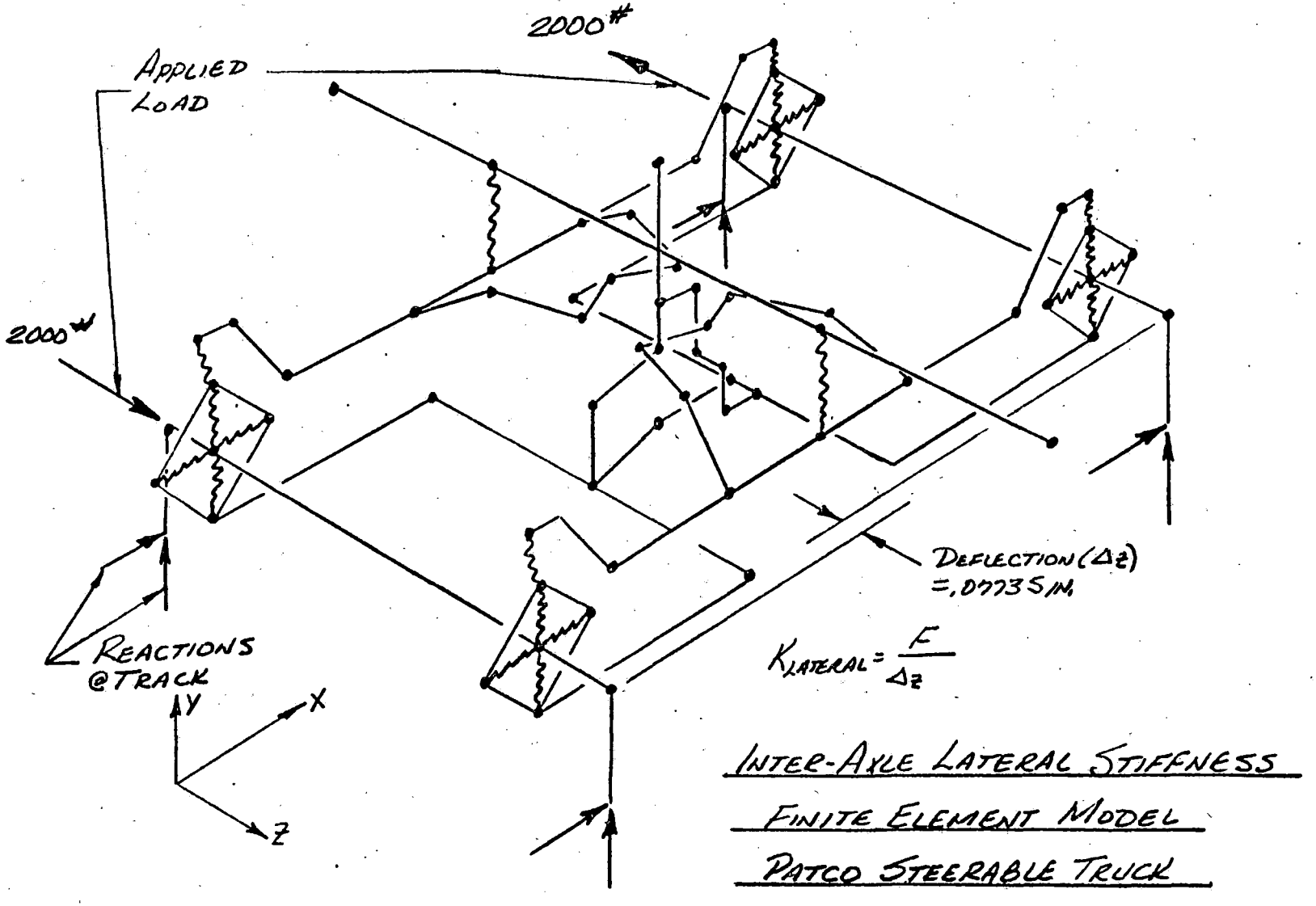
2000#
APPLIED LOAD
2000#
DEFLECTION (Δz) =.07735 IN.
REACTIONS @TRACK
Y
X
Z
K LATERAL = F/Δz
INTER-AXLE LATERAL STIFFNESS
FINITE ELEMENT MODEL
PATCO STEERABLE TRUCK

FIGURE 4-5.8

5.0 COST BENEFIT ANALYSIS

5.1 Introduction

The technical analysis provided data which supports the technical feasibility of modifying the PATCO P-III truck to a steerable configuration. The cost analysis will provide data that will be used to establish the overall cost effectiveness or net worth of the proposed steerable truck concept for the PATCO system. The basic trade-off will be the increased capital cost and increased maintenance cost because of the added assemblies versus the potential savings from reduced rail wear in curves, elimination of rail lubricators, elimination of wheel skid-flats caused by lubricant finding its way onto the rail head, and reduced energy consumption in curves. The additional benefit of steering will be the reduction or elimination of the noise and squeal associated with negotiating sharp curves. However, this cost analysis will not attempt to determine a dollar value for reduced noise levels.

5.2 Capital Costs

Capital costs have been determined for three steerable truck configurations. The first configuration represents a modification of two existing trucks. The preliminary design and description report and the technical analysis describe this first configuration as the proposed steerable truck.

The second configuration represents a full scale effort aimed at retrofitting 400 existing trucks. The third configuration represents a new design that is not constrained by the requirement to interface with existing equipment.

The capital costs are made up of manufacturing hours and rate, material cost, tooling cost, and assembly cost.

5-2.1 Prototype Test Trucks

The capital cost estimate of modifying two existing trucks to a steerable configuration represents part of the cost of confirming the predicted performance levels presented in the technical analysis. This configuration is best described as a prototype test truck. The prototype test truck was designed to mate with existing traction equipment, brake equipment, and bolster so that these parts are interchangeable. Initially it was thought that the existing truck frame assembly could be modified to a configuration that would be compatible with the requirements for steering. However, as the preliminary design progressed it became obvious that it was not feasible nor economically practical to modify the existing truck frame. A new truck frame assembly is required for the prototype test truck and represents a sizeable cost.

The requirement for mating directly with existing traction equipment represented a major design constraint for the steering arms. It was learned from PATCO that an earlier gear box mounting design had to be changed in order to extend motor life.

The existing design does provide the environment for extended motor life; therefore, it was strongly recommended that the existing motor/gear box mounting design be carried over to the prototype steerable test truck design. This requirement added complexity and weight to the steering arm design and resulted in increased material cost and labor cost.

The manufacturing cost of the prototype test truck design consists primarily of the cost of the steerable truck frame assembly which includes two independent side frame assemblies and two steering arm assemblies. The total cost of one prototype steerable truck frame (including material, stress relief, and labor) is $105,100. In addition to the manufacturing cost, there is a prototype tooling cost that has been estimated at $80,000.

The total manufacturing cost of prototype test trucks is $290,200 per car set plus engineering.

5-2.2 Retrofit Truck Design

The capital cost estimate of modifying 400 existing trucks to a steerable configuration was also determined. This cost estimate would be representative of a full scale effort aimed at the retrofit of entire fleets. The cost estimate of the retrofit design was also based on using existing traction equipment, brake equipment, and bolster. However, a simplified interface between the motor/gear box and the steering arms was considered. This would require modification to the mounting arrangement used on existing traction equipment.

The manufacturing cost of the steerable truck frame assemblies, which include two independent side frames and two steering arm assemblies, was estimated at $14,120 each.

The tooling cost associated with the retrofit of 400 trucks was estimated at $390,000. The amortized tooling cost per truck is $975. The total manufacturing cost of the retrofit design is $15,095 per truck plus engineering. The scrap value of the existing truck frames would help defer the retrofit expense and was estimated at $150 per truck. The manufacturing cost would then be $14,945 per truck or $29,890 per car set plus engineering.

5-2.3 New Truck Design

A new truck design with steering capability would not be constrained by existing equipment. Therefore, refinements could be made in the areas of interface between traction equipment and steering arms. A new design would also offer the potential for cost reduction by combining the functions of the various links that are required in the retrofit design. The manufacturing cost of a new steerable truck frame (designed for high production - 400 trucks) was estimated at $7300 more than the manufacturing cost of the conventional truck frame.

The tooling cost of a new cost design was estimated to be $270,000. The amortized tooling cost per truck is $675 (assuming 400 trucks). The steerable feature would represent

a premium cost of approximately $7975 per truck, or $15,950 per car set plus engineering.

5-2.4 Capital Cost Summary

The capital cost of manufacturing prototype test trucks was estimated at $290,200 per car set. The capital cost of manufacturing steerable truck frame assemblies for retrofit was estimated at $29,890 per car set. The capital cost premium of the steerable feature on a new design was estimated at $15,950 per car set. There is an engineering cost associated with all three approaches that would tend to raise the individual costs.

Section 5.4 of this report discusses the cost trade-off between capital costs and operating costs.

5.3 Operating Costs - PATCO System

The PATCO system accumulated a total of 3,983,000 car-miles during 1979, or 53,106 miles per year per car (75 cars). Since the system is 14.2 miles long, the total yearly car mileage results in 280,500 one-way trips or 3740 one-way trips per year per car. During the same year, 11,078,000 passengers rode the system. This averages out to about 40 passengers per car per one-way trip. Assuming 155 lbs per passenger, the average car weight is 86,260 lb. The total traffic is then about 6 million gross tons per year past any given point along the system.

The operating cost areas that would be affected by the addition of steering include rail, wheel, and truck maintenance, and power consumption. Rail maintenance costs include rail

grinding, rail replacement, and rail lubrication. Wheel maintenance costs include wheel truing during the life of the wheel as well as the replacement cost. The maintenance costs of a steerable truck will increase somewhat because of the added complexity and the increase in the number of parts. However, the potential exists that the total steerable truck maintenance costs will be the same as the existing truck maintenance costs if wheel life can be extended. Several truck components (including journal shock rings and motor mounts) are replaced during wheel changeout because the truck is disassembled and not because their useful life is spent. The total power consumption should be lower because of reduced curve resistance.

5-3.1 Rail Maintenance

The PATCO system has 28.4 miles of revenue track which include: 21.6 miles of surface and 2.0 miles of bridge track consisting of 132-pound ASCE welded rail on wood tie and ballast and 4.8 miles of subway track consisting of 100-pound ASCE jointed rail on wood half ties imbedded in concrete. Rail lubricators are installed on the subway curved track sections, some with radii of 190 feet. Track gauge is 4 feet, 8 1/2 inches.

Steerable trucks can have an effect on three areas of rail maintenance including: rail grinding, rail lubrication, and rail replacement on curved track. These areas and their related costs are discussed below.

Rail Grinding

Rail grinding is performed primarily to reduce noise on the PATCO system. There is no measurement or fixed schedule applied to this program. The Superintendent of Way and Power determines the need for grinding based on inspection of rail corrugation. Rail corrugation occurs on the curves, especially the 190-feet radius curves near City Hall and Ninth Street Stations. Approximately 280,000 revenue cars pass over the revenue track between grindings.

Typically, a SPENO bus power unit and several buggies, with two dozen grinding stones, are contracted to grind all revenue rail in 60 hours over 7 days. The grinder operates at approximately 1 mph and usually requires two passes to accomplish the task. Approximately 0.0015 inches of rail surface is removed with each pass. Single track operation is necessary during grinding. The grinding train has exclusive occupancy of only one traffic block.

Prior to commencement of revenue service, PATCO contracted the grinding of all track to assure good shunting. The time and cost of all rail grinding to date is given in Table 5-3.1.

Table 5-3.1: PATCO Rail Grinding Costs

1968	$ 8,000
1972	2,000
1975	7,800
1977	11,600
1979	16,000

In support of the contracted rail grinding operation, PATCO assigns a foreman to coordinate track operation, de-energize third rail and perform liaison/witnessing functions. At $14.30 per hour (including benefits), this cost is about $1000 (1980 labor/benefits rate). This brings the total cost of the last grinding operation to about $17,000. The latest grindings have occurred approximately every 2 years. Assuming this to be reasonably typical, then the average rail grinding cost on a yearly basis is about $8500 per year. A fleet of steerable trucks would certainly reduce the severity of rail corrugation on sharp curves and possibly eliminate the need for rail grinding. It was assumed that a fleet of steerable trucks could prolong the need to grind by at least a factor of three. This would reduce the average yearly rail grinding cost to about $2833.

Rail grinding is necessary to remove rail corrugations; however, rail grinding reduces the life of the rail because of material removal. There is a long term rail replacement cost associated with the grinding operation that is not included in the average yearly grinding cost estimate discussed above.

Rail grinding of the PATCO system does not represent a major cost; however, a fleet of steerable trucks would reduce and possibly eliminate curved rail corrugation.

Rail Replacement

Table 5-3.2 shows the costs incurred by PATCO for replace-

ment of curved track sections. These costs include both material and labor.

Table 5-3.2: PATCO Rail Replacement Costs

1978	$ 13,200
1979	22,300

The 1978 and 1979 rail replacement costs were used to determine an average yearly rail replacement cost of $417,750. This cost represents only curved track sections. The primary reason for replacement of curved track is loss of gauge face due to excessive wear caused by wheel flange contact.

A fleet of steerable trucks would certainly reduce the severity of gauge face wear on curved rail sections. Since rail gauge face wear is caused by wheel flange contact, the wheel flange wear index can be used to estimate the reduction of rail gauge wear from a fleet of steerable trucks. It has been conservatively estimated that a fleet of steerable trucks could reduce rail gauge face wear on very sharp curves by a factor of four. This would make the estimated yearly cost $4438 for curved rail replacement. This results in a yearly savings of $13,312 if a fleet of steerable trucks are used.

Rail Lubrication

Rail lubrication is a method commonly used to reduce squeal, flange wear, and rail gauge face wear on sharp curves. The PATCO system has 10 lubricators installed on various curves in the subway. When the lubricators are working properly, they do

in fact reduce the squeal and wear associated with sharp curves. However, when the lubricators are not functioning properly they can create problems. If the lubricators are not providing sufficient lubricant, the noise or squeal will increase dramatically. The excessive noise will alert the train operator that the lubricators are not functioning properly and maintenance can be scheduled. If the lubricators are providing excessive amounts of lubricant, the excess will find its way to the rail head surface and cause wheel slide which results in wheel flats.

Lubricator maintenance requires 8 man-hours per month per lubricator. The hourly rate with benefits for a maintenance man is $10.47 per hour. The maintenance of all 10 lubricators results in a monthly cost of $838, or a yearly cost of $10,051 plus $5000 per year for grease and other consumables. This brings the total to $15,051 per year.

A fleet of steerable trucks would not need a lubricator system. Therefore, the entire yearly cost of $10,051 could be viewed as a savings effected by steerable trucks.

5-3.2 Wheel Maintenance

Wheel flats are the principal wheel wear mode at PATCO, followed by flange wear and other types of tread wear such as spalling. Rail lubrication reduces flange wear, although wheel flats remain a problem if lubricant is over-applied or improperly applied (both of which are difficult to prevent in practice). Wheel flats are usually removed by wheel truing.

PATCO has maintained a wheel truing program since system start up, utilizing an above floor wheel lathe which accommo-

dates a complete truck. Wheels are visually inspected whenever noise is reported and at each scheduled car inspection: monthly and at 12,000-mile intervals. They are checked with AAR wheel gauges at the 50,000-mile inspection or whenever visual inspection indicates irregular wear. A typical wheel is trued every 55,000 to 70,000 miles (every 12 to 14 months), averaging four truings over a typical 240,000- to 300,000-mile life.

Wheels are trued to 0.003-inch tolerance between wheels on the same axle. All wheels on a car are required to be within 0.5-inch diameter. PATCO condemning limit is 25.5-inch diameter.

Additionally, small dime size flat spots are frequently removed with abrasive shoe brakes. Typically, a mechanic changes the brake shoes in the shop and operates the car within the yard up to 30 mph with dynamic braking disconnected. This effort spans 2 hours, 1 hour in action running the car and the remaining changing brake shoes and disconnecting/connecting dynamic braking.

Wheel Truing Procedure and Cost

All wheels at PATCO are trued in the Lindenwold Shop. Table 5-3.3 lists the categories and hourly wages of personnel involved in wheel truing and wheel changing at PATCO.

TABLE 5-3.3: PATCO PERSONNEL WHEEL TRUING/CHANGING

Employee	Hourly/With Wage/Benefits	Tasks
Foreman	$11.00/$15.07	Operate lift for detrucking
Electrician	$ 8.09/$11.08	Disconnect/reconnect trucks; disconnect on press/boring machine
Machinist	$ 7.89/$10.81	Detruck, operate overhead crane; qualified to set up segmented abrasive brake shoes/ operate car
Yard Motorman	$ 7.70/$10.55	Move disconnected car around yard/shop with other available car
Helper	$ 6.48/$ 8.88	Qualified on overhead crane and assists at lathe set up

Wages and Benefits Reflect 1980 Dollars

The procedures and manpower expenditures associated with wheel truing are listed in Table 5-3.4. A total of 36 man-hours is required to true one car set of eight wheels. This effort represents a labor cost of $384 per car set.

Wheel Changing Procedure and Cost

Table 5-3.5 lists the procedures and manpower expenditures associated with wheel changing. A total of 111 man-hours is required to change eight wheels (one car set). This represents a labor cost of $1198 per car set.

TABLE 5-3.4: PATCO WHEEL TRUING PROCEDURE

Step Operation	Elapsed Time (hr)	Personnel	Time (hr)	Man-Hours	Labor Cost (C)	Remarks
1. REMOVE TRUCKS	1	1 electrician	0.5	0.5	$ 5.54	Working both trucks
a. Receive car over pit disconnect trucks		2 mechanics	1	2	21.62	
b. Move car to lifting bary	1	1 yard motorman	1	1	10.55	Use another revenue vehicle as available
		2 mechanics	1		21.62	to push/pull
c. Raise car on left	2	1 shop foreman	1	1	15.07	Foreman operates lift
		2 mechanics	2	4	43.24	
Subtotal	4			10.5	117.64	For two trucks
2. TRUE WHEELS (TRUCK SET OF FOUR WHEELS)						
a. Set up one axle set truck in lathe	0.5	1 machinist	0.5	0.5	5.41	Either man operates
		1 helper	0.5	0.5	4.44	crane
b. Turn one axle set	1.25	1 machinist	1.25	1.25	13.51	Operate lathe
c. Reverse truck to set up other axle set	0.5	1 machinist	0.5	0.5	5.41	Either man operates
		1 helper	0.5	0.5	4.44	crane
d. Turn one axle set	1.25	1 machinist	1.25	1.25	13.51	
e. Remove truck from lathe	0.5	1 machinist	0.5	0.5	5.41	
		1 helper	0.5	0.5	4.44	
f. Sharpen lathe tools	2	1 helper	2	2	17.76	Normally sharpens four sets for two cars during one day
Subtotal	4			7.5	74.33	For one truck set
3. REINSTALL TRUCKS (reverse procedure of REMOVE TRUCKS above)						
Subtotal	4			10.25	117.64	For two trucks

TABLE 5-3.5: PATCO WHEEL CHANGING PROCEDURE

Step Operation	Elapsed Time (hr)	Personnel	Time (hr)	Man Hours	Labor Cost (C)	Remarks
1. REMOVE TRUCK	1.0	See Table --		2.63	$ 29.41	Prorated for one axle set
2. REMOVE AXLE	2.0	1 electrician	0.5	0.5	5.54	Electrician disconnects/
		2 mechanics	2.0	4.0	43.24	removes motor; mechanics operate crane
3. CLEAN AXLE	1.0	1 helper	1.0	1.0	8.88	Scrapes and Steam cleans outside shop on drainage slab
4. PRESS OFF WHEELS (axle set-2 wheels)	1.0	1 machinist	1.0	1.0	10.81	Machinist operates press;
		3 mechanics	1.0	3.0	32.43	most of this time is handling
5. BORE WHEEL (axle set-2 wheels)	2.0	1 machinist	2.0	2.0	21.62	Operates boring machine;
		1 helper	0.5	0.5	4.44	assists handling wheel
6. PRESS ON WHEEL (axle set-2 wheels)	1.5	1 machinist	1.5	1.5	16.22	Machinist operates press;
		3 mechanics	1.5	4.5	48.65	most of this time is handling
7. INSTALL AXLE	2.0	See remarks	-	4.5	48.78	Reverse of REMOVE AXLE above
8. INSTALL TRUCK	1.0	See remarks	-	2.63	29.41	Reverse pf REMOVE TRUCK above
TOTAL	11.05			27.76	299.43	For one axle set

Wheel Life Cycle Cost

If the average wheel life at PATCO is about 270,000 miles and the average mileage per year per car is 53,106 miles, then the average wheel life in time is 5.08 years. Table 5-3.6 lists the costs incurred during the life of a wheel.

TABLE 5-3.6: WHEEL LIFE CYCLE COSTS - EXISTING TRUCK

Item	Cost Per Car Set
Wheel Material Cost ($470 each - 1979 pricing)	$3760
Wheel Changeout Labor Cost	$1198
Wheel Truing Cost 4 Times ($384 each truing per car)	$1536
TOTAL	$6494

$$\text{Yearly Cost} = \frac{\$6494}{5.04 \text{ yrs}} = \$1278 \text{ per year per car}$$

Steerable trucks would eliminate the need for lubrication and, therefore, eliminate the skid flats that are caused by lubrication. Since skid flats are a major reason for truing wheels, it seems reasonable that the total number of truings could be reduced from four to two during the life of the wheel.

Steerable trucks will also reduce flange wear significantly. This will have a major impact on wheel life because so much tread metal must be removed to restore flange thickness. Reduced flange wear is a result of low angles of attack during curving.

An additional benefit of steering is the capability to use a worn wheel profile without incurring truck hunting. This extends the useful life of the wheel tread between truings.

Steering also has a major impact on wheel tread wear as well as rail head wear. Studies by Kuman (2)* at ITT are showing a substantial connection between tread wear and angle of attack. Studies by EMD (3) are showing that longitudinal wheel/rail creep must increase dramatically to transmit a given rail horsepower if lateral creep is present. Recent tests by Canadian National (4) on steerable 100-ton freight cars have shown 50% reduction in flange wear and 30% reduction in tread wear.

From the above considerations, it seems likely that the effect of steering on the wheel life of a transit car could easily be to increase the life by more than a factor of two. For the purpose of this study, it seemed reasonable to expect that PATCO wheel life could be extended from 270,000 miles to 500,000 miles if steering were added. This would extend the wheel life time to 9.42 years. Table 5-3.7 lists the estimated wheel costs for a steerable truck.

* Numbers in brackets refer to references

TABLE 5-3.7: WHEEL LIFE CYCLE COSTS - STEERABLE TRUCK

Item	Cost Per Car Set
Wheel Material Cost ($470 each - 1979 pricing)	$ 3760
Wheel Changeout Labor Cost	$ 1198
Wheel Truing Cost 2 Times ($384 each truing per car)	$ 768
TOTAL	$ 5726

Yearly Cost = $\frac{\$5726}{9.42 \text{ years}}$ = $608 per year per car

Based on the above considerations, the addition of steering would reduce the yearly wheel cost per car set from $1278 for the existing truck to $608 for the steerable truck. This results in a yearly savings of $670 per year per car, or $50,250 per year for the PATCO system (75 cars).

Power Consumption

During 1979, PATCO used a total of 38,118,700 kilowatt hours at a cost of $1,561,529. The power breakdown was: 70% traction, 14% lighting, heating and air conditioning, 14% station operation, and 2% maintenance. The cost of traction power alone for 1979 was $1,093,070. A fleet of steerable trucks could reduce the total traction power cost because of reduced curve resistance.

To prevent the stalling of trains in curves, it is a widespread practice to compensate grades on the basis that

rolling resistance increases .8 lb per ton per degree of curvature (5). Thus, the curve resistance in a 4-degree curve would be twice the curve resistance in a 2-degree curve. On the other hand, to achieve a given change in direction, a 2-degree curve must be twice the length of a 4-degree curve. Therefore, the total energy tends to be a function of the amount of direction change.

The above suggests a method for using savings data on one system to estimate savings on another. For each system, the total direction change for all curves can be divided by total miles to give a "curvature index" having the units of degree per mile. Car-mile maintenance costs associated with curvature, i.e., wheel wear and rail wear, could be extended from one system to another on the basis of the ratio between the two curvature indicies.

Table 5-3.8 shows the various curves for the West Bound track at PATCO. The first column gives the curve number, the second column gives the curve length in feet, and the third column gives the curvature in degrees (degrees per 100-foot segment or chord). The fourth column gives the angle of direction change for the particular curve. The angle of direction change is the product of the curve length and curvature. The curvature index was calculated by dividing the total angle of direction change by the length

Table 5-3.8: WEST BOUND TRACK - PATCO

Curve No.	Curve Length (ft)	Curvature (deg/100 ft)	Angle of Direction Change (deg)	Curve Resistive Effort (ft-lb/ton)	
				$\theta > 4°$	$\theta < 4°$
1	4,651	0.58	26.97	-	1,890
2	2,829	0.98	27.72	-	2,020
3	2,656	1.4	37.18	-	2,818
4	2,087	0.77	16.07	-	1,147
5	2,033	2.0	40.66	-	3,253
6	1,674	0.73	12.22	-	869
7	1,654	0.93	15.38	-	1,115
8	1,651	1.58	26.09	-	2,010
9	1,598	1.07	17.10	-	1,257
10	1,358	1.98	26.89	-	2,147
11	1,260	7.17	90.34	10,497	-
12	1,063	1.03	10.95	-	802
13	888	0.7	6.22	-	441
14	798	2.6	20.75	-	1,747
15	700	0.28	1.96	-	133
16	662	2.55	16.88	-	1,415
17	579	1.6	9.26	-	715
18	535	21.6	115.56	25,100	-
19	438	19.0	83.22	16,561	-
20	421	13.0	54.73	8,593	-
21	391	11.3	44.18	6,411	-
22	330	29.0	95.7	25,743	-
23	317	0.55	1.74	-	122
24	251	1.3	3.26	-	245
25	218	28.6	62.35	16,597	-
26	205	9.6	19.68	2,621	-
27	142	13.3	18.89	3,005	-
	31,389		901.95	115,128	24,146

of the track in miles or, 902 ÷ 14.2 = 63.5 degrees per mile Since there are 52.8 100-foot segments of chords per mile, the average curvature for the system can be calculated by dividing the curvature index by 52.8, or 63.5 ÷ 52.8 = 1.20 degrees curvature.

A fleet of steerable trucks could reduce the curve resistance effort significantly and, therefore, reduce energy consumption. Curve resistance was mentioned previously as 0.8 lb per ton per degree, however, a more accurate estimate is given by King (4) as $(0.66 + 0.07\theta)\theta$ where θ is the curvature in degrees. Using this curve resistance estimate and the curve length, the curve resistive effort for the PATCO curves is given in Table 5-3.8. The curve resistive effort for curves greater than 4 degrees is given in Column 5 and for curves less than 4 degrees in Column 6. The total curve resistive effort for the West Bound Track is then 115,128 + 24,146 = 139,274 ft-lb/ton. In order to determine what percentage of the energy is dissipated in curving, an estimate of the energy consumed per trip on a per ton basis must be calculated.

During 1979, a total of 3,983,000 car-miles were accumulated. Since the system is 14.2 miles long, the total mileage is equivalent to 280,500 one-way car trips. In order to determine the energy dissipated per car trip, the total

traction power (which is 70% of the total) must be divided by the total one-way car trips.

$$\frac{(38{,}118{,}700 \text{ kw-hrs})\ 70\%}{280{,}500 \text{ one-way car trips}} = 95.1 \text{ kw-hrs per car trip}$$

This is equivalent to 2.52×10^8 ft-lb per car trip. Dividing the energy per car trip by the average car weight (86,260 lbs) yields 5.84×10^6 ft-lb/ton. This number represents the energy required per car per one-way trip on a unit ton basis.

The energy per trip can now be compared to the curve resistive effort to determine what percent of the total power cost is spent for curving. Dividing the total curve resistive effort for the West Bound PATCO Track by the total energy required per one-way trip yields:

$$\frac{139{,}274 \text{ ft-lb/ton}}{5.84 \times 10^6 \text{ ft-lb/ton}} = 2.4\%$$

This represents an energy cost of $26,234 per year for curving alone.

It has been stated before that a fleet of steerable trucks could reduce curve resistance and, therefore, the total energy cost somewhat. It has been conservatively estimated that a steerable truck could eliminate the curve resistance on curves less than 4 degrees and reduce the curve resistance by 75% on curves greater than 4 degrees. Using the above criteria

and referring to the track resistive effort given in Table 3.3.1, Columns 5 and 6, the following calculation can be made to determine the percent of curve resistance reduction:

$$\frac{(115{,}128 \times .75) + 24{,}146}{115{,}128 + 24{,}146} = 79\%$$

From the above calculation and assumptions, it seems reasonable to expect a 79% reduction in curve resistive effort on the PATCO system. Multiplying the current curving energy cost($26,234) by 79% yields a potential power cost savings of $20,735. This represents an energy cost savings per year that could be realized if the PATCO fleet had steerable trucks.

5-3.3 Truck Maintenance

Table 5-3.9 presents a breakdown of the truck maintenance costs for the PATCO fleet using 1979 labor and material rates. The table shows that the truck maintenance cost neglecting wheel maintenance is about $390,800 per year, or $5210 per year per car. Wheel maintenance costs are handled as a separate item (See Section 5-3.2).

Table 5-3.9: 1979 Truck Maintenance Cost Breakdown for the PATCO Fleet

Item #	Description	Cost
1	Motor rebuild	$142,700
2	Gear unit rebuild	118,000
3	Motor-gear coupling	27,000
4	Motor-gear mounting	1,100
5	Motor suspension	10,400
6	Gear unit suspension	700
7	Third rail	11,700
8	Unit tread brakes	20,300
9	Hand brake	800
10	Frame related	4,000
11	Bolster related	10,000
12	Side bearings	3,000
13	Shock absorbers	20,000

Item #	Description	Cost
14	Journal bearing	$ 13,000
15	Journal rubbers	5,100
16	Miscellaneous	3,000
	SUBTOTAL	$390,800
17	* Wheel Maintenance	95,850
	TOTAL	$486,650

* See Section 5-3.2: Wheel Life Cycle Cost - Existing Truck, for a detailed breakdown of this cost.

The maintenance cost breakdown estimate for a steerable truck would be similar to the first 16 items of Table 5-3.9 plus additional items directly related to the steering mechanism. Table 5-3.10 gives a breakdown of the additional maintenance items for a steerable truck. The table shows that the steerable truck would increase the maintenance cost for the fleet (75 cars) by about $14,000 per year. However, the potential exists that the steerable truck maintenance cost, neglecting wheel maintenance, will be the same as the existing truck maintenance. Several truck components such as motor suspension mounts, gear suspension mounts, and

journal rubbers are replaced during wheel changeout because the truck is disassembled and not because their useful life is spent. If wheel life can be extended,as estimated in Section 5-3.2, then it seems likely that the increased cost due to steering can be offset by a cost reduction resulting from extended useful life of the rubber components cited above. Therefore, it seems reasonable to expect very little if any change in truck maintenance costs resulting from steering. However, wheel maintenance costs would reduce dramatically if steering were added.

Table 5-3.10: Additional Maintenance Cost Items for a Steerable Truck Fleet (75 cars)

Item #	Description	Cost
1	Steering Arm	$ 4,000
2	Shear/Pad Slider	6,000
3	Rubber Joints	2,000
4	Links/Hangers	2,000
	TOTAL	$14,000

The next section summarizes all operating costs.

5-3.4 Operating Cost Summary

Table 5-3.11 shows that if the PATCO system were

equipped with steerable trucks, a potential savings of $105,015 per year could be realized. The potential operating cost savings must now be traded off against the capital cost outlay required to retrofit.

Table 5-3.11: Operating Cost Summary in Dollars

Description	Existing Truck	Steerable Truck	Savings
Rail Maintenance Costs			
Rail Grinding	8,500	2,833	5,667
Curved Rail Replace.	17,750	4,438	13,312
Rail Lubrication	15,051	-	15,051
Wheel Maintenance Costs (75 cars)	95,850	45,600	50,250
Traction Power Costs	1,093,070	1,072,335	20,735
Truck Maintenance Costs	390,800	390,800	-
TOTAL	$1,621,021	$1,516,006	$105,015

5.4 Cost Analysis Summary

The capital cost summary (Section 5-2.4) stated that the cost to retrofit existing trucks with steering would be about $29,890 per car set or $2,241,750 for the entire fleet (75 cars). The operating cost summary (Section 5-3.5) stated that steering could reduce the yearly operating costs by approximately $105,015 per year. The question then becomes

what is the pay back period for the retrofit.

Payback is the period required to recover initial outlay and has traditionally been an important consideration for revenue-producing projects. A rough approximation may be obtained by dividing the annual savings into the first cost. This results in what is commonly called the base payback period.

$$\text{Base Payback Period (Retrofit)} = \frac{2,241,750}{105,015} = 21.3$$

The base payback period ignores the time value of money and could over or understate the actual payback period. A more accurate figure could be obtained if the payback definition is interpreted as the period needed to recover outlay from the cost savings discounted. This latter period may be called the true payback period. The true payback period will be the same as the base payback period if the cost savings escalate at the same rate as they are being discounted. However, rather than guess at inflation rates for labor and material, costs associated with the projected yearly savings, and the interest rates at which a transit property could borrow money, the base payback period will be used.

The base payback period for the premium cost of steering added to new trucks can be calculated in a similar way. The capital cost summary puts the premium cost of

steering for a new truck design at $15,950 per car set or $1,196,250 for the entire fleet.

$$\text{Base Payback Period (new design)} = \frac{\$1,196,250}{\$105,015} = 11.4$$

Keep in mind that this analysis did not attempt to put a dollar value for reduced noise levels during curving.

6.0 SUMMARY AND CONCLUSIONS

This report presents data which shows that it is technically feasible to modify an existing heavy rapid rail truck to a steerable configuration with dramatically improved curving performance without adversely affecting its high speed stability or ride quality. The improved curving performance is brought about by yawing the axles to a radial position during curve negotiation. The axles are forced-steered by a linkage arrangement between the axles and carbody. The stability is obtained by providing the required dynamic axle yaw restraint. Axle yaw restraint comes from the primary longitudinal spring element and the forced steering link. Ride quality is preserved by retaining the existing secondary suspension without significantly changing the input to this suspension.

This report also presents data which shows that the cost benefit of steering for a particular transit system depends on the number of curves. In the case of the PATCO system, significant savings in the areas of wheel maintenance, track maintenance, and energy consumption could be realized with the addition of steering; however, the cost to retrofit the entire PATCO fleet in terms of the base payback period made steering appear less attractive.

Based on the technical and cost analysis studies, the following conclusions have been reached:

CONCLUSIONS

1. It is mechanically feasible to modify an existing truck to a steerable configuration.

2. Steering arms provide a practical method of mounting traction and brake equipment so that the entire assembly can yaw with the axle.

3. Analysis shows that because of the high unsprung mass due to the steering arms and the traction and brake equipment mounted on the steering arms, a primary longitudinal stiffness of 30,000 lbs./in. is required to provide stability for the self-steered design configuration (assuming λ = 1/7, f = full Kalker).

4. Curving studies show that the self-steered design configuration requires a 2000-lb. friction slider in series with the 30,000 lbs./in. primary longitudinal stiffness for improved curving performance on curves down to 28 degrees (assuming a friction coefficient $\mu \geq 0.3$).

5. Curving studies show that the performance of the self-steered design configuration with 2000-lb. sliders degrades as the wheel/rail adhesion level (coefficient of friction, μ) drops significantly below 0.3.

6. Curving studies show that self-steering performance improves with increased wheel conicities.

CONCLUSIONS (Cont'd)

7. Analysis of the friction sliders shows that the self-steered design configuration with 2000-pound sliders may have stability problems on rough track if slider breakout occurs.

8. Increasing the slider breakout force level would enhance stability but would degrade curving performance of the self-steered design configuration.

9. The addition of a steering link from the carbody bolster to the outer steering arm can convert the self-steered design configuration to a force-steered design configuration.

10. The force-steering link lateral stiffness increases the effective inter-axle bending stiffness of the truck and, therefore, increases the critical speed or stability margin of the design.

11. Analysis shows that the forced-steered design configuration with 30,000-lbs./in. longitudinal primary stiffnesses in series with 2,000-lb. sliders can provide excellent curving performance (angles of attack nearly zero) without sacrificing high speed stability (assuming $\lambda \geq 1/20$ $f \geq 1/2$ Kalker).

12. Self-steering action will be present (assuming sufficient wheel/rail adhesion levels) and will actually aid the performance of the force-steered design configuration. This will result in lower force levels in the force-steering link.

CONCLUSIONS (Cont'd)

13. Force-steered operation in curves will ensure radial performance (nearly zero angle of attack) with or without the aid of self-steering action under all wheel/rail adhesion conditions.

14. Linear analysis shows that force-steered design configuration has the possibility of kinematic instability at low values for the Kalker coefficient associated with creep and low values for the wheel conicities.

15. It is not known whether such low values of creep coefficients are possible or not. This can best be answered by full scale testing on wet or lubricated rail.

16. It is also not known to what wheel profile a steerable truck will wear. This can be answered only by full scale testing of a steerable truck.

17. If necessary, alternate force-steered design configurations can be used to prevent kinematic instability caused by low values of creep and low values of wheel conicities, but this approach will result in sacrificing improved curving performance.

18. Based on a reduced wear index, it has been estimated that the addition of steering can significantly reduce wheel flange wear and curved rail wear during curving.

CONCLUSIONS (Cont'd)

19. Because of the reduced angle of attack during curving, the force-steered configuration should significantly reduce the noise levels typically associated with negotiating sharp curves.

20. It is anticipated that the force-steered truck design could result in improved ride quality because of its ability to track the rail center better than a conventional truck with an equivalent secondary suspension.

21. The capital cost for manufacturing two prototype trucks for road testing was estimated at $290,200.

22. It is common practice that before a prototype truck design is released for field testing one truck frame undergo structural fatigue testing. This cost has been estimated at $111,900 and should be part of the total prototype truck costing.

23. The capital cost for retrofitting the PATCO trucks with steering was estimated at $15,095 per truck (based on 400 trucks).

24. The capital cost premium for steering on a new truck design was estimated at $7300 per truck (based on 400 trucks).

25. Steering could reduce PATCO wheel maintenance costs by about $50,250 per year.

CONCLUSIONS (Cont'd)

26. Steering could reduce PATCO rail maintenance costs by about $34,030 per year.

27. Steering could reduce PATCO tractive power consumption by about 2% or $20,735 per year.

28. The base payback period for retrofitting the PATCO fleet was estimated at 21 years.

29. The base payback period for the premium cost of steering on a new truck design was estimated at 11 years for the PATCO system.

30. The cost benefit of steering, with respect to a specific transit system, depends on the total number of sharp curves (greater than 4 degrees) and the railcar fleet size to be retrofitted.

7.0 REFERENCES

1. Hedrick, J.K., et al., "Performance Limits of Rail Passenger Vehicles: Evaluation and Optimization," Final Report, U.S. Department of Transportation Contract No. DOT-OS-70052, November 1978.

2. Kumar, S., "Some Wheel-Rail Interaction Factors Influencing Vehicle Dynamics," Proceeds of ASME, Winter Meeting, December 7, 1979.

3. Logston, D.F. and G.S. Itami, "Locomotive Friction-Creep Studies", ASME Paper No. 80-RT-1, January 1980.

4. King, F., "Testing of Type 1I Freight Car," Canadian National Railway Report, 1979.

5. Marks, L.S. and T. Baumeister, "Standard Handbook for Mechanical Engineers," 7th edition, copyright 1979, Chapter II, p. 38.